Integrating Carbon Capture and Blast Furnace Technologies

Edward J Long

A thesis submitted for the degree of Doctor of Philosophy

School of Engineering
Newcastle University
United Kingdom

September 2023

Acknowledgements

I would like firstly to thank both Prof. Steve Bull and Dr. Adrian Oila, my research supervisors at Newcastle University, for their invaluable guidance and patience.

The support of my employer, Primetals Technologies Limited, has been highly appreciated both financially and in providing me with time to carry out this research work and reminding me of its importance to Steel producers.

I would also like to offer thanks to the staff and students within the School of Chemical Engineering and Advanced Materials at Newcastle University for their help and feedback.

Finally, my greatest thanks go to my wife, Sophie. Her support and encouragement have made the writing of this document possible more than any other.

Abstract

It is now widely acknowledged that industrial emissions play a large part in the increase of global temperatures. One industry yet to show significant signs of reducing emissions of CO_2 is the steel industry despite accounting for approximately 7% of industrial emissions. There is however a wide range of research available on carbon capture and utilisation techniques from several other industries. This gives confidence that such technologies could also be applied to the steel industry.

The aim of this project was to suggest methods to reduce CO_2 emissions per tonne of steel produced by considering likely changes in steel production methods up to 2050. By assessing eleven combinations of crude steel production methods, the average CO_2 emission intensity was derived. This was based on applying best available techniques to existing processes and increasing the proportion of crude steel generated by scrap recycling and directly reduced iron. These options are limited by the availability of raw materials and therefore the effect of a new, undeveloped, technology was also considered. This would allow for a greater reduction in average CO_2 intensity of crude steel but is unlikely to be available for widescale adoption before 2050. This leads to the conclusion that existing technologies will need to be augmented to meet binding 2050 CO_2 emission reduction targets.

The technological compatibility of several available and soon to be available techniques for the treatment of blast furnace gas were considered. This was carried out using a flowsheet approach combining the blast furnace process with gas treatment technologies. These technologies included CO_2 removal using chemical absorption, physical absorption and physical adsorption with the effect of water gas shift to maximise CO_2 removal also considered. Technologies to utilise this captured CO_2 were also analysed such as regeneration of CO_2 using plasma catalysis, solid oxide electrolysis and reverse water gas shift. In many cases the resulting gas streams were recycled back to the blast furnace to displace other fuels. Six metrics were used to assess each of the flowsheet cases with an approximate operating cost for utilities also considered. By assessing the options based on these considerations and technological compatibility with the established blast furnace process, the most attractive options to a steelmaker were determined. This leads to the conclusion that chemical absorption for CO_2 capture is the most compatible technology although not necessarily the lowest operating cost option.

The work also presents an analysis of different chemical absorption amines on the capital cost of such a system for treating blast furnace gas. This analysis was carried out by developing models within Aspen HYSYS to estimate operation considering three types of amine solution and a further three mixtures of amines. Factors such as equipment size and regeneration energy were used to determine the effect of the different amines to treat the blast furnace gas. The equipment size was used to prepare an approximate capital cost for eleven different options considering different concentrations of the amines and amine blends. By comparing these costs to a benchmark of 28wt% monoethanolamine, the most promising amine for treating blast furnace gas was identified to be piperazine. This amine reacts quickly with CO_2 in the gas stream resulting in smaller equipment size and hence capital cost. However, this case also produced one of the highest levels of solvent loss driven by the high temperature of gas leaving the absorber vessel. This will either increase operating costs or the complexity of the gas cooling section of the absorber column.

Contents

Nomenclature

ΔH^{o}_{298}	Enthalpy of Reaction

Abbreviations

AIST	American Institute of Science and Technology
AMP	2-amino-2-methyl-1-propanol
APEA	Aspen Process Economic Assessment
ASME	American Society of Mechanical Engineers
ASU	Air Separation Plant
BAT	Best Available Technique
BAU	Business As Usual
BF	Blast Furnace
BFG	Blast Furnace Gas
BOF	Basic Oxygen Furnace
BOFG	Basic Oxygen Furnace Gas
CCS	Carbon Capture and Storage
CCU	Carbon Capture and Utilisation
CDQ	Coke Dry Quenching
CFC	Chlorofluorocarbons
COG	Coke Oven Gas
COP	Conference of the Parties
CSP	Concentrated Solar Power
CV	Calorific Value
d	Day
DR	Direct Reduction
DRI	Directly Reduced Iron
e	Electron
E_a	Activation Energy
EAF	Electric Arc Furnace
eNRTL	Electrolyte Non-Random Two Liquid
EOR	Enhanced Oil Recovery
ETS	Emissions Trading Scheme
EU	European Union
eV	Electron Volt

FGR	Flue Gas Recycle
g	grams
GDP	Gross Domestic Product
GHG	Greenhouse Gas
GJ	Gigajoule
Gt	Gigatonnes
h	hour
H_2	Hydrogen
HBI	Hot Briquetted Iron
HIsmelt	High Intensity Smelting
HM	Hot Metal (product from a blast furnace)
HSS	Heat Stable Salts
ID	Internal Diameter
IEA	International Energy Agency
IPCC	Intergovernmental Panel on Climate Change
kg	Kilograms
kJ	Kilojoules
km^2	square kilometre
KPI	Key Performance Indicators
kWh	Kilowatt hours
m^2	square metres
mm	millimetres
MMBtu	Million British Thermal Units
mt	Million Tonnes
mol	moles or molar basis
MOE	Molten Oxide Electrolysis
Mt/y	Million tonnes per year
MW	Megawatts
NG	Natural Gas
Nm^3	cubic meter of gas under 0°C and atmospheric pressure
NOAA	National Oceanic and Atmospheric Administration
OECD	Organisation for Economic Co-operation and Development
PA	Physical Absorption
PEG	Polyethylene Glycol
PCI	Pulverised Coal Injection

ppm	Parts per Million
RPB	Rotating Packed Bed
RWGS	Reverse Water Gas Shift
s	second
SEWGS	Sorption Enhanced Water Gas Shift
SOEC	Solid Oxide Electrode Cell
SSAB	Svenskt Stål AB
t	tonnes
TGR-BF	Top Gas Recycling Blast Furnace
tHM	Tonnes of Hot Metal
TRL	Technological Readiness Level
TRT	Top gas energy Recovery Turbine
TSA	Temperature Swing Adsorption
UAE	United Arab Emirates
UK	United Kingdom
ULCOS	Ultra Low CO_2 Steelmaking
UN	United Nations
USA	United States of America
WGS	Waste Gas Shift
wt%	percentage by weight
VDEh	Association of German Steel Manufacturers
VLE	Vapour Liquid Equilibrium
Vol%	Percent by volume
VPSA	Vacuum Pressure Swing Adsorption
YSZ	Yttria-Stabilized Zirconia

List of Figures

List of Tables

Chapter 1. Introduction

This chapter is intended to introduce the background of the research project. Section 1.1 provides the context for the thesis covering climate change driven by CO_2 emissions and the steel industry. Section 1.2 explains the aims and objectives of the study and Section 1.3 outlines the scope considered within the different assessments. Finally, Section 1.4 lists the software packages used to develop the results reported later within this thesis.

1.1 Thesis Context

1.1.1 Emissions and Climate Change

Global warming is commonly accepted as predominately caused by industrial activities. These activities have given rise to an increase of greenhouse gasses emitted to the planet's atmosphere. Although not the solely responsible species, carbon dioxide (CO_2) is the most widely recognised and emitted greenhouse gas. It is the product of combustion of carbon and is therefore produced from a wide range of industries. Some of these processes can adopt new technologies which do not involve carbon at all and therefore will not emit CO_2 to the atmosphere. Other industries have a more fundamental relationship with carbon sources and are therefore labelled as "hard to abate". In these cases, process improvement and retro fit technologies must be considered to reduce emissions in line with the Paris Agreement (Melorose, 2015) guidelines. It is hoped that this will show willingness to improve whilst allowing time for new processes to be researched and deployed at scale.

Steel production is arguably one of the major developments made during the industrial revolution allowing larger structures and equipment to be constructed. This industry was developed and retains its reliance on fossil fuels to refine raw iron ore into a finished steel product.

1.1.2 From the Steel Industry's Perspective

The steel industry is responsible for approximately 10% of global greenhouse gas emissions (IEA, 2020). To meet strict guidelines for the reduction of CO_2 by 2050 laid out in the Paris Agreement (Melorose, 2015) the steel industry must begin to act within the coming decade. This action may include replacing existing production routes with less polluting alternatives or the application of retro-fit technologies to

reduce the emissions from existing facilities. The global steel industry is difficult to typify due to the differing ages and predominant technologies installed in different geographical locations. This report focuses on the European steel industry due to the increasingly high financial penalty for emitting CO_2 within this region. References will be made to China as it accounts for around half of the world's steel production (IEA, 2020). North America will also be discussed as this location already has a high proportion of low emission technologies.

Discussion around the decarbonisation of the steel industry is divisive, as it is a globally manufactured and traded commodity. Steel making either from recycling or virgin materials is reportedly carried out in 88 (out of 195) countries at various scales (WorldSteel, 2020). As mentioned previously, China produces the majority of steel yearly with countries such as India and Japan providing the second and third most steel respectively.

Several countries have or are planning to apply some form of CO_2 taxation. The aim of these schemes is to encourage industrial emitters to invest in carbon reduction schemes or risk financial penalties for continuing to release CO_2 unabated. Were these schemes to be applied equally for each location, then they would provide a serious incentive to decarbonise many industries. Currently, the cost of emitting CO_2 and therefore the cost of producing steel is not the same globally. This may encourage steelmaking companies to relocate carbon intensive facilities to regions without such strict CO_2 permitting while abandoning facilities with too high a CO_2 penalty. An example of this is the differing approaches taken by the European union and India. The former is seeing a shift of production from existing technologies to natural gas, hydrogen and scrap melting routes to meet binding reduction targets in 2030. India has one of the latest decarbonisation targets, aiming to meet the Paris Agreement targets by 2060. For this reason, blast furnaces are still being built within India, which will have an operating life of at least 20 years. Furthermore, the state-controlled steel industry is planning to invest heavily to replace aging infrastructure with new blast furnaces. This scenario of CO_2 intensive production of steel relocating from one geographical region to another is unlikely to have a deep impact on the global average emissions intensity of steel production.

One method which could decrease CO_2 emissions from steelmaking is the adoption of directly reduced iron and electric arc furnaces. This is already being seen in North America where scrap recycling accounts for a large portion of steel production. In Europe there are also plans for large scale investment to increase capacity in directly

reduced iron and scrap melting. Once operational, these new facilities will replace existing blast furnaces within Europe.

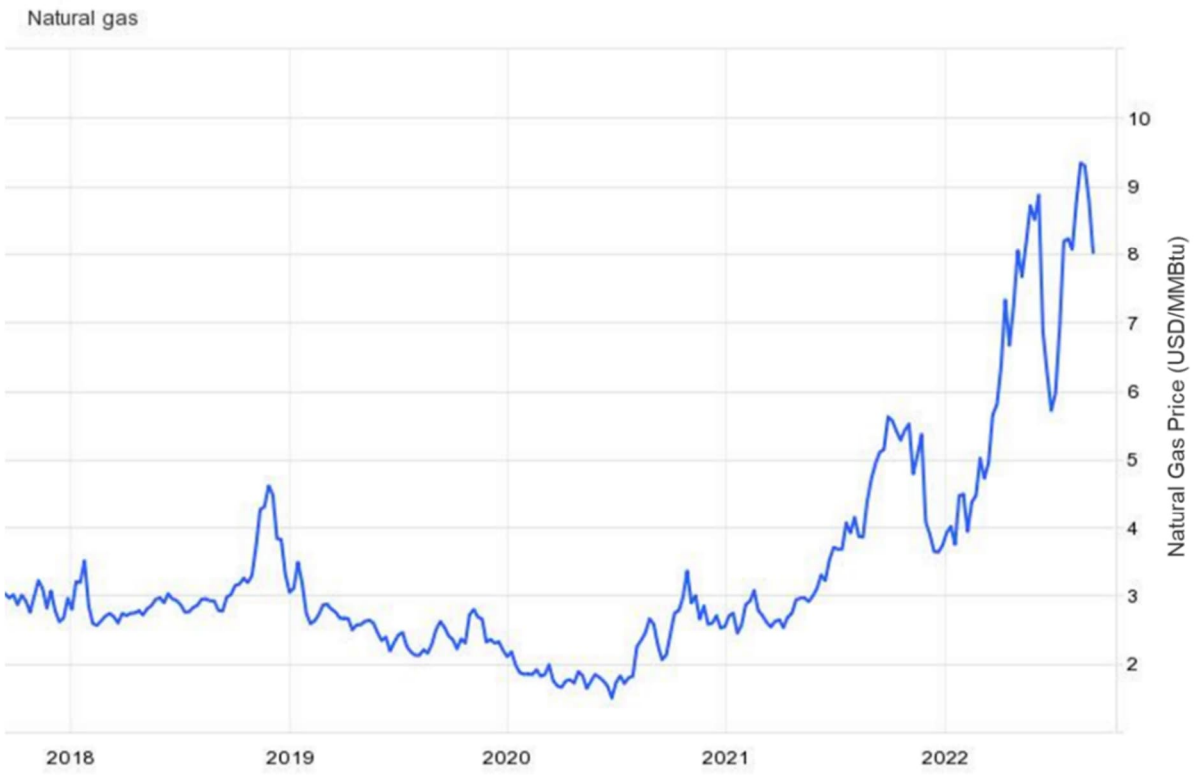

Figure 1.1: Natural Gas Price from 2018-2022 (Trading Economics, 2022)

Directly reduced iron plants currently rely on natural gas and electrical energy respectively to reduce iron ores and produce crude steel. Recent increases in the cost of natural gas, as shown in Figure 1.1, have incurred a significant escalation in operating costs of such processes. The impact of this is the temporary closure of the only directly reduced iron plant currently located within the EU. The rising natural gas price has also increased electrical energy prices as natural gas is often used to generate electricity.

An alternative to using a carbon-based fuel source is hydrogen fuelled direct reduction. This would result in very low CO_2 emissions per tonne of steel produced and is therefore the subject of much industry interest. There will be many industries looking to use hydrogen to reduce their emissions which will place steelmakers into competition with other industries who are better able to pass on costs to their customers.

Within Europe a carbon trading scheme is in place which requires emitters to buy permits to allow the emission of a tonne of CO_2. The price of these permits has

steadily increased in recent years as shown in Figure 1.2, reaching a high of almost 100 euros per tonne of CO_2 in August 2022.

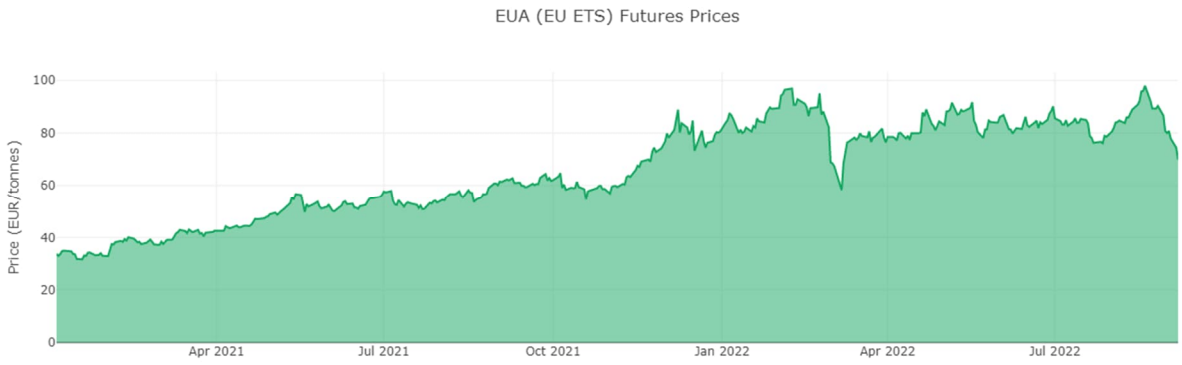

Figure 1.2: Cost of emitting CO_2 within Europe (Ember, 2022)

This cost of emitting CO_2 is forecast to increase further to encourage large scale emitters to convert their processes to cleaner production routes. Alternatively, industries may look to install a method of reducing CO_2 emission from existing processes while new production routes are developed.

1.1.3 Carbon Capture and Storage and Utilisation

Removal of CO_2 from gas streams was first proposed in the 1930's to purify natural gas (Bottoms, 1930). This technology has since been developed for use in hydrogen production and power generation. Three families of carbon capture will be considered within this work, namely:

- Chemical Absorption
- Physical Absorption
- Physical Adsorption

The methods above were chosen because of their reference of use at large scales similar to that required to treat blast furnace gas. Other methods of removing CO_2 from a gas stream are possible but are less suited to the gas flowrates from a blast furnace. These include membrane separation and cryogenic separation which will only briefly be explained within this thesis.

CO_2 captured from fertiliser production, to name but one source, is currently sold to the food and drink industry. This CO_2 is used both in the slaughter of animals and packaging of meat and in the carbonation of drinks. A further use of CO_2, developed over the past decade, is to enhance the recovery of oil from depleted hydrocarbon reservoirs. This has provided a major economic driver for carbon capture within Northern America where most carbon capture plants are currently located. It is important to note that while there are multiple uses for CO_2 currently, the amount of CO_2 available by adopting carbon capture would far outweigh what is required by these various uses.

CO_2 can also be stored in geological formations without being used to produce new chemicals or fuels. While this saves the energy required to utilise CO_2, significant energy may be required to transport the CO_2 to a suitable location for storage. Furthermore, while storage volumes are estimated to be vast, they do not provide an endless capacity. A further disadvantage to CO_2 storage is the level of monitoring to ensure that the injected gas remains stored within the reservoir.

1.2 Aim of This Work

The purpose of this work is to identify potential pathways to significantly reduce CO_2 emissions from the production of steel. The outcomes of this work aim to support the steel industry with their ongoing plans for decarbonisation of steel production. The aim is to suggest which of the many routes available to produce steel should be developed further to offer the largest reduction in CO_2 emissions while considering practical limitations on the availability of raw materials such as scrap steel.

1.2.1 Assessment of Steel Production Routes

In Chapter 4, the global average emissions of CO_2 per tonne of steel produced is determined based on the split of production over different manufacturing routes. The analysis is carried out considering available literature data for the various production steps within the different manufacturing routes. These are combined to determine the total CO_2 emissions generated by producing one tonne of crude steel from a given route. Different routes are considered in parallel with the amount of steel produced from each adjusted to meet the total steel consumption predicted for the year 2050. By changing the mixture of established production routes, significant reductions in average CO_2 intensity of steel can be realised without waiting for new technologies to

be developed. The purpose of this chapter was to identify ways to reduce current levels of CO_2 emissions by 80% based on technology and raw materials which are forecast or assumed to be available by the year 2050. Relying on currently available technologies will allow the steel industry to begin reducing its CO_2 emissions. The alternative is to wait for the development of new technologies which are currently not available at scale. This second approach would mean a greater capital expenditure in order to meet the 2050 deadline.

1.2.2 Assessment CO_2 capture and utilisation technologies

In Chapter 5, different technologies were assessed to treat blast furnace gas to remove, store or utilise CO_2. The analysis was carried out using heat and mass balances and simplistic literature data available for the various technologies investigated. By combining technologies, a flowsheet was created which detailed the different process steps and their effect on a blast furnace gas stream. The utility cost for each flowsheet, quantity of CO_2 removed, energy requirement and exported energy were all used to identify promising combinations. The technologies considered were mostly at a high technological readiness level, although some were not yet available at sufficient scale to treat the full flow of blast furnace gas from a steelworks. The aim of this chapter was to determine complimentary process steps which offer CO_2 reduction from an existing blast furnace. These technologies should be suitable to be applied to blast furnace gas within the next decade to significantly reduce the CO_2 emissions from existing steelmaking facilities. In addition, these technologies should have a minimum impact on operating costs and disruption to the steelwork energy balance.

1.2.3 Assessment of Chemical Absorption

In Chapter 6, detailed process modelling will be assessed to identify promising chemical absorption amines or blends of amines. Aspen HYSYS (Chang, 2018) was used to carry out the process modelling due to the software's large range of validated conditions with several different amine types. A standard flowsheet for removing CO_2 from natural gas was used as a basis and modified to suit the treatment of blast furnace gas. Details of the changes made and the model set-up are given in Chapter 3. The equipment duty was determined based on meeting 90% CO_2 removal from blast furnace gas. Using these equipment duties, an approximate capital cost for each different amine was determined using Aspen Process Economic Assessment

(APEA). The aim of this chapter was to determine whether chemical choice truly has an impact on capital cost of a chemical absorption plant. A further aim was to investigate whether compression of blast furnace gas prior to entry into the chemical absorption system offers a benefit to the capital cost of the plant.

1.3 Scope of the study

Within this study the following scope has been considered for each of chapters:

1.3.1 Assessment of Steel Production Routes

The scope for Chapter 4 includes the raw material preparation processes through to the crude steel output from either a basic oxygen furnace (BOF) or electric arc furnace. Casting and rolling processes are excluded from the scope of this section due to being almost constant regardless of the upstream processing steps.

The mining and transportation of raw materials to the steelworks are omitted from the assessment within Chapter 4. This may penalise production routes which require fewer different raw materials such as scrap metal, which could also be sourced more locally than high quality coal and iron ores.

All the process gasses generated by the different processing steps are expected to be fully combusted and sent to atmosphere. Such gasses are typically used to generate both steam and electricity for a steelworks. The chapter considers that electricity is purchased entirely from outside of the steelworks and carries its own CO_2 burden. While this may be true for scrap recycling processes, the blast furnace – basic oxygen furnace route generates significant portions of combustible gas which is used for on-site power generation.

The only utility gas considered in the scope is oxygen which is generated within the steelworks (and therefore the scope of this assessment) at an air separation plant by consuming electrical energy.

1.3.2 Assessment CO_2 capture and utilisation technologies

In Chapter 5 the blast furnace process becomes the focus and therefore the scope changes from the previous chapter. In this chapter the raw materials which are specifically used in the blast furnace are considered as inputs. These include coke, coal, iron ores, steam, compressed air, oxygen and in some cases hydrogen. Outputs from the model include CO_2, fuel gasses generated by removing CO_2 from

blast furnace gas or regenerating CO_2 and flue gasses produced by burning gasses to generate heat.

Electrical energy is supplied from outside of the scope of the study to power equipment to compress the blast furnace gas stream and remove CO_2 from it. This energy will be supplied either by the on-site power plant or be purchased from the national grid. In both cases the utility cost would be the same.

1.3.3 Assessment of Chemical Absorption

In Chapter 6, the scope of the study narrows once more to consider only the carbon capture process. In this case, the boundary conditions are the gas inlet and outlet of the absorber column, the inlets and outlets of the lean amine cooler and the inlet and outlet of the reboiler at the base of the regenerator column. In addition, captured CO_2 leaves the confines of the model from the top of the regenerator column after having been cooled in a condenser. No further removal of water or other impurities from the CO_2 stream is considered as the acceptable level for these components will depend on the transportation and use of CO_2.

The boundaries identified above is supplemented by supply and drain lines to maintain the correct flow and concentration of amine within the chemical absorption system and the water wash system, if present, at the top of the absorber column.

Energy requirements for regenerating the amine and heat removed via the heat exchanger and condenser steps were all determined within the model. Although amine pump size and capital cost were considered within the assessment, the electrical energy consumption was not considered as a method to rank the different amines from most to least favourable.

1.4 Tools to be used in this Work

The study on steel production routes reported in Chapter 4 is based on data analysis with Microsoft Excel. This software package was chosen due to its ability to handle large quantities of simple calculations while allowing for data handling and reporting.

Work on the combination of technologies with the existing blast furnace process was also carried out in Excel. This allowed many simple calculations to be carried out with separate excel files used for separate flowsheets. Within each file, different sheets were used to determine the blast furnace gas composition and electrical equipment duties. A summary sheet combining the outputs of all these sheets was included to aid the reporting of the ranking criteria for each flowsheet. A separate Excel file was

prepared to summarise the output from all the cases prepared to allow direct comparison. This summary file also allowed the calculation of utility costs and ranking criteria for the cases and reported in Chapter 4.

The study of different amines for chemical absorption from blast furnace gas forms the final chapter within this work. Aspen HYSYS was chosen for the detailed process design of this plant. The reasons for this are that Aspen HYSYS has been proven to be able to simulate the absorber and regenerator column operation. This ability is due to the detailed property databases which support thermodynamic modelling and physical properties required for simulating chemical absorption. Separate Aspen case files were prepared for the different concentrations of the amines and blends of amines considered. The key figures from these different cases were compiled in an Excel file to allow for easy comparison between the different cases.

Aspen Process Economic Analyser (APEA) is a part Aspen HYSYS used to develop the capital costs reported in Chapter 6. This software was used due to the ease of transferring the process duties for equipment determined within Aspen HYSYS into a capital cost within APEA. In addition, APEA uses historical project data to reach cost estimates. The results of the different capital costs were recorded in a separate Excel summary file. This allowed a comparison of the results for all the cases considered which is reported within Chapter 6.

Chapter 2. Literature Review

This chapter sets out the research performed as a basis for the results presented in Chapter 4, Chapter 5 and Chapter 6 of this dissertation. An outline of relevant research is provided, split into sections to cover steelmaking processes, carbon capture and carbon dioxide storage and utilisation. After considering the background research, the objectives of this work are then recorded.

2.1 Chapter Introduction

2.1.1 Climate Change

In October 2021, the conference of the parties (COP) 26 Climate Change Conference was held in Glasgow in the UK (UKCOP26, 2021). This event was the first chance to test the readiness and commitment of countries to meet the Paris Agreement designed to limit further global temperature rises. This agreement was reached after it was now widely regarded that the increase in global temperatures is due to interference from mankind's industrial revolution (IPCC, 2013). Emissions of so-called greenhouse gasses (GHGs) into the atmosphere are overloading the delicate natural carbon cycle. This in turn is causing atmospheric and sea temperatures to rise. The most widely recognised GHG is carbon dioxide (CO_2), which is the most commonly emitted species due to being a product of combustion for all carbon-based fuel sources. Recorded levels of this gas in the atmosphere have risen by approximately 120 parts per million (ppm) in the last 200 years (NOAA, 2016).

The European Union and many individual countries have agreed to reduce CO_2 emission levels to 80% of 1990 levels by the year 2050 (HM Government, 2011). In 2015, global climate change discussions were held, with a target of limiting further sea temperature increases to 2°C (Melorose 2015). This has since been ratified by the European Union, the United States and China. The treaty has become the successor to the Kyoto treaty which expired at the end of December 2012. However even this limit is viewed by many small island nations as too high a temperature rise leading to further loss of habitable islands around the South Pacific (Ford 2015). In an effort to appease such communities, an aspirational target temperature rise of 1.5°C has also been included within the latest Treaty - The Paris Agreement (Melorose, 2015). However, analysis by the UN in 2021 suggested that the world is not on track to limit an increase in global temperatures to even 2ºC above pre-

industrial levels. Some industries, such as power generation, can adopt new processes which do not involve carbon at all and therefore will not emit CO_2 to the atmosphere. However, industries such as steel and cement have a more fundamental relationship with carbon sources and have been labelled as “hard to abate”. For these industries, process improvement and retro fit technologies must be considered in order to reduce their emissions in line with the Paris Agreement (Melorose, 2015) guidelines whilst new processes are researched and adopted.

There are many different forms of greenhouse gases. These include carbon dioxide, methane, nitrous oxide, ozone, chlorofluorocarbons (CFCs) and hydrochlorofluorocarbons (HCFCs) (Carbon Capture, Storage and Use, 2015). All of these compounds trap heat within the planet’s atmosphere which shifts the balance between heat energy received from the sun and that reflected back from the planet. The use of CFCs has been banned globally for the past 10 years in an effort to reduce the release of this family of chemicals into the environment (Montreal Protocol). The use of HCFCs is also being phased out with a target date of 2030 for the cessation of their use (Miller, 2011).

Limits exist in the majority of countries on the emission levels of nitrous oxide (or NOx) and most power stations are now equipped to meet these regulations. Methane has approximately 25 times greater global warming potential than CO_2 on the atmosphere over a timescale of 100 years (Myhre, 2013). Most recently, members of the COP26 conference agreed to combat methane emissions from industrial and agricultural sources.

The remaining significant greenhouse gas is a product of combustion of carbon. For this reason, emission of CO_2 from various industries is coming under increasing scrutiny.

The EU, Australia and China have all adopted some form of carbon credit system (Baranzini, 2000). This is a method of regulating the levels of CO_2 emission which allows for high level emitters to be penalised. However, both the cost and availability of credits has proved divisive with the relatively low cost within the EU leading to little motivation to seek out mitigating technologies. Strategic industries, such as steel, have been allowed greater flexibility in order to retain production within the EU. This is due to the realisation that steel demand and production is a global industry at risk of large scale relocation. It is hoped that by limiting the cost rise to produce steel within the EU, production will not move to countries which do not require carbon

credits. This scenario is called carbon leakage, as potentially higher emissions would be emitted with the loss of EU gross domestic product (GDP) and jobs (Pardo, 2012).
The majority of CO_2 emissions can be attributed to the power generation sector who rely heavily on coal and gas fired power plants to provide baseload power and account for surges in power grid demand. This leads to the industry accounting for approximately 78% (Metz, 2005) of all stationary sources of CO_2. It is not the intention of this document to discuss the deployment of renewable energy sources and nuclear power in any great lengths, except where parallels can be drawn between the power and steel industries.
At around 7% of global GHG emissions, the Steel Industry is one of the larger industrial sectors by emissions. This is closely followed by the cement industry which, in many countries, is closely linked with the steelworks.

2.1.2 The Steel Industry

Steel production generates large quantities of carbon dioxide (CO_2) emissions. Steel is used to produce coils, plates, rods, bars, structural beams and sections supporting the automotive to construction industries. Therefore, it is unlikely that production rates will decline between now and 2050. In fact, in 2005, the global steel production was estimated to be 1144 million tonnes (Conejo, 2020), whereas in 2018 it was estimated to be 1808 million tonnes. The production rate fell during the coronavirus (COVID19) pandemic of 2020 then recovered in line with demand from other industries. Yearly production is expected to increase further, reaching a predicted 2100 million tonnes by 2050 (International Energy Agency, 2020). After this time, there may be some stagnation in growth as steel begins to be replaced by advanced polymers and natural materials.
The reliance of different electrical energy generation technologies on steel is shown visually in Figure 2.1. This highlights that more traditional generation methods such as gas and coal fired power plants generally have a lower steel consumption per megawatt of capacity than renewable energy sources such as wind or concentrated solar power (CSP). This highlights that decarbonisation by the power industry will increase the demand for steel from existing processes and equipment.

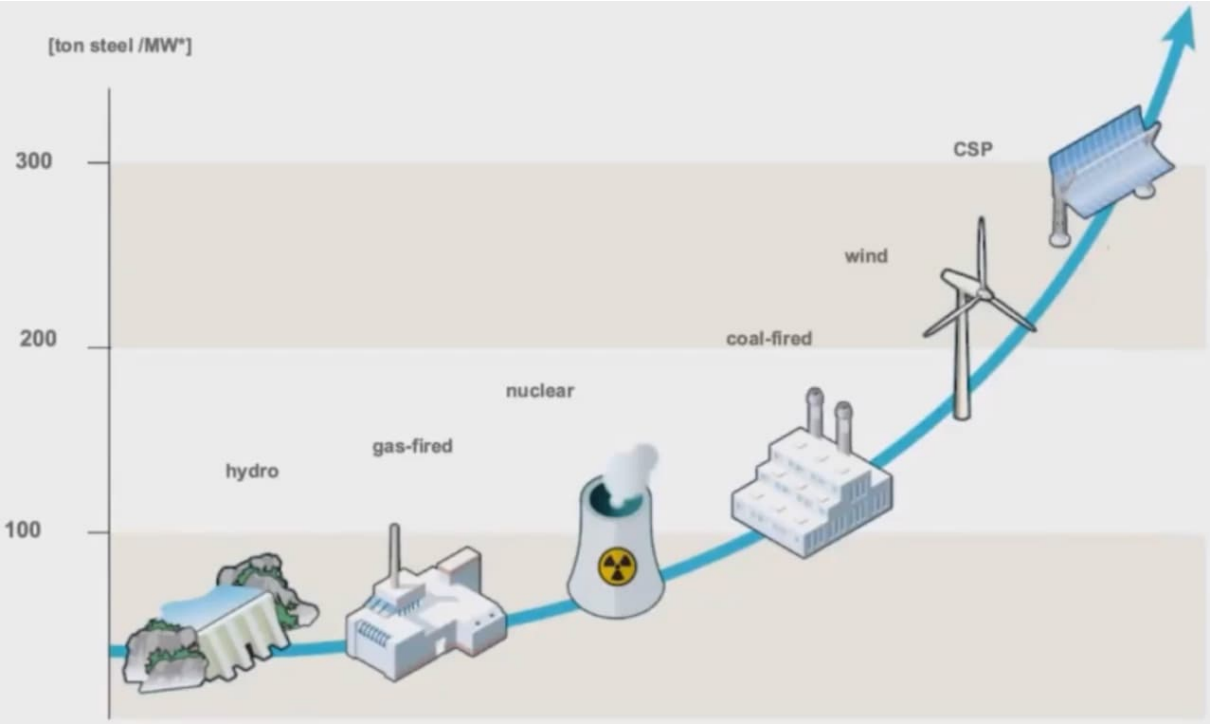

Figure 2.1: Steel required per MW of installed electrical capacity (de Mare, 2021)

Alternatively, industries who must look to carbon capture to reduce emissions will also require a supply of, often high grade, steel to build such facilities. For these reasons, emissions from steelmaking processes on a global scale must be reduced to meet increasingly legally binding CO_2 targets.

Many different processing routes are used to produce steel globally. The age of equipment and efficiency of operation also varies geographically. To determine a baseline for any improvements, an average CO_2 generation for steel production has been determined as 1.83 tonnes of CO_2 per tonne of steel (Gielen, 2020). However, there are multiple routes to produce steel, each generating a different amount of CO_2. In 2019 the blast furnace route accounted for 71.5% of the steel produced globally (WorldSteel, 2023) with electric arc furnaces (EAF) accounting for 28.2%. It is unrealistic to assume that this share will shift completely to a steel recycling route due to scrap availability and limitations on steel grades produced. Industrial analysis (Doyle, 2021) instead predicts that the EAF route is likely to account for roughly 45% of steel production by 2050. Regardless of steelmaking route, it is likely that scrap recycling will increase both in the blast furnace (or equivalent) route and through the EAF process. A limit will need to be imposed though to control impurities in the steel, especially in the case of copper as this will reduce the range of products that can be produced (JFE Steel, 2013). If the copper content of the produced steel exceeds 0.06% by weight then it can no longer meet the high quality required for the

automotive industry (Takeuchi, 2009). This leads to a theoretical maximum of 20% scrap input to the basic oxygen furnace (BOF) process based on low quality (and therefore cheapest) scrap.

A separate issue is the average life of steel products being around 20-30 years (Gielen, 2020). This means that the maximum volume of steel scrap available for recycling will be equal to the production rate 20-30 years earlier. This leads to the maximum production of steel via scrap alone in 2050 being limited to 1,350 million tonnes per year (Mt/y) (Birat, 2010) assuming all scrap can be used. This leaves a short fall of at least 750 million tonnes per year which needs to be accounted for by other sources. These may include the use of Directly Reduced Iron (DRI) to bolster scrap supplies or from processes yet to reach commercialisation. But taking a process from trial stage to even 5% market penetration can take at least 30 years (Allwood, 2010). Due to the competitive nature of the steelmaking industry, a process offering a clear advantage may obtain a faster diffusion rate. The BOF, for example, accounted for 10% of steel production after 8 years of commercialisation (Arens, 2014). This new process was replacing a less efficient, and more costly alternative and therefore had a large economic advantage. As well as gains in profitability, management attitude and access to capital funding will also increase diffusion rates of a technology (Arens, 2014). However, newer technologies, which may still be perceived as risky, generally have a slower diffusion rate. Although it is not the intention of this work to discuss funding and government support, clearly the implementation of these measures would accelerate changes in steelmaking processes.

The average life of a blast furnace installation means that steelmakers will be unwilling to abandon these facilities unless there is a clear benefit in doing so. Taking a typical life of a blast furnace as 15 years indicates that a total of 86 facilities (outside of China) will retain their primary steelmaking capacity up to 2030. This value excludes any further rebuilding or repair works which may take place between now and this date.

Steel production is carried out via a number of discreet processes. Generally, these rely on either a BOF or an EAF to convert intermediate iron products into crude steel. However, the combination of steps to reach these end processes can vary depending on end product quality and economic factors. A simplified map of process steps to reach crude steel is included in Figure 2.2 below.

The most common, conventional, route is the blast furnace and basic oxygen furnace (BF-BOF) route. This involves the preparation of iron ore and carbon fuel raw materials for use in the BF which supplies a liquid iron to the BOF. The BOF then further purifies the iron by removing carbon to produce liquid steel.

Alternatively, iron ore can be reduced without being melted to form directly reduced iron (DRI) which can be melted alongside scrap metal in an EAF. This produces liquid steel with less CO_2 emissions but requires a high quality of scrap and iron ore. Iron may also be directly reduced using hydrogen instead of natural gas or coal. This would offer the potential to further reduce CO_2 emissions, depending on the source of the hydrogen.

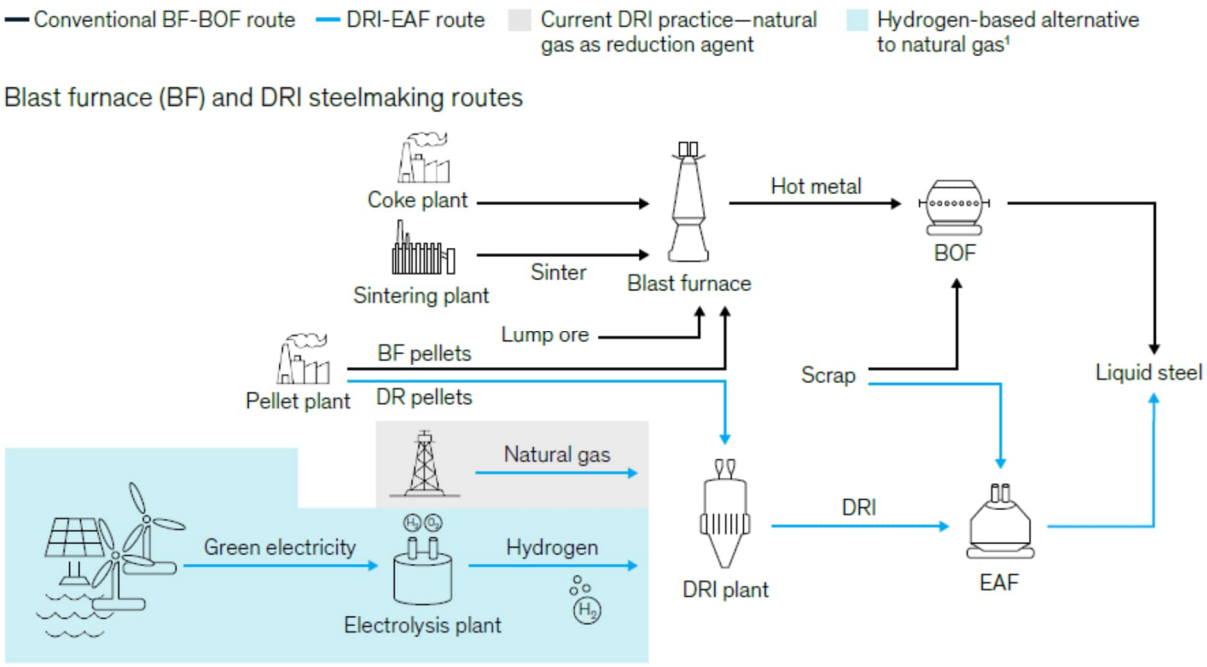

Figure 2.2: Common steelmaking routes from (Doyle, 2021)

It is also possible to mix these steps with DRI and scrap metal sometimes used in the blast furnace. In addition, the hot metal from the blast furnace can also be used in an EAF alongside scrap or DRI.

The individual steps will be explained below, with a focus on the source of emissions and potential mitigation options.

2.2 Steelmaking Processes

2.2.1 Coke Production

Metallurgical grade coal is heated up to 1300ºC in an oxygen free environment to drive off volatile materials and form coke. The hot coke is then rapidly quenched to

prevent the carbon fuel from burning. This acts as both fuel and a chemical reactant to reduce iron ore in the blast furnace process and even aids the gas distribution through the blast furnace vessel. Due to the heating process, a flue gas is generated which contains CO_2 based on the combustion of carbon monoxide (CO) and methane (CH_4) as per Equation 2.1 and 2.2 below.

$$2CO + O_2 = 2CO_2 \qquad \text{Equation 2.1}$$

$$CH_4 + 2O_2 = CO_2 + 2H_2O \qquad \text{Equation 2.2}$$

The process also generates a stream of coke oven gas (COG) which can be combusted to produce heat and power within the steelworks. The crude coke oven gas is generated at high temperatures by the coke oven process and is quenched to around 80^{o}C. On cooling, the gas releases condensates including naphthalene and (heavy and light) tars. By employing wet chemical scrubbers, hydrogen sulphide (H_2S) and ammonia (NH_3) can also be removed from the gas stream. By determining the CO_2 content of the flue gas and the CO_2 generated by burning the exported gas, an amount of CO_2 per tonne of coke produced can be assessed. Table 2.1 lists a typical gas composition for the process gas generated at the coke ovens – coke oven gas. It is predominately made up of hydrogen with notable amounts of methane also present. The balance of the species are nitrogen, carbon dioxide and monoxide with small amounts of oxygen also present.

Component	H_2	CH_4	N_2	CO	CO_2	O_2	H_2O
Composition (wet, molar basis)	59.53%	23.04%	5.76%	3.84%	0.96%	0.19%	3.98%

Table 2.1: Composition of Coke Oven Gas from (Santos, 2013)

Electrical energy is also required to drive fans to generate combustion air with which to burn the fuel gasses. Further energy is required to power equipment to produce the coke such as conveying equipment. Substitution of ~5% metallurgical grade coal is possible with charcoal to reduce the coal consumption in this stage (MacPhee, 2009). However, this will not change the emissions from the coke ovens themselves and only provides a more carbon neutral feedstock. Such considerations are not made within this work. This is due to concerns about the sourcing of sufficient quantities of biomass being likely to compete with food production (Piketty, 2009).

Best available techniques (BATs) to reduce energy consumption and by extension CO_2 emissions include quenching the hot coke with nitrogen instead of water. As the water is substituted, the technique has been named Coke Dry Quenching (CDQ). It allows the recovery of heat energy from the coke which can be used to generate steam or electricity (Sundqvist, 2018). Examples of this technology are currently only found in the newest installations in Asia where it is reported that 75 kWh/t_{coke} can be saved (Chen, 2014). Basic input and output material flow information on a per tonne basis is included in Table 2.2 below from three separate sources. The third source has the benefits of the Best Available Techniques (BATs) applied to it:

Reference	**McBrien (2016)**	**He (2017)**	**Santos (2013)**	**BAT**	**Units**
IN					
Coal	1250	1326	1400	1400	kg/t
Coke Oven Gas	65	0	490	490	kg/t
Blast Furnace Gas	0	1310	610	610	kg/t
Combustion Air	1050	-	1470	1470	kg/t
Electricity	83	35	35	-40	kWh/t
OUT					
Coke	1000	1000	1000	1000	kg/t
Coke Oven Gas	193	180	142	180	kg/t
Tar	56	-	42	42	kg/t
Flue Gas	1100	2600	2130	2630	kg/t

Table 2.2: Material Flows to generate 1 tonne of coke

The above shows a wide range of different fuel gasses used to heat the coal. It is this choice of fuel gasses which will have the greatest effect on the CO_2 emissions from this process. The first reference reports using pure coke oven gas which, due to the high gas calorific value and hydrogen content, lowers gas consumption, flue gas generation and CO_2 emissions. The second reference considers using blast furnace gas instead of coke oven gas. This results in the gas consumption and CO_2 emissions increasing to account for the reduced gas calorific value. The final reference considers a mixture of coke oven and blast furnace gasses and therefore provides a mid-range of CO_2 emissions per tonne of coke.

Values for CO_2 emissions per tonne of coke reported elsewhere range from 97 kg (Fan, 2021) to 824 kg (Pardo, 2012). This highlights the need to be clear on the system boundaries considered and whether the CO_2 emissions (or credit) from electricity consumption or generation are also included. It is important to note also that only around 420 kg of coke are required to support the production of 1 tonne of liquid steel – the system boundary considered in this work. This results in the CO_2 emissions contribution from this step of the steelmaking process being around 344 kg per tonne of steel.

2.2.2 Sinter Production

Iron ore can be charged directly into the various ironmaking processes. However, most ores contain only a small portion of iron oxides and therefore require large amounts of energy to melt the impurities so they can be separated from the steel or iron. To improve both the iron oxide content and adjust the chemistry, iron ores are often beneficiated in a sinter plant. Sinter plants also allow some recycling of fine dust particles from the ironmaking processes. These dusts and iron ore are blended with a small portion of fine coke and limestone which is heated on a moving grate to sinter the materials together. To agglomerate the material, bed temperatures of 1300-1480^{o}C are required. The resulting hot fused mass is cooled, crushed and screened before it is sent to the blast furnace.

This process produces CO_2 from the combustion of the fuel gas but also the thermal decomposition of limestone to lime. The resulting sinter is relatively fragile and therefore unsuitable for long distance transport. For this reason, it is usually consumed in a blast furnace in the same steelworks. Due to the heating of the raw and recycled materials, a waste gas stream is emitted to the atmosphere. Electricity is required to power exhaust fans which suck air into the process and maintain the flame at the correct position within the material bed. Best available techniques to reduce energy consumption rely on waste heat recovery from sinter cooling stages. This can allow the preheating and recirculation of air for the sinter plant but also the generation of electricity. Basic input and output material flow information on a per tonne basis is included below in Table 2.3. The information is based on two separate literature sources and published operating data for European installations from the Association of German Steel Manufacturers (VDEh) for the year 2009:

Reference	*Operating Data (VDEh, 2009)*	*Santos (2013)*	*McBrien (2016)*	BAT	units
IN					
Iron Ore	807	840	1000	1000	kg/t
Coke	41	50	50	50	kg/t
Combustion Air			600	600	kg/t
Coke Oven Gas	2	2	-		kg/t
Limestone	140	10	200	200	kg/t
Electricity	34.5	32	111	104	kWh/t
OUT					
Sinter	1000	1000	1000	1000	kg/t
Waste Gas	-	*410*	*650*	620	kg/t

Table 2.3: Basic Material flows required to produce 1 tonne of Sinter

Table 2.3 above shows a significant range in iron ore requirements to produce 1 tonne of sinter. This will be due to the variety of ore grades used as a feedstock for this process. By comparison, coke consumption remains relatively constant across the available data. As the sintering process does not generate a process gas used anywhere else within the steelworks, the accounting of the CO_2 generated by this step is straight forward as it is solely the CO_2 emitted from the sinter plant chimney. However, the gas steam also contains harmful components such as dioxins (Jones 2012) which are currently diluted by the CO_2. By removing this component, the gas stream may require further treatment to limit the exposure levels to these chemicals. The CO_2 content of the flue gas will vary depending on the raw materials such as limestone and fuel gasses used by a sinter plant. CO_2 emissions per tonne of sinter produced has been estimated at between 90 kg (Brunke, 2014) and 260 kg (Fan, 2021). As with the coke making process described previously, this will no doubt be due to either considering or excluding electricity emissions, different fuel gasses and facility operating ages. By considering best available techniques it is expected that emissions can be lowered. Estimates (Carpenter, 2012) predict these reductions to be in the order of 94kg of CO_2, leading to around 166kg of CO_2 begin emitted per tonne of sinter produced.

Unlike the coke making process, a large proportion of sinter is required to support the manufacture of one tonne of liquid steel. This is determined by considering both the

consumption of sinter by the blast furnace reported in Table 2.5 and the consumption of hot metal to produce one tonne of crude steel reported in Table 2.11. These values, result in 1093 kg of sinter being required to produce one tonne of crude steel which leads to a contribution per tonne of liquid steel of 284 kg of CO_2.

2.2.3 Pellet Production

Pellets are a further form of iron ore which can be used to produce molten iron in the blast furnace and directly reduced iron at the DRI plant. Around two thirds of all pellets produced are used to produce molten iron with the remainder used for DRI production (Carpenter, 2012). Although the grade of pellet varies depending on it's intended use, this work will consider the same manufacturing process and emissions for producing both types of pellet. BF grade pellets typically contain less iron oxide by weight than DR grade pellets and also include a higher level of acidic impurities. While these impurities can be melted and separated in the blast furnace process, it results in a reduced yield in the DR process which does not separate slag from the directly reduced iron.

The manufacturing steps are shown graphically in Figure 2.3 and starts with the mining and crushing of iron oxides. The resulting material is ground to form a slurry of the iron ores. A binding agent is then mixed with the slurry and agglomerated to form green, unfired, pellets. These raw pellets are cured by induration where magnetite iron ores are oxidised to hematite. This takes place at temperatures above 1250^{o}C which requires either gas or oil burners to be used. The pellets can then be cooled and screened with particles smaller than 9mm recycled back to the grinding stage. In addition, pellet plants consume electricity to operate process fans, compressors and conveyor belts. Pellets are much more resilient than sinter material allowing them to be transported large distances without a significant deterioration in quality.

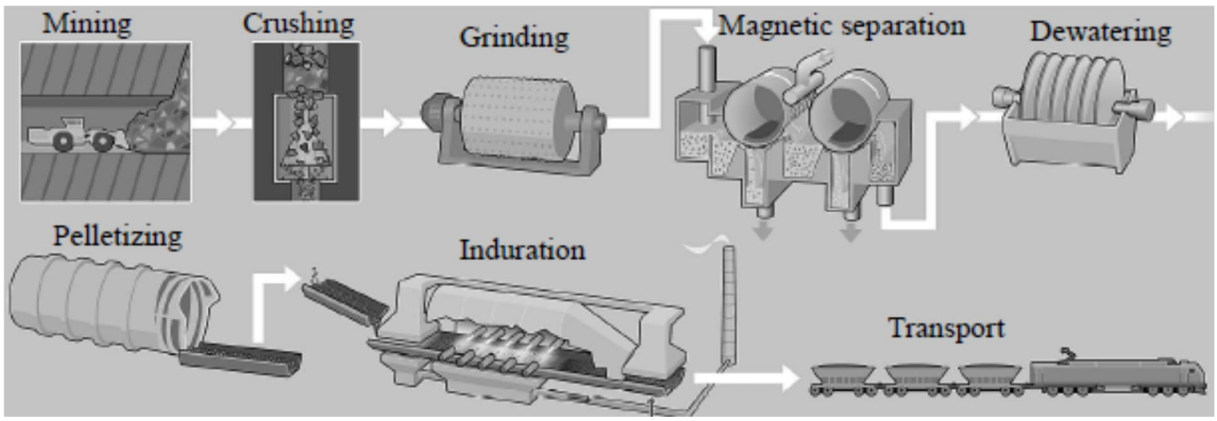

Figure 2.3: Process units in the pellet making process (Riesbeck, 2013)

Basic input and output material flow information on a per tonne basis is included from two separate literature sources in Table 2.4 below. Unlike the coke and sinter production, no data for best available techniques has been included as very little energy efficiency can be gained.

Reference	**Lv (2019)**	**Costa (2001)**	**units**
IN			
Iron Ore	990	1000	kg/t
Coal	20	10	kg/t
Electricity	22	40	kWh/t
OUT			
Pellets	1000	1000	kg/t

Table 2.4: Basic Material flows required to produce 1 tonne of pellets

Table 2.4 above shows that obtaining complete data sets from literature is a challenge with only one reference including a waste gas flow quantity but omitting the corresponding fuel consumption. Emissions of CO_2 per tonne of pellet produced have been calculated at between 35kg (Fan, 2021) and 75 kg (Pardo, 2012). It is less common to use large quantities of pellets to feed the blast furnace. By combining the pellet consumption figure at the blast furnace in Table 2.5 and the hot metal consumption figure in Table 2.11 a pellet use per tonne of crude steel can be determined. This value is around 350kg of pellets per tonne of liquid steel. This then results in a contribution of only 26kg per tonne of steel which is by far the lowest of all the steps. This study also considers that pellet making facilities have generally been

installed more recently than sinter plants and therefore do not have a best available technique which can further reduce emissions from this step.

2.2.4 Blast Furnace

By far the most common method of making iron, an intermediate of steel, is the blast furnace. This process uses coke to heat and reduce iron oxides to form a liquid iron product. Layers of fuel and iron oxides are added to the top of the blast furnace vessel where they slowly descend whilst undergoing numerous reduction reactions indicated below:

$$3Fe_2O_3 + CO = 3Fe_3O_4 + CO_2 \qquad \text{Equation 2.3}$$

$$Fe_3O_4 + CO = 3FeO + CO_2 \qquad \text{Equation 2.4}$$

$$FeO + CO = Fe + CO_2 \qquad \text{Equation 2.5}$$

Towards the bottom of the blast furnace, oxygen enriched air is added at high temperature to burn the coke and form a reducing gas comprising of CO, H_2 and N_2. Due to the internal temperature of the vessel, the Boudouard reaction below ensures that a constant source of CO is maintained:

$$2CO \leftrightharpoons CO_2 + C \qquad \text{Equation 2.6}$$

Liquid iron and slag produced by the process are stored in the hearth of the blast furnace which is periodically drained into a mobile ladle. These refractory lined containers transport the liquid iron to the steelmaking process. The slag produced contains all the impurities separated from the iron ores. These include sulphur and oxides of calcium, magnesium, aluminium. The slag is typically rapidly cooled with water to create a glassy material which can be sold to cement makers as a raw material for their process.

The blast furnace process has been in use and developed over the past century and therefore has limited scope to reduce energy intensity and emissions further. The process can be further split down into sub-processes highlighted in Figure 2.4. These include the hot blast stoves and the coal grinding plant, which as they generate a flue gas emission to atmosphere are described as follows:

Hot blast stoves heat the compressed air “blast” which enters the blast furnace. They do so by sequential cycles of heating by burning blast furnace gas and cooling with the compressed air. The blast furnace gas used is often enriched with a higher calorific gas which may include coke oven, basic oxygen furnace or natural gas. Some hot blast stoves instead recover some of the heat from the waste gasses and use this to preheat the incoming gas and air streams prior to combustion. Although this technology may offer increased energy efficiencies, it does not always reduce CO_2 emissions from this part of the steelworks. Flue gasses from the Hot Blast Stoves are difficult to typify as the age of the installation and exact combination of fuel gasses combusted will all have an effect on the flue gas composition. Generally, the gas will contain a larger proportion of CO_2 and smaller percent of O_2 than from a gas fired power plant.

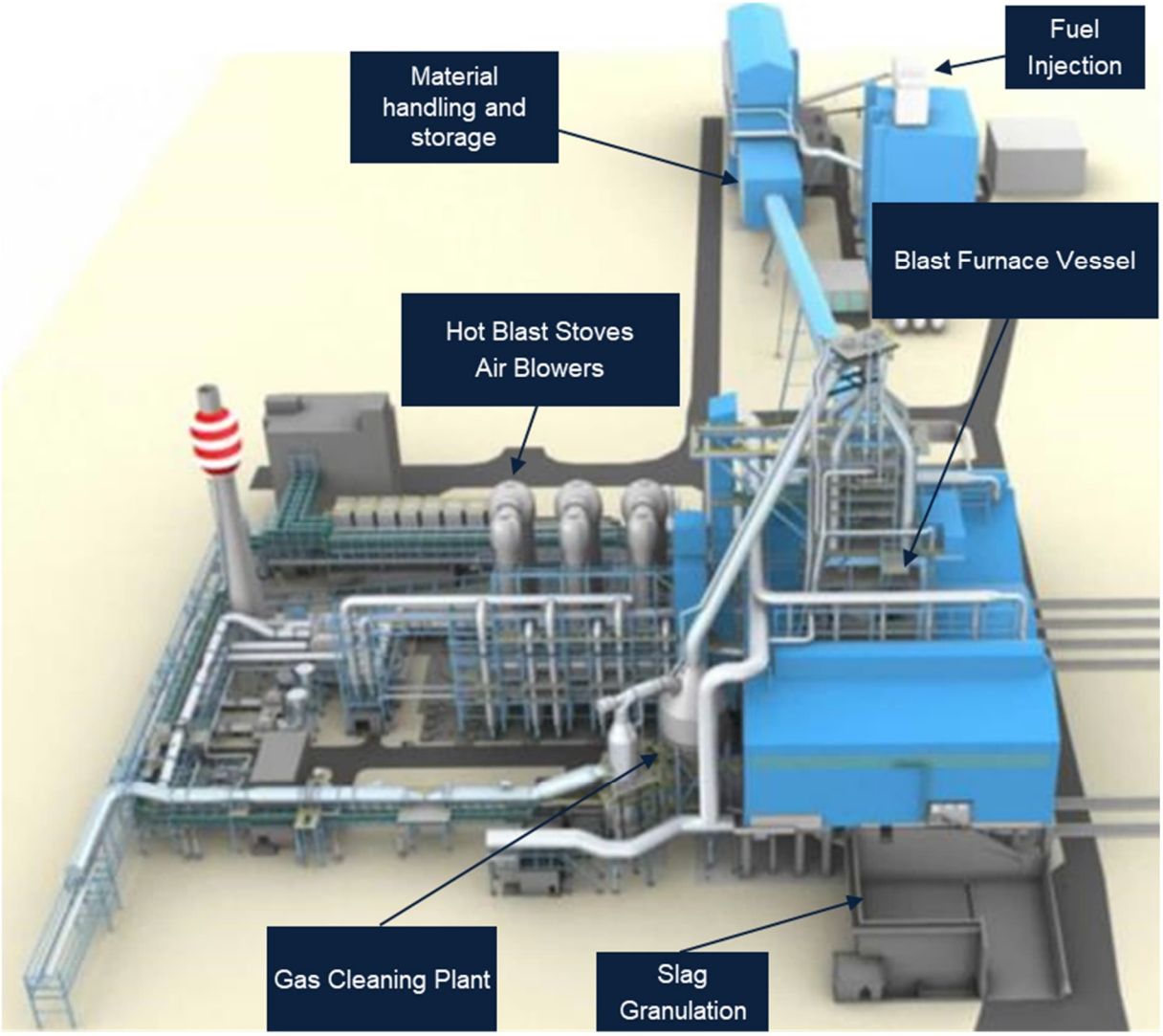

Figure 2.4: Blast Furnace sub-processes

The coal grinding plant represents a widely adopted method of reducing the coke consumption of the blast furnace. By drying and grinding coal to a fine size (below 1.5mm) and injecting it into the blast furnace, the resulting carbon source can be used to reduce the coke rate of the blast furnace. But the drying process requires a small amount of fuel gas to be combusted to generate the necessary heat. This means that a further small atmospheric emission is created. By using ground coal the operating costs can be lowered by utilising a cheaper quality of coal, which also saves emissions from the coke oven process. However, the replacement of coke by coal is not on a 1:1 basis. This means that an increase of coal injected into the blast furnace by 100 kg per tonne of hot metal (tHM) represents a reduction of between 80-100 kg/tHM coke required. Despite this, coal has become the most predominant tuyere injectant. There is a theoretical maximum amount of coal which can be injected into a blast furnace to replace coke. It is thought that this level is 270 kg/tHM (Ribbenhed, 2008 from Carpenter, 2012) due to the thermochemical conditions within the blast furnace.

Natural gas can also be injected into blast furnace as a fuel either instead of or alongside coal. Within North America and Russia the availability and therefore price means this is more common than elsewhere. Natural gas has a higher replacement ratio than for coal of between 900-1150 kg per tonne of coke (Cairns, 1998 from Carpenter, 2012). In addition, the combustion of 1 gigajoule (GJ) of natural gas generates 55% of the CO_2 emissions than 1 GJ of coke. Unfortunately, the maximum injection rate into a blast furnace is limited as it significantly lowers the flame temperature, requiring an increase in oxygen consumption. Considering an injection rate of 140kg of natural gas per tonne of hot metal an estimated 55kg of CO_2 per tonne of hot metal will be reduced.

In addition, a variety of waste plastics, tyres and bio-fuels can also be injected into the blast furnace. These will all have varying replacement ratios and introduce their own impurities. Waste plastic, for example, will generally contain low amounts of sulphur and alkalis which need to be removed from the blast furnace in the waste, slag, product. But, use of plastic may increase the chlorine input and increase the concentration in the gasses leaving the blast furnace. This may lead to corrosion of the steel gas mains if the chloride content is allowed to rise too much.

Sources of emissions are twofold – from combustion of fuel gasses to generate heat and those contained within the exported blast furnace gas. Some pilot plants have

been designed specifically for capturing CO_2 from Blast Furnace gas. Generally, though, these facilities have looked at the feasibility of capture and energy requirement rather than any long-term assessment of operating and capital cost. These plants (Han (2014), Goto (2011), Blostein (2011), Rhee (2011)) cater for CO_2 capture rates up to 10 tonnes per day. This is significantly less than the figure of around 3900 tonnes of CO_2 per day for a full-scale plant. Therefore, scale up work is still required for which the conservative steel industry will need further encouragement and support.

Due to the wide adoption of the blast furnace process, a large range of literature data is available. Several sub-units are included in this step, which further increases the variability of available data. The discrepancies will be due to the exact quality and mixture of materials added to the blast furnace and used to heat the air blast. The fuel gas and electrical energy requirements are considered a part of the overall blast furnace step. Finally, the blast air supplied to the blast furnace through the hot blast stoves can be generated by either steam or electrically driven compressors. For this assessment, electrically driven units are considered as a more modern solution. Available technologies to reduce emissions include the installation of a top gas energy recovery turbine. This is a gas expander which reduces the pressure of the gas leaving the blast furnace to generate electricity. This can generate around 30.6 kWh of electricity per tonne of hot metal produced by the blast furnace (Carpenter, 2012). A further technology of lower technological readiness is heat recovery from the molten slag. Although under development since 1985 (Pickering, 1985), a full-scale plant has yet to be brought into operation. This technology is assumed to be able to save around 20 kg of CO_2 per tonne of hot metal (Xie, 2010). Two independent references for material and electrical energy consumption per tonne of hot metal from the blast furnace are recorded in Table 2.5:

Reference	McBrien (2016)	Santos (2013)	BAT	units
IN				
Coke	410	370	370	kg/t
Coal	102	165	165	kg/t
Sinter	1394	1120	1120	kg/t
Pellets	0	359	359	kg/t
Iron Ore	0	132	132	kg/t
Oxygen	29	68	68	kg/t
Electricity	85	104	48.1	kWh/t
OUT				
Hot Metal	1000	1000	1000	kg/t
Blast Furnace Gas	1600	1513	1513	kg/t
Slag	300	318	320	kg/t
Flue Gas	210	1110	1110	kg/t

Table 2.5: Basic Inlet and outlet flows from a blast furnace

The differences between the two references shown above in Table 2.5 highlight the large discrepancy between blast furnace operation. The best example is the fact the data reported in column 2 does not include any ore or pellets in the raw materials and considers only a modest level of coal injection at the tuyeres of the blast furnace. By comparison, column 3 includes a more balanced blend of sinter, pellets and ore to produce hot metal. Furthermore, the coal injection and therefore oxygen consumption is more in line with modern practice.

The sources of CO_2 from this process step are twofold coming from both the waste gas from heating the compressed air to the furnace and the combustion of the resulting process gas. The composition of the Blast furnace gas will vary depending on the level of oxygen enrichment of the air stream fed to the process and efficiency of operation. The gas composition in Table 2.6 can be taken as a “typical” value for the blast furnace process:

Component	N_2 + Ar	CO_2	CO	H_2
Composition (dry, molar basis)	49%	23%	23%	5%

Table 2.6: Composition of Blast Furnace Gas (Tobiesen, 2007)

Total emissions from the blast furnace process are considered to be equivalent to between 1279kg (Pardo, 2012) and 1476kg (Fan, 2021) per tonne of hot metal produced. The range of values is relatively small considering the possible range of raw materials used within the blast furnace. Because the hot metal produced forms the bulk of the feedstock to the final steelmaking process, 901kg are required to produce 1 tonne of liquid steel (Santos, 2013). To determine the emissions contribution from this step the CO_2 content in the flue gas from the hot blast stoves and the CO and CO_2 content of the exported blast furnace gas and electrical energy consumption were all considered. This leads to a total of 1330kg of CO_2 produced per tonne of steel with 1280kg from the gas streams and the remainder attributable to the electricity generation.

Several best available techniques could be deployed with further techniques under development. The industry believes that further emission reductions of 20% are feasible, primarily through fuel substitution (Carpenter, 2012). In addition, scrap metal and directly reduced iron can also be used in the blast furnace to lower coke and iron ore consumption. This has the advantage of separating out any impurities from the directly reduced iron before they enter the final steelmaking process. Scrap usage in the blast furnace has been recorded as high as 160 kg/tHM (AIST, 2015). Alternatively, DRI can be used to increase productivity and reduce coke rate. This offers the additional advantage of separating the molten iron from the waste slag before the iron is converted to steel at either the BOF or the EAF. To date, the maximum recorded utilisation of DRI in a blast furnace has been 184 kg/tHM (AIST, 2019).

Recently, hydrogen injection into the blast furnace has been trialled in order to reduce the amount of carbon required to reduce iron ore. These trials (Watakabe, 2013) are all at an early stage and widescale implementation will require a significant increase in the current levels of hydrogen produced today. The long term success of this strategy remains unclear, as the industry will need a large supply of hydrogen and will compete with other industries to secure this decarbonised source of energy. Considering this, steel producers are starting to explore options of upgrading coke oven gas already available at most steelworks to increase its hydrogen content from approximately 55% to 83% by volume (Chen, 2011).

2.2.5 Corex

Corex (Hasanbeigi, 2014) is an alternative smelting process which splits the traditional blast furnace process into two separate vessels as shown in Figure 2.5. The main benefit of this approach is that the fuel does not need to be pre-treated in the coke ovens to support a weight of material above it. In a reduction shaft, the iron ore is converted to directly reduced iron (DRI) using reducing gasses. The reducing gas is produced in the melter gasifier vessel which also converts the solid DRI to a liquid product similar to that from the traditional blast furnace process. It is for these reasons that the corex process is one of very few alternative ironmaking processes to be commercialised.

This technology has been adapted at a small scale in South Korea and China but has struggled to gain a foothold in older steelworks in Europe and America. This is mainly due to the increased oxygen consumption compared to a blast furnace. This processing route already includes a CO_2 removal stage to lower the CO_2 of the top gas. The CO_2 lean portion is recycled back to the process with the CO_2 rich part used as a fuel gas elsewhere.

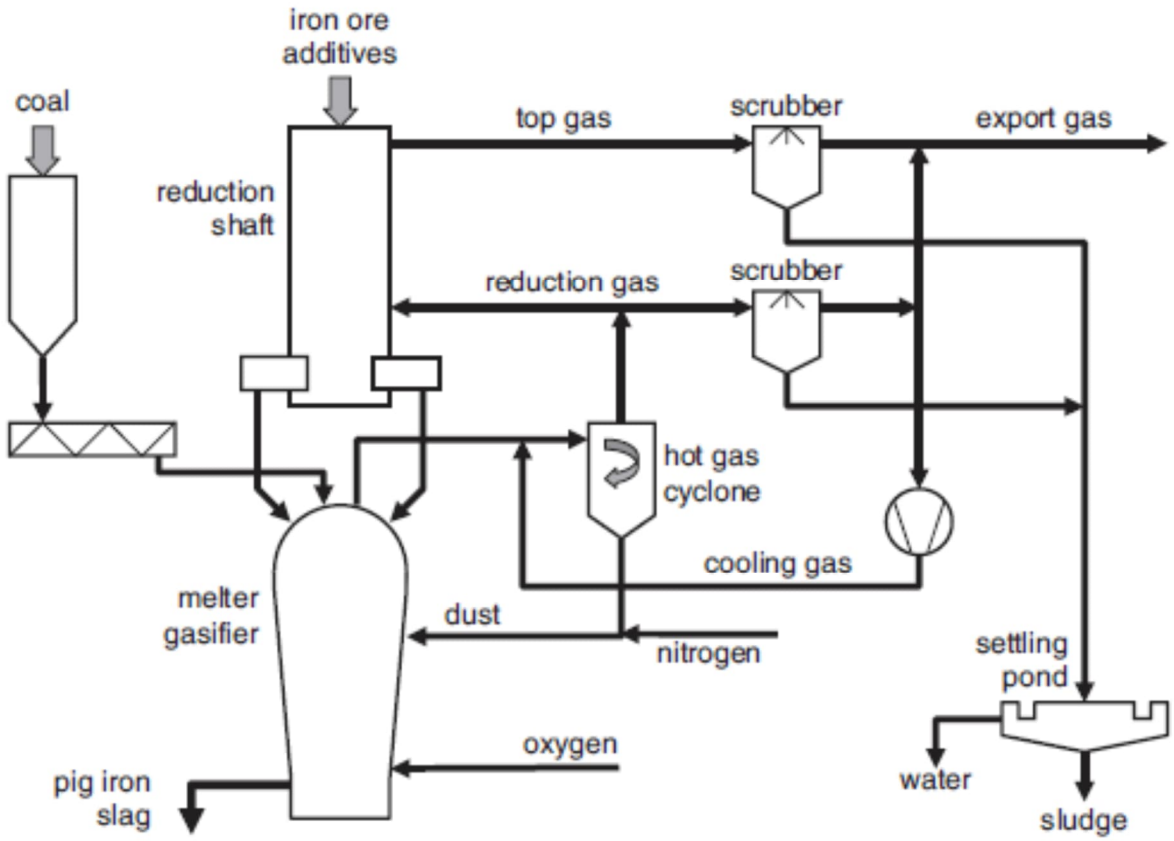

Figure 2.5: Schematic diagram of the corex process (Lampert, 2007)

The blast furnace process uses oxygen enriched air whereas the corex process uses pure oxygen to melt the DRI and form a reducing gas containing CO and H_2. This has the advantage of lower gas flows through the Corex process as less N_2 is present in the system. This leads to a gas which is richer in both CO and CO_2 than from the blast furnace process from which removing the CO_2 becomes more economically favourable. Basic input and output flows from literature are recorded in Table 2.7:

Reference	**Hu (2009)**	**Costa (2001)**	**Units**
IN			
Coal	1000	990	kg/t
Pellets	750	932	kg/t
Iron Ore	750	444	kg/t
Oxygen	757	800	kg/t
Electricity	90	75	kWh/t
OUT			
Hot Metal	1000	1000	kg/t
Corex Gas	1630	-	kg/t
Slag	350	-	kg/t

Table 2.7: Basic Inlet and Outlet flows for the corex process

As with the coke making and blast furnace processes, the gas exported from the corex plant can be used either in a DRI plant or to raise steam and electricity within the steelworks. a typical gas composition is given below in Table 2.8 which shows a higher portion of both CO_2 and CO. This is due to the use of oxygen instead of air which limits the input of N_2 to the corex process.

Species	CO_2	N_2	CO	H_2	CH_4
Corex Gas dry vol%	30-35	Balance	38-45	15-23	1-2

Table 2.8: Typical corex gas composition (Lampert, 2007)

The total emissions from a corex plant are estimated to be between 1212.3kg (Hu, 2009) and 1420kg per tonne of hot metal (Srinivasa Rao, 2007) produced by the process. Hu (2009) does not distinguish clearly between the corex gas amount produced and the amount exported to other users. This may then provide a

significant overestimate of CO_2 emissions as this accounts for the main source of emissions from this process. Because the hot metal produced forms the bulk of the feedstock to the final steelmaking process, 901kg are required to produce 1 tonne of liquid steel (Santos, 2013). To determine the emissions contribution from this step the CO and CO_2 content of the exported corex gas and electrical energy consumption were considered. This leads to a total of 1,583kg of CO_2 produced per tonne of steel with 1543kg from the gas streams and the remainder attributable to the electricity generation. This is the highest emission value of any individual process step but does remove the requirement for a coke oven and sinter plant and their associated emissions as discussed in sections 2.2.1 and 2.2.2.

2.2.6 Top Gas Recovery Blast Furnace

A further development of the blast furnace process is the so-called top gas recycling blast furnace, or TGR-BF. This involves the treatment of the gas from the process to remove CO_2, with the resulting CO rich gas recycled back to the blast furnace as a fuel. The benefit of this process configuration is that it reduces the carbon fuel rate added to the top of the blast furnace and creates a stream containing a high proportion of CO_2 which can be further purified and compressed for storage.

This concept was trialled as part of the ULCOS research project in 2007 (van der Stel, 2013) with a pilot plant employed to prove the idea. The initial design focused on vacuum pressure swing adsorption as the separation method although more recent studies (Chung, 2018) have also considered chemical absorption systems. The initial research proposed a CO_2 reduction of up to 50% compared to a traditional blast furnace. Because of the recycling of gas back to the blast furnace, there is less gas available to be exported to other users in the steelworks. The original work focussed on the maximum recycling rate of gas at the blast furnace but did not consider the requirement to replace this lost energy source at the other users such as the on-site power plant.

This is the most technologically advanced option to reduce emissions from the traditional BF-BOF steel production route but still requires to be scaled up from the experimental to commercial scale. This was planned to take place at two sites within Europe (Pettersson, 2012) with both projects being cancelled for economic reasons. Basic input and output material flows from literature are recorded in Table 2.9:

Reference	Sen (2013)	Jin (2017)	Units
IN			
Coke	199	190	kg/t
Coal	173	170	kg/t
Sinter	550	920	kg/t
Pellets	0	374	kg/t
Iron Ore	1034	237	kg/t
Recycled Gas	-	200	kg/t
Oxygen	274	307	kg/t
Electricity	-	252	kWh/t
OUT			
Hot Metal	1000	1000	kg/t
Export Gas	-	301	kg/t
Slag	364	-	kg/t

Table 2.9: Basic Inlet and Outlet material flows for the TGR-BF process

The two references show similar fuel consumptions although the volume of gas re-injected into the process is not specified by the first reference. The electricity consumption from the second reference is predicted to far exceed that of the traditional BF and COREX routes. This is due to the TGR-BF requiring additional energy to recirculate the gas stream and remove CO_2. Depending on the exact operation, the process may also fully consume the export gas, resulting in less emissions elsewhere in the steelworks. This may lead to steelmakers having to purchase additional natural or hydrogen gas to meet their power and heat requirements. Overall, emissions from this process are estimated to be between 504 and 1,243 kg of CO_2 per tonne of hot metal (IPPC, 2012 & Pardo, 2012). The large difference between these two references is due to the inclusion of carbon capture (IPPC, 2012) or the release of separated CO_2 to atmosphere (Pardo 2012). This route offers the largest advantage in terms of CO_2 reduction if the separated CO_2 is stored or utilised.

This ironmaking method has already incorporated carbon capture into its flowsheet in order to recycle combustible gasses generated by the process. A barrier to this was that the original design included a vacuum pressure swing adsorption (VPSA) plant

to separate the CO_2 rich stream from the recycled gasses. This relies on both vacuum pumps and compressors with a suitable rating for full scale gas flows.

A further offshoot from the ULCOS program is the HIsarna plant (Zeilstra, 2014). This design builds on the commercially available HIsmelt process and adds a cyclone reducing section. The process is based on the use of coal and raw iron ores which eliminates CO_2 emissions generated to convert coal to coke. Most recent production rates from this process were in the region of 180 tonnes of hot metal per day (Van der Stel, 2020) which is still someway short of the 5,000 to 10,000 tonnes of hot metal per day that can be produced by a blast furnace. The HIsarna process does allow for the use of higher proportions of scrap metal and biomass-based carbon than the blast furnace and produces a waste gas with a higher CO_2 content. All these factors suggest that, when combined with carbon capture technologies, CO_2 emissions could be reduced by at least 80% (Meijer, 2013) compared to the blast furnace process. This technology will not be discussed further or considered in this work. This is because it is deemed unlikely that steelmakers will choose to adopt a new coal based production route which would completely replace existing infrastructure.

2.2.7 Directly Reduced Iron

Directly reduced iron (DRI) is produced either using coal or natural gas. It generates a solid metallic iron product which can be briquetted to allow it to be transported greater distances. The coal-based routes are predominately operated in India, but it is assumed that these facilities will only continue to operate up to the end of their working life. The gas-based production is more widespread and is considered likely to become the sole production route for DRI. This is because the existing technology already allows a large portion of natural gas to be replaced with hydrogen. This was first achieved in 1999 in Trinidad (Elmquist, 2002) by passing hydrogen through a bed of iron ore at a velocity above the minimum fluidisation velocity. This creates a fluidized bed reactor to encourage good mixing of the iron ore and good contact between the gas and solid phases. Other suppliers have also achieved pilot plant operation with 90% of the natural gas fuel replaced with hydrogen (Duarte, 2019). This information means that the development of DRI plants utilising almost exclusively hydrogen is at a high technological readiness level.

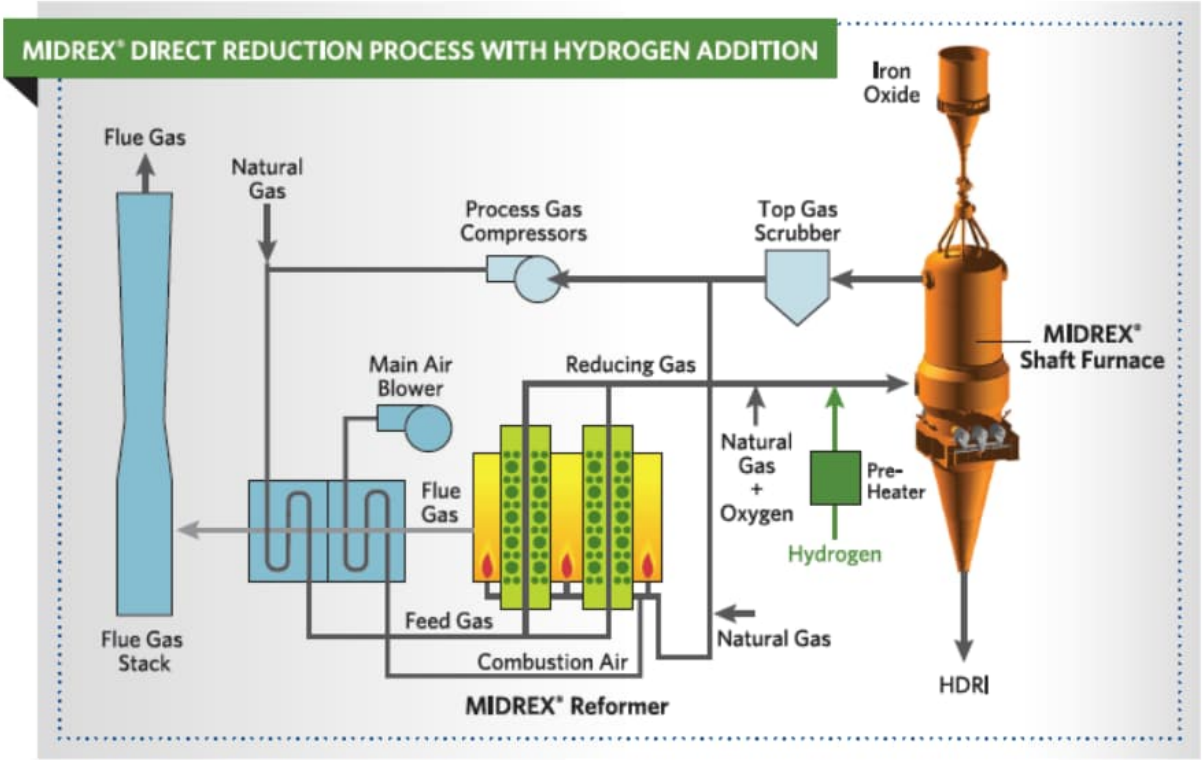

Figure 2.6: DRI plant with H_2 addition (Millner, 2017)

A typical flowsheet of a current DRI plant is included in Figure 2.6 above. High grade iron ore in the form of pellets are added to the top of the shaft furnace with the DRI leaving from the bottom of the vessel. Gas enters the vessel above the DRI discharge point and rises through the shaft furnace. The gas is a mixture of hydrogen and carbon monoxide which reduces the iron oxide to iron without melting it. This results in the solid product containing both metallic iron and impurities which will require removing in a future processing step. The gas leaving the furnace is first cleaned to remove any dust, enriched with natural gas and compressed in order to recycle it back to the furnace. The recycled gas stream is preheated and passed through a reformer in order to produce the reducing gas containing hydrogen and carbon monoxide. Further enrichment with oxygen, natural gas and hydrogen can be carried out before the gas stream enters the furnace again. Despite the recycling of the gas stream, there is still a source of emissions from this process. Natural gas is combusted to achieve the necessary operating temperatures within the reformer stage. The flue gas from this combustion step is used to preheat the recirculated gas stream before being sent to a chimney and emitted to atmosphere.

The DRI product is currently used in electric arc furnaces where insufficient scrap capacity is available to meet production demands. DRI has also been used in blast

furnaces to reduce the fuel consumption there. This becomes a promising route if the DRI has been produce through a green or near green route. The DRI-EAF route needs high quality DR-grade pellets with a lower level of impurities than in the BF grade pellets. The reason for this is that the EAF is not able to process large amounts of slag generated when the DRI is melted and releases the impurities within. Basic input and output material flows from Literature are recorded in Table 2.10:

Reference	**Kumar (2020)**	**Costa (2001)**	**units**
IN			
Ore	1313	0	kg/t
Pellets	0	1418	kg/t
Natural Gas	77	215	kg/t
Coal	344	0	kg/t
Air	1329	-	kg/t
O2	0	-	
Electricity	-	105	kWh/t
OUT			
DRI	1000	1000	kg/t
Off Gas	2063	-	kg/t

Table 2.10: Basic Inlet and Outlet material flows for the DRI process

Waste gases from the process are drawn off with a portion recycled back as a feed gas. The remaining gas is burnt in a reformer vessel which convert the recycled gas to a mixture of CO and H_2. The waste gas stream from the reformer is used to preheat the recycled gasses before being sent to a chimney. It is therefore this off gas that is the sole source of emissions from the DRI process. Emissions are estimated to be in the order of 435kg per tonne of DRI produced (Rechberger, 2020). This is significantly lower than for both the blast furnace and corex process but a higher quantity is required to produce 1 tonne of liquid steel. This is due to the end product containing both useable iron and waste slag which must be separated in the electric arc furnace. By adopting best available techniques for this process it will be possible to reduce emissions, with the potential to further reduce emissions through substitution of natural gas for pure hydrogen. It is estimated that this will reduce the

emission of CO_2 to a mere 40kg per tonne of DRI produced (Rechberger, 2020). This figure highlights that a small quantity of natural gas will still be required to reduce the pellets and produce DRI.

The DRI-EAF route needs high purity DR-grade iron ore pellets. DR-grade pelletising capacity would need to massively increase (by 10x) for the global steel industry to completely convert to the DRI-EAF process route (Lefebvre, 2021). This would require significant investment to secure the iron ore resources and pre-processing steps. Given the above, it seems unlikely that a full conversion from the conventional BF-BOF route to DRI-EAF steelmaking will occur.

The DRI process is the only route to include carbon capture to date (IEA, 2020). In this case, the captured CO_2 stream was compressed and used for enhanced oil recovery.

Finally, electrical methods of reducing iron oxides are being developed such as the American Iron & Steel Institute led CO_2 Breakthrough Project (Quader, 2016).

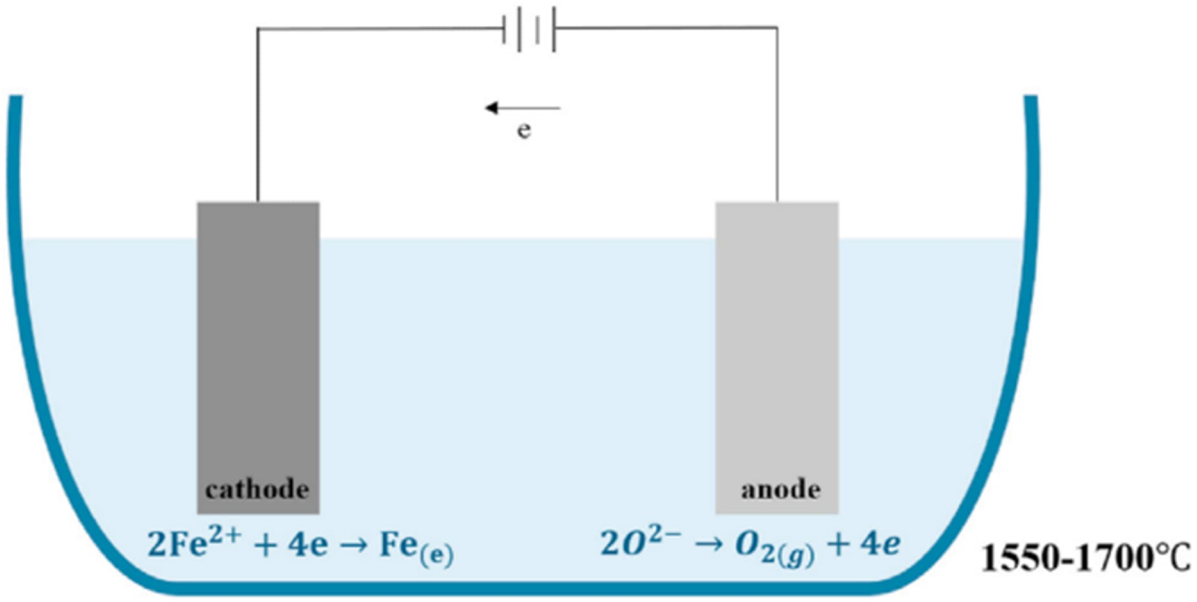

Figure 2.7: Molten Oxide electrolysis principle (Zhang, 2021)

This involves molten oxide electrolysis (Wiencke, 2018) as shown in Figure 2.7 which operates at high temperatures. The process uses electricity and therefore requires no carbon to produce the iron product. In addition, the process will produce large amounts of high purity O_2 as a by-product which could also be sold commercially. The researchers hope that this technology can replace blast furnaces once the current bench scale experiments have been developed to a competitive level. But,

due to the lack of scale up at the time of writing, this technology is excluded from this study.

2.2.8 Basic Oxygen Furnace

Taking molten iron from either the blast furnace or corex process, the basic oxygen furnace (BOF) is the most common method of producing crude steel. The molten iron is combined with a small portion of scrap metal to cool the batch and oxygen is introduced at high velocity to stir the liquid and reduce the carbon content of the molten iron. The ratio of scrap to molten iron depends on the availability of scrap and hot metal, chemistry of the hot metal and desired steel quality. Various fluxes are also added to remove the remaining impurities and alter the composition of the steel to reach the desired grade. This generates a gas stream with a varying chemical composition depending on the stage of the process, but that includes CO and CO_2. As with the coke oven and BF process the gas can be captured and utilised in other areas of the steelworks. Due to the wide range of possible scrap inclusions in this process step, multiple references from published data have been summarised in Table 2.11 on a per tonne of liquid steel basis:

Reference	**McBrien (2016)**	**Jin (2017)**	**He (2017)**	**Santos (2013)**	**Costa (2001)**	**Units**
IN						
Hot Metal	976	959	950	901	720	kg/t
Scrap	12	7	140	190	380	kg/t
Pellets	0.0		0	5	21	kg/t
Oxygen	43	86	73	74	71	kg/t
Natural Gas	0		0	0	4	kg/t
Electricity	83.3	88.89	35.5	45	20	kWh/t
OUT						
Liquid Steel	1000	1000	1000	1000	1000	kg/t
BOF gas	100	99	133	104	-	kg/t
Slag	30	-	85	114	-	kg/t

Table 2.11: Basic Inlet and Outlet material flows for the BOF process

As with previous production steps, the off gas produced by the BOF plant can be captured and used to generate steam and electricity within the steelworks. Unlike the

previous processes, the batchwise nature of the BOF means that a portion of the gas produced at the start of operation is not recoverable due to the high O_2 content. It is considered that the gas recovered will have a typical composition as recorded in Table 2.12 below and that it is flared completely to account for the CO_2 emissions from this stage. Any other sources of CO_2 from scrap preheating are ignored as they are significantly smaller than the sources considered within the other processing steps.

Species	CO_2	N_2	CO	H_2	H_2O	CH_4
BOF gas vol%	14.4	13.8	56.9	2.6	12.2	0

Table 2.12: Typical BOF gas composition (Santos, 2013)

Emissions are estimated at between 193kg (Fan, 2021) and 202kg (Pardo, 2012) of CO_2 per tonne of liquid steel produced. Considering the wide range of possible scrap to hot metal ratios, these emission values are remarkably similar. Instead, the slight difference is likely due to the level of automation of the process and operator knowledge and experience.

2.2.9 Electric Arc Furnace

The electric arc furnace (EAF) offers a lower emissions route to steelmaking (European Commission 2010). Mixtures of steel scrap, DRI and pellets are melted using electrodes to form liquid steel. Despite this, the use of EAF in global steelmaking still only accounts for 33% (Xu, 2010). Traditionally this has been due to the limited number of steel grades which could be produced by the EAF. With a greater focus on high quality, well sorted scrap metal this route is now able to produce most of the high grade, carbon, steels required by the construction industry. As the main energy source for this process is electricity, regions which suffer from high prices per kWh are also dissuaded from converting to EAF production methods. An EAF may also be designed to utilise molten iron from the blast furnace or corex process. In fact, by using a liquid iron source, the resulting electrical consumption at the electrodes may be significantly reduced, whilst the range of end products increases. The EAF process is less able to deal with slag than the BOF process as some of the iron and iron oxides become lost to the slag component. This results in high amounts of slag tending to reduce the productivity of the EAF unit as it not only needs energy to melt the slag but also tends to lose FeO into the slag component. As

with the BOF process, the scrap to hot metal ratio can vary significantly. A range of this ratio are included in Table 2.13:

Reference	**Kumar (2020)**	**Costa (2001)**	**Yang (2017)**			**Units**
IN						
Scrap	110	870	330	740	1050	kg/t
DRI	1050	200	0	0	0	kg/t
Hot Metal	0	0	760	320	0	kg/t
O2	30	40	-	-	-	kg/t
Natural Gas		10	-	-	-	kg/t
Electricity	595	500	60	275	420	kWh/t
OUT						
Steel	1000	1000	1000	1000	1000	kg/t
Slag	210					kg/t
Gas	80		100			kg/t

Table 2.13: Basic Inlet and Outlet material flows for the EAF process

As with the BOF process, the EAF is a batch process with the resulting off gas composition and flow varying depending on the stage of production. A typical gas composition is given in Table 2.14 below:

Species	CO_2	N_2	CO	H_2	H_2O	O_2
EAF gas mass%	40.0	56.0	0.0	0.0	1.0	3.0

Table 2.14: Typical EAF gas composition from (Ho, 2013)

Emissions from the EAF are estimated to be around 300kg per tonne of liquid steel (IEA, 2020). This value includes scope 2 emissions from the generation of the large quantities of electricity required by the process. Therefore, with the implementation of near zero emission electricity, the emissions to generate one tonne of liquid steel using an EAF will reduce compared to current reference values. Because of the low emissions and simpler production route, it is widely accepted that the EAF will become more widespread by 2050. Limits on scrap quantity and quality mean it is not feasible to expect all steel to be produced in this manner. This is especially true as the lifecycle of steel increases from its current 20-30 year level, meaning that even

with an increase in overall production, the level of available scrap will likely remain similar to today's levels.

2.2.10 Casting and Rolling

Once the liquid steel has been produced from either the BOF or EAF process, it must be cast into a desired thickness and width, cooled and cut into intermediate products. Depending on the end product required, the casting process may generate a variety of intermediate products such as slab, billet, etc (Griffin, 2019). This intermediate product is then hot rolled and formed into an end product with the required shape and metallurgical properties. Further processing may then be carried out in a cold rolling mill such as pickling, annealing, tempering, and coating. There are emissions generated during these processes from the burning of fuel gasses to heat the intermediate products and from electrical consumption. As with other stages, energy efficiency improvements are possible through the increased use of automation systems and waste heat utilisation. This section of the steelworks is assumed to be independent of any changes in configuration of the upstream equipment and is therefore excluded from the analysis within this work.

2.2.11 Steelmaking summary

In the previous sections, operating data published by several authors have been recorded.

Some works (Costa 2001, Kumar 2020) sought to compare exergy losses for different steelmaking routes. To achieve this, material balances were created which are reported within this work. In this case, no CO_2 emissions were reported, but were inferred based on the composition of the waste gasses from the various processes.

Other literature sources (McBrien 2016) used mass and energy balances to identify heat recovery potentials from the various steelmaking processes. This work also helped in choosing the best available techniques to be applied to the various processes.

Some work did consider CO_2 emissions specifically (Santos 2013) to determine the effect of post combustion CO_2 capture. However, it was limited to processes substituting the traditional blast furnace which are still some time away from commercialisation.

As there are no working references for the TGR-BF process described in section 2.2.6, a literature source (Jin 2017) was used which developed a detailed heat and

mass balance for this technology. The purpose of this was to analyse whether swapping the BF for the TGR-BF process would reduce the CO_2 emissions from a steelworks. The conclusions were that emissions are reduced both with and without carbon capture from the process gas but that electrical energy requirement increased by a factor of 1.7.

Generally, the literature focusses on either detailed heat and mass balances for a particular technology and substitution of one processing step for a newer technology. There does not appear to be any assessment of the emissions from a full production route or the combination of different routes to meet the level of steel demand predicted by 2050.

2.3 Carbon Capture

Traditionally, the power industry has been the focus of carbon capture and storage (CCS) technologies. Therefore, their technologies have influenced the development and nomenclature of CCS. This is reflected in the following definition of the three broad types of CCS technologies (IPCC, 2005):

1. Post Combustion Capture – This is the removal of CO_2 from a waste gas stream containing a mixture of CO_2, N_2 and water. The aim of this family is to prevent CO_2 produced during combustion of hydrocarbons from being emitted to the atmosphere. This technology is the most suited to being retrofitted on to an existing plant.
2. Pre Combustion Capture – This is the removal of CO_2 from a Synthetic Gas (Syn Gas) which may, for example, be produced by coal gasification or water shift reaction. The aim of this family of technologies is to convert a hydrocarbon source into a clean burning fuel and reduce the amount of inert CO_2 sent to the combustion process.
3. Oxy-Fuel Combustion – This is the replacement of air used to combust a gas with pure oxygen. This then creates a waste gas stream with very high CO_2 content mixed with residual water which is relatively easy to separate. To control the flame temperature at the burner, some of the waste gasses may be recycled in order to provide a cooling effect. A further benefit to this scheme is that there is no N_2 component in the waste gas. This option is likely to require significant redesign of a facility to incorporate this technology.

Removal of CO_2 from a gas stream can be carried out in several different ways. These include chemical absorption, physical absorption, physical adsorption, cryogenic distillation and membrane separation. Of these, cryogenic distillation and membrane separation have been excluded from this study based on excessive cost for the scale of CO_2 separation required for the steel industry. The remaining methods will be discussed and explained in the following sections.

2.3.1 Chemical Absorption

The oldest form of Carbon Capture Technology is Chemical Absorption using dilute monoethanolamine (MEA) which chemically reacts with CO_2 to remove it from a gas stream. Originally developed for removing CO_2 from natural gas, chemical absorption has been in use since the 1930's (Bottoms, 1930).

In an absorber column, containing packing material, the gas stream to be treated is contacted with a liquid solvent which chemically reacts with the CO_2 to remove it from the gas stream. The rich solvent leaving the bottom of the absorber column is then pumped to a regenerator (or stripper) column in which it is heated to reverse the chemical reaction and release CO_2 back into the gas phase. The regenerated, lean, solvent is then pumped back to the absorber to remove further CO_2 from the gas stream. The solvent temperature is generally controlled prior to its entry to the top of the absorber column and system efficiency is improved by using the lean solvent heat to warm the rich solvent prior to its entry to the regenerator column. This basic arrangement is shown in Figure 2.8.

More complex iterations may include wash sections being located at the top of the absorber column where water is used to quench the gas and limit solvent loss, cool the purified gas and maintain a water balance within the capture system. In addition, several studies have been carried out to determine the effect of intercoolers (Sachde, 2014), where a portion of the solvent is collected from the absorber column to be cooled before being readmitted into the column. The perceived advantage is that, as the chemical reaction between the solvent and CO_2 is exothermic, a cooler solvent temperature will increase the rate of reaction. These studies tend to ignore heat losses from the column to atmosphere which for a vessel in the order of 8 metres wide and 25 metres tall are likely to be significant.

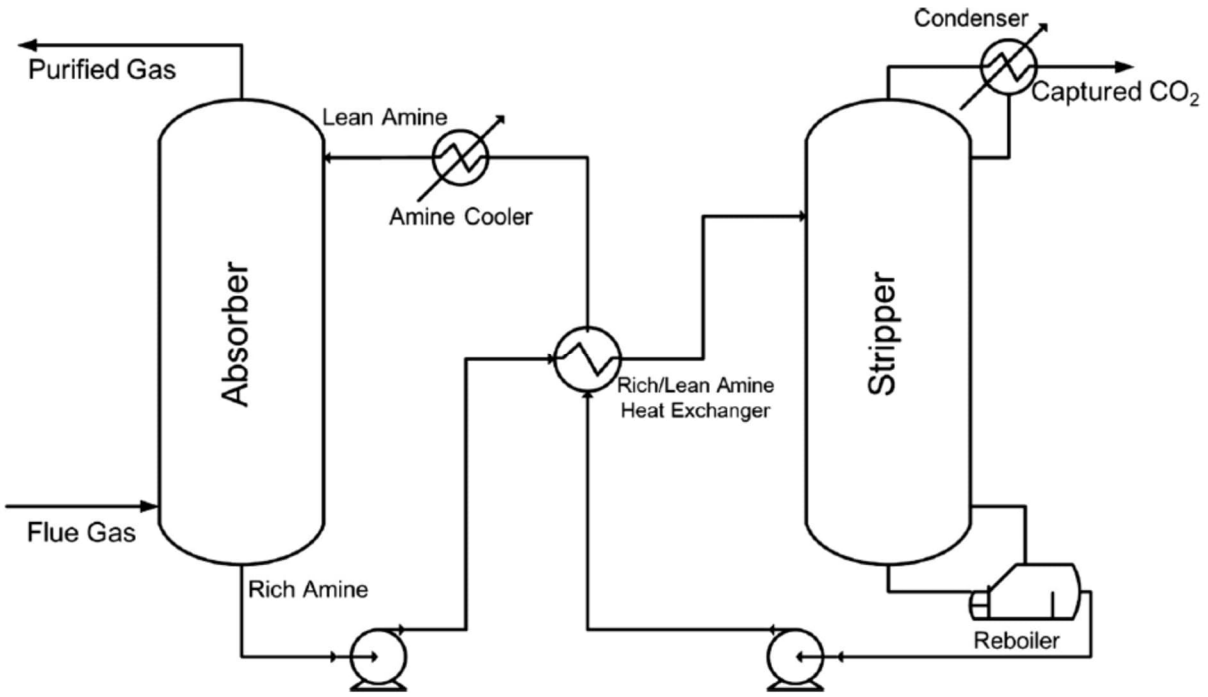

Figure 2.8: Basic Flowsheet of Chemical Absorption CO_2 capture (Oh, 2016)

Although ammonia, carbonates and ionic liquids may also be used to separate CO_2 from a gas stream, this study will focus on amines as the predominate and most widely developed family. Even within this group, a wide range of individual and blends of solvents have been considered within academia leading to several main categories being established. Monoethanolamine (MEA) is an example of a primary amine. It has two N-H bonds as shown in Figure 2.9 allowing it to react quickly with CO_2 but releases a large amount of heat during the reaction.

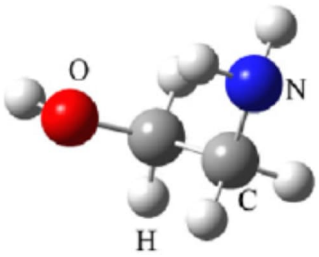

Figure 2.9: Representation of MEA (blue-N, grey-C, red-O, white-H) (Zhang, 2018)

The capacity of primary amines to react with CO_2 is lower than other types of amines. In addition, a strong chemical bond is formed during the reaction which requires a large amount of heat energy to reverse. The concentration of these types of amine used to capture CO_2 are generally low (less than 40% by weight) with higher

concentrations resulting in corrosive, flammable or viscous mixtures. This can lead to damage of equipment, present a safety concern or be hard to pump and distribute equally over the full diameter of the absorber and regenerator columns. Despite these drawbacks, MEA is seen as the benchmark amine, is available commercially (Reddy, 2003) and has been installed at the CO_2 Technology Centre Mongstad (Hamborg, 2014) in Norway.

Alternatively, tertiary amines such as methyldiethanolamine (MDEA), react more slowly as they can only react with CO_2 once it has dissolved into the liquid phase. Once the CO_2 is available as a bicarbonate a tertiary amine can react with it. The advantages of these solvents are that they require less thermal energy to release the CO_2 and regenerate the amine, are less prone to degradation and can maintain a higher loading of CO_2 (Mohamadirad, 2011). These solvents are also less corrosive which allows higher concentrations of the amine.

Finally, commercially available solvents such as 2-amino-2-methyl-1-propanol (AMP) shown in Figure 2.10 below and the Mitsubishi Heavy Industries KS-1 tend to adopt sterically hindered amines (Mimura, 1995) which retain the benefits of the primary amines whilst offering lower energy requirements for regeneration of the solvent. The exact composition and mixtures of these commercial solvents are, however, rarely published within academia for comparison against traditional solvents.

Figure 2.10: Representation of AMP (blue-N, grey-C, red-O, white-H) (Zhang, 2018)

Regardless of the solvent category, all require large quantities of thermal energy in order to regenerate the rich solvent which can either be provided by steam from the power plant or a dedicated gas fired boiler. In the first case, the electrical output of the power plant will be reduced and in the second case, additional gas must be burnt at a further operating cost and generate extra CO_2 emissions.

A wide variety of research has been carried out in the power sector, particularly on the loss of electrical output to support the carbon capture system. This is because chemical absorption technologies can be retro-fitted to existing processes as a so-called end of pipe solution. The technology also produces a relatively pure CO_2 stream which requires little further purification to meet the required gas quality for transportation and storage. A multitude of industrial and pilot plants have been installed based on this form of technology with a range of different solvents. Operating data from these sites (Thimsen, 2014; Miyamoto, 2017; Wilson, 2004) has been used to assess the typical barriers to wide scale adoption, namely:

- Rate of corrosion of the equipment by the various solvents.
- Emission of solvent into the treated gas stream.
- Slow reaction time to changes to the inlet gas conditions (composition, flowrate).
- Degradation rate of the solvent by oxygen and sulphur dioxide.
- High energy consumption to release the CO_2 from the solvent.

The corrosion rate of MEA has been widely studied with the result that most pilot plants utilising high concentrations of MEA tend to use stainless steel for the various vessels and equipment (Brigman, 2014). This choice of material becomes necessary to counteract the corrosivity of MEA. But adopting stainless steel increases the capital cost of the vessels and equipment by a factor of between 2x and 3.5x (Fischer, 2017) compared to using carbon steel.

For the power generation industry, emission of amine into the treated gas stream would release the solvent into the atmosphere. As the majority of these chemicals are toxic to marine life, representing an environmental concern. The main cause of this is a fine aerosol attaching itself to particles within the gas stream (Morken, 2014) which can be very difficult to remove in a washing section.

Due to the quantity of solvent within the absorber and regenerator columns, the reaction time of the chemical absorption plant to changes in gas flow or composition can be slow. The response times to changes in a number of operating parameters have been determined in a pilot plant (Montañés, 2018). This work concluded that the rates of CO_2 capture and desorption from the liquid phase were not significantly affected by changes in the inlet gas flowrate. Furthermore, the chemical absorption process was found to reach equilibrium again 55 minutes after the change in gas flowrate.

The effect of impurities is important as the liquid solvent is gradually degraded by oxygen and sulphur dioxide (SO_2) entering the absorber vessel in the gas stream. This results in the formation of heat stable salts which take no part in the absorption reaction between the CO_2 and solvent. The salts will then require treatment which recovers some, but not all, of the degraded solvent. The portion of salts that cannot be recovered becomes a waste stream from the capture plant.

The chemical absorption process requires significant amounts of heat in order to regenerate the solvent and release CO_2 back into the gas phase. This energy requirement is generally between 2.3 and 4.1 GJ per tonne of CO_2 captured (Brown, 2016 & Hamborg, 2014) but varies significantly with the solvent chosen. Furthermore, a higher CO_2 concentration in the inlet gas or a more complicated capture plant arrangement will also decrease this energy requirement.

Recently, further work has focused on the mass transfer of gas into the solvent with such methods as rotating packed beds (RPBs) or Higees investigated (Jassim, 2002). Whereas traditional absorber columns allow gas and liquid to contact each other in stational packed bed, the RPB increases the mass transfer between the two phases by rotating the packing as shown in Figure 2.11.

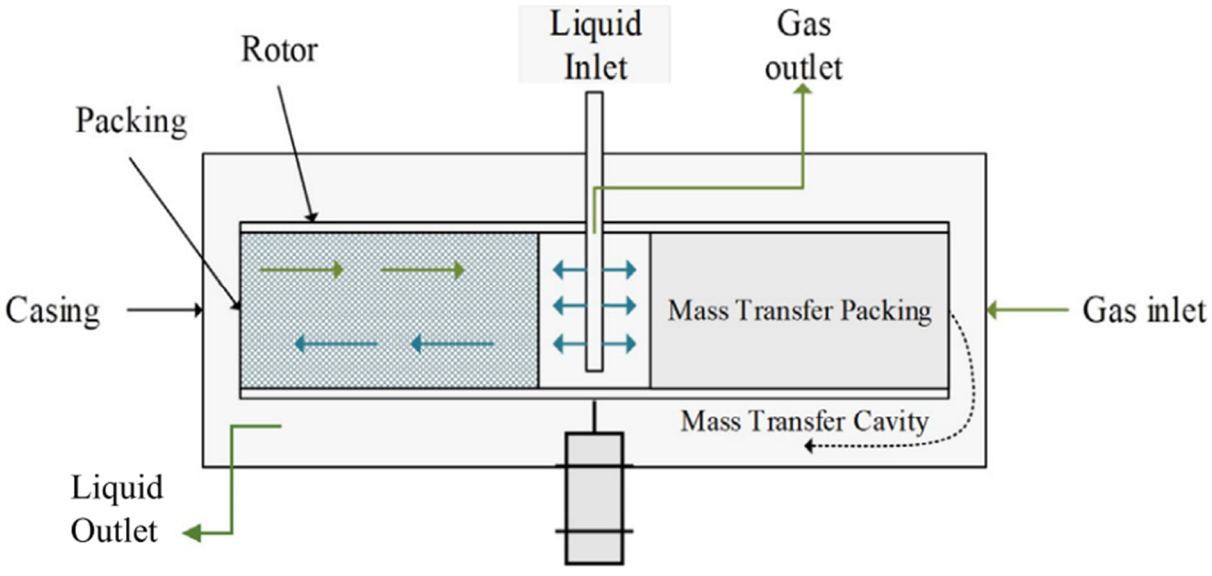

Figure 2.11: Schematic of a rotating packed bed (Esmaeili, 2022)

As the mass transfer can be the rate limiting step in the reaction between an amine and CO_2, this allows the overall footprint of the capture plant to be reduced. As RPBs

are not currently available at the scale required by steelworks, they have been excluded from this study.

2.3.2 Physical Absorption

A second process involving the circulation of liquid solvent is physical absorption. Instead of amines which chemically react with the CO_2 a mixture of polyethylene glycol (PEG) is used to physically capture the CO_2. This provides the advantage that the removal of CO_2 from the gas stream is not limited by reaction stoichiometry and reaction rates. As with chemical absorption, the physical absorption process is an exothermic reaction requiring solvent temperature to be controlled within the absorption column.

The process is currently viewed as the benchmark in pre-combustion capture to generate a carbon free fuel gas stream. The gas stream enters the absorber vessel at elevated pressure of around 20 bar gauge where it is contacted by the liquid solvent. Instead of increasing temperature, the pressure of the solvent leaving the bottom of the absorber vessel is reduced in stages to release the captured CO_2. The CO_2 released from the solvent is over 99% pure (Kunze, 2010) with the main impurity being water which must be removed before the CO_2 stream can be transported for storage or utilisation. The fuel gas stream leaving the top of the absorber vessel will have a sufficient pressure to directly feed a modern gas turbine. A flowsheet of a typical physical absorption process is included below in Figure 2.12.

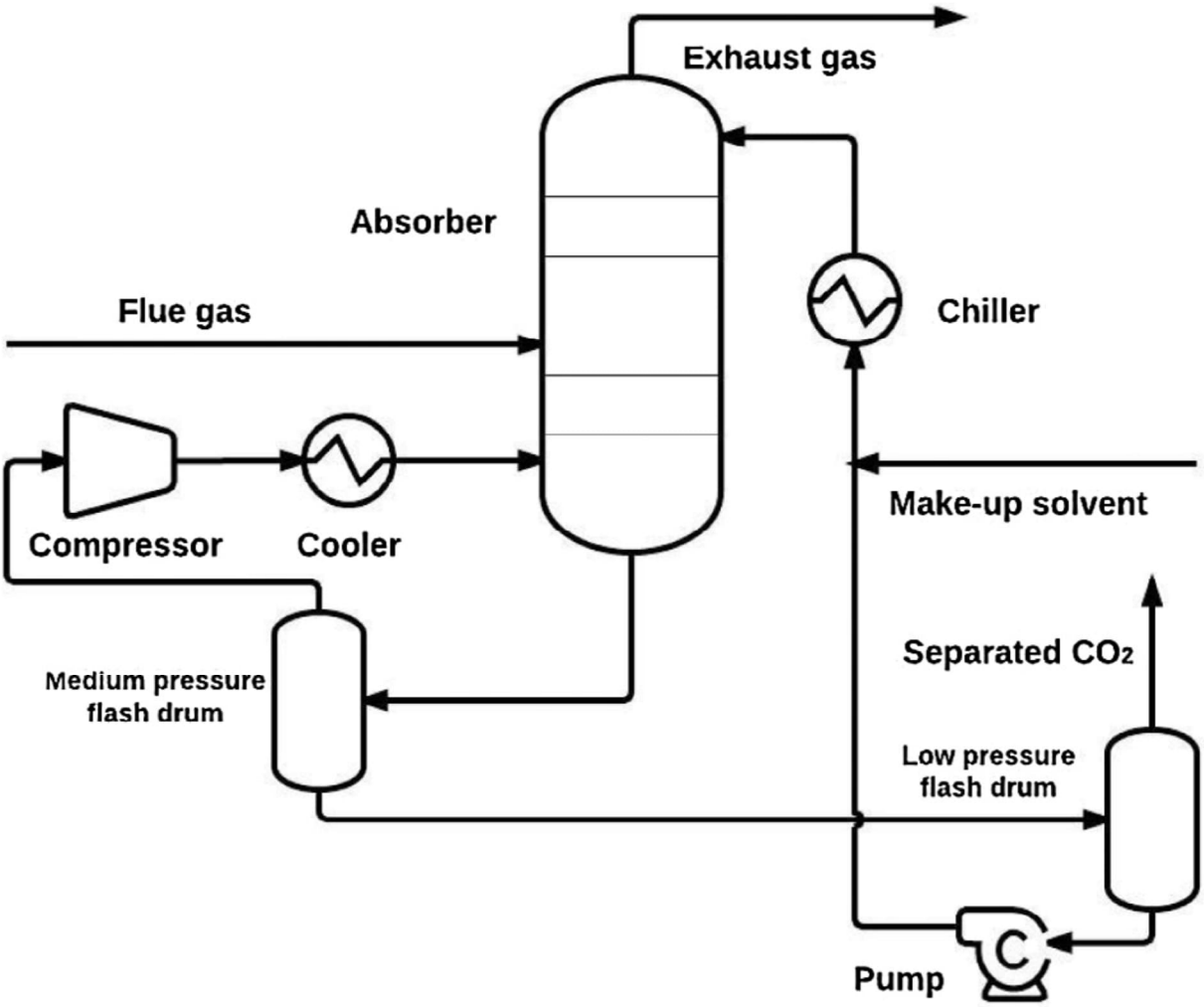

Figure 2.12: Flowsheet of the Physical Absorption process (Tan, 2016)

Proprietary solvents such Rectisol and Selexol are already used commercially at industrial scale to remove CO_2 from syngas (Markewitz, 2015). But, due to the proprietary nature of these solvents, there is limited process information available within literature. For analysis of this capture method the retention factors given in Table 2.15 were considered:

Gas Component	CO_2	CO	N_2	H_2	H_2O
Retention Factor	17%	99.9%	99.9%	100%	8.8%

Table 2.15: Gas retention factors for Selexol process (Progressive Energy, 2015)

Although there are significant savings in terms of heat energy, there will be electrical energy consumption to boost the gas pressure prior to treatment and to restore the solvent pressure once the CO_2 gas been removed. For applications where the compression of the feed gas is commonplace, such as the power generation

industry, this technology is likely to require little changes to existing equipment. For the steel industry, where most indigenous gasses are generated at only slightly above atmospheric pressure, it would require the installation of a dedicated gas compressor station.

2.3.3 Physical Adsorption

In this design, CO_2 from the gas is adsorbed onto a solid, often porous material as it passes across it. The selectivity of the porous material can be tuned by changing its composition and pore size but 100% selectivity is unrealistic. The pressure or temperature conditions within the adsorber vessel are then changed in order to release the captured CO_2 and prepare the porous material for the next capture cycle. Two options will be considered within his work, namely pressure swing adsorption (PSA) and vacuum pressure swing adsorption (VPSA).

Physical adsorption offers a midpoint between chemical and physical absorption, as gas compression is still required, but to a lower level than with physical absorption. This is coupled with the potential to require steam to remove the CO_2 from the porous solid in the case of temperature swing adsorption. For analysis of this capture method the following retention factors, i.e., the amount of gas left within the fuel gas shown in Table 2.16 were considered:

Gas Component	CO_2	CO	N_2	H_2	H_2O
Retention Factor (PSA)	3%	78.5%	100%	86.5%	0%
Retention Factor (VPSA)	3%	95%	100%	99%	0%

Table 2.16: Gas retention factors for PSA and VPSA processes (ULCOS, 2009)

Pressure swing absorption designs have already been employed in corex plants to separate the process gas into CO_2 rich and poor streams. The focus has been on the recycling of CO and H_2 back to the process with the result that the purity of the CO_2 stream is below than that required for most end users. This would lead to an additional purification step being required before the CO_2 stream could be sold to a consumer.

The purity of the CO_2 stream can be increased by installing a vacuum pump, as shown in Figure 2.13, allowing a greater pressure swing. The maximum capacity of this equipment has historically limited the maximum gas flow which can be treated by such systems.

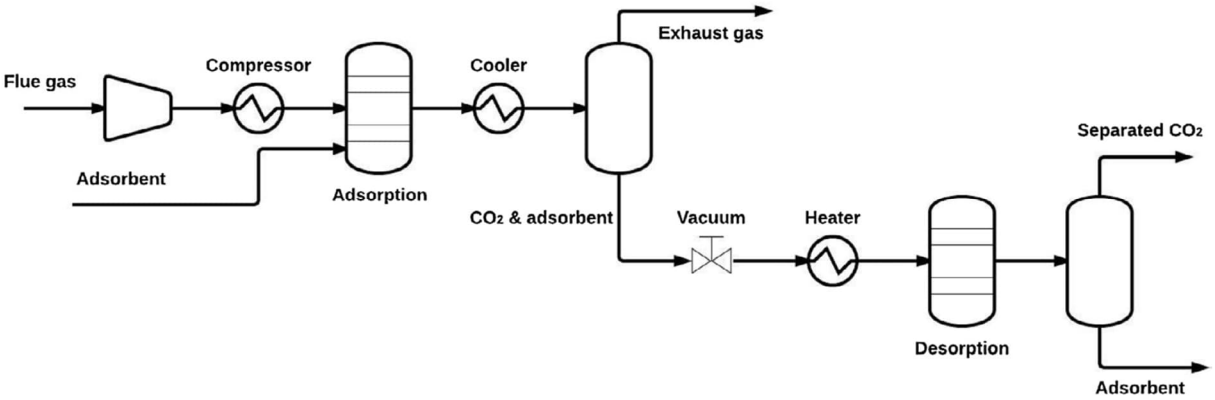

Figure 2.13: Flow diagram of a conventional VPSA capture process (Tan, 2016)

Whereas pressure swing absorption operates in a cyclic manner, a continuous temperature swing adsorption (TSA) based on a fluidized bed process is being developed (van Paasen, 2021). It is hoped that the combination of a solid adsorbent used in a fluidised bed will lead to the delivery of high capture performance, lower capture costs and low emissions.

CO_2 is first adsorbed at low temperatures in a multi-staged fluidized bed where heat is released during the adsorption reaction between CO_2 and the adsorbent. The hotter adsorbent is transported to a second multi staged fluidized bed via heat exchangers, where the captured CO_2 is released using steam. The steam regenerates the adsorbent before it is returned to the adsorber where it is again available for CO_2 capture.

The ideal characteristics for the adsorbent material are that it allows CO_2 to be selectively bound to it; be fluidizable; suitable for production at tonne scale; display high temperature and mechanical stability. Compared to chemical and physical absorption processes, the TSA process contains no liquid water, and therefore, lower-cost construction materials can be used.

2.4 CO_2 Utilisation

The largest obstacle to capturing CO_2 from process or flue gasses is finding a purpose for it. Without consideration of transport to and injection at a storage site or utilisation there is no economic driver to separate CO_2 from the gas stream. Although most test sites currently release the CO_2 into the atmosphere (Moser, 2020 & Notz, 2012) the most successful developments are able to sell the separated CO_2 to an end user. The only full-scale carbon capture plant operating on a steelworks in the UAE (Ramírez-Santos, 2018) is a good example of this as the CO_2 is sold for

enhanced oil recovery (EOR). There are also a number of chemical and other processes which currently require CO_2.

These processes will place different purity requirements on the captured CO_2 with gas used for drinks and food packaging, for example, requiring high purity CO_2. It must be mentioned that these traditional users of CO_2 utilise a relatively small amount compared to what could be supplied by the Steel industry if it was to adopt carbon capture on a wide scale. This means that new methods to utilise CO_2 must also be developed with the ideal scenario being utilisation local to a steelworks to limit the distance the CO_2 must be transported. A number of such alternatives are discussed in the following sections which may gain acceptance after further development.

2.4.1 Geological Storage (Offshore)

The oldest conceived idea for mitigating CO_2 emissions to the atmosphere remains one of the most contentious. By compressing CO_2 to high pressures, it can be injected deep underground into either depleted oil and gas reservoirs or saline aquifers (Leung, 2014). Whilst this has been achieved at several sites globally (Rosenbauer, 2010 & Turan, 2020) critics of this concept are quick to point out that this is not a permanent solution. Long term monitoring is also required to identify any escape of CO_2 from the storage site. From Table 2.17 it can be seen that the CO_2 purity requirement for both geological storage and EOR are similar indicating that the transportation of the gas stream is the determining factor. For CO_2 captured from blast furnace gas, potential contamination may include H_2O, CO and N_2. This is due to the relatively large amounts of these chemicals in the untreated blast furnace gas.

	Geological Storage	EOR
H_2O	500 ppm	500 ppm
H_2S	200 ppm	200 ppm
CO	2000 ppm	2000 ppm
SO_x	100 ppm	100 ppm
NO_x	100 ppm	100 ppm
O_2	4% vol	1000 ppm
CH_4	4% vol	2% vol
N_2+Ar +H_2	4% vol	4% vol

Table 2.17: Required CO_2 purity for Geological storage and EOR (Visser, 2010)

Global storage capacity has been estimated between 400-10,000 Gigatonnes (Gt) of CO_2 for deep saline aquifers and a further 920 Gt of CO_2 from depleted oil and gas reservoirs (International Energy Agency, 2004). But this volume is not spread equally around the world. Use of this storage capacity will also attract competition with sites closest to shore likely to be prioritized for hydrogen storage. This leaves storage locations at some distance from the shoreline. These locations will either need a permanent pipeline stretching hundreds of kilometres, or a fleet of CO_2 tankers to ferry the CO_2 from land to an injection wellhead. From various studies on the compression of CO_2 (Carpenter, 2012) a figure of 115 kWh/t_{CO2} can be assumed to determine the power requirements for storing CO_2. If the oil or gas reserve is not fully depleted, then injecting CO_2 can increase the yield of oil. This is known as Enhanced Oil Recovery (EOR) and is currently the most financially attractive option for using CO_2 (Bachu, 2010). Estimates vary on the ratio of CO_2 stored to the CO_2 released when the recovered oil is burnt. Furthermore, this use of CO_2 to generate further fossil fuels is frowned upon by many advocates of net zero emissions. This is because it potentially encourages fossil fuel consumption instead of investing in alternative technologies. For the short term at least, this solution is providing a market for captured CO_2 in North America and the United Arab Emirates.

2.4.2 Algae Feedstock

Photosynthesis is a natural method of removing CO_2 from the atmosphere. Based on this, some researchers (Styring, 2012) have looked to grow algae using captured CO_2 and then process it into biofuels a potential schematic of such a process is

included in Figure 2.14. This has the potential to offer an environmentally friendly way of converting a waste product into a useable commodity.

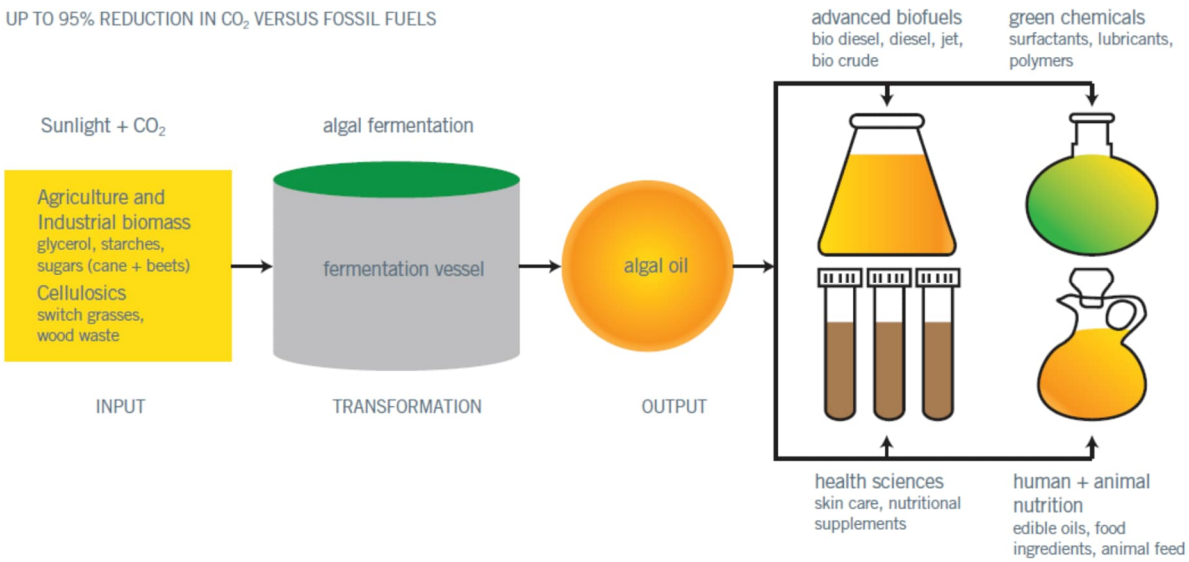

Figure 2.14: Schematic of Algae use in CO_2 separation (Global CCS Institute, 2011)

Ideally, the CO_2 would be supplied by dissolving the gas into a non-toxic liquid to aid the mass transfer of CO_2. This would also result in better growth of the algae, a higher algal oil output and better utilisation of CO_2. As the algae will only take up CO_2 during daylight hours, some buffering of the captured CO_2 must be installed. An alternative would be to simulate daylight using electric lighting with the drawback of additional electrical energy consumption. The largest drawback with algae though is the required space to treat the volume of CO_2 which could be captured from a typical steelworks. Some researchers claim this relationship is in the order of 50 grams per m^2 per day (g/m^2d) (Sun, 2011). This would equate to some 55.79km^2 of land required to utilise 2790 tonnes of CO_2 per day.

Products from this process could replace fossil sources of oil but would still produce CO_2 emissions if used as fuel for combustion in addition to the emissions created by the processing of the algae.

2.4.3 Slag Mineralisation

A by-product of steelmaking is slag which contains the impurities removed from the iron ore during the iron and steelmaking processes. The slag contains large amounts of Calcium Oxide (CaO) and Magnesium Oxide (MgO) as shown in Table 2.18 which can be mineralised to capture CO_2 as show in equations 2.7 and 2.8.

$$CaO + CO_2 = CaCO_3 \quad \Delta H^o_{298} = -177.9 \text{ kJ/mol} \qquad \text{Equation 2.7}$$

$$MgO + CO_2 = MgCO_3 \quad \Delta H^o_{298} = -100.7 \text{ kJ/mol} \qquad \text{Equation 2.8}$$

This mimics the natural slow acting mineralisation process but on a larger and faster scale which requires higher temperatures and pressures. Studies carried out on this method have concluded that 3.3 tonnes of slag are required to capture one tonne of CO_2 (Dri, 2014). This slag must be ground to both maximise the surface area for reaction with CO_2 and to disrupt the smooth glassy layer on the surface of the slag particles produced at the granulation facilities of the blast furnace.

Composition	CaO	SiO_2	MgO	Al_2O_3	Fe_2O_3
Content (wt%)	30 – 60	10 – 20	5 – 10	1 – 10	5 - 20

Table 2.18: Chemical composition of blast furnace slag (Humbert, 2019)

On approximately 400kg of slag are produced for every tonne of steel (Horii, 2015) which is far less than the 1.8 tonnes of CO_2 for the same amount of steel. Therefore, this concept is unlikely to account for all the emissions from a steelworks, although may highlight slag as a useful commodity for other industries who produce a smaller volume of CO_2. The mineralisation process has also been reported to require approximately 20 MW of energy per tonne of CO_2 captured. Most of this requirement comes from a water evaporation stage (Dri, 2014), with the actual CO_2 mineralisation step being exothermic.

A final consideration is that blast furnace slag is currently used by the cement industry as a raw material which generates less CO_2 than clinker. By using slag to capture emissions from one source it may therefore increase the emissions from another industrial process.

2.4.4 Recycle to Blast Furnace

The blast furnace and alternative technologies work in a similar manner to a gasifier in that coke and oxygen are burnt to form CO gas. The CO and hydrogen are then used to reduce the iron oxides. In the case of corex and TGR-BF, the CO_2 lean gases are recycled to the blast furnace. A novel alternative, yet to be investigated within literature, would be to recycle the CO_2 rich gasses and allow the process temperatures and coke fuel to reduce the CO_2 to CO. This would mean an increase

in the concentration of CO and CO_2 in the top gas and a lower volume to be treated. Within the blast furnace, the reaction of CO with coke is exothermic whereas the reaction of CO_2 with coke is endothermic. This means that there would be an overall increase in coke consumption to generate the necessary heat inside the blast furnace.

2.4.5 Water Gas Shift Reaction

Although not strictly speaking a CO_2 utilisation technology the water gas shift reaction may offer benefits to the steel industry. In this process, a stream of CO and water is passed over a catalyst which promotes the following reaction (Basile, 2015):

$$CO + H_2O = CO_2 + H_2 \quad \Delta H^o_{298} = -41.1 \text{ kJ/mol} \qquad \text{Equation 2.9}$$

This could lead to the blast furnace being a net producer of H_2 which could be used to reduce the carbon fuels at the blast furnace, produce greener electricity on site or be sold to offset the cost of carbon capture. The reaction in Equation 2.9 is exothermic and, with a carefully designed heat exchanger network, can preheat the incoming gas stream (Sanz, 2015). In fact, the required temperature of 200^{o}C can be reached using the heat generated by the reaction of CO with water. Because of the exothermic reaction, some chemical energy is lost during this process. But the outlet gas would contain a high proportion of CO_2 which could easily be separated from the other main constituent (by volume), hydrogen. As shown in Figure 2.15, the water-gas shift is split into two phases to increase the conversion rate of water to H_2. The first reactor operates at high temperatures which reduces the CO content of the blast furnace gas from around 25% to 6% by volume (van Dijk, 2018). This increases both the H_2 content and the CO_2 content and consumes steam. Prior to the gas entering the second reactor it must be cooled as the catalysis within the second reactor operates at a lower temperature. This second stage reduces the CO within the gas stream to near zero to maximise the H_2 and CO_2 content. After the second water gas shift reactor the gas stream must be cooled both to condense out any excess moisture from the gas and to allow the CO_2 to be removed.

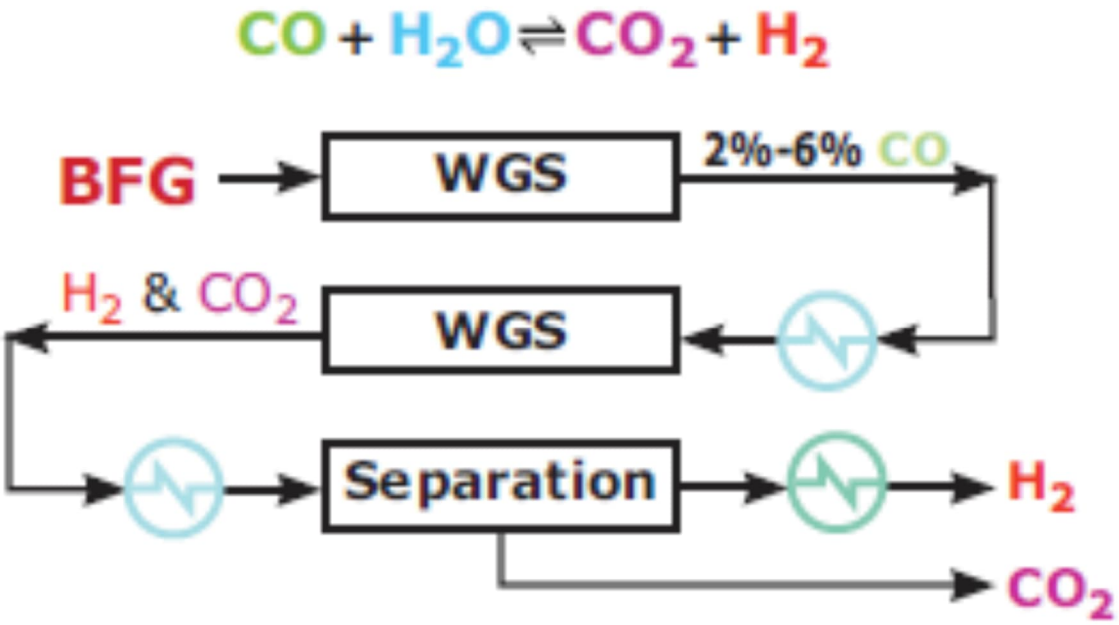

Figure 2.15: Layout of WGS and carbon capture system adapted from van Dijk (2018)

By adopting a solid sorption enhanced water gas shift (SEWGS), the water-gas shift and the CO_2 separation steps can be combined. This reduces the number of process steps through which the gas stream must pass and the number of cooling steps to pre-condition the gas. As CO_2 is removed from the gas stream, the shift reaction is driven further to completion allowing a lower steam to CO ratio (Fernández, 2017). Unlike the traditional WGS process, the product gas leaves the SEWGS process at high temperatures which provides a greater level of heat energy to the end users of the gas. The process becomes cyclic as the solid adsorbent will reach its capacity of CO_2 and require regeneration with steam. This then requires multiple SEWGS vessels which allow for constant treatment of the gas by alternating between regeneration and SEWGS operation.

2.4.6 Solid Oxide Electrolysis Cell

A solid electrolysis cell (SOEC) can convert CO_2 to CO using an electrical current at high temperature. Introducing CO_2 at the cathode leads to the negatively charged oxygen being conducted through the electrolyte and oxidised to O_2. This reaction is required to take place under high temperature conditions of around 800°C (Suzuki, 2015). This temperature is significantly higher than the temperature of most CO_2 streams from capture processes. Some of the consumed electrical energy is converted into heat within the electrolysis cell which makes up part of the heat input

but additional energy will be required to heat the CO_2 before it enters the electrolysis cell. By adopting such a high temperature, the overall electrical energy requirement is slightly lowered and non-noble metal catalyst such as nickel supported on yttria-stabilized zirconia (YSZ) can be used which reduces the capital cost (Hu, 2013). Solid Oxide Electrolysis Cells (SOECs) are capable of converting H_2O and CO_2 into a syngas suitable for fuel generation such as through the Fischer-Tropsch process. The basic schematic of this process is given in Figure 2.16.

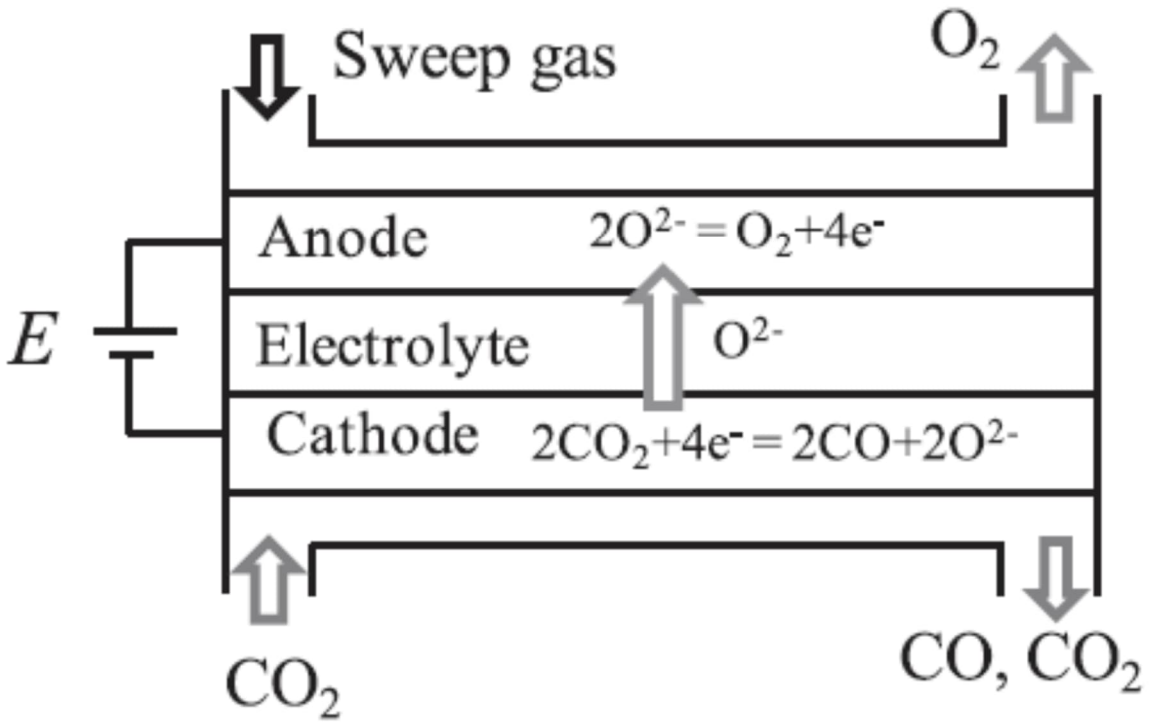

Figure 2.16: Schematic of a Solid Oxide Electrolysis Cell (Suzuki, 2015)

Research (Suzuki, 2015) has estimated the electrical consumption for this process to be 189 kilojoules per mole (kJ/mole) of CO_2 but with good conversion rates between 60 to 70%. For this work, it is assumed that the CO_2 stream will be preheated to the required temperature by combustion of a small portion of fuel gas creating a small additional emission source. The catalyst stability, cell lifespan and electrical energy consumption for this technology remain limitations to adopting this application on a widescale (Hu, 2013).

2.4.7 Reverse Water Gas Shift Reaction

By reversing the water gas shift reaction in Equation 2.9, CO can be produced from CO_2 and H_2 over a copper-based catalyst (Hu, 2013). This offers the potential to

allow recycling of the CO_2 produced during the steelmaking process steps by forming gas with a high CO content.

$$CO_2 + H_2 = CO + H_2O \quad \Delta H^o_{298} = +41.2 \text{ kJ/mol} \qquad \text{Equation 2.10}$$

The reaction given above (Yilmaz, 2017) is slightly more favourable than the SOEC and proceeds at lower temperatures. For the reverse water gas shift (RWGS), operating temperatures of 400°C are stated in literature (Saravanan, 2021). As with the solid oxide electrolysis cell it is assumed that a fuel gas is burnt to generate the necessary heat. The process will require a stream of hydrogen to reach a ratio of 1:1 H_2 to CO_2. This ratio has been reported to allow conversion rates of the CO_2 of between 20-35% (Kim, 2014). The treated gas stream will have a high calorific value due to both the CO generated from the CO_2 and the unreacted H_2 and can therefore be used for heat or electrical energy generation around the steelworks. Although the concept of recycling CO_2 into a usable fuel is of interest, it sparks debate over the lifetime of the fuel before it is eventually burnt and the carbon is released to the atmosphere. Because energy is required both to generate H_2 and preheat the feed gases, the process itself will emit CO_2.

2.4.8 Plasma Catalysis

Non-thermal plasma technology has the potential to supply the considerable energy required to convert CO_2 into fuels and chemicals (Paulussen, 2010). Non-thermal plasma consists of a room temperature stream containing highly energetic electrons containing a typical mean energy of 1-10 eV (Tu, 2012). This high energy can easily break the C-O bonds in CO_2 molecules. A catalyst is also required to limit the produced species to mostly CO, however conversion rate is quoted as a maximum of 38% in literature (Mei, 2016). By using a coaxial dielectric barrier discharge pure CO_2 can be converted into CO and O_2 at low temperatures. A proposed arrangement showing the position of electrodes and packing material at a laboratory scale is shown in Figure 2.17. Significant further work would be required to develop the technology to the capacity required to treat separated CO_2 on a steelworks.

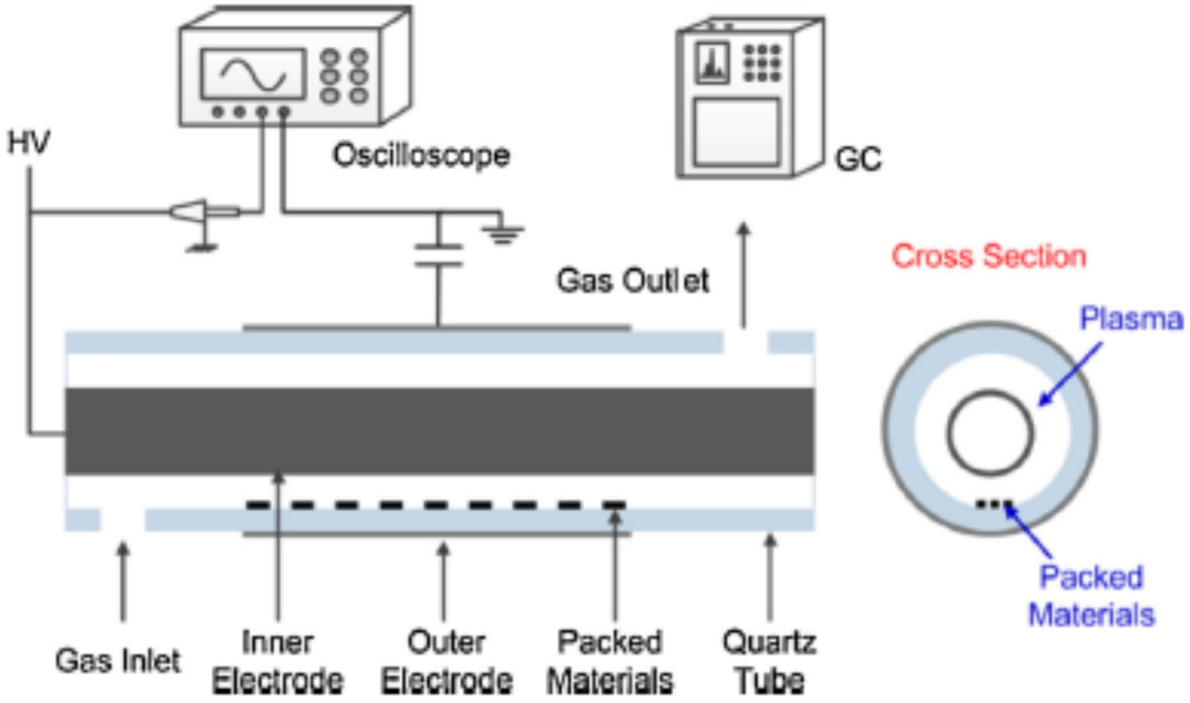

Figure 2.17: Schematic of a Plasma-Catalysis System (Mei, 2016)

A large energy requirement of 1.6 kilojoule per millimole (kJ/mmol) of CO_2 converted (Mei, 2016) is seen due to the inefficiencies of plasma technology. The resulting gas stream leaves the plasma converter at around 150°C and consists of a mixture of Oxygen, CO, CO_2 and any other species in the inlet gas stream. An additional step may therefore need to be introduced to remove the oxygen to make the gas safer to handle. This would also increase the chemical energy value per volume in the gas stream. Finally, the resulting gas does not fully convert the CO_2 to CO, meaning that the consumer of this gas will likely emit a high portion of CO_2.

2.4.9 Flue Gas Recycle

Mimicking the oxy-fuel combustion technique under consideration by the power generation industry, some combustion-based processes within the steelworks are considering recycling their flue gases. The benefits of this technology are that a reduction in the quantity of high calorific gas can be made without impact on the flame temperature (Mathur, 2021). This means that these gasses become available for other processes which might displace purchased fuel gasses or may allow greater on-site power generation. Perhaps most critically for this work, the unrecycled flue gas will contain a higher CO_2 content making capture from the gas stream more economical than from the input process gasses. The process will increase electrical

consumption both to power additional recirculation fans and to provide an O_2 stream to the process, replacing the combustion air currently used.

The schematic in Figure 2.18 exemplifies flue gas recycling applied to the hot blast stoves of a blast furnace. In this case, a stream of blast furnace gas is combusted with a synthetic air made by mixing oxygen with a portion of the flue gasses generated by the combustion. This creates a flue gas stream with a higher CO_2 content which reduces the energy consumption and cost per tonne of CO_2 separated. Furthermore, because of the higher CO_2 content, a small increase in heat transfer efficiency is observed in the hot blast stoves which results in a reduction in fuel gas consumption.

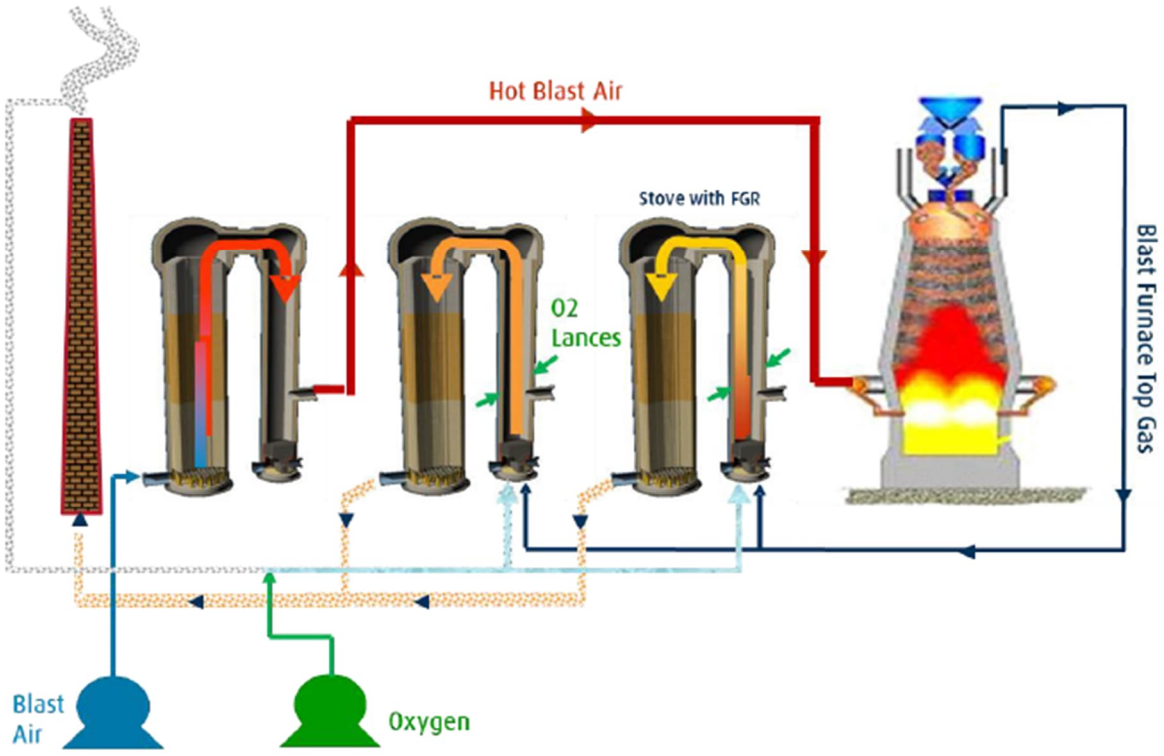

Figure 2.18: Schematic of flue gas recycling for the blast furnace stoves (von Schéele, 2008)

2.4.10 Other Processes

Care has been taken during the research stage of this work to identify and consider the most promising technologies for carbon mitigation of existing steelmaking processes. It should be recognised that new concepts and technologies are being constantly developed due to the level of interest this topic holds within academia. Other ideas which are currently unproven or at a low technological readiness level (TRL) may yet prove more advantageous than those considered in this work.

2.4.11 Carbon Capture Summary

The literature referenced within this work focusses on in-depth studies of a particular type of technology (Saima, 2013) to calculate specific capture costs or show future improvements. Not all of technologies are at sufficient commercial readiness that operating data is readily available. In these cases, theoretical or laboratory scale data has been reported (Mei 2016, Suzuki 2015). Relatively few publications are available detailing carbon capture from blast furnace gas. Those that do (Rochelle 2014, Saima 2013) focus on one technology with some statement as to why this is the best choice. The reviews of carbon capture technology have compared different types of capture technology on a generic level, but without considering advantages or disadvantages to applying them to blast furnace gas. Furthermore, these comparisons are mostly qualitative, with no clear quantification of benefits or drawback to adopting a specify technology. There does not therefore appear to be a clear assessment of the "best" technology for removing CO_2 from blast furnace gas.

2.5 Investigation Objectives

By undertaking the research presented in this chapter, the following objectives were identified to fulfil the aim of this dissertation:

- An assessment should be made to compare the emissions of carbon dioxide from various steelmaking routes. This should identify whether process substitution has the potential to drive a reduction in carbon dioxide emissions without the development of removal or utilisation technologies. This assessment and its results are reported in Chapter 4.
- Multiple, different technologies should be considered to reduce the emissions from the predominant BF-BOF route. This part of the study will focus on approximate operating costs for the various schemes to determine a list of preference for steelmakers. The results of this analysis are reported within Chapter 5 of this thesis.
- Finally, a range of chemical absorption solvents will be considered to identify ideal solvents for removal of carbon dioxide from blast furnace gas. This part of the study will also develop an order of magnitude costs for such a facility which can be used by steelmakers in their financial planning for reducing carbon dioxide emissions. The results of this assessment are reported in Chapter 6.

Chapter 3. Experimental Design

3.1 Chapter Introduction

To assess the design and cost of the chemical absorption-based carbon capture plant, Aspen HYSYS® and Aspen Process Economic Analyser (APEA) were used. This chapter will explain the development of the flowsheets undertaken and the basis for the various inputs required to drive the software. The results of the various cases are reported in Chapter 6.

3.2 Aspen HYSYS®

Aspen HYSYS® V11 software (Chang, 2018) was used to model the carbon capture from blast furnace gas. An example case for acid gas cleaning via monoethanolamine (MEA) was used as a basis.

3.2.1 Chemical Components considered

The chemical components within Table 3.1 were considered within the component list. Only a single amine or a combination of two amines being studied were added to the component list for a particular case.

Chemical Formula	Name	Chemical Formula	Name
H_2O	Water	HCl	Hydrochloric Acid
CO_2	Carbon dioxide	HSCN	Thiocyanic acid
H_2S	Hydrogen Sulphide	H_2SO_4	Sulfuric acid
O_2	Oxygen	H_3PO_4	Phosphoric acid
N_2	Nitrogen	NaOH	Sodium Hydroxide
H_2	Hydrogen	CH_2O_2	Formic acid
CO	Carbon monoxide	CH_3COOH	Acetic acid
CH_4	Methane	**Amines**	
C_2H_6	Ethane	DGA	Diethanolamine
C_2H_8	Propane	MDEA	Methyldiethanolamine
C_4H_{10}	n-Butane	MEA	Monoethanolamine
C_4H_{10}	i-Butane	PZ	Piperazine

Table 3.1: Table of chemical names and formulas considered

The list in Table 3.1 above is based on the standard component list for the software package with the following components removed; COS, CS_2, M-mercaptan and E-mercaptan as they are not present within the blast furnace gas stream entering the absorber.

A standard Aspen HYSYS® property package was chosen for handling chemical solvents for simulating the removal of acid gases such as CO_2 from gas streams. The "Acid Gas – Chemical Solvents" package is based on extensive research (Zhang, 2009) on rate based chemical absorption process simulation and molecular thermodynamic models for aqueous amine solutions. This package combines the Peng-Robinson equation of state, given in Equation 3.1, for the vapour phase and electrolyte non-random two liquid (eNRTL) activity coefficient model for electrolyte thermodynamics (Song, 2009).

$$p = \frac{RT}{V_m - b} - \frac{a\alpha}{V_m^2 + 2bV_m - b^2} \qquad \text{Equation 3.1}$$

Where:

$$a = \frac{0.45724 R^2 T_C^2}{P_C}$$

$$b = \frac{0.07780 R T_C}{P_C}$$

$$\propto = \left(1 + (0.37464 + 1.54226\omega - 0.26992\omega^2)(1 - T_r^{0.5})\right)^2$$

$\kappa = 0.37464 + 1.54226\omega - 0.26992\omega^2$ when $\omega \leq 0.49$

$\kappa = 0.379642 + 1.48503\omega - 0.164423\omega^2 + 0.016666\omega^3$ when $\omega > 0.49$

V_m = Molar Volume

$$T_r = \frac{T}{T_C}$$

T_C = Critical Temperature (K)

P_C = Critical Pressure (MPa)

T = Temperature (K)

R = Ideal Gas Constant (8.314 J/mol.K)

ω = acentric factor

Regression of both thermodynamic and physical properties for aqueous amine solutions (Zhang, 2011) was used to identify the necessary model parameters. This

regression was performed using available data on vapour liquid equilibrium (VLE) and heats of absorption for the supported amine, namely diethanolamine (DEA), diglycolamine (DGA), diisopropanolamine (DIPA), methyldiethanolamine (MDEA), monoethanolamine (MEA), piperazine (PZ) and triethanolamine (TEA).

In addition to major amine and acid gas components, contaminants such as heat stable salts can also be accounted for. Further consideration is also made for inert gases, hydrocarbon components and petroleum fractions. These latter components were not considered in the modelling as they are not present within the blast furnace gas or generated during the CO_2 removal process.

The package requires a minimum of one of the supported amines, CO_2, H_2S and H_2O to function. The default valid phases of vapour and liquid were assigned for the model with temperature limits of -123.1^oC and 9726.85^oC and default pressure limits of 0 – 100,000 bar. These ranges are the default values for the software models and (more than) sufficient to cover the ranges of temperature and pressures expected when removing CO_2 from blast furnace gas which are discussed in section 3.2.8.

The default inside-out flash convergence algorithm was chosen with a default maximum of 100 iterations specified. These types of algorithm use a simple equilibrium and enthalpy model in an inner calculation loop which then solves overall component heat balances in an outer loop. This outer loop of calculations then updates the thermodynamic models with the results from the rigorous models. The maximum number of calculation iterations was maintained at a default value of 10,000. If the calculated values do not converge within this number of iterations, then it will return an error.

3.2.2 Heat Stable Salts

Although the option to consider the presence and formation of heat stable salts in the liquid phase was included within the model, no concentration of salts was specified within the model runs. The reason for this is the lack of reference data from operating plants for loading of heat stable salts within the circulating amine solution. Assessment of treatment of other gasses (Freguia, 2003) showed that a small concentration of heat stable salts can reduce the energy requirement to break the chemical bond between the amine and CO_2. Excessive formation can reduce the absorption capacity and aggravate operational problems such as foaming, corrosion, amine loss, and change in the vapor-liquid equilibrium (Hai, 2020).The content of

heat stable salts must be controlled within the amine solution, which would require additional reclaiming units, not considered in the basic acid gas treatment flowsheet.

3.2.3 Chemical Reactions considered

A standard set of reactions were used to capture the chemical reactions between the defined components. These reactions can be further split into equilibrium and kinetic reaction types. For the equilibrium reactions, the constants and coefficients are fixed within the model and cannot be modified.

The equilibrium reactions for models containing MEA as the amine (Chang, 2018) are:

$$MEA + H_3O^+ = MEAH^+ H_2O \quad \text{Equation 3.2}$$

$$2H_2O = H_3O^+ + OH^- \quad \text{Equation 3.3}$$

$$H_2O + HCO_3^- = H_3O^+ + CO_3^{-2} \quad \text{Equation 3.4}$$

$$H_2O + NH_3 = OH^- + NH_4^+ \quad \text{Equation 3.5}$$

$$NH_3 + HCO_3^- = H_2O + NH_2COO^- \quad \text{Equation 3.6}$$

A number of kinetic reactions are included within the software models. These were not used within this work as a Rate based approach was taken to increase calculation speed whilst retaining an error deviation within 5% (Isa, 2021). For reference, reactions involving MEA as the amine (Chang, 2018) are included below:

$$CO_2 + OH^- = HCO_3^- \quad E_a = 5.547x104 \text{ kJ/kgmol} \quad \text{Equation 3.7}$$

$$HCO_3^- = CO_2 + OH^- \quad E_a = 1.074x105 \text{ kJ/kgmol} \quad \text{Equation 3.8}$$

$$MEA + H_2O + CO_2 = H_3O^+ + MEACOO^- \quad Ea = 4.126x104 \text{ kJ/kgmol} \quad \text{Equation 3.9}$$

$$H_3O^+ + MEACOO^- = MEA + H_2O + CO_2 \quad Ea = 6.916x104 \text{ kJ/kgmol} \quad \text{Equation 3.10}$$

The kinetic reactions above are valid even when MEA was substituted for different amines supported by the Aspen HYSYS® property package. For the kinetic reactions a complete list of activation energies is given below in Table 3.2 for the amine species considered in this work:

Amine	Equivalent reaction to 3.8 or 3.9 above	Activation Energy (kJ/kgmol)
MEA	8	$4.126x10^4$
MEA	9	$6.916x10^4$
PZ	8	$3.360x10^4$
PZ	9	$9.154x10^4$
MDEA	8	$3.780x10^4$
MDEA	9	$9.255x10^4$
DGA	8	$6.621x10^4$
DGA	9	$1.142x10^5$

Table 3.2: List of activation energies for the range of amines considered (Chang, 2018)

3.2.4 Alterations to example case

The original flowsheet contained a flash separator unit in order to simulate the rapid loss of pressure to release captured CO_2 from the rich amine leaving the absorber column. As the blast furnace gas inlet pressure is significantly lower than considered in the original model, the flash separator was replaced with a pump unit and the light hydrocarbon sink was removed. The sour gas stream was updated to match process conditions typical for blast furnace gas, which are included in Table 3.3:

Parameter	units	value
Molar flow	kgmole/h	13119
Temperature	°C	40
Pressure	bar	1.10
Composition		
CO_2	mole %	22.5
CO	mole %	23.2
N_2	mole %	45.0
H_2	mole %	2.70
H_2O	mole %	6.60

Table 3.3: Absorber Column Inlet Gas Conditions

It should be noted that blast furnace gas composition is dependent on several operating parameters and will vary over the course of a day. As the software

considers steady state calculations, a typical, fixed composition is given in Table 3.3 above. Figure 3.1 below shows the recorded dry composition of blast furnace gas from an operating unit within the UK. This data is included to indicate typical variations over a 24 hour period. The data shows that there is a relationship between the amount of CO and CO_2 within the gas with a decrease in CO_2 often corresponding to an increase in CO. Within Figure 3.1, the H_2 content can be seen to be gradually increasing. This is due to a slow increase in the amount of coal injection into the blast furnace which is atypical of stable operation.

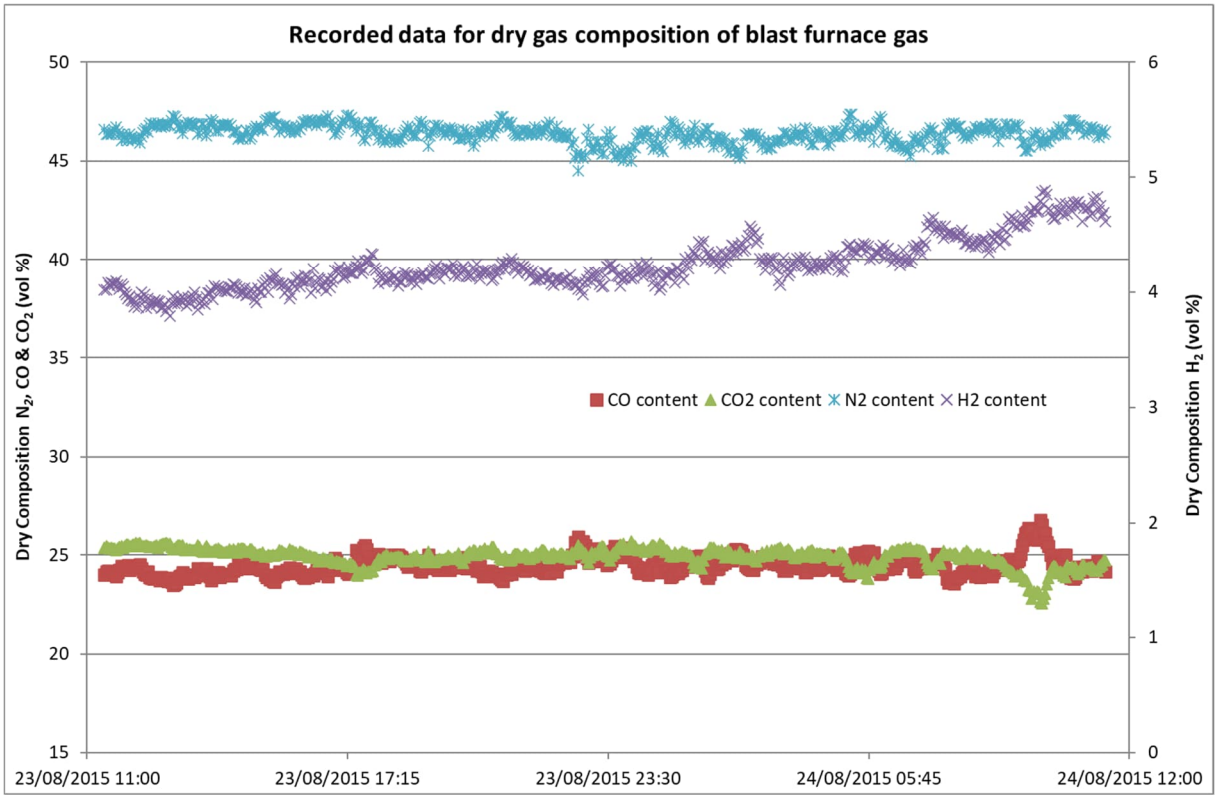

Figure 3.1: Graph of blast furnace gas components over a 24 hour period

3.2.5 Absorber Column

The absorber column unit settings were mostly left as per the example case, except for the column packing. The packing type was changed from tray type to a packed type which considered a random packed bed. This was specified based on experience within the steel industry of this type of design for demisting purposes. Due to an increase in both gas and liquid flows compared to the example case, the diameter of the absorber column was increased to limit pressure drop. The number of theoretical stages within the column was maintained at 20 from the example case being counted from the top down. The first 2 stages were dedicated to a water wash

section with Lean amine entering the column at stage 3 and leaving the column at the last stage. Stage 20 was also where the feed gas enters the column. The average stage height across the cases considered was 775mm and ranged from 215 to 2,000mm. The number of stages was chosen to provide a detailed description of the temperature, pressure and concentration profiles through the absorber and regenerator columns.

A pressure drop across the column was calculated based on the column diameter and height and flowrates of gas and liquid. This pressure drop was used to determine the operating pressure at each stage. The wash section was set to remove all liquid leaving stage 2 of the column by specifying a liquid flowrate of 0.0 kg/s between stage 2 and 3.

The pressure profile of the column was set using the calculated pressure drop through the 20 stages. The more common “Efficiency” option was selected as it uses rate-based calculations in the background to calculate stage efficiencies of CO_2 absorption. These values are then used to solve the column. The accuracy and ease of use of this method is suitable for this modelling due to the small number of variables considered in this work and the exclusion of mercaptans, COS and CS_2. The more rigorous advanced modelling setting would be required to consider these components which uses rate-based calculations to calculate the column itself. A packed type of column was considered with a Pall ring type of random packing manufactured from metal (Afkhamipour, 2013).

The height of each stage was set to be equal considering the chosen height of packing in each model. The component efficiencies from the example case were left unchanged.

The column diameter was set manually to avoid flooding based on the packing dimension of 50mm. The packed height was then adjusted in order to reach the target CO_2 removal.

The heat model was left inactive as per the standard model set up to simplify the column environment. The remaining inputs were kept as per the example case.

An estimate for each component on each stage in the absorber column was derived by the model. The values were plotted graphically up the height of the absorber column in Figure 3.2 below. Components with estimated fractions below $1x10^{-5}$ are excluded for clarity.

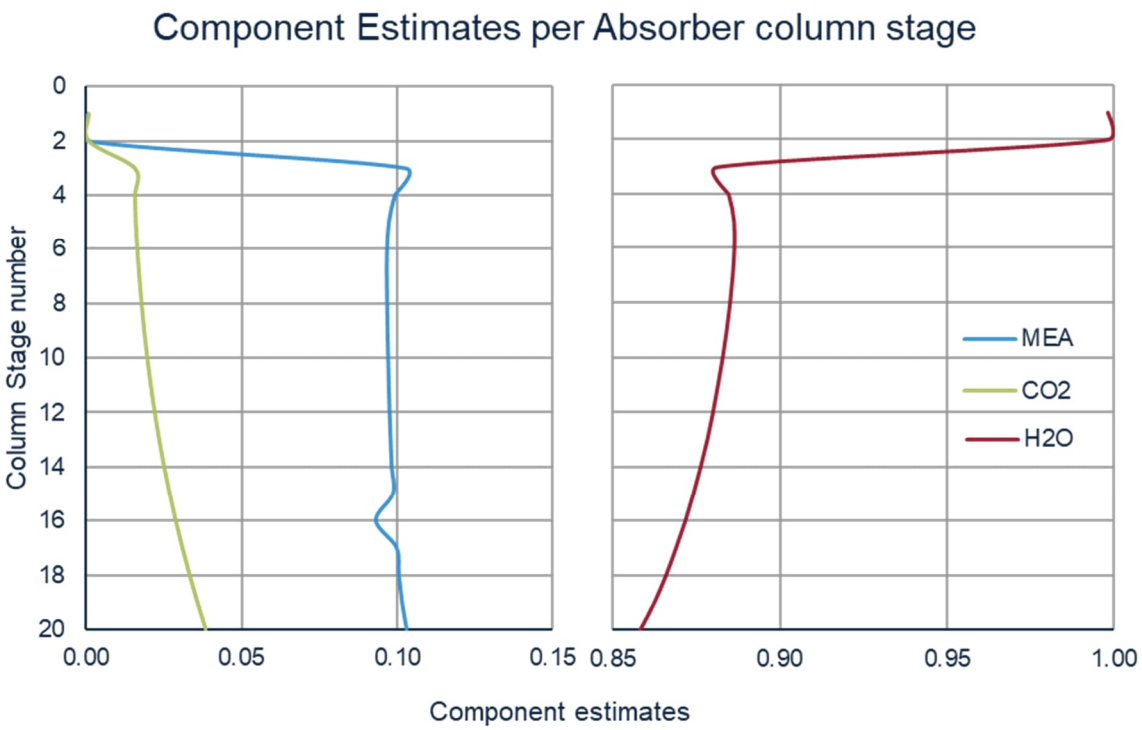

Figure 3.2: Graphical representation of Absorber Column Estimates per stage

Efficiency values are also given for CO_2 removal at every stage within the absorber column. These are shown graphically in height order in Figure 3.3.

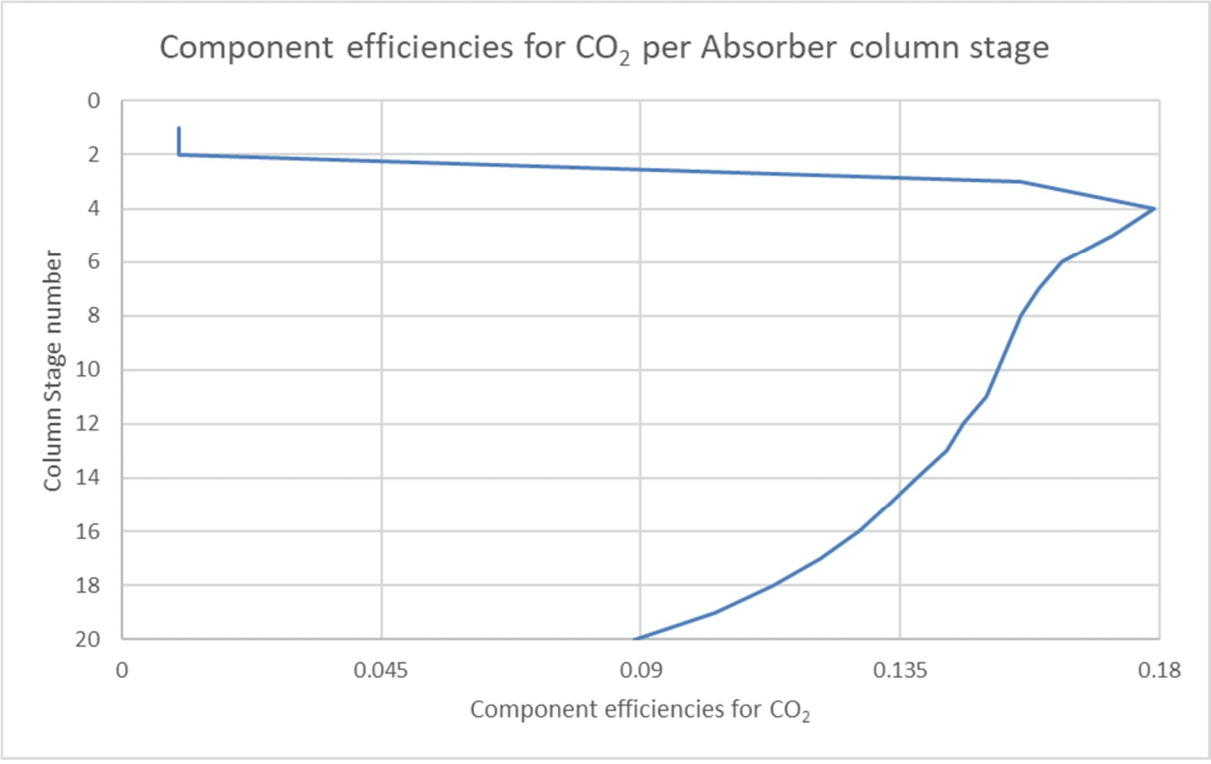

Figure 3.3: Graph of Absorber Column Efficiencies per stage

The trend of component efficiencies in Figure 3.3 shows the column position where CO_2 is actively removed in stages 3-20 and the wash section in stages 1 & 2. The component efficiencies for CO_2 are markedly less in the wash section than the remaining stages as no significant CO_2 removal takes place in the wash section.

The flow model was based on validated mass transfer coefficients between gas and liquid phases in packed columns from established methods (Onda, 1968). Factors for interfacial area, heat transfer, liquid and vapour mass transfer coefficients are all left at the default values of 1. These values are used to allow the model to be "tuned" to accurately reflect true operating data. As no real operating data is available for chemical absorption from blast furnace gas, these values were retained as per their default settings. The software process all the equations governing gas and liquid flows at each stage within the column. Including the rate based expressions to account for the chemical reactions at each stage too can lead to convergence problems. To avoid this, a set of default convergence criteria and calculation parameters are set within the model (Øi, 2007). These include flow model factors for the top and bottom of the column, set to 0.5, and a transition factor, set to 0.2 which were maintained at their default values. No mixed flow was considered on the feed stages.

The software attempts to solve the multitude of mass and heat balances for a maximum of 10,000 times. This figure was the standard value within the example case and was retained to allow the model to reach a solution considering different gas inlet conditions and amine types. The software will reach a solution if the remaining error in the equilibrium calculations is below 1.0×10^{-5} and the remaining error in the heat balance calculations are below 5.0×10^{-4}.

These are the default values for HYSYS which are already considered to be very small (Aspentech, 2005). Furthermore, relaxing these tolerances is not advised due to any time savings being limited and the risk of additional difficulty in solving the recycle blocks within the flowsheet.

HYSYS cannot use the equation of state or activity model in the supercritical range, so an alternate method must be used. The default method was selected which allows HYSYS to calculate vapour pressures (K values) for the components based on the vapour pressure model being used. Using this method, the K-values which are calculated are ideal K-values.

A general-purpose solving method was used to solve the column equations as it provides a good level of accuracy for most problems (Aspentech, 2005). Within the software there is the option to employ an acceleration program to decrease convergence time of K values and enthalpy parameters. By default, this option is not selected and should only be used if the equilibrium error decreases slowly during model conversion. The modelling carried out resulted in fast convergence of the equilibrium models but a slower conversion of the heat and specification errors, therefore the acceleration option was left deselected. To decrease the convergence time of the heat and specification errors, a damping factor was applied in an adaptive manner with a period of 10 seconds. This damping factor controls the step size between iterations and was set to adaptive to allow HYSYS to automatically update this value. For this reason, the initial damping factor varies between the cases.

3.2.6 Regenerator Column

The regenerator column unit was again left mostly as per the example case. The packing was changed from tray to packed type and the operating pressure was increased to 2 bar to match literature (Johnsen, 2018). As with the absorber column, the number of stages was maintained at 20 from the example case being counted from the top down. The rich amine enters the column at stage 1 and leaves the column at the last stage. A pressure drop across the column was calculated based on the column diameter, column height and flowrates of gas and liquid. This pressure drop was used to determine the operating pressure at each stage. A reflux ratio of 2 was specified in the models which controls the relative amounts of liquid leaving the base of the regenerator column to the vapour sent back to the column to remove CO_2 from the rich solvent. This value is in line with available literature for reflux ratios (Sun, 2015). The gas temperature leaving the condenser of 40^{o}C was also specified to reach the necessary degrees of freedom in the model to allow it to converge to a solution. This temperature was chosen as it was deemed to be an achievable target which would limit the water content in the CO_2 stream leaving the condenser.

The pressure profile of the column was determined by the calculated pressure drop through the 20 stages. An efficiency type mode was used as it produces results comparable to the more intensive Advanced mode. The advanced mode is only recommended when contaminants other than H_2S and CO_2 (Dyment, 2015) are present in the feed gas due to the computational time required being significantly longer. A packed type column was considered with a Pall type of packing

manufactured from metal. The height of each stage was set to be equal considering the chosen height of packing in each model. The component efficiencies from the example case were left unchanged. The flow model was set to a mixed method which is reported to generate the most reliable results (Pouladi, 2016). The effect on the results of using these different models was investigated and found to be negligible.

Factors for interfacial area, heat transfer, liquid and vapour mass transfer coefficients are all left at the default values of 1. These values are used to allow the model to be "tuned" to accurately reflect true operating data. As no real operating data is available for chemical absorption from blast furnace gas, these values were retained as per their default settings. The software process all the equations governing gas and liquid flows at each stage within the column. Including the rate based expressions to account for the chemical reactions at each stage too can lead to convergence problems. To avoid this, a set of default convergence criteria and calculation parameters are set within the model (Øi, 2007). These include flow model factors for the top and bottom of the column, set to 0.5, and a transition factor, set to 0.2 which were maintained at their default values. No mixed flow was considered on the feed stages. This is true if the rich amine is supplied to the regenerator at sufficient pressure to avoid it becoming a two phase (liquid and vapour) system. To ensure this, the rich amine pump pressure was adjusted between the cases to maintain a single phase at the feed stage of the regenerator column.

The column diameter was set manually to avoid flooding based on a packing dimension of 38mm. The packed height was then adjusted in order to reach the target CO_2 removal.

The heat model was set to none to simplify the column environment. The remaining inputs were kept as per the example case.

An estimate for each component on each stage in the regenerator column was derived by the model. The values were plotted graphically up the height of the absorber column in Figure 3.4 below. Components with estimated fractions below $1x10^{-5}$ are excluded for clarity.

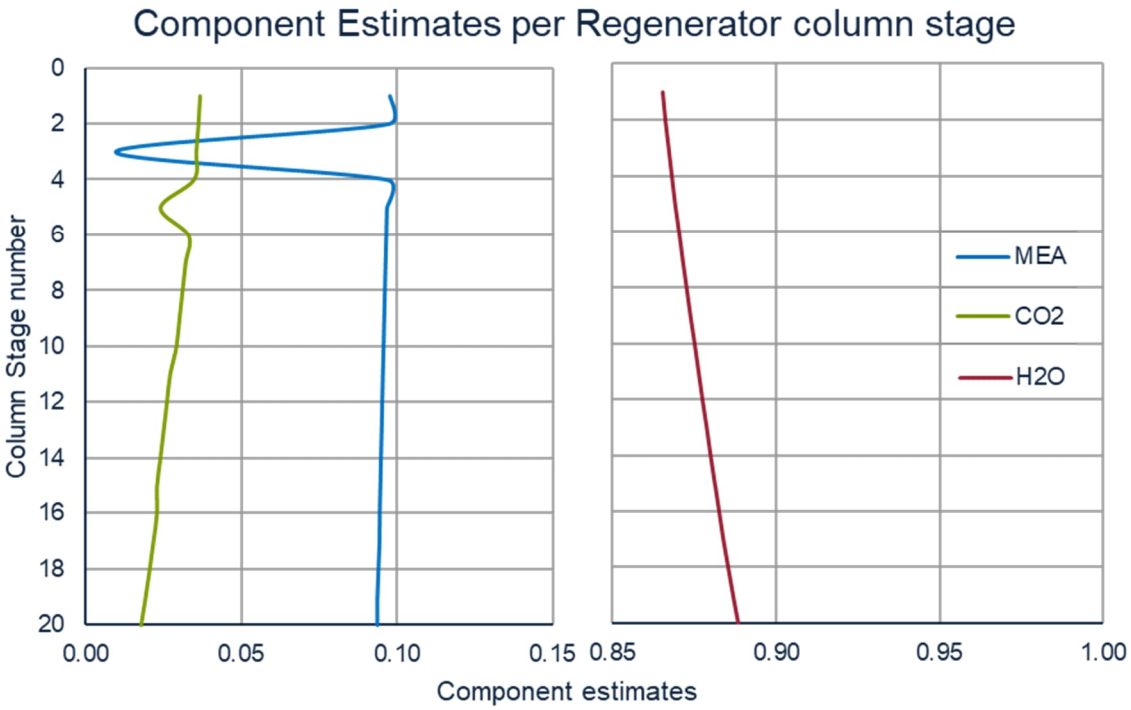

Figure 3.4: List of Regenerator Column Estimates per stage

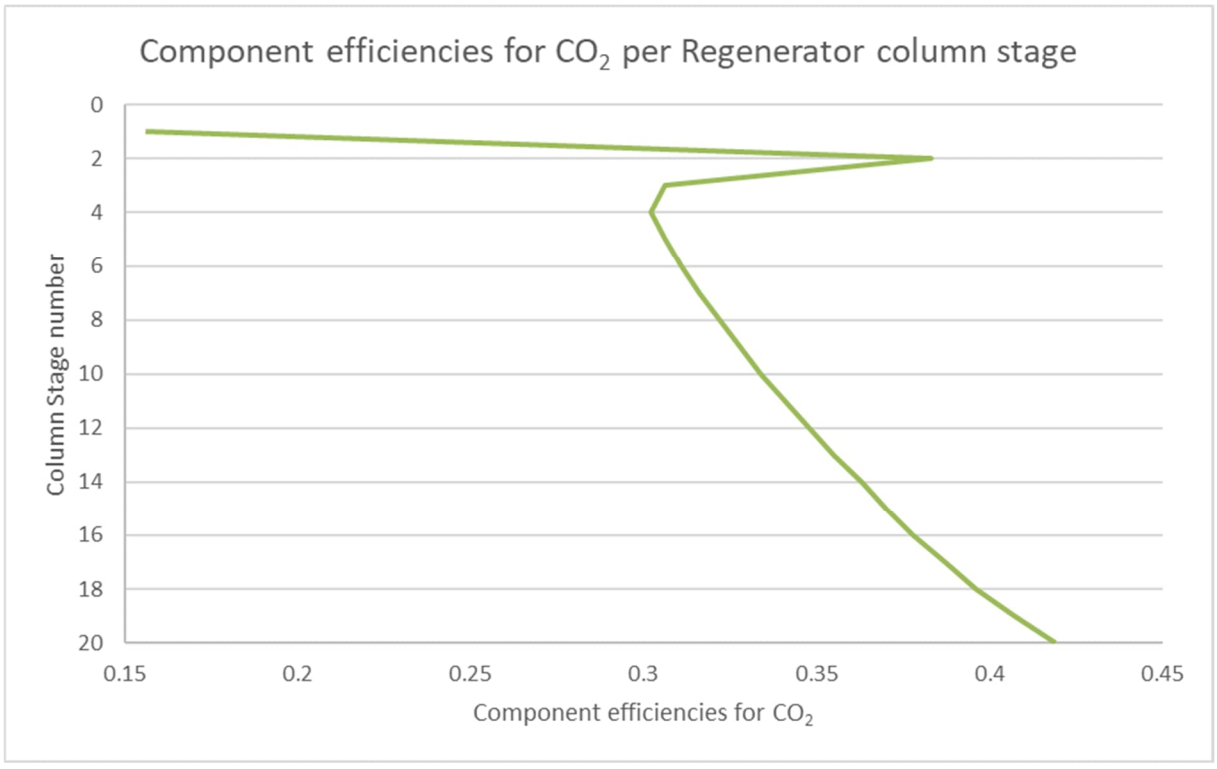

Figure 3.5: Graph of Regenerator Column Efficiencies per stage

Efficiency values are also given for CO_2 removal at every stage within the regenerator column. These are shown graphically in Figure 3.5 with values for the condenser at the top of the column and reboiler at the bottom set to 1 and excluded

from the graph. The results show that there is a general increase in CO_2 efficiency ascending the column until the entry stage for the rich amine.

3.2.7 Other Flowsheet Blocks

The lean amine pump was located between two streams to specify a pump differential pressure of 1.85 bar. This pressure is an estimate to pump the lean amine approximately 10 m to the top of the absorber column while still providing a greater pressure than in the gas phase. This enabled the electrical energy required by the pump to be calculated and a rough equipment size to be generated. The true differential pressure will depend on the height of the regenerator column and the distance between the absorber and regenerator column. For this study, the differential pressure was kept constant regardless of regenerator column height.

The lean/rich heat exchanger model was based on providing a specified temperature rich amine to the top of the regenerator column. The specified value varies based on the amine used as some chemicals are more prone to thermal degradation than others. For simplicity, it was assumed that the pressure drops of both lean and rich amine through the heat exchanger system would be zero.

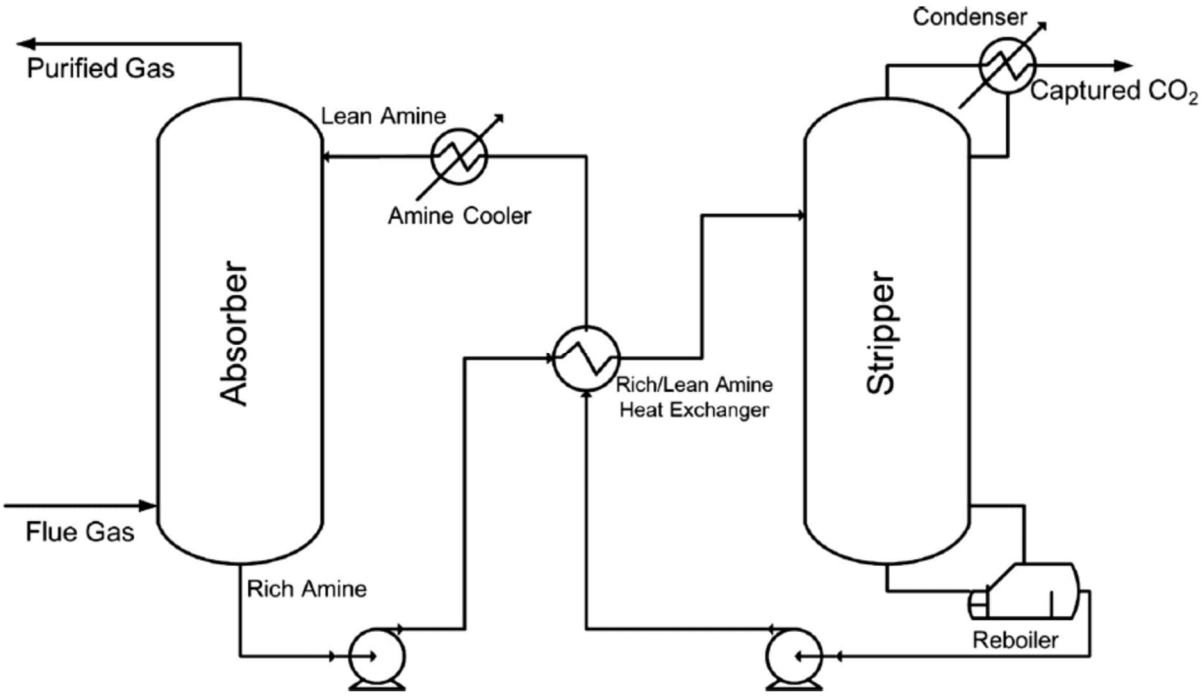

Figure 3.6: Basic Flowsheet of Chemical Absorption showing key equipment (Oh, 2016)

The amine concentration and total flowrate was controlled by a make-up block which added water and amine to the system to maintain flows and concentration. A drain for water is also included as a part of this block to prevent an increase in water content of the recirculated liquids. These variables are specific to each model depending on the amine type used.

A heat exchanger was used to control the lean amine temperature before it entered the top of the absorber column as shown in Figure 3.6. By specifying a temperature in the exit stream, the cooler determined the necessary energy removal to reach the target liquid temperature. For all models, this temperature was set to 40°C to balance the heat exchanger duty against the CO_2 removal efficiency in the absorber column.

A second make-up block was also present in the wash water system. This maintained a specified flow of water and prevented a build-up of solvent in the wash water circuit by blowing down contaminated water from the system. The total flowrate was adjusted for the different cases to control the gas temperature leaving the absorber column. For all cases the amine concentration was set at 0.25 mass% to allow the wash water to remove amine from the gas stream.

3.2.8 Model Validation

A basic sensitivity analysis was carried out considering two absorber column gas pressures, temperatures and flowrates. All other specified values were kept the same with only the parameter of interest being varied between the cases.

The pressure of the gas entering the absorber column was considered as 1.03 and 3.5 bar. This represents operation at a location significantly removed from the Blast Furnace or very local to the Blast Furnace with the minimum of gas pressure loss during the upstream cleaning process. No change in regenerator operating pressure was considered.

Sour Gas Pressure	bar absolute	1.03	3.5
Lean Solvent Loading	mol_{CO2} / mol_{amine}	0.2821	0.291
Rich Solvent Loading	mol_{CO2} / mol_{amine}	0.4599	0.4912
CO_2 Captured	%	88.6%	~100%
Specific Energy Consumption	GJ/t_{CO2}	4.37	3.89

Table 3.4: Comparison of low and high pressure sour gas results

Table 3.4 shows that a higher gas pressure increases the amount of CO_2 captured. It is expected that this was due to the greater partial pressure of CO_2 within the absorber column, allowing a greater saturation of the amine by CO_2. This is evident in the increase in rich amine solvent loading. In both cases the regenerator column had the same operating pressure and therefore a similar regeneration rate. The energy consumption for both cases was the same which leads to a higher specific energy requirement for the lower pressure case due to less CO_2 being removed in this scenario.

Gas temperatures of 25°C and 80°C were considered. This covers the range of temperatures at which blast furnace gas is likely to enter the absorber column. The lower range represents an upstream wet cleaning process and ambient temperatures typical for the UK climate. The upper range represents either the less common dry gas cleaning process or a temporary loss of water to a wet cleaning process.

Sour Gas Temperature	°C	25	80
Lean Solvent Loading	mol_{CO2} / mol_{amine}	0.2834	0.2825
Rich Solvent Loading	mol_{CO2} / mol_{amine}	0.4703	0.4657
CO_2 Captured	%	93.2%	91.3%
Specific Energy Consumption	GJ/t_{CO2}	4.15	4.25

Table 3.5: Comparison of low and high temperature sour gas results

Table 3.5 shows that an increasing gas temperature decreases the amount of CO_2 captured by the solvent. This was expected, as the chemical reaction between CO_2 and the amine is exothermic and therefore the equilibrium was shifted away from the complete reaction of CO_2 with the amine. This is shown in the lower loading of the rich solvent in the higher temperature case. As the reboiler energy was kept the same for both cases, the specific energy requirement was lower for the cooler gas temperature case due to a great amount of CO_2 being removed from the blast furnace gas.

Depending on the consumption of gas by other users and the amount of gas produced by the furnace, the flow available at the absorber column will vary. Unlike composition and pressure, gas flow from the blast furnace is not often measured.

Instead it is usually calculated based on process models. This leads to a greater difficulty in assigning a range of flows which the capture plant may experience.
An ideal gas flow turn-down of 5:1 was considered to account for different operating cases at the blast furnace and a reduction of production levels. Below this flow, it would make sense that the absorber column would be bypassed.

Sour Gas Flow	kg/s	22.04	110.2
Lean Solvent Loading	mol_{CO2} / mol_{amine}	0.2035	0.2834
Rich Solvent Loading	mol_{CO2} / mol_{amine}	0.2442	0.4681
CO_2 Captured	%	99.9%	92.1%
Specific Energy Consumption	GJ/t_{CO2}	4.05	4.21

Table 3.6: Comparison of low and high sour gas flow results

Table 3.6 above shows that as the flow of blast furnace gas decreases, the rate of CO_2 capture increases. This is due to the ratio of gas to liquid decreasing which results in a lower rich solvent loading. The reboiler energy for both cases were the same but due to the increased amount of CO_2 captured in the lower flow case, the specific energy consumption is lower. The energy consumption could be lowered further to reduce the CO_2 capture rate from 99.9 to 90% of that in the blast furnace gas. This assessment did not consider the effect of allowable pressure drop on the column internal packing which will limit the range of allowable flows through a given column design. If such a large range of flows are typical then it may become more feasible to install multiple absorption columns in parallel.

3.3 Purity of CO_2 captured

As blast furnace gas contains sizable amounts of CO and H_2 alongside CO_2, scenarios to estimate the capture rate of these components were prepared within Aspen HYSYS®. Simplified gas cases were established to determine the capture rate of these compounds from the blast furnace gas by removing the CO_2 component of the gas stream.
In section 5.2.3 of Chapter 5 it will be assumed that no CO or H_2 would be removed from the blast furnace gas stream in the absorption column. To test this a standard 30% by weight MEA case was taken as a basis and the inlet gas composition was changed to represent a stream of either CO or H_2 saturated with water.

The results suggest that around 0.075% of the incoming CO and H_2 was removed from the gas stream by the liquid phase. This is likely to be through the dissolving of the gas phase into the liquid solvent and will be far lower when the CO and H_2 are diluted with N_2 and CO_2 in the blast furnace gas mixture.

A further case using blast furnace gas as the inlet gas composition was run to confirm this. The resulting H_2 and CO content in the separated CO_2 stream leaving the regenerator column was estimated as 55ppm and 227ppm respectively on a dry basis. Although no limit is stated on H_2 content for either geological storage or enhanced oil recovery (EOR), CO quantity should be controlled to below 2000ppm (Visser, 2010). The modelling to date therefore provides confidence that negligible amounts of CO & H_2 are removed from the blast furnace gas stream. The captured CO_2 stream will still be suitable for storage or EOR applications. This is despite the higher CO and H_2 content in the blast furnace gas stream than most power plant flue gasses.

3.4 Model Development

The initial assessment assumed a fixed regeneration energy per tonne of CO_2 captured. Originally, Aspen HYSYS® models were set up based on a given reboiler heat input and a fixed reflux ratio. This resulted in the acid gas leaving the regenerator column being below 0°C which is colder than would be expected. To prevent this, the specification of the regenerator column was changed to calculate the required reboiler duty. To maintain the required degrees of freedom within the model the regenerator column exit gas temperature was specified as 40°C. The regenerator column pressure was also increased from 1.1 bar absolute to 2 bar absolute which is similar to that reported within literature (Johnsen, 2018). The pressure drop through the column was calculated by the model based on the column dimensions, gas and liquid flowrates. For simplicity, the wash section at the top of the absorber column was also removed to determine the effect on sweet gas temperatures leaving this column. This led to the following comparison in Table 3.7:

Parameter	Units	Original	Modified
Sour Gas Flow	kmol/h	13120	13120
Solvent Flowrate	m^3/h	3000	2500
Lean Solvent CO_2 Loading	mass/mass	0.3331	0.1509
Rich Solvent CO_2 Loading	mass/mass	0.4473	0.3725
Sweet Gas Flow	Kgmol/h	10390	11027
Sweet Gas Temperature	°C	38.98	55.33
Sweet Gas Pressure	Bar abs	1.066	1.075
Sweet Gas CO_2 content	mol%	3.91	2.75
Sweet Gas Solvent content	mol%	0.01	0.01
Acid Gas Flow	Kgmol/h	3250	2755
Acid Gas Pressure	Bar abs	1.1	1.975
Acid Gas Temperature	°C	63.51	39.99
Acid Gas CO_2 content	mol%	78.51	96.18
Reboiler Heat Addition	MW	140	178.6
Condenser Duty	MW	67.7	71.95
Solvent Cooler Duty	MW	67.4	97.93
Solvent Make-Up Rate	m^3/h	0.00	0.08
Absorber packing Height	m	20	7.8
Absorber column Diameter	m	8.6	9
Regenerator packing Height	m	20	9.5
Regenerator column Diameter	m	8.2	8

Table 3.7: Comparison of initial and modified simulations with 30%wt MEA

Table 3.7 above shows that by allowing the model to calculate reboiler duty, the energy requirement increases to that more in line with reported literature figures (Moser, 2020). The modified model also predicts lean and rich amine loadings comparable with figures available in literature (Haribu, 2014). The original values were deemed excessively high. The sweet gas temperature increases due to the lack of a wash section at the top of the absorber column, which accounts for the increase in make-up rate of the solvent. The lower acid gas temperature means the gas leaving the regenerator column has a lower moisture content and leads to a corresponding increase in CO_2 percentage. The increase in reboiler energy requirement leads to the cooling duty of both condenser and solvent cooler increasing in order to maintain a thermal balance in the system. Finally, the absorber

and regenerator column heights are dramatically smaller in the modified models which represents both a reduction in pressure drop through the columns and a reduced capital expenditure.

3.5 Aspen Process Economic Analysis (APEA)

Once the flowsheets had been finalized for several different amine types and concentrations, the rough capital cost of the equipment was calculated using APEA V11. The equipment shown on the Aspen HYSYS® flowsheet was imported into APEA as a list of equipment, except for the make-up blocks for the amine and water wash system.

A construction project was generated for each amine case based on the following parameters in Table 3.8. Each item of equipment was then sized to determine an approximate installed (direct) cost. These costs were used for comparison of the different cases as they include site manpower for installation as well as the cost to supply the equipment to the worksite.

The largest driver to adopt carbon capture equipment is seen within the EU. For this reason, the project location is specified as within the EU and all costs are quoted in euros. Although no full-scale carbon capture facility is in operation to treat blast furnace gas, the capital costs consider the process to be proven and of only a standard complexity. This is due to the operation of several small scale carbon capture facilities for the steel industry and large scale examples operating within the power generation industry.

In order to match the operation of blast furnaces within a steelworks, 8000 operating hours per year are specified for the carbon capture plant, with 24 hour per day operation foreseen.

An economic life of ten years is chosen as this timeframe should allow the adoption of alternative steelmaking processes and amine blends which may supersede designs currently under consideration. This economic life is shorter than the average blast furnace campaign life of 15 years between repairs and therefore represents steelmakers installing carbon capture equipment part way through a, potentially final, blast furnace campaign.

Parameter	Value
Units of measure	Metric
Project Country Base	EU
Project Currency Name	EUR
Process Description	Proven Process
Process Complexity	Typical
Project Type	Clear (Green) field
Contingency Percent	18%
Soil condition	Soft Clay
Pressure Vessel Design Code	ASME
Vessel Diameter Specification	ID
P&I Design Level	Full
Tax rate	40%
Interest Rate	20%
Economic life of project	10 years
Project Capital Escalation	5%
Working capital percentage	5%
Facility Type	Chemical Processing Facility
Operating mode	Continuous Processing – 24 hours/day
Length of start-up period	20 weeks
Operating hours per year	8000
Process Fluids	Liquids and Gasses
Pricing Basis	1st Quarter 2018

Table 3.8: List of parameters required for generating capital costs

All prices generated by APEA are based on a database of costs from the first quarter of 2018. Since this time both raw material and manufacturing costs will have trended upwards driven by the aftereffects of COVID19 and ever-increasing energy prices. For this reason, the costs quoted within Section 6.4 will be considered on a comparative basis rather than as absolute values.

3.6 Conclusions

A combination of Aspen software was used to define the operating requirements for a chemical absorption type carbon capture plant to treat blast furnace gas. The

packages were used to assess the use of different amines and concentrations on the approximate capital cost of such a plant. The simulation package was validated as part of its deployment by the developer and again in this work. The modelling of carbon capture from blast furnace gas was not validated against real operating data. This is due to the lack of available data of sufficient detail to carry out this analysis. The same is true for the economic analysis where a reference database of costs from 2018 was used. More recent pricing has not been sought to validate the costs generated by the software as it is intended to provide a comparison of costs rather than true costs for each amine or blend of amines considered.

Chapter 4. Routes to Steel

The multiple process routes to the production of one tonne of crude steel were briefly explained within Chapter 2. Each of these routes will generate a unique level of CO_2 emissions. The simplest solution for the steelmaking industry is to adopt a manufacturing route which meets the EU's aspirational target of reducing CO_2 emissions by 80% (Hummel, 2014). This would require a reduction from a current average of 1.83 tonnes of CO_2 per tonne of crude steel (Gielen, 2020) to 0.37 tonnes of CO_2 per tonne of crude steel. Only limited change in current manufacturing routes are likely globally between now and 2050. It is not the intention of this chapter to discuss financial incentives and penalties for maintaining current production routes. Only to assess what the split of technologies responsible for global steelmaking may look like by 2050 and the average CO_2 emissions for these options.

4.1 Chapter Introduction

Many researchers have developed models or investigated operating data to derive CO_2 production intensities for primary and secondary steelmaking routes (Pardo 2012, Hasanbeigi 2014, Arens 2016, Zhang 2018 amongst others). Depending on the boundary conditions used though, the results of these studies vary widely.

This chapter uses reported data to determine the CO_2 intensity of producing one tonne of liquid steel. This liquid steel must be solidified before it can be exported. For the purposes of this study the casting and rolling processes are excluded as there will be little impact from altering the upstream process routes. Intermediate cast products such as steel slab or billets are traded internationally. This allows the final rolling and forming into steel products to happen at a separate location to the crude steel production. In fact, it is reasonable to expect this geographical separation of crude steel production and final product forming as areas such as Europe look to reduce greenhouse gas emissions. This will not necessarily lead to a reduction in global average CO_2 intensities per tonne of crude steel. This is due to crude steel producing facilities outside of the EU not always requiring a focus on low CO_2 intensity.

Not all steel is produced via the same method. Different production routes have been considered in order to monitor the perceived CO_2 intensity of steelmaking across a wide variety of scenarios. Whilst the blast furnace – basic oxygen furnace (BF-BOF) route and direct reduction – electric arc furnace (DRI-EAF) route have been widely

researched, a cross over option of blast furnace – electric arc furnace (BF-EAF) may represent a “stepping stone” between current carbon-based production routes and future electric based routes.

Alternative commercial technology for producing iron such as the corex process will not be considered. This technology could feed both BOF and EAF processing routes but does not represent a significant change in emissions from the blast furnace fed BOF route.

New technology based on the yet to be commercialised top gas recycling blast furnace (TGR-BF), will be considered as an alternative to the blast furnace. For the purposes of this assessment, it will be assumed that this technology uses coal instead of coke and generates half the CO_2 emissions of a traditional blast furnace. This results in the removal of emissions from the coke oven stage in addition to the reduction in CO_2 generated during the ironmaking step.

It should be noted that there are also a wide range of technologies either at pilot phase or lab scale which may offer zero or near zero emission routes to producing steel. These technologies, such as HIsarna (Zeilstra, 2014) and Electrowinning (Quader, 2016) are at best 10 years away from full scale facilities and hence have been excluded from this review. This is due to adoption of any significant percentage of global steelmaking being likely to occur after the 2050 timeframe of this study.

Finally, it is unlikely that the global steel production will adopt one common route of steel production. This is due to limits on the amount of scrap which can be recycled, and raw materials of the necessary quality for DRI production. Blast furnaces are still being built most notably in India and it is unlikely that these new production facilities will be decommissioned by 2050. This means that the future is likely to balance multiple different steel production routes, each with their individual level of CO_2 emissions. By looking at an average level of CO_2 emissions, the effect of production shifts and adoption of new technologies or carbon capture and storage can be analysed. This allows the average emission intensity to be compared to the recorded value for 2020 to determine improvement on a global scale.

4.2 Methodology

4.2.1 Scope of Analysis

The scope for this analysis excludes mining of raw materials and transportation to the steelworks. It incorporates the raw material preparation including the coke ovens, sinter plant and pellet plant, ironmaking including blast furnace (BF) and DRI plant

and steelmaking including basic oxygen furnace (BOF) and electric arc furnace (EAF). The air separation unit (ASU) is also included although this stage only requires electricity for the gas compression and chilling required to separate oxygen from air. The electrical energy consumption for each process stage is summated as this electricity will be generated at least in part by combustion of a fossil fuel. Due to this consideration, no emissions from the on-site power plant will be derived. General electrical consumption of the site, such as for lighting, office buildings and communication are excluded from this analysis as it is expected that these will be constant across the routes considered. Direct and Indirect emissions from the transport of raw or intermediate products around the steelworks are also excluded, although it is noted that a reduced number of process steps is likely to require less transportation of material. Emissions arising from the conversion of limestone into lime are excluded from this study as it is assumed that this activity will be carried out on a separate site with the lime being transported to the steelworks. The study assumes that all materials are produced on site, with the only raw materials being coal, iron ores, lime, scrap and natural gas.

The combinations of process steps to form a production route are shown below in Table 4.1:

	Coke Production	Sinter Production	Pellet Production	Ironmaking	Steelmaking
BF-BOF	X	X	X	BF	BOF
BF-EAF	X	X	X	BF	EAF
DRI-EAF			X	DRI	EAF
DRI-BF-BOF	X	X	X	DRI & BF	BOF
EAF					EAF
NEW TECH			X	New Tech	BOF

Table 4.1: Table of process steps to reach crude steel

For each of the routes above, the total emission of CO_2 to the atmosphere was determined per tonne of liquid steel produced at the basic oxygen furnace or electric arc furnace. These values will be compared to determine the lowest possible emission level with this being compared to legally binding targets for CO_2 reduction. As full adoption of any one route to the manufacture of steel is unlikely, the ratio of production routes will then be considered to determine the average CO_2 emission per

tonne of crude steel. This will then be compared to the current average CO_2 emissions to determine scale of improvement. Eleven different scenarios have been considered and each are explained in the following sections. For details of the calculation methodology, please refer to the Appendix where a worked example is given.

4.2.2 BF-BOF Route

Firstly, a typical baseline operation for the BF-BOF steelmaking route was assessed by combining the individual process steps highlighted in Figure 4.1 together to produce one tonne of crude (liquid) steel at the BOF plant.

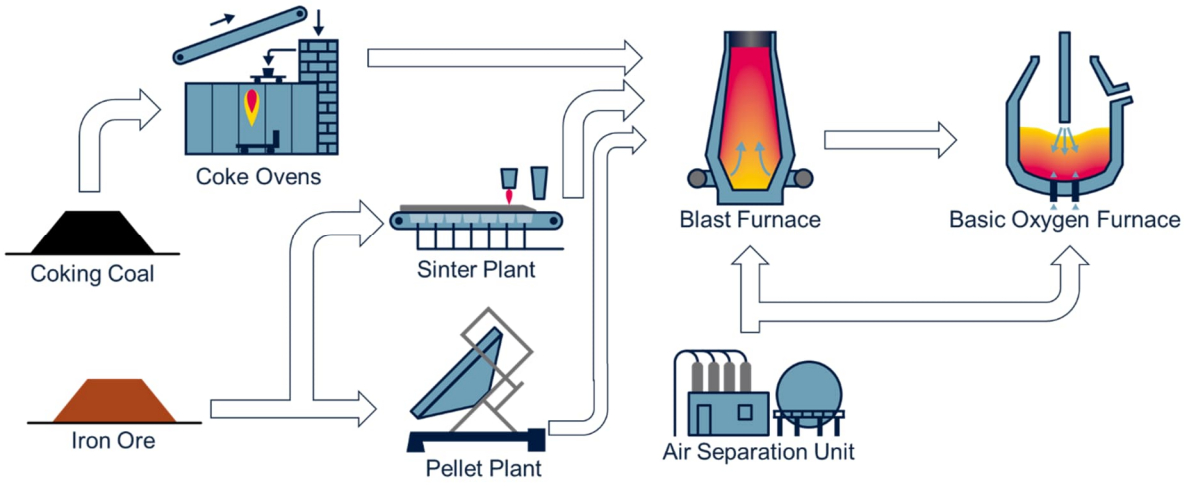

Figure 4.1: Flowsheet of processes in the BF-BOF steelmaking route (after Primetals)

For comparison, a further case is evaluated, to indicate the use of best available techniques as highlighted within literature (Sundqvist, 2018 & Carpenter, 2012). From the possible options the following were selected:

- For the coke ovens, coke dry quenching was chosen as the best available technique to recover energy for electricity generation. This results in the coke ovens becoming an electrical energy exporter and a slight drop in CO_2 emissions per tonne of coke produced of 81kg.
- For the sinter plant, waste heat recovery and selective flue gas recirculation were identified as the best available techniques. Electrical energy reduction is limited due to the extra recirculation fans, but CO_2 emissions are lowered by 38kg per tonne of sinter.

- For the pellet plant, no best available techniques are identified within literature and hence this step remains unchanged.
- For the blast furnace, a gas expansion turbine (also referred to as a TRT) and slag heat recovery are determined to be the applicable best available techniques. Of these, the first is already widely adopted on blast furnaces with a top gas pressure above 1.5 bar g. The second technology has been under development for many years but there is no current commercial technology to fulfil this roll. The combination of these two technologies results in the electrical energy consumption being halved and a decrease in CO_2 emissions per tonne of hot metal produced of 45kg.
- For the basic oxygen furnace, improved control systems are the sole best available technique. This does not mitigate CO_2 emissions but does reduce the electrical energy requirement by around 10%.
- Finally, for the air separation unit, a more modern design of plant is assessed which reduces electrical energy requirement by around one third.

The breakdown of CO_2 emissions for each step is included below.

Case	Current BF-BOF	Best Available Techniques	Units
Coke Ovens	0.25	0.22	t_{CO2} / t_{steel}
Sinter Plant	0.10	0.06	t_{CO2} / t_{steel}
Pellet Plant	0.02	0.02	t_{CO2} / t_{steel}
Blast Furnace	1.28	1.16	t_{CO2} / t_{steel}
Basic Oxygen Furnace	0.09	0.09	t_{CO2} / t_{steel}
Electricity	0.17	0.04	t_{CO2} / t_{steel}
TOTAL	1.91	1.60	t_{CO2} / t_{steel}
Reduction from BFG	0.43	0.40	t_{CO2} / t_{steel}

Table 4.2: CO_2 emissions per tonne of crude steel for current BF-BOF operation and implementation of best available techniques

The results above in Table 4.2 are slightly higher than those reported in literature which might indicate some double counting of emissions. These are likely to be around the flaring of process gasses and additional emissions from electrical energy

consumption. Process gasses would be used to generate a large portion of electricity on the steelworks and therefore reduce the extra emissions from purchased electricity. Ignoring this consideration, we can see a reduction from 1.91 to 1.58 tonnes of CO_2 per tonne of crude steel (around 17.2%) is possible by applying the best available techniques to each process step. When introducing CO_2 capture from the blast furnace gas stream to remove 90% of the CO_2 the reduction could be increased to 38% if all the captured CO_2 is completely stored or utilised.

4.2.3 DRI-EAF routes

A commonly mentioned alternative to the smelting routes shown previously is the combination of direct reduction with scrap metal in an EAF as shown below in Figure 4.2. This has the greatest potential to move steelmaking away from its current reliance on carbon based fuels.

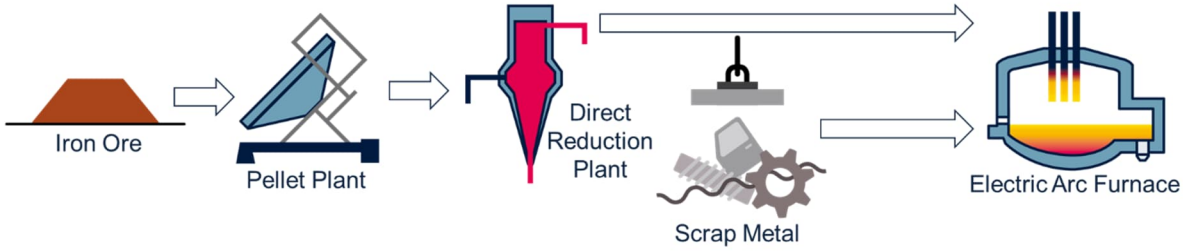

Figure 4.2: Flowsheet of Process steps for DRI-EAF steelmaking route (after Primetals)

The use of DRI also reduces the amount of scrap consumed and allows lower grades to be utilised. The DRI contains slag as well as iron which leads to a reduction in productivity at the EAF as it must also melt and then separate the slag. A single ratio of 9.5:1 DRI to scrap metal forms the basis of the emission intensity values given in Table 4.3. This is compared to the best available techniques which in this case consider a halved CO_2 intensity of the electrical energy compared to current global average figures. The DRI cases are based on using natural gas as a fuel instead of coal. Further improvement would be possible by converting to near or 100% hydrogen fuelled DRI plants. In this case, emissions from the DRI step are predicted to reduce by 90% as some CO_2 sources will always remain.

Case	Baseline DRI-EAF	Best Available Techniques	Units
Pellet Plant	0.09	0.09	t_{CO2} / t_{steel}
DRI	0.46	0.46	t_{CO2} / t_{steel}
EAF	0.07	0.07	t_{CO2} / t_{steel}
Electricity	0.34	0.17	t_{CO2} / t_{steel}
TOTAL	0.95	0.78	t_{CO2} / t_{steel}
Reduction from H_2 based DRI	0.41	0.41	t_{CO2} / t_{steel}

Table 4.3: Estimates of CO_2 emissions per tonne of crude steel for each process step in routes with DRI production

The information in Table 4.3 above shows that, there are relatively few steps from raw material to crude steel via this route. The only portion affected by applying best available techniques is the CO_2 from electrical energy, there is a relatively small difference of only 0.17 tonnes of CO_2 per tonne of crude steel (around 18% reduction) between the two cases. The right hand column of Table 4.3 represents a reduction of 51% compared to the emissions from the best available techniques applied to the BF-BOF route described in section 4.2.2. Further reductions could be achieved by converting from natural gas to hydrogen as the main fuel for the DRI plant. In this case, it is estimated that emissions would reduce by 90% for this step down to 0.05 tonnes of CO_2 per tonne of crude steel.

There is a limit on the current availability of DRI grade pellets which would need to increase by a factor of ten to support the DRI-EAF route becoming the sole source of steel production.

4.2.4 EAF Route

The largest reduction in CO_2 emissions from steel production would be achieved by converting to Electric Arc Furnaces as it shifts the energy requirement from carbon fuels to electricity. Two cases are reported in Table 4.4 with 100% scrap used as a raw material to produce crude steel. The second case includes best available techniques which in this case is the halving of current CO_2 emissions from electrical generation.

Case	Baseline EAF	Best Available Techniques	Units
Electric Arc Furnace	0.04	0.04	t_{CO2} / t_{steel}
Electricity	0.19	0.09	t_{CO2} / t_{steel}
TOTAL	0.23	0.14	t_{CO2} / t_{steel}

Table 4.4: Estimates of CO_2 emissions per tonne of crude steel for each process step in a EAF route

Table 4.4 above shows that this production route contains only one step and its associated electrical energy consumption. The emissions per tonne of crude steel are 1.48 tonnes of CO_2 lower from the EAF route than from the BF-BOF route described in section 4.2.2. By adopting best available techniques, CO_2 emissions are estimated to reduce by a further 0.09 tonnes of CO_2 per tonne of crude steel (around 39% reduction for the EAF processing route).

4.2.5 BF-DRI Route

A further alternative is to use DRI in a blast furnace which will then separate out the slag from the iron in the DRI material. This route has the disadvantage of introducing an additional processing step, but it is already employed at blast furnaces in the USA, Mexico and Austria. The benefit comes from both an increase in productivity and reduction of emissions from the blast furnace process.

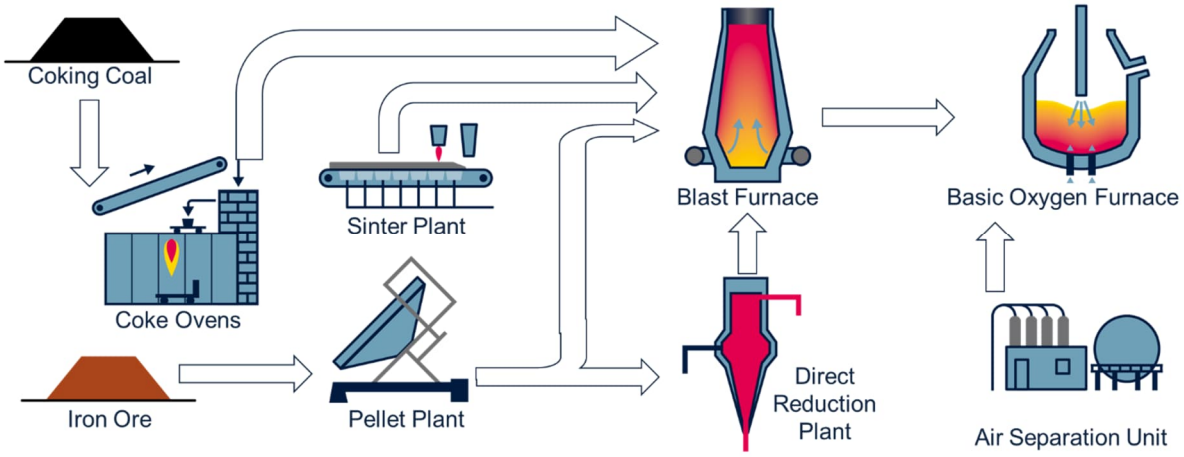

Figure 4.3: Process steps which form the DRI-BF-BOF steelmaking route (after Primetals)

Case	Baseline BF-DRI	Best Available Techniques	Units
Coke Ovens	0.25	0.19	t_{CO2} / t_{steel}
Sinter Plant	0.06	0.04	t_{CO2} / t_{steel}
Pellet Plant	0.04	0.04	t_{CO2} / t_{steel}
DRI Plant	0.07	0.07	t_{CO2} / t_{steel}
Blast Furnace	1.02	1.00	t_{CO2} / t_{steel}
BOF	0.09	0.09	t_{CO2} / t_{steel}
Electricity	0.13	0.04	t_{CO2} / t_{steel}
TOTAL	1.60	1.48	t_{CO2} / t_{steel}
Reduction from BFG & H_2 based DRI	0.44	0.33	t_{CO2} / t_{steel}

Table 4.5: Estimates of CO_2 emissions per tonne of crude steel for each process step in routes involving blast furnaces partially fed with DRI

Table 4.5 above compares the baseline BF-DRI case with the use of best available techniques. The results show that by adding in the extra process step of DRI production, overall CO_2 emissions can be reduced. This allows the increase in emissions from the DRI plant are outweighed by lower emissions from the blast furnace and coke ovens.

4.2.6 New Technology

There are several alternative processes to the blast furnace. For this study, new technology is considered as a combination of Top Gas Recycle Blast Furnace, where gases are recycled back to the process to reduce carbon consumption and HIsarna which can use coal instead of coke as a fuel. As this technology is already considered to be the best available, only the figure for emissions attributable to electricity varies between the two columns in Table 4.6. No additional line is included for the effect of carbon capture as it is expected that this will already be integrated into the new technology.

Case	New Tech-BOF	Best Available Techniques	Units
Pellet Plant	0.08	0.08	t_{CO2} / t_{steel}
New Technology	0.23	0.23	t_{CO2} / t_{steel}
Basic Oxygen Furnace	0.09	0.09	t_{CO2} / t_{steel}
Electricity	0.06	0.03	t_{CO2} / t_{steel}
TOTAL	0.47	0.44	t_{CO2} / t_{steel}

Table 4.6: Estimates of CO_2 emissions per tonne of crude steel for each process step involving new technology

Table 4.6 above shows that the presumed new technology has a large potential to reduce CO_2 emissions per tonne of steel. The predicted emissions intensity for this future production route almost matches that derived for the EAF steelmaking route. The reduced number of process steps from raw material to crude steel and a decrease in emissions from the step replacing the blast furnace enable this.

4.2.7 BF-EAF Route

A potential stepping-stone to reducing the CO_2 emissions from steel production may be to incorporate Electric Arc Furnaces into the existing steelmaking pathways.

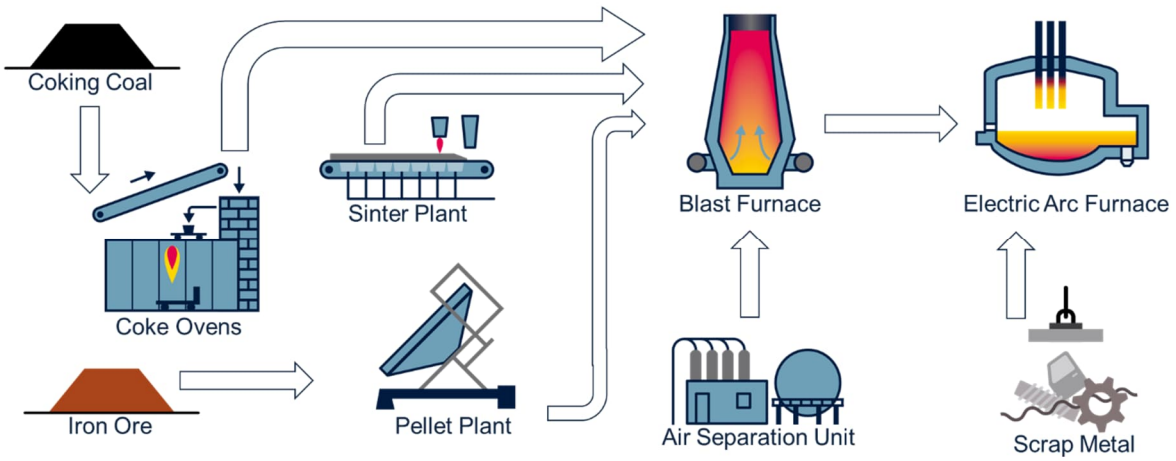

Figure 4.4: Process steps included in the BF-EAF steelmaking route (after Primetals)

Two cases are reported below in Table 4.7 with a hot metal to scrap ratio of 2.3:1 used as an input to the EAF. The second case applies best available techniques to all relevant steps. In addition, it considers low carbon electricity.

Case	Baseline BF-EAF	Best Available Techniques	Units
Coke Ovens	0.19	0.17	t_{CO2} / t_{steel}
Sinter Plant	0.08	0.05	t_{CO2} / t_{steel}
Pellet Plant	0.06	0.06	t_{CO2} / t_{steel}
Blast Furnace	0.86	0.84	t_{CO2} / t_{steel}
Electric Arc Furnace	0.04	0.04	t_{CO2} / t_{steel}
Electricity	0.13	0.04	t_{CO2} / t_{steel}
TOTAL	1.34	1.21	t_{CO2} / t_{steel}
Reduction from BFG	0.27	0.27	t_{CO2} / t_{steel}

Table 4.7: Estimates of CO_2 emissions per tonne of crude steel for each process step in a BF-EAF route

The results above show that, a reduction in emissions by 0.57 tonnes of CO_2 per tonne of steel produced is possible by adopting a BF-EAF route to replace the current BF-BOF route. Compared to using DRI, there will be less slag for the EAF plant to handle as the blast furnace provides a low level of impurities in the hot metal. Because of this, a greater level of scrap impurities could be processed than that with a pure scrap charged vessel. The electrical consumption per tonne of crude steel is approximately the same for the BF-BOF baseline case and the high scrap BF-EAF route. More of this electrical energy will need to be purchased though, as the available process gasses from the blast furnace and coke ovens will be reduced leading to a shortage of on site electricity generation.

4.3 Results

The routes described earlier within this chapter were combined and assigned a percentage of the predicted steel production in the year 2050. The best available techniques were considered for all routes as by this time, there should be a wide adoption of these into the various process steps both to reduce emissions and operating costs. Eleven potential scenarios for the production of steel by 2050 were considered, each with a base case and an additional case considering carbon capture from any remaining blast furnace facilities and hydrogen fuel for any operational direct reduction plants. The cases are described individually below.

4.3.1 Business as Usual (BAU)

The first scenario (BAU) considers the current production split of approximately 66% BF-BOF, 10% DRI-EAF and the remainder via scrap recycling. This is approximately the same as the current production split and therefore represents no increase in investment in alternatives to the predominant BF-BOF route. To represent continual improvement by steelmakers globally, best available techniques are assumed to have been applied to all operating units. The effect of applying these for each of the production routes can be seen in section 4.2. The case described above can be considered as a minimum investment option as expenditure is limited to upgrading existing facilities.

	Units	BF-BOF	DRI-EAF	EAF	TOTAL
Steel Produced	mt	1390	210	500	2100
Scrap used	mt	260	20	530	810
Total Emissions	mt	2190	160	70	2420
Emissions intensity	tCO_2 / t_{steel}	1.58	0.78	0.14	1.15
Emissions with CCS and H_2	mt	1630	80	70	1780
Emissions intensity	tCO_2 / t_{steel}	1.18	0.37	0.14	0.85

Table 4.8: Combination of processing routes in the Business as Usual case showing overall average CO_2 emission intensity

Table 4.8 shows the quantity of steel produced by each route and the total emissions of CO_2 in millions of tonnes. Emissions include those from electricity which are assumed to be halved from the current global average of 0.45kg/kWh. This can be achieved either by purchasing greener electricity or through carbon capture from the on-site power plant flue gasses. An additional emissions value is derived to indicate the effect of carbon capture from the blast furnace gas stream and conversion of DRI plants to use hydrogen. Both of these steps are designed to reduce the amount of CO_2 emitted into the atmosphere.

4.3.2 DRI-BF

The use of DRI in the blast furnace instead of a feedstock for an EAF would reduce the emissions from the blast furnace. Use of DRI in the blast furnace is assessed in scenario 2 (DRI-BF). It considers that the BF-BOF route would maintain its current 66% share of steelmaking production with an increase in DRI capacity to feed blast

furnaces with 184 kg/tHM of DRI. The basis for using this value is the current record for DRI consumption by a blast furnace recorded in North America (AIST, 2020). The scenario also considers that no investment to increase EAF capacity will be made between now and 2050. This would require an increase in DRI production and its pellet precursor above what is currently available. The case described above represents a continuation of measures announced by several steelmakers who intend to increase DRI capacity, with a number of steelmakers in North America and Europe already using DRI in their blast furnaces (AIST, 2020).

	Units	DRI-BF	DRI-EAF	EAF	TOTAL
Steel Produced	mt	1390	210	500	2100
Scrap used	mt	285	23	527	834
Total Emissions	mt	2053	164	70	2287
Emissions intensity	tCO_2 / t_{steel}	1.48	0.78	0.14	1.09
Emissions with CCS and H_2	mt	1520	78	70	1667
Emissions intensity	tCO_2 / t_{steel}	1.10	0.37	0.14	0.79

Table 4.9: Combination of processing routes in the DRI-BF case showing overall average CO_2 emission intensity

Table 4.9 shows the quantity of steel produced by each route and the total emissions of CO_2 which includes those from electrical energy production. The emissions from electricity production are again assumed to halve by 2050 from current levels due to a wider availability of low carbon electricity. A separate value is given for average emission intensity which indicates the effect of carbon capture from the blast furnace and use of hydrogen for DRI production.

4.3.3 Max DRI

A further scenario (Max DRI) considers that some production via BF-BOF routes will be substituted for production via the DRI-EAF route by 2050. This scenario is based on a tripling of the current market share for DRI-EAF to 30% while the scrap recycling production share remains the same as for the case described in section 4.3.1. DRI will be produced exclusively using natural gas with best practices adopted by all operating units. The Max DRI case represents a realistic increase in DRI capacity considering the availability of iron ore pellets of the appropriate quality required as a

feedstock and the difference in capacity between a large modern blast furnace and a DRI plant.

	Units	BF-BOF	DRI-EAF	EAF	TOTAL
Steel Produced	mt	966	630	504	2100
Scrap used	mt	184	69	527	780
Total Emissions	mt	1523	493	70	2085
Emissions intensity	tCO_2 / t_{steel}	1.58	0.78	0.14	0.99
Emissions with CCS and H_2	mt	1135	234	70	1439
Emissions intensity	tCO_2 / t_{steel}	1.18	0.37	0.14	0.69

Table 4.10: Combination of processing routes in the Max DRI case showing overall average CO_2 emission intensity

Table 4.10 shows the quantity of steel produced by each route and the total emissions of CO_2 which includes those from electrical energy production. Electrical energy emissions are assumed to be half the current global average to represent the increase in green energy availability and CCS adoption by the power generation industry. A separate value is given for average emission intensity which indicates the effect of carbon capture from the blast furnace and use of hydrogen for DRI production.

4.3.4 New Tech

A scenario considering the adoption of a new technology to replace the blast furnace was also considered (New Tech). The case is assumed to be indicative of a TGR-BF process rather than a completely zero emissions process. For the purposes of this assessment, the CO_2 emissions are considered as 20% of the traditional BF process (Meijer, 2013). This would be achieved by a combination of carbon capture and the removal of the coke and sinter plant emissions. The new technology will take time to become adopted globally, hence the scenario considers that only 20% of global steel production will switch from BF-BOF to the new technology (Allwood, 2021). No increase in capacity of DRI or EAF plants are considered which results in their share of global steel production remaining the same as described in section 4.3.1.

	Units	BF-BOF	New Tech	DRI-EAF	EAF	TOTAL
Steel Produced	mt	966	420	210	504	2100
Scrap used	mt	184	80	23	527	813
Total Emissions	mt	1523	183	164	70	2085
Emissions intensity	tCO_2 / t_{steel}	1.58	0.44	0.78	0.14	0.92
Emissions with CCS and H_2	mt	1135	176	78	70	1219
Emissions intensity	tCO_2 / t_{steel}	1.18	0.42	0.37	0.14	0.69

Table 4.11: Combination of processing routes in the New Tech case showing overall average CO_2 emission intensity

Table 4.11 shows the quantity of steel produced by each route and the total emissions of CO_2 which includes those from electrical energy production. Separate values are given for average emission intensity which indicates the effect of carbon capture from the blast furnace and use of hydrogen for DRI production.

4.3.5 BF-EAF

Instead of blast furnaces feeding BOF plants, this scenario considers EAFs fed with hot metal from blast furnaces. This route is based on the complete replacement of the BF-BOF route for steel production by a BF-EAF route. The DRI-EAF or scrap recycling capacities however are retained at present levels. By increasing the scrap consumption per tonne of crude steel, the blast furnace capacity will be reduced from 1250 to 1050 million tonnes. The corresponding increased consumption of scrap from 813 to 1002 million tonnes, is still below the maximum thought to be available by 2050. The BF-EAF case offers the potential as a stepping stone between current blast furnace based steel production and future scrap based production. For the purposes of this study an approximate ratio of 2.3:1 hot metal to scrap is used as the basis for determining the EAF emissions.

	Units	BF-EAF	DRI-EAF	EAF	TOTAL
Steel Produced	mt	1386	210	504	2100
Scrap used	mt	452	23	527	1002
Total Emissions	mt	1677	164	70	1911
Emissions intensity	tCO_2 / t_{steel}	1.21	0.78	0.14	0.91
Emissions with CCS and H_2	mt	1303	78	70	1451
Emissions intensity	tCO_2 / t_{steel}	0.94	0.37	0.14	0.69

Table 4.12: Combination of processing routes in the BF-EAF case showing overall average CO_2 emission intensity

Table 4.12 shows the quantity of steel produced by each route and the total emissions of CO_2 which includes those from electrical energy production. A separate value is given for average emission intensity which indicates the effect of carbon capture from the blast furnace and use of hydrogen for DRI production.

4.3.6 DRI + New Tech

Another scenario combining the basis for those given in section 4.3.3 and 4.3.4 was also assessed. In this case, EAF capacity is forecast to remain at 24% of global steel production. By comparison, the BF-BOF route is predicted to produce only 26% of global steel in 2050 as both new technology and DRI replace current capacity. This must result in a reduced average CO_2 intensity of global steelmaking as the most polluting route accounts for a smaller portion of steelmaking than it does currently.

	Units	BF-BOF	New Tech	DRI-EAF	EAF	TOTAL
Steel Produced	mt	546	420	630	504	2100
Scrap used	mt	104	80	69	527	780
Total Emissions	mt	860	185	493	70	1607
Emissions intensity	tCO_2 / t_{steel}	1.58	0.44	0.78	0.14	0.77
Emissions with CCS and H_2	mt	641	183	234	70	1128
Emissions intensity	tCO_2 / t_{steel}	1.17	0.44	0.37	0.14	0.54

Table 4.13: Combination of processing routes in the DRI + New case showing overall average CO_2 emission intensity

Table 4.13 shows the quantity of steel produced by each route and the total emissions of CO_2 which includes those from electrical energy production. A separate value is given for average emission intensity which indicates the effect of carbon capture from remaining blast furnaces and use of hydrogen for DRI production.

4.3.7 Max Scrap

Instead of maximising DRI capacity, this case (Max Scrap) considers maximising scrap consumption by increasing EAF capacity. Of all the cases considered maximisation of scrap utilisation is a widely touted option for decarbonising the steelmaking industry. Many researchers, however, fail to consider that there is a practical limit to the amount of scrap that will be available for recycling. This is estimated to be 1350 million tonnes based on figures reported in section 2.1.2 (Birat, 2010). To utilise this amount of scrap, the EAF capacity is forecast to increase to cater for 54% of global steel production. The DRI-EAF route is predicted to maintain its current 10% market share with BF-BOF capacity declining. It is important to note that the BF-BOF route also consumes a small amount of scrap and this is also considered within the 1350 million tonnes limit on scrap availability.

	Units	BF-BOF	DRI-EAF	EAF	TOTAL
Steel Produced	mt	758	210	1132	2100
Scrap used	mt	144	23	1183	1350
Total Emissions	mt	1195	164	157	1515
Emissions intensity	tCO_2 / t_{steel}	1.58	0.78	0.14	0.72
Emissions with CCS and H_2	mt	891	78	157	1125
Emissions intensity	tCO_2 / t_{steel}	1.17	0.37	0.14	0.54

Table 4.14: Combination of processing routes in the Max Scrap case showing overall average CO_2 emission intensity

Table 4.14 shows the quantity of steel produced by each route and the total emissions of CO_2 which includes those from electrical energy production. A separate value is reported which assesses the effect of hydrogen based DRI plants and carbon capture for the remaining blast furnace gas streams. As the market share of DRI-EAF remains unchanged and the BF capacity reduces, it is expected that this number will represent less of a change than in other scenarios. With a smaller

number of DRI and BF plants in operation, applying these changes to all of them would become more likely.

4.3.8 DRI-BF + Scrap

A further scenario combines the basis' given in sections 4.3.2 and 4.3.7. This determines the global average emission intensity from steelmaking when DRI is used to feed blast furnaces and the maximum amount of scrap recycled via the EAF route. It forecasts that DRI-EAF capacity remains at 10% of steel production and that EAF capacity replaces around 29% of production via the BF-BOF route. The remaining BF-BOF production is considered to include DRI as described in section 4.3.2. The increased use of DRI and scrap represents a likely scenario for steel production in 2050. DRI is already being developed for use in blast furnaces and EAF capacity is already planned to replace much of the BF-BOF production route in North America.

	Units	DRI-BF	DRI-EAF	EAF	TOTAL
Steel Produced	mt	772	210	1118	2100
Scrap used	mt	158	23	1168	1350
Total Emissions	mt	1152	164	155	1470
Emissions intensity	tCO_2 / t_{steel}	1.49	0.78	0.14	0.70
Emissions with CCS and H_2	mt	855	78	155	1087
Emissions intensity	tCO_2 / t_{steel}	1.11	0.37	0.14	0.52

Table 4.15: Combination of processing routes in the DRI-BF + Scrap case showing overall average CO_2 emission intensity

Table 4.15 shows the quantity of steel produced by each route and the total emissions of CO_2 which includes those from electrical energy production. As in previous scenarios, carbon capture and hydrogen fuels are considered with the resulting emissions intensity reported as a separate number.

4.3.9 Max scrap and DRI

A combination of scenarios described in sections 4.3.3 and 4.3.7 results in a further case in which market shares for both EAF and DRI-EAF routes increases to replace the BF-BOF route. But since there is a limit on scrap availability and a consideration that the DRI capacity can only treble by 2050, 14% of steel production will still be carried out via the BF-BOF route.

	Units	BF-BOF	DRI-EAF	EAF	TOTAL
Steel Produced	mt	299	630	1171	2100
Scrap used	mt	57	69	1224	1350
Total Emissions	mt	470	493	162	1125
Emissions intensity	tCO_2 / t_{steel}	1.57	0.78	0.14	0.54
Emissions with CCS and H_2	mt	350	234	162	746
Emissions intensity	tCO_2 / t_{steel}	1.17	0.37	0.14	0.36

Table 4.16: Combination of processing routes in the Max Scrap and DRI case showing overall average CO_2 emission intensity

Table 4.16 shows the quantity of steel produced by each route and the total emissions of CO_2 which includes those from electrical energy production. The capacity of blast furnaces reduces significantly which makes applying carbon capture to the remaining gas streams more likely but results in less of an impact on average emission intensity. By comparison, with the increase of DRI capacity conversion to use hydrogen as the main fuel source has a greater potential to reduce emissions. For this reason, the emissions which result from the combination of both these technology steps is reported as a separate number.

4.3.10 New Tech + Max scrap

By combining the scenarios described in sections 4.3.4 and 4.3.7, EAF capacity is increased and a new technology is adopted to partially replace the BF-BOF route. Due to the relatively short time remaining until 2050, it is presumed that new technology will only account for 20% of steel production globally. The level of adoption is based on the uptake of the BOF accounting for 10% of steel production after 8 years (Arens, 2014). The diffusion of this new technology over the 28 year period between 2022 and 2050 could be as high as 35%. However, it is important to realise that diffusion will be dependent on the remaining lifetime of the existing blast furnace facilities and the current lack of available technologies for adoption. For these reasons, a lower estimate of 20% uptake of new technology is considered in this work. Once again, this scenario considers that there will be no increase in DRI-EAF capacity from 2020.

	Units	BF-BOF	New Tech	DRI-EAF	EAF	TOTAL
Steel Produced	mt	338	420	210	1132	2100
Scrap used	mt	64	80	23	1183	1350
Total Emissions	mt	532	183	164	157	1036
Emissions intensity	tCO_2 / t_{steel}	1.57	0.44	0.78	0.14	0.49
Emissions with CCS and H_2	mt	397	183	78	157	814
Emissions intensity	tCO_2 / t_{steel}	1.17	0.44	0.37	0.14	0.39

Table 4.17: Combination of processing routes in the New + Max Scrap case showing overall average CO_2 emission intensity

Table 4.17 shows the quantity of steel produced by each route and the total emissions of CO_2 which includes those from electrical energy production. The combination of steelmaking routes proposed in this scenario would appear unlikely and require significant development and implementation of the new technology. Although technologies do exist with the potential to reduce CO_2 emissions, the scale up and commercial adoption of these technologies remains a challenge.

4.3.11 New Tech + Max scrap and DRI

A final scenario combines the considerations made in sections 4.3.4 and 4.3.9 and therefore adopts an increase in DRI-EAF and EAF production routes. Furthermore, the introduction of new technology means, this is the only scenario where no global steel will be produced via the BF-BOF route. While this case will undoubtedly attract the maximum investment cost for the steel industry, it should have the greatest potential to reduce CO_2 emissions per tonne of crude steel. Nevertheless, the scenario is viewed by the author as relatively unlikely as it would require the current predominate steelmaking route to be completely replaced by a combination of new and alternative technologies within a relatively short timeframe.

	Units	New Tech	DRI-EAF	EAF	TOTAL
Steel Produced	mt	299	630	1171	2100
Scrap used	mt	57	69	1224	1350
Total Emissions	mt	130	493	162	785
Emissions intensity	tCO_2 / t_{steel}	0.44	0.78	0.14	0.37
Emissions with CCS and H_2	mt	130	234	162	526
Emissions intensity	tCO_2 / t_{steel}	0.44	0.37	0.14	0.25

Table 4.18: Combination of processing routes in the New + Max Scrap and DRI case showing overall average CO_2 emission intensity

Table 4.18 shows the quantity of steel produced by each route and the total emissions of CO_2 which includes those from electrical energy production. As with previous scenarios, a discrete emissions intensity value is reported which considers hydrogen based DRI. As there are no operating blast furnaces within this scenario, there is no requirement for carbon capture from their gas stream. Carbon capture is predicted to be part of the standard flowsheet for the new technology and is therefore considered in the base emission intensity value.

4.4 Options for Steelmaking for 2050

Considering the limitations of scrap and DRI availability, eleven different scenarios have been prepared to show what steel production in 2050 might look like. Each case is compared to the average emissions intensity reported for the year 2020 (Gielen, 2020) of 1.83 tonnes of CO_2 per tonne of crude steel.

The results in Figure 4.5 below show that, by maintaining the current production routes and adopting best available techniques, CO_2 emissions per tonne of steel are unlikely to fall by more than 40% compared to the levels reported for 2020. By adopting carbon capture for use on blast furnace gas streams and converting DRI plants to use hydrogen, a 54% reduction on current emissions intensity is possible. Therefore, it is exceptionally unlikely that the current split of production routes globally will be retained to up and beyond 2050. In fact, steelmakers are already shifting from BF-BOF routes to EAF and DRI routes to reduce their CO_2 emissions. The major exception to this is Asia where the number of new blast furnaces continues to increase.

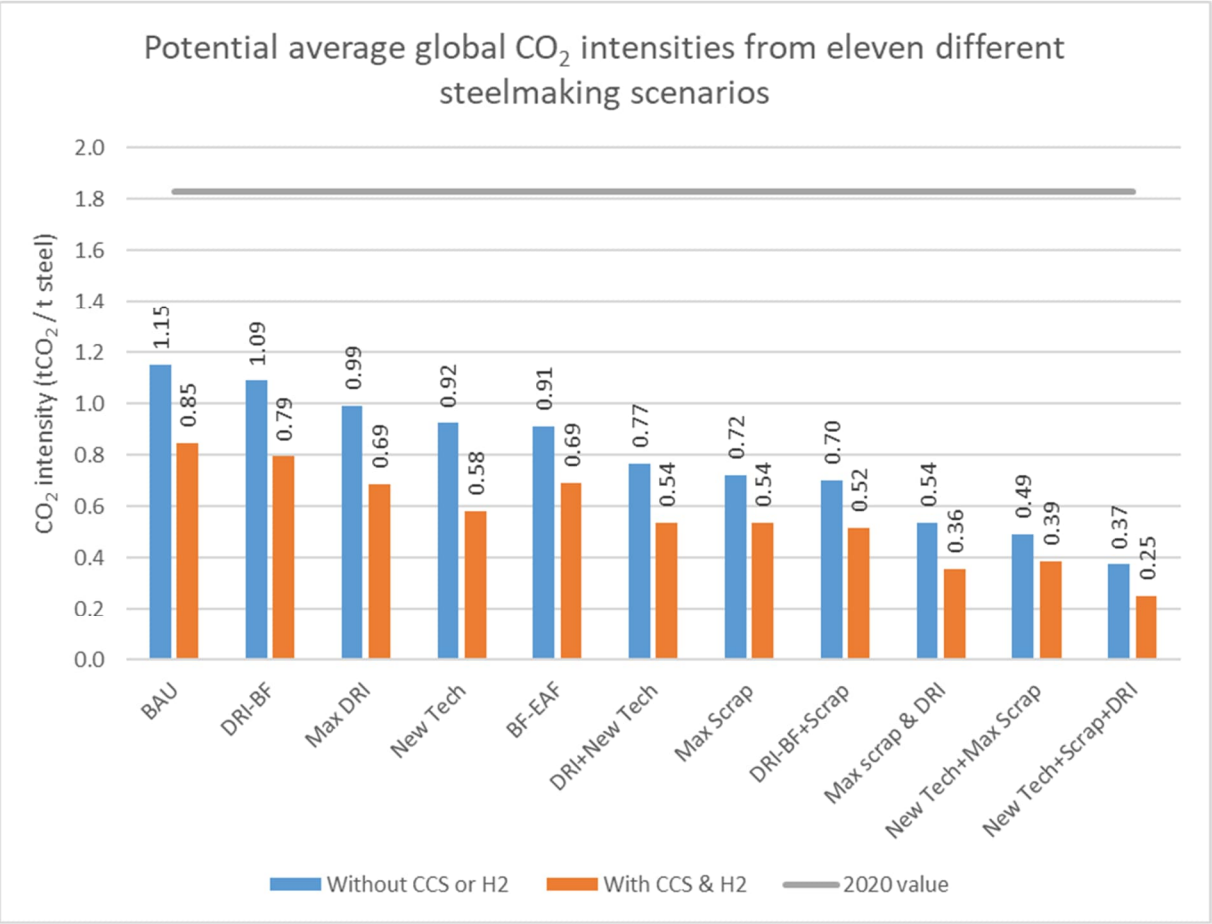

Figure 4.5: Graph of average CO_2 emissions per tonne of steel produced from each of the scenarios considered

By increasing global DRI production for use as a feedstock in blast furnaces, CO_2 intensity can be reduced further still. If all blast furnaces were to be charged with DRI, there would only be a small step change of around 3% in emissions of CO_2 per tonne of steel compared to the first case considered. Therefore, this second scenario will need to be combined with other considerations to make significant reductions in global emissions intensity.

Instead, many producers will most likely choose to adopt a DRI-EAF route to supplement scrap steel as assessed in the third case. The CO_2 intensity for this scenario is reduced further to around 46% of 2020 values. To achieve this, 20% of global steel production would shift from BF-BOF to DRI-EAF. This forecast is reliant on the feedstock to and DRI production capacity tripling between now and 2050.

By adopting a new technology, emissions intensity could be lowered further than by maintaining current production methods or by increasing the DRI-EAF route production share by 20%. Any new technology is presumed to only replace 20% of BF-BOF production due to the time it will take to scale up and gain trust in a new

technology. A relatively small decrease in CO_2 emissions of 50% compared to today's value is observed, considering the large scale investment required to develop and adopt a new technology.

An alternative to adopting a new technology would be to reduce the capacity of blast furnaces globally and use their hot metal to produce steel in EAFs alongside scrap. To achieve this would require around a 3-fold increase in the capacity of EAFs globally but would not consume as much scrap as replacing blast furnaces outright with EAFs. Interestingly, the average electrical consumption per tonne of steel would remain roughly the same as currently achieved. The reason for this is that the hot metal supplied to the EAF contains enough energy to begin the melting of the scrap metal. This in turn notably reduces the electricity requirement to melt the scrap and refine it to the required composition. As the ratio of hot metal to scrap decreases compared to current levels the global blast furnace capacity would reduce by 15%. The reduction allows the oldest and most inefficient units to be decommissioned. The combination of blast furnace and EAF would have the ability to halve CO_2 emissions per tonne of steel compared to 2020 values. The reduction relies on all operating units having best available techniques applied to them. If carbon capture were to be applied to blast furnaces and hydrogen used for DRI production, emissions would decrease to almost a third of the 2020 value. Combining carbon capture with a reduced number of blast furnaces offers the potential for a large reduction in emissions without investing in new production technologies or large scale demolition of existing facilities.

By pairing an increase in DRI-EAF routes with new technologies as described in section 4.3.6, CO_2 emissions could be driven lower than the current global average. The reduction in this scenario would be achieved by reducing steelmaking via the BF-BOF route from around 66% to 26% with new technologies and DRI-EAF routes increasing by 20% each. But the resulting reduction in emissions of 58% compared to current values is disappointing, considering the level of investment required to develop and adopt a new technology.

The greatest reduction in emissions intensity is seen through the maximisation of scrap recycling. By increasing the production share of the EAF route from 24% to 54% of global steel production, it is predicted that all available steel scrap will be utilised. In addition to the EAF capacity more than doubling, considerable thought would need to be given to the transportation and sorting of scrap to allow the maximum recycling of this waste stream. The above would result in CO_2 emissions

reducing by 61% compared to 2020 values which could increase to 71% if carbon capture and hydrogen were deployed at the blast furnaces and DRI plants respectively. By also considering DRI as a feedstock at the remaining blast furnaces, emissions only fall by a further 1%, indicating that the shift to EAFs represents the largest single reduction in CO_2 emissions.

Combining both the maximum scrap recycling and the maximum production of DRI for use in EAFs results in a 71% reduction in emissions per tonne of steel. In this case, the BF-BOF route would be responsible for the production of only 14% of global steel output. By applying carbon capture and hydrogen to blast furnaces and DRI plants, emissions drop to 81% of 2020 levels. This highlights the importance of developing carbon capture or other CO_2 reducing technologies which can be implemented into the existing blast furnace process.

The remaining 14% of production could be accounted for by a new technology to completely halt BF-BOF as a steelmaking route. CO_2 emissions would still only reduce to around 80% of 2020 values, although by converting DRI plants to use hydrogen, a reduction of 86% would seem feasible. But, given the relatively short timeframe between today and 2050, it is unrealistic to expect a complete shift away from blast furnaces. An example of this is the fact that blast furnace units are currently being planned which will have operating lives of 20+ years.

4.5 Conclusions

From the work reported within this chapter there appear to be several alternative process routes which offer lower emissions than the current dominant steel production route. But full replacement of the BF-BOF route is unlikely due to limitations on both scrap and DRI availability. Therefore, multiple production routes will need to be combined to meet the level of steel demand predicted by 2050. Of the eleven combinations considered in this chapter it is unlikely that any one of the scenarios considered will fully represent steel production in 2050. It is expected that scrap recycling and DRI will account for a higher proportion of steelmaking production than in 2020, but both rely on EAFs with a high electrical energy consumption. In these cases, the securing of cheap, low carbon electrical energy sources becomes critical to the expansion of the current global production capacities. Furthermore, the study has presumed that all DRI will be produced using either natural gas or hydrogen. As with electricity, hydrogen must become available in sufficient quantity and cost from low carbon sources to become a viable fuel source.

New technology has the potential to significantly reduce carbon emissions from steelmaking without requiring large scale expansion of existing EAF based routes. There is no “game changing” technology ready for widescale adaptation by the steel industry. This results in a significant technical risk which is likely to prevent steelmakers investing and slowing adoption of any new technology.

The results of this work suggest that the increased use of scrap recycling is the key to reducing CO_2 emissions from the global steel industry. Expansion of EAF capacity will come at the expense of the traditional BF-BOF route and further expansion of DRI routes. There would also still be opportunities to allow further incremental reductions through new technology replacing blast furnaces and the adoption of carbon capture on these older technologies.

There is no single viable technology capable of reducing CO_2 emissions below 90% of 2020 levels. This conclusion matches that made within A Steel Roadmap for Low Carbon Europe (Eurofer, 2013). Therefore, methods of reducing CO_2 from the traditional blast furnace process should be investigated in parallel with increased scrap use in the EAF process. Generally, the incorporation of a secondary process, such as carbon capture, is more likely to be implemented than a wholesale shift to a new, and as yet unproven, technology.

Other assessments looking only at improving the efficiency of existing technologies and a small increase in scrap usage within EAFs estimated that the average emissions intensity could fall to 724kg CO_2 per tonne of crude steel (Woertler, 2013). This value is lower than that reported in the Business and Usual case in Figure 4.5 due to the increased EAF production compared to that currently seen.

Chapter 5. Optioneering to Reduce CO_2 Emissions

Having reviewed the CO_2 emissions generated to produce one tonne of liquid steel in the previous chapter, further work was then undertaken to identify possible improvements to the blast furnace process. This chapter focusses on the effect of installing different technologies to remove CO_2 from the blast furnace gas or reduce the amount of CO_2 emitted to the atmosphere.

5.1 Chapter Introduction

As discussed in section 2.1.2, the blast furnace route is currently the most common method of generating steel. In fact, this step alone is reported to produce approximately 69% of the total CO_2 emissions from a steelworks (Santos, 2013). As the blast furnace is likely to continue to provide a large proportion of steel up to 2050, it is logical to determine which technologies can be combined to reduce the CO_2 generated by this process step to make it fit for a low carbon future.

To this end, four different carbon capture methods and a further nine process steps will be investigated to reduce CO_2 emitted to the atmosphere. Combinations of these technologies will be analysed within a flowsheet to determine the effect on CO_2 removal, (thermal and electrical) energy consumption, energy loss from the gas stream and a rough operating cost.

It is hoped that by assessing these multitude of cases and ranking them according to the criteria above that clear candidates will be identified for integration into the blast furnace process.

5.2 Methodology

A flowsheeting exercise was carried out, using Microsoft Excel, to determine the best fit in terms of technology for removing CO_2 from blast furnace gas. Two locations for this carbon capture within the gas network were also explored.

Options for either converting or storing the CO_2 were also considered but became secondary to the capture position and unit type.

The calculations common to all cases in this assessment are given in the Appendix.

A flowsheet can be split into the following sub-sections:

5.2.1 Blast Furnace Heat and Mass Balance

A blast furnace Heat and Mass Balance Model, developed by Primetals Technologies based on literature (Peacey, 1979) was used to estimate the exit gas stream volumetric flow and composition. This model has been continuously updated with the latest version developed in 2021 to accurately replicate data from operating blast furnaces.

The inputs to the model are based on an operating unit within the UK and considers a mixture of sinter and pellets as a feedstock to produce molten iron.

The model includes the facility to recycle and inject gasses back into the blast furnace process which will affect fuel rate and blast furnace gas composition.

Outputs from the heat and mass balance used in the flowsheet include the air blast volume, coke and coal consumption. The air blast volume is used by the Hot Blast Stove heat balance to determine the volume of combustible gasses required to heat the air to a target temperature.

The analysis considers that gas from the blast furnace would not be treated until it had passed through a wet Gas Cleaning process. Before this cleaning step, the dust content of the gas may range from 3 to 10 g/m^3 (at 273K and 1 atmosphere). At this level of solids in the gas any equipment will begin to suffer from blockages and require frequent cleaning cycles. This basis also allowed the gas conditions to be fixed as saturated with water at approximately 40°C. Two supply pressures are possible, depending on the placement of the capture step within the gas network. If the separation step were to take place immediately after the gas cleaning plant, a higher pressure would be available on most modern blast furnaces. In practice it will be more likely that the separation step takes place at the boundary of the blast furnace. Therefore, the gas pressure was taken to be 0.1 bar gauge due to there being a recycle of blast furnace gas (BFG) back to the hot blast stoves which are supplied with low pressure gas.

5.2.2 Hot Blast Stoves Heat Balance

The energy required to heat the blast from 150 to 1150°C was calculated considering the change in sensible heat and used to determine the fuel requirements at the hot blast stoves. A typical thermal efficiency for a hot blast stove of 80% was used to determine the heat input. This is slightly lower than available literature (Danloy, 2009) to allow consideration for the age of infrastructure typically seen in the steel industry. In addition, a flame temperature was determined based on the composition of the

blast furnace gas and a secondary, enrichment, gas such as coke oven gas. The flame temperature was set to 200°C above the target hot blast temperature, i.e. 1350°C. To reach this value with low calorific gas blast furnace gas, coke oven gas is added to increase the flame temperature. In cases where the blast furnace gas has CO_2 removed from it, nitrogen is added to the combustible gas to dilute it and lower the resulting flame temperature.

In all cases, the volume and composition of the resulting flue gas at the stoves was also calculated. This provides an estimate of any change in CO_2 emissions from this part of the flowsheet. Most cases do not consider capture from this source of emissions, as the flow is relatively low and more similar in composition to a power plant flue gas stream. Compositions of typical gasses considered within this sub-model are included in Table 5.1 below:

Species	units	CO_2	N_2	CO	H_2	H_2O	CH_4
Coke Oven Gas	mol%	1.5	3.8	6.2	59.3	4.2	24.9
Blast Furnace Gas	mol%	22.4	44.7	23	2.7	7.3	0.0

Table 5.1: Composition of Gas at the Hot Blast Stoves

The flame temperature is calculated at an excess air ratio between 5 and 50%, presuming a combustion air temperature of 35°C and moisture content of 1.9%. This corresponds broadly with an ambient air humidity of 73% which is average for the UK and 22°C ambient air temperature. The air temperature then increases to 35°C during compression by the combustion air fans. Although combustion air flow is determined within this model, no fan duty is calculated to assess the effect of different operating regimes. This is due to the power consumption of this equipment being very small when compared to new equipment for CO_2 capture and utilisation.

5.2.3 Chemical Absorption

Modelling of the chemical absorption stage for CO_2 capture is based on removing 90% of the CO_2 in the incoming gas. The remaining species (CO, N_2 & H_2) are considered to be untouched by the chemical absorption stage and leave within the fuel gas stream. The energy requirement to regenerate the chemical solvent is 2.5 GJ/t_{CO2} (Brown, 2016) and is supplied by saturated steam at 2.2 bar. To determine the solvent flowrate, a maximum CO_2 load of 0.3 moles of CO_2 per mole of solvent was considered (Sachde, 2014). The chemical absorption plant is directly fed with

blast furnace gas and does not require compression or further cleaning of the incoming gas stream.

5.2.4 Gas Compressor & Vacuum pump

To determine an approximate gas compressor and vacuum pump duty a separate calculation block can be added into the case file. The compressor uses the inlet gas temperature, pressure, flow and composition along with the outlet pressure to determine electrical energy consumption.

The calculation steps for deriving electrical duty from the inlet gas conditions and outlet pressure are listed in the appendix.

5.2.5 Other Carbon Capture Technologies

To estimate the separation of the various components in the inlet gas stream, retention factors, given in Table 5.3, were used for physical adsorption and absorption steps. The inverse of the above factors is used to determine the gas composition of the CO_2 stream. All three require a gas compressor to increase the blast furnace gas pressure at the inlet of the capture stage. The formula and factors for the outlet gas species are included in Equation 5.1 below:

$$x_{\mathrm{i}} = \frac{Q_{\mathrm{in}} \times y_{\mathrm{i}} \times retention_{\mathrm{i}}}{Q_{\mathrm{out}}} \qquad \textit{Equation 5.1}$$

Where,

x_i = mole percent of component i in outlet gas

Q_{in} = Volume flow of Inlet Gas (m^3/h)

y_i = mole percent of component i in inlet gas

$retention_i$ = Retention factor of component i

Q_{out} = Volume flow of Outlet Gas (m^3/h)

	Pressure Swing Adsorption (PSA)	Vacuum pressure swing adsorption (VPSA)	Physical Absorption (PA)
Inlet Pressure	6 bar gauge	4 bar gauge	18 bar gauge
CO_2 Outlet Pressure	1.16 bar actual	0.15 bar actual	16 bar gauge
Retention Factors			
CO_2	0.03	0.03	0.17
N_2	1.0	1.0	0.999
CO	0.785	0.95	0.999
H_2	0.865	0.99	1.0
H_2O	0.0	0.0	0.088

Table 5.2: Retention factors for various chemical species for different carbon capture types (ULCOS, 2009 & Progressive Energy, 2015)

From Table 5.2 above, we can see that the Physical absorption model is likely to capture the least amount of CO_2 from the inlet gas stream. This is indicated by the retention factor for CO_2 being the highest of the three capture methods. The resulting CO_2 stream from the physical absorption step will be the purest of the three methods above as the retention factor for the other gas components are the highest. By creating a purer CO_2 stream the chemical energy lost from the fuel gas is reduced. Any further processing of the CO_2 before it can be compressed and transported to an end user is also reduced.

Vacuum pressure absorption also requires an additional vacuum pump sub-model to determine the electrical requirement of this additional equipment. For the physical absorption model, the solvent pump duty was estimated based on a figure of 51.1 kWh/t_{CO2} (Progressive Energy, 2015) to account for the ratio of solvent to CO_2.

In the case of Temperature Swing Adsorption (TSA), the inlet gas stream was compressed, this time to around 4.7 bar to account for pressure losses through the adsorption column. Steam was chosen as the regeneration medium, saturated at 150°C. The regeneration energy was taken as 4.4 GJ/t_{CO2} (Joss, 2017) and it was presumed that the maximum loading of the porous material would be 0.526 t_{CO2}/m^3 (Elfving, 2017). As with Chemical Absorption, it is expected that 90% of the incoming CO_2 will be separated.

5.2.6 Geological Storage (Offshore)

The bases case for CO_2 utilisation is the scheme to compress captured CO_2 to approximately 100 bar gauge, which is the current industry norm. A figure of 115 kWh/t_{CO2} (Birat, 2010) is considered to determine the power requirement. The power requirement is based on compressing the CO_2 stream to a pressure of 40 bar gauge. As most Steelworks have access to their own sea port, it is expected that transport of CO_2 will be by tanker to an injection wellhead. This is justifiable, as final compression can be carried out at the injection wellhead. It is important to note that only compression energy is estimated with no impact of final gas processing to meet sufficient quality for transportation. For example, physical adsorption methods would require further treatment to limit CO and H_2 content. Chemical and physical absorption generate a purer stream of CO_2 with the main impurity being water. In this case the CO_2 stream from the carbon capture plant will require de-humidification to meet requirements for both transportation and injection into a storage well.

5.2.7 Algae Feedstock (Offshore)

An alternative to geological storage would be to use the CO_2 as a food source for Algae. This plant matter could in turn be processed into oils and plastics. The major advantage considered of this method over storage is the much lower CO_2 pressure required. Due to the sheer size of the Algae plantation required, it is expected that CO_2 will still require compressing to above it's critical pressure to reduce storage volumes during shipping.

For the considerations of the flowsheet, there is negligible energy consumption at the algae plantation resulting in no real difference between this case and the geological storage options. The only change is an estimate of land usage based on a figure of 50 $t/d/km^2$. Based on the capture of 2790 tonnes per day from a typical blast furnace gas stream, an area the size of 55.79km^2 is required when capture is carried out by chemical absorption. This is just under half of the land attributable to Newcastle upon Tyne. At the time of writing, there are four operating blast furnaces within the UK, with each potentially requiring this space for utilising captured CO_2 as an algae feedstock. Therefore, this utilisation method is not feasible for large scale adoption for CO_2 captured from a steelworks.

5.2.8 Slag Mineralisation

A final storage method for CO_2 includes the mineralisation of components within Steelwork slags. This has the benefit that the CO_2 would be compressed to a pressure of around 6 bar gauge as Slag mineralisation could be carried out on the steelworks site. Due to the lower CO_2 compression the electrical energy consumption will also be reduced when utilising the captured CO_2 in this manner. No additional energy consumption is accounted for as the slag will be available from existing processing routes. The slag would be ground to increase surface area for mineralisation and therefore speed up this reaction, however energy consumption to achieve this will be minimal. A final consideration in this flowsheet is the relative amounts of captured CO_2 and available slag from the blast furnace. The flowsheet excludes additional slag from the basic oxygen furnace or electric arc furnace processes, which will have a slightly different composition and therefore uptake of CO_2.

5.2.9 Recycle to Blast Furnace

Instead of sending captured CO_2 to storage or for processing, the concept of re-injecting the CO_2 into the Blast Furnace was assessed. In this case, the Nitrogen within the heated compressed air stream to provide oxygen to the Blast Furnace is replaced with recirculated CO_2. Due to the reduction of Nitrogen supplied to the Blast Furnace, the top gas from the Blast Furnace would then include a greater percentage of CO_2 and CO. Furthermore, the required export CO_2 pressure would be relatively low at 4.5 bar gauge or less. The full effect of this scheme is determined in the heat balance for the hot blast stoves and the heat and mass balance for the blast furnace. As the purity of the CO_2 recycled back to the blast furnace is relatively unimportant, this scheme is likely to favour physical adsorption as the CO_2 separation method as the purity of the CO_2 is less important than other CO_2 utilisation methods.

5.2.10 Water Shift Reactor (WGS)

Another method of maximising CO_2 for capture is the water gas shift reaction, where water and CO form hydrogen and CO_2. The resulting hydrogen and CO_2 content of the blast furnace gas would increase but at the expense of gas calorific value. The scheme assessed in this study is that of a low temperature water shift reaction, which due to its exothermic nature, requires no energy input for gas preheating. For the

flowsheet purposes, it is expected that the total portion of CO in the inlet gas is converted into CO_2 and that a stoichiometric amount of steam is required.

5.2.11 Solid Oxide Electrolysis Cell (SOEC)

Solid Oxide Electrolysis cells are still under development, but offer a method to convert CO_2 to CO using electrical power at high reaction temperatures of around 600°C. For the flowsheet assessment it was presumed that the CO_2 stream was preheated by burning a portion of the fuel gas from the CO_2 separation plant. A heat balance model was used with a thermal efficiency of 80% used as a basis. The fuel gas is expected to be combusted in a stream of hot oxygen generated as a by-product at the SOEC. The estimated electrical consumption is 189 kJ per mole of CO_2, but with good conversion rates in the order of 60 to 70% (Suzuki, 2015). The flowsheets assess the regenerated CO_2 stream leaving the SOEC being burnt at the hot blast stoves to increase the amount of chemical energy exported from the blast furnace. But because the calorific value of the regenerated CO_2 stream is high, it must first be diluted with nitrogen before being combusted.

5.2.12 Reverse Water Gas Shift (RWGS)

By reversing the water gas shift reaction described in section 5.2.10, CO_2 can be converted back to CO using thermal & chemical energies. For the flowsheet assessment it was considered that the CO_2 stream was preheated to 400°C by burning a portion of the fuel gas from the CO_2 separation plant. As with the SOEC cases, a thermal efficiency of 80% was used as a basis. A 1:1 ratio of Hydrogen to CO_2 was assumed to be sufficient for the relatively low CO_2 conversion rates of 20% (Kim, 2014). The unreacted Hydrogen also adds to the calorific value of the converted CO_2 stream which is used to enrich the unrefined blast furnace gas at the hot blast stoves.

5.2.13 Plasma-Catalysis

One last method considered to convert CO_2 to CO, is the use of plasma as an energy source. A catalyst is also required to limit the number of produced species to mostly CO. Even with the use of a catalyst the conversion rate is typically low, being quoted as a maximum of 36.5% (Tu, 2012). Furthermore, an excessively large energy requirement of 1.6 kilojoule per millimole (kJ/mmol) of CO_2 converted is reported (Tu, 2012) due to the inefficiencies of plasma technology. The resulting gas stream leaves

the plasma converter at around 150°C and consists of Oxygen, CO, CO_2 and any other species in the inlet gas stream (Mei, 2016). The flowsheets with plasma catalysis assess the regenerated gas stream being used to fuel the hot blast stoves, once the oxygen has been removed. No additional energy consumption is included for the oxygen removal stage with this step removing 100% of the O_2 selectively without reducing any other component in the gas stream.

5.2.14 Flue Gas Recycle

By recycling CO_2 rich waste gasses, the concentration of CO_2 will increase and make removal of this compound easier and more cost effective. Within this study the waste gasses generated by combustion at the hot blast stoves is assessed. The scheme fits broadly with the oxy-fuel combustion proposals for gas fired power plants and involves the flue gasses being recycled and enriched with oxygen before being used as a source of oxygen in the combustion process. The flowsheet also considers some recovery of the flue gas sensible heat to preheat the incoming fuel gas stream. By doing this, the target flame temperature can be reached without introducing any enrichment gas to the system. The flue gas composition is calculated within the hot blast stove heat balance model described within section 5.2.2.

5.3 Results and Discussions

For each combination of technologies, several resulting factors were considered.

The amount of CO_2 captured per tonne of hot metal from the blast furnace (tCO_2/tHM) was one of the measures used to compare the different flowsheet cases. This allows the identification of combinations of technologies able to remove the largest and smallest amounts of CO_2 from the blast furnace process. The metric was calculated using the formula given in Equation 5.2:

$$t_{CO_2} = Q_{CO_2} \times y_{CO_2} \times \rho_{CO_2}$$ *Equation 5.2*

Where,

t_{CO2} = tonnes of CO_2 captured (t/tHM)

Q_{CO2} = Volume flow of CO_2 (m^3/tHM)

y_{CO2} = Volume percent of CO_2

ρ_{CO2} = Density of CO_2 (t/m^3)

The amount of electrical energy required per tonne of product from the blast furnace (kWh/tHM) was also calculated using the formula in Equation 5.3. By comparing the values for electrical energy consumption for the different cases the largest and lowest electrical consumptions can be quickly identified. This is especially important for steel producers as supply of electrical energy is often limited with a large increase requiring additional electricity to be purchased.

$$Energy_{Elec} = E_{pumps} + E_{compressors} + E_{SOEC} + E_{Plasma} - E_{TRT} + (115 \times t_{CO_2})$$ *Equation 5.3*

Where,

$Energy_{Elec}$ = overall electrical energy consumption (kWh/tHM)

E = electrical energy consumption of pumps, compressors, SOEC, plasma generator and expansion turbine (kW/tHM)

t_{CO2} = tonnes of CO_2 captured from the incoming gas stream (t_{CO2}/tHM)

The amount of steam energy required per tonne of product from the blast furnace (kWh/tHM) was also calculated using the formula in Equation 5.4. This allows the heat energy requirements for the different cases to be ranked which highlights cases where chemical absorption and the water gas shift reaction are considered.

$$Energy_{\text{Steam}} = Q_{\text{Steam}} \times H_{\text{Steam}}/3600 \qquad \textit{Equation 5.4}$$

Where,

$Energy_{\text{Steam}}$ = Thermal energy requirement in the form of steam (kWh/tHM)

Q_{Steam} = Mass Flow of Steam (kg/tHM)

H_{Steam} = Enthalpy of Steam (kJ/kg)

The specific energy consumption (kWh/t_{CO2}) is the amount of energy input to capture 1 tonne of CO_2 from the blast furnace process. It combines both electrical and steam energy requirements as shown in Equation 5.5. This allows total energy requirements to be considered regardless of whether the predominant energy requirement is met through electrical or steam use.

$$Specific\ capture\ energy = \frac{Energy_{\text{Elec}} + Energy_{\text{Steam}}}{t_{\text{CO}_2}} \qquad \textit{Equation 5.5}$$

Where:

Specific capture energy = total energy required to capture 1 tonne of CO_2 (kWh/t_{CO2})

$Energy_{\text{Elec}}$ = Electrical Energy Requirement (kWh/t_{CO2})

$Energy_{\text{Steam}}$ = Thermal Energy (steam) requirement (kWh/t_{CO2})

t_{CO2} = tonnes of CO_2 captured from the incoming gas stream (t_{CO2}/tHM)

The Export Gas Energy is the thermal energy released from the gas on combustion (MW_{th}). This allows the impact of the technologies within a flowsheet on the overall steelworks energy balance to be identified. In cases where the export energy is significantly lower than in the base case, additional natural gas will need to be purchased by the steelmaker to meet the energy demands of the steelworks. In cases where the export energy increases, the steelmaker may be able to reduce their reliance on bought in gas. The metric was calculated using the formula given in Equation 5.6:

$$\textit{Export Energy} = Q_{\text{Fuel}} \times CV_{\text{Fuel}} \qquad \textit{Equation 5.6}$$

Where,

Export Energy = amount of chemical energy exported (MW)

Q_{Fuel} = Volume flow of Fuel Gas (m^3/tHM)
CV_{Fuel} = Calorific Value of Gas (MJ/m^3)

By considering both the electrical energy requirement and the exported energy, the (parasitic) energy requirement can be determined. This value is reported as a percent of the energy generated by the upgraded blast furnace gas. The metric was calculated using the formula in Equation 5.7 and allows further analysis of the impact on the energy balance of the steelworks.

$$Parasitic\ Energy = \frac{Energy_{\mathrm{Elec}}}{(Export\ Energy \times Generation\ Efficiency)} \qquad Equation\ 5.7$$

Where,
Parasitic Energy = electrical energy requirement as a percent of export energy
$Energy_{Elec}$ = Electrical energy consumption (kWh/tHM)
Generation Efficiency = Efficiency of power generation plant, taken as 30% (Khallaghi, 2022)
Export Energy = amount of chemical energy exported (MW)

For some technologies, a negative impact could be foreseen even without completing a full flowsheet. A list of the cases and the capture and CO_2 utilisation technologies each consider is included in Table 5.3.

Case Number	Capture Technology	CO_2 utilisation method	CO_2 captured	Electrical Energy	Steam Energy	Export Gas Energy	Parasitic Energy	Specific Energy
			t_{CO2}/tHM	kWh/tHM	kWh/tHM	MJ/tHM	%	kWh/t_{CO2}
Base	None	None	0	173	0	3018	19.1%	-
1	MEA	Storage / EOR	0.37	218	259	3018	24.1%	1288
2	MEA	Storage / EOR	0.60	245	419	2339	34.9%	1106
3	MEA	BF Recycle	0.83	272	576	6258	14.5%	1021
4	MEA	BF Recycle	0.6	262	415	5503	15.9%	1129
5	MEA	Storage / EOR	0.76	263	833	2616	33.5%	1443
6	MEA	Storage / EOR	1.23	319	1348	1694	62.7%	1355
7	MEA	SOEC	0.44	623	414	4456	46.6%	2357
8	MEA	RWGS	0.38	175	299	5317	11.0%	1246
9	MEA	RWGS	0.56	174	414	7113	8.2%	1051
10	MEA	RWGS	0.43	175	343	7184	8.1%	1204
11	MEA	Storage / EOR	0.63	248	428	5190	15.9%	1073
12	MEA	Storage / EOR	0.43	224	296	2175	34.3%	1208
13	MEA	Storage / EOR	0.49	231	341	3017	25.6%	1168
14	PSA	Storage / EOR	0.40	297	0	2390	41.4%	742
15	PSA	Storage / EOR	0.65	301	0	3349	30.0%	464
16	PSA	BF Recycle	0.92	371	0	5132	24.1%	403
17	PSA	BF Recycle	1.33	302	0	5911	17.0%	227
18	PSA	Storage / EOR	0.82	362	308	2263	53.4%	817

Case Number	Capture Technology	CO_2 utilisation method	CO_2 captured	Electrical Energy	Steam Energy	Export Gas Energy	Parasitic Energy	Specific Energy
			t_{CO2}/tHM	kWh/tHM	kWh/tHM	MJ/tHM	%	kWh/t_{CO2}
19	PSA	Storage / EOR	1.32	327	498	1120	97.4%	625
20	PSA	SOEC	0.55	568	0	3265	58.0%	1033
21	PSA	RWGS	0.6	301	0	6216	16.1%	501
22	PSA	RWGS	0.45	253	0	7181	11.7%	562
23	PSA	Storage / EOR	0.67	334	0	3895	28.6%	499
24	PSA	Storage / EOR	0.46	230	0	2175	35.3%	501
25	VPSA	Storage / EOR	0.40	304	0	2878	35.2%	759
26	VPSA	Storage / EOR	0.65	309	0	4115	25.1%	476
27	VPSA	BF Recycle	0.96	399	0	6322	21.0%	416
28	VPSA	Storage / EOR	0.82	378	308	2590	48.7%	837
29	VPSA	Storage / EOR	1.32	383	498	1647	77.6%	668
30	VPSA	SOEC	0.50	707	0	4059	58.1%	1414
31	VPSA	RWGS	0.58	333	0	6711	16.6%	575
32	VPSA	RWGS	0.45	261	0	7188	12.1%	581
33	VPSA	Storage / EOR	0.69	351	0	4946	23.7%	509
34	PA	Storage / EOR	0.34	342	0	3015	37.8%	1004
35	PA	Storage / EOR	0.56	314	0	3928	26.6%	560
36	PA	BF Recycle	0.78	330	0	6383	17.2%	423
37	PA	BF Recycle	1.13	303	0	6363	15.9%	268

Case Number	Capture Technology	CO_2 utilisation method	CO_2 captured	Electrical Energy	Steam Energy	Export Gas Energy	Parasitic Energy	Specific Energy
			t_{CO2}/tHM	kWh/tHM	kWh/tHM	MJ/tHM	%	kWh/t_{CO2}
38	PA	Storage / EOR	0.70	375	308	2616	47.8%	976
39	PA	Storage / EOR	1.13	374	498	1694	73.6%	772
40	PA	SOEC	0.39	816	0	4390	62.0%	2092
41	PA	RWGS	0.49	324	0	6390	16.9%	661
42	PA	RWGS	0.38	268	0	6808	13.1%	706
43	PA	Storage / EOR	0.59	405	0	5298	25.5%	686
44	TSA	Storage / EOR	0.37	284	456	3018	31.4%	1999
45	TSA	Storage / EOR	0.60	352	737	4881	24.1%	1816
46	MEA	Algae Feed	0.37	218	259	3018	24.1%	1288
47	MEA	Mineralisation	0.37	176	259	3018	19.4%	1174
48	MEA	Plasma Catalysis	0.4	1740	277	4018	144%	5042
49	MEA	Plasma Catalysis	0.6	2565	415	2735	313%	4966
50	MEA	Plasma Catalysis	0.86	3622	598	4536	266%	4907

Table 5.3: List of Flowsheet cases and resulting ranking factors

5.3.1 Amount of CO_2 Captured

From the results in Table 5.3, PSA & VPSA have the potential to capture a larger amount of CO_2 than chemical and physical absorption and temperature swing adsorption. The assessment presumes that the chemical absorption plant is only able to capture 90% of the incoming CO_2. Should the equipment be designed to capture a higher percentage, then this method would become comparable to the physical adsorption methods.

Physical absorption offers the least amount of CO_2 captured from the cleaned blast furnace gas as the assessment is made based on a typical capture rate. It is feasible to believe that a specifically designed capture plant for the blast furnace gas stream would be able to remove a higher percentage of CO_2 from the incoming gas.

The highest amount of CO_2 captured is shown in cases where the entire gas flow from the blast furnace is treated by water gas shift to convert CO into CO_2. This configuration is shown in cases 6, 19, 29 and 39 within Table 5.3 where capture rates exceed 1 tonne of CO_2 per tonne of product from the blast furnace regardless of capture plant type.

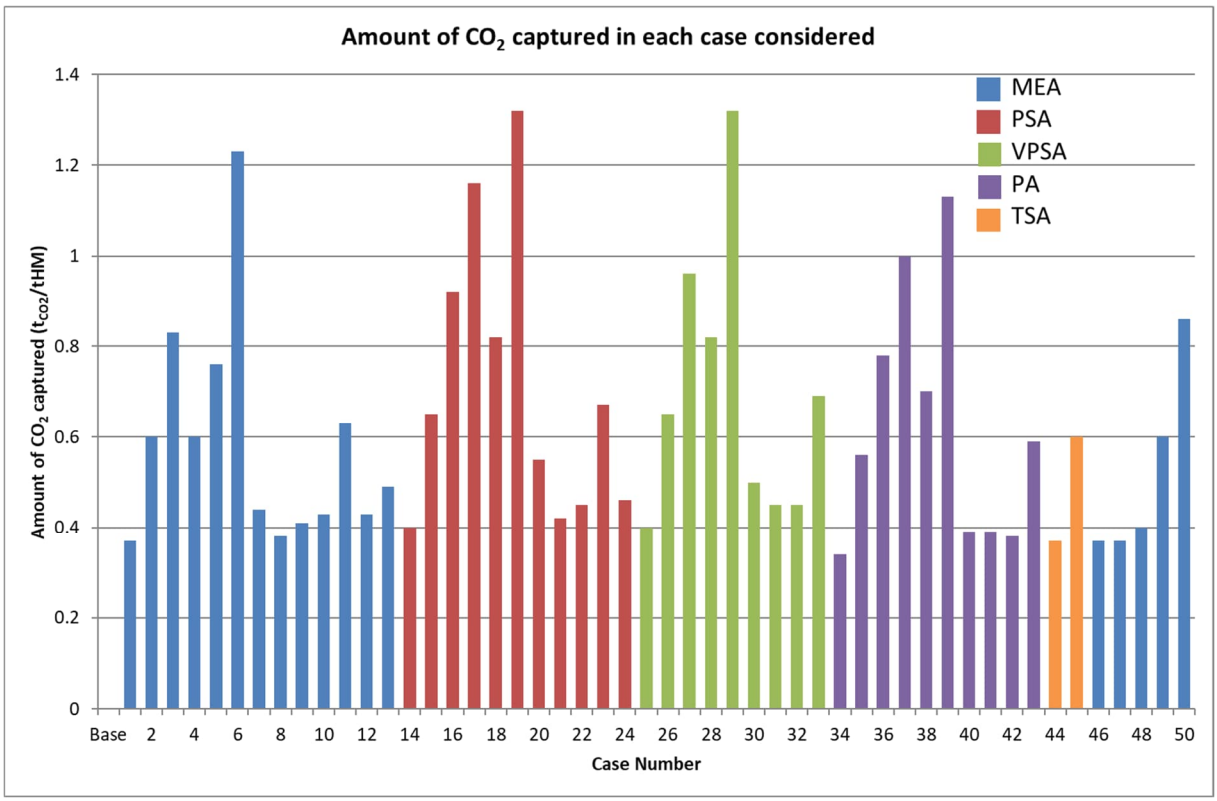

Figure 5.1: Graph of the amount of CO_2 captured for all the cases considered

In Figure 5.1, the lowest amount of captured CO_2 is shown in cases considering removing CO_2 by physical absorption. When CO_2 is removed from the exported blast furnace gas without any other technology (cases 1, 25, 34 & 44) less than 0.4 tonnes of CO_2 are captured per tonne of product from the blast furnace. These scenarios represent an end of pipe solution to capture CO_2 from the blast furnace gas exported and therefore represents a “Business as Usual” scenario with a minimum impact on blast furnace operation. As the target is to capture the highest possible amount of CO_2 from the blast furnace gas stream, then an additional technology will be required to compliment the capture technology. But by introducing multiple processing stages, the capital and operating cost will increase.

5.3.2 Electrical Energy Requirement

For the base case, a conservative energy consumption was taken to include all the Blast Furnace auxiliary equipment. The results shown in Figure 5.2 indicate that chemical absorption requires the least electrical energy to capture CO_2 due to only requiring relatively small motors to recirculate the liquid solvent.

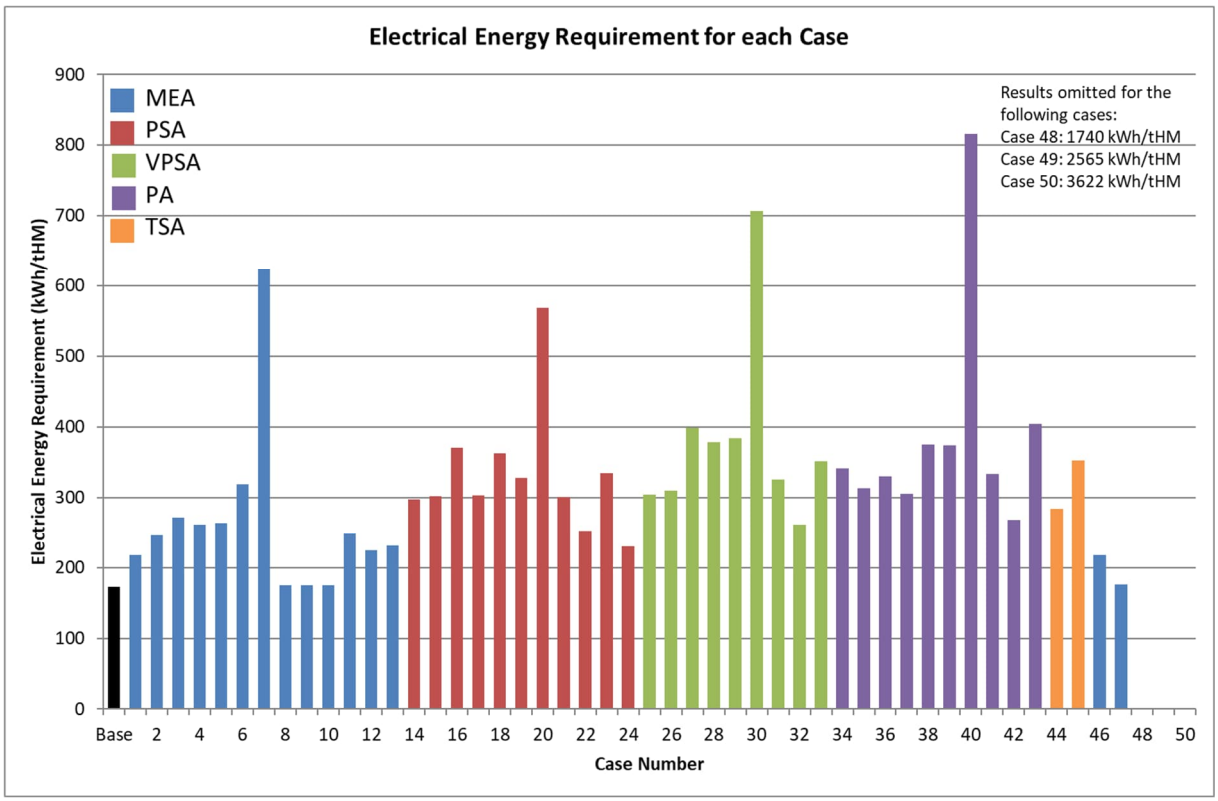

Figure 5.2: Graph of Electrical Energy for each case

By comparison, the other CO_2 separation technologies all require gas compression and therefore have higher electrical energy usage.
The electrical power consumption of the remaining technologies generally increases with the size and number of gas compressors with Physical Absorption requiring the highest levels of electrical power.
Cases which regenerate the captured CO_2 via electrical means such as solid oxide electrolysis cell (cases 7, 20, 30 & 40) and plasma catalysis (cases 48-50) incur further power usage. This is particularly notable when plasma catalysis is used to regenerate the CO_2 due to the low electrical efficiencies involved.

The electrical energy is a key parameter in this assessment of options as the majority of steelworks operate aging and inefficient power plants. These facilities generally have a power generation efficiency of around 30%. By comparison, steam generating boilers have thermal efficiencies of around 80%, making steam a more available energy source for most steelworks. Any excess electricity which exceeds the available on-site supply capacity must be sourced from a third party. As well as affecting operating costs for the site it also increases scope 2 emissions per tonne of steel produced.

5.3.3 Steam Energy Requirement

For the base case, no steam was considered, although the compressed air stream to many European blast furnaces is enriched with small quantities of steam. The steam requirement usually varies throughout the year (Colclough, 1959) to counteract the seasonal ambient air humidity.

Many of the cases shown in Figure 5.3 have a zero additional steam requirement if the capture stage is either physical adsorption or physical absorption.

For the capture stages, neither physical adsorption nor physical bbsorption require steam to regenerate the capture medium. Of the remaining two technologies, chemical absorption has a lower regeneration energy than temperature swing adsorption (TSA). In cases where water gas shift (WGS) was also considered additional steam is required as a feedstock. Therefore, the cases with the highest consumption of steam are those considering chemical absorption as the separation

step after a water gas shift step has taken place. No flowsheet case combining TSA and WGS was prepared as ultimately temperature swing was not seen to be as viable as the other separation technologies. Had such a case been prepared, it would have resulted in a higher steam consumption than any listed in Table 5.3.

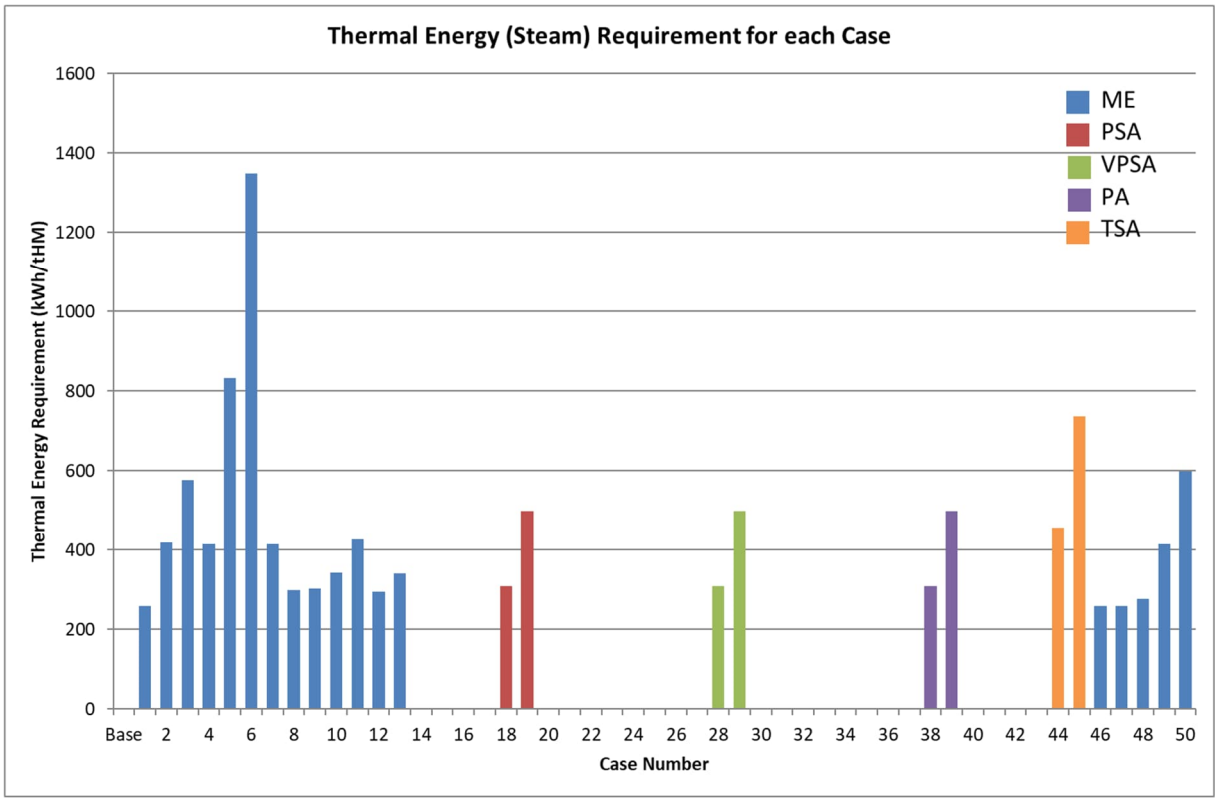

Figure 5.3: Steam Requirement for each case

5.3.4 Specific Capture Energy

The results shown in Figure 5.4 indicate that the highest energy consumptions generally occur with reduction of CO_2 through either solid oxide electrolysis or plasma catalysis. Both of these technologies use a large amount of electrical energy in order to convert CO_2 into CO. CO_2 capture via temperature swing adsorption also generates a high energy consumption. In this case it is the large amounts of thermal energy required to regenerate the porous adsorption material. Chemical absorption has only a slightly lower overall energy requirement due to the large steam consumption offsetting the small electrical energy requirement. PSA is shown to be the least energy intensive. The current assessment does not include for any further process to purify the CO_2 stream prior to compression and transportation.

The lowest specific capture energies are generally in cases where the inlet concentrations of CO_2 are high. Notable exceptions to this are chemical and physical absorption capture methods which use a fixed energy per tonne of CO_2 captured in this assessment. In reality, the equipment design of such capture plants would be adapted to take advantage of the higher inlet CO_2 concentrations.

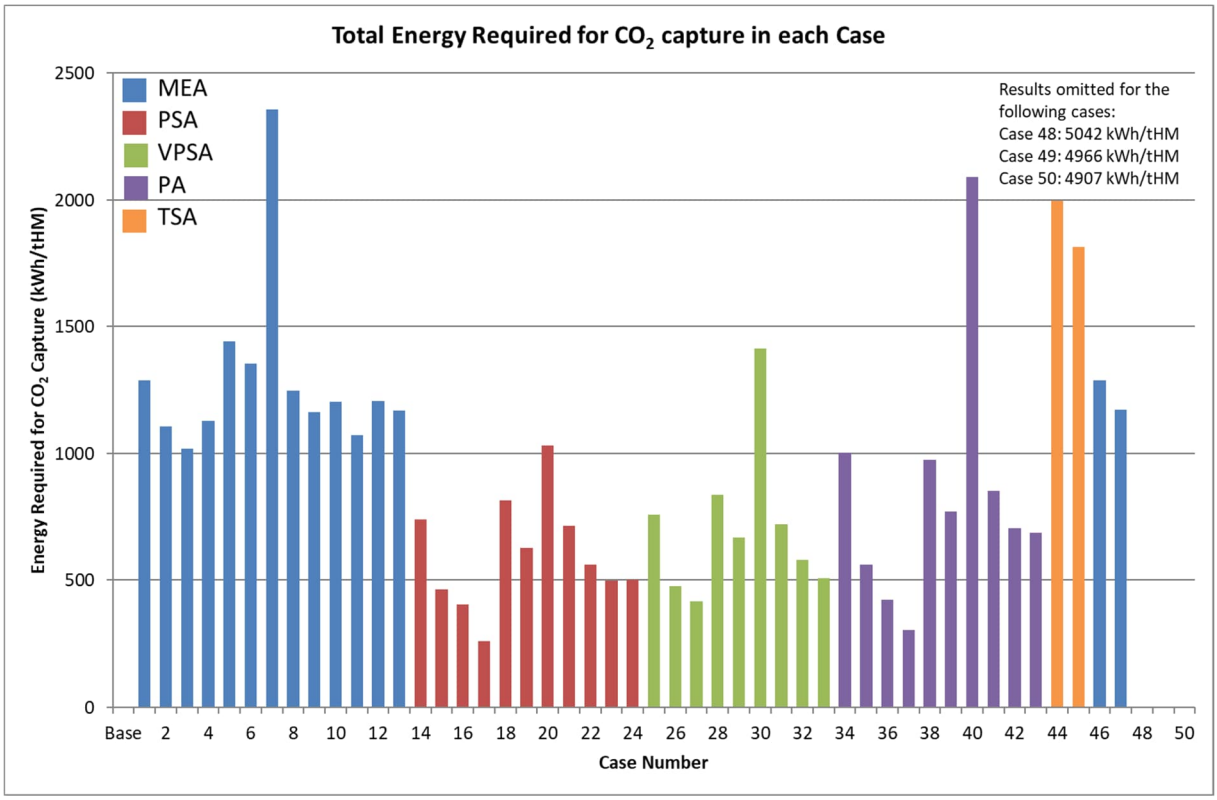

Figure 5.4: Graph of required energy to capture CO_2 for each case considered

5.3.5 Export Gas Energy

The base case considers a typical blast furnace operation in the UK to derive a gas flow and calorific value. In general, the results in Figure 5.5 show that chemical absorption and physical absorption export a greater energy within the gas stream to other users within the steelworks. By comparison, physical adsorption processes remove a small portion of H_2 and CO from the exported fuel gas stream and therefore provide less energy for other users. When the complete flow of gas from the blast furnace has the CO_2 removed from it then a higher fuel gas energy results. In these cases, the flow to the hot blast stoves decreases. In most of these cases, excess air or nitrogen must also be considered at the hot blast stoves to limit the resulting flame temperature.

The lowest export gas energy cases consider the use of WGS to convert CO & H_2O into CO_2 & H_2 (cases 5, 6, 18, 19, 28 & 29 in Figure 5.5). Despite containing a large amount of H_2 within the gas stream the conversion process is exothermic which results in a loss of a small amount of calorific value (in the form of heat).

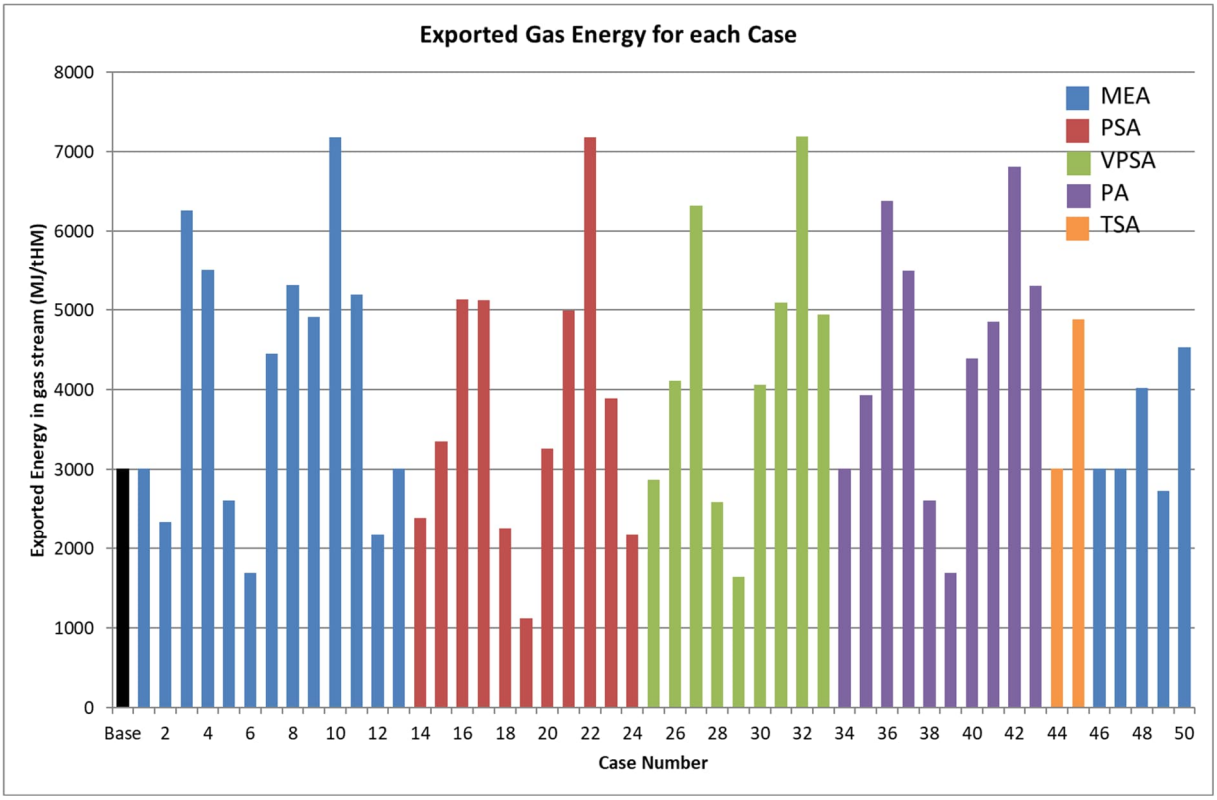

Figure 5.5: Exported energy for each case

The highest export energy cases consider the use of RWGS to regenerate the captured CO_2 (cases 8-10, 21, 22, 31, 32, 41 & 42 in Figure 5.5). In these cases, both the generation of CO from CO_2 and the addition of H_2 into the flowsheet. The supply of H_2 is likely to come at a penalty to the operating cost as demand of H_2 struggles to keep pace with demand from multiple industries in the near-term future. As with electrical energy, imported H_2 will also carry a CO_2 burden as it is unlikely that all sources of H_2 will be carbon neutral.

5.3.6 Energy Loss

It is important to note that the base case also has some energy consumption driven by the electrical energy consumption of the blast furnace process. Of all the cases considered in Figure 5.6, 68% have a higher energy loss than the base case. This

can be explained by the cases requiring more electrically driven equipment to be added to the flowsheet either to capture or utilise CO_2.

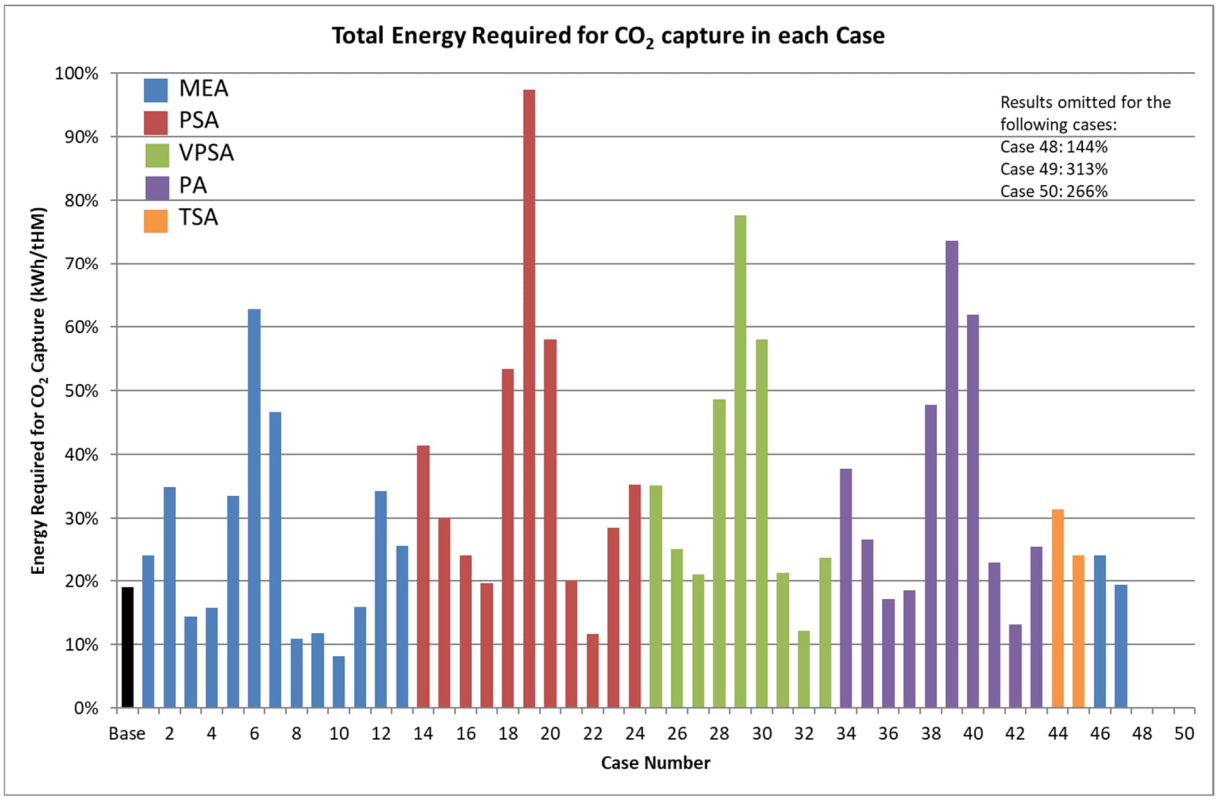

Figure 5.6: Parasitic Energy Loss for each case

As discussed in sections 5.3.2 and 5.3.4, the highest values appear in the cases considering plasma regeneration of CO_2. In these cases, the very high electrical energy requirement does not provide a comparative increase in CO_2 removed from the blast furnace. The lowest energy loss levels occur with high export gas energies, typically characterised by recycling CO or CO_2 containing gasses back to the blast furnace to lower the N_2 content in the cleaned blast furnace gas.

5.4 Operating Cost

By using utility costs from a UK based steelworks (British Steel, 2018), operating costs for each of the flowsheets can be estimated. This adds a further element to rank the various cases and identify the most promising.

5.4.1 Utility Costs

The list in Table 5.4 was provided by a UK steelworks to indicate the internal prices for each utility used to produce steel.

Utility	Units	Cost
Electricity	£/MWh	70.0
Steam	£/tonne	10.994
Oxygen	£/m^3	1.404
Nitrogen	£/m^3	0.544
COG	£/m^3	3.887
BFG	£/m^3	3.761

Table 5.4: Utility costs based on actual internal costs for a Steelworks in the UK dated 2018

In addition, a H_2 cost of 0.164 £/m^3 is considered which equates to around 8 USD/kg. Currently H_2 is not required by most steelworks and therefore, new supply contracts would need to be drawn up.

It is important to note that non-domestic electricity prices have increased by approximately 2.5 times on average from 2018 to 2023 (Department for Energy Security & Net Zero, 2023) driven by a similar increase in cost for Natural Gas. Electricity prices will have a direct impact on the utility cost for oxygen and nitrogen due to their supply via an electrical energy intensive cryogenic air separation process. The cost of combustible gasses including COG and BFG are typically index linked to the price of natural gas too as a short-fall of these gasses will require natural gas to be purchased. As steam is typically generated on a steelworks by combustion of a combustible gas, it's utility cost will also increase in line with the combustion gas. Only H_2 is likely to have maintained or reduced its utility cost since 2018. This is due to development work into hydrogen supply and electrolyser development.

Using the information in Table 5.4 and an estimated hydrogen cost the operating costs for each case can be derived and are shown in Figure 5.7.

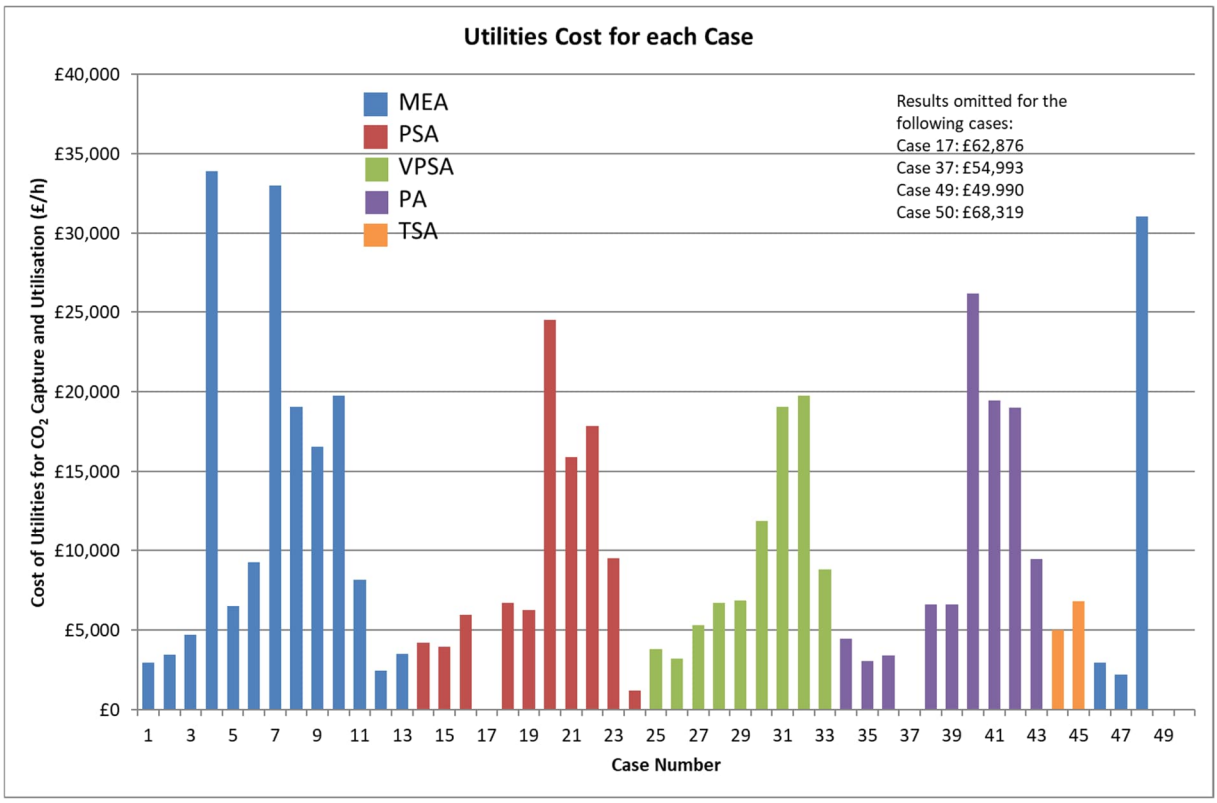

Figure 5.7: Graph of Derived Utility costs for each case considered

Figure 5.7 shows that the cases requiring the lowest cost of utilities are unsurprisingly those where CO_2 is removed from the blast furnace gas and compressed for transport to a utilisation or storage site. Cases where a water shift stage is included also have low utilities cost, considering the large amounts of steam required in this process step. If the steam consumption exceeds the availability within the steelworks then the low value of steam considered in this study may increase.

Utility costs can also be represented per tonne of CO_2 removed from the process. This is an interesting metric as it can be compared to the cost of emitting one tonne of CO_2 to the atmosphere. If the cost to capture the CO_2 is lower than the cost of emitting it, then there becomes a financial incentive to build and operate a CO_2 capture facility. Such a comparison is made in Figure 5.8 and shows that for most cases considered, the calculated utility cost is below the current EU carbon price of 85 EUR/t_{CO2} (OECD, 2021), considering an exchange rate of £1 = €1.15. The analysis does exclude other cost factors such as maintenance and manning but indicates that there is already a business case to investigate carbon capture from blast furnace gas.

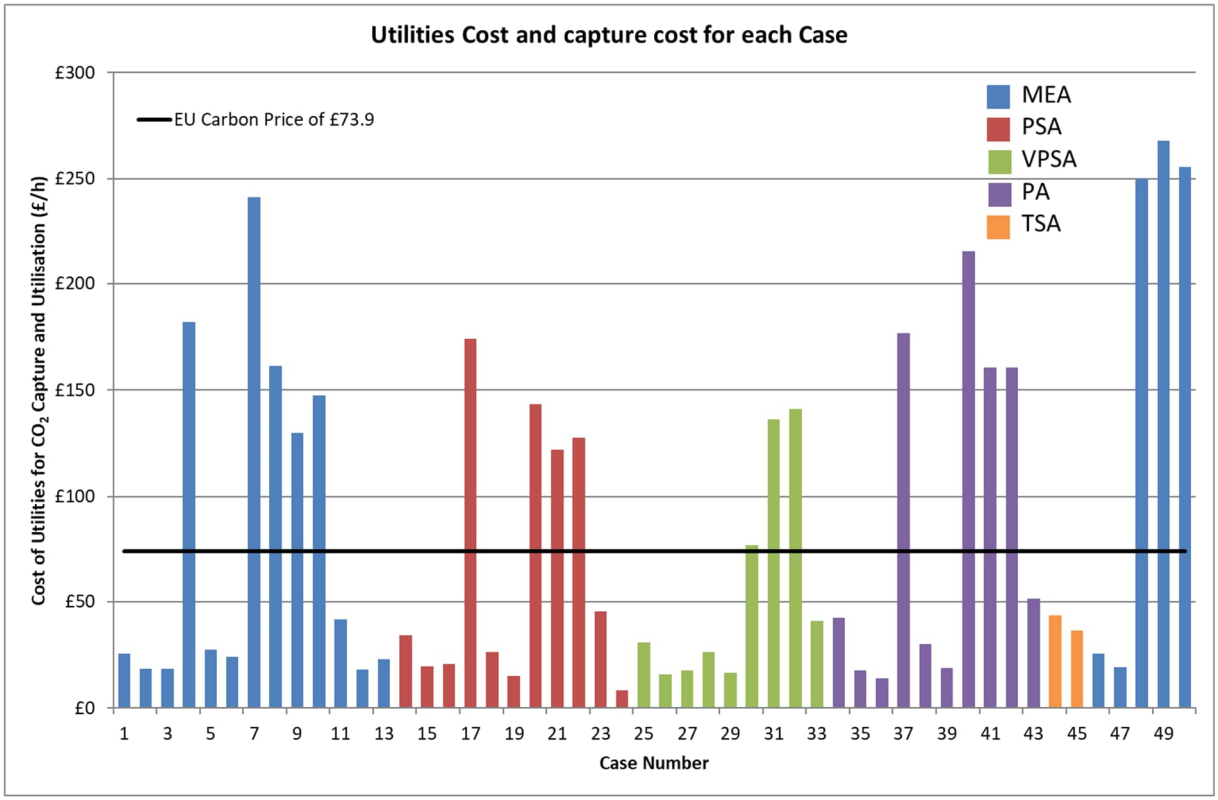

Figure 5.8: Cost to Capture 1 tonne of CO_2 for each case considered & current EU carbon price

By considering costs of capturing one tonne of CO_2, the cases involving the water shift process become increasingly attractive. This is due to its potential to increase the amount of CO_2, which can be captured without using an expensive utility such as electricity or hydrogen.

All utility costs bar H_2 are index linked to the cost of natural gas. This means that most utility costs will be 2.5 times higher than that calculated in this work. As the cost applies a credit for exported blast furnace gas, the costs are expected to rise equally across all cases.

5.5 Conclusions

From the work to date, some technologies offer clear advantages in the CO_2 capture stage. Chemical Absorption was identified as the most promising option due to the following considerations:

- The absorber operating pressure is in line with supply pressure of blast furnace gas. Therefore, no large gas compressor would be required to increase the gas pressure prior to the CO_2 removal plant. This compressor would incur significant capital cost to meet the gas flow duty. Removing this equipment from the capture plant will allow a reduced capital equipment cost.
- Separated CO_2 purity is higher than with other technologies. The main contaminant is gaseous water which is more easily removed than CO and N_2 prior to onward transportation. Therefore, purification costs will be reduced and a wider range of CO_2 utilisation options will be available when chemical absorption is used to capture the CO_2.
- There is a high retention of useful CO and H_2 components in the blast furnace gas. Because of this, there is less loss of chemical energy to the other users within the steelworks. Consequently, there is little need to purchase costly natural gas from outside of the steelworks.
- It is a mature technology used by a variety of industries. There is significant research in a variety of chemical solvents and process improvements. These would need to be investigated further to define the best technical solution for treating blast furnace gas.
- Most steelworks have a high-capacity steam network, capable of supporting the flow required to the regenerator column. This results in relatively low operating costs compared to using scarcer electrical energy based separation methods.

Chemical Absorption does have a potential drawback of a slower response time to changes in the inlet gas composition. Some comprehension of the effect of variable inlet conditions has been gained through pilot scale tests (Montañés, 2018 & Moser, 2020), but not for gasses of a similar composition and variation to blast furnace gas. It is therefore likely that the capture plant location will be driven downstream of a gas holder to buffer changes in gas flow and composition. Furthermore, the variation will likely depend on the design and dimensions of the capture plant itself, especially the solvent inventory. To truly understand these factors, a more in-depth analysis of the capture process would be required.

PSA and VPSA routes have been shown to capture a higher percent of CO_2 from the gas stream than chemical absorption. The separated CO_2 is generally contaminated with CO and H_2. These impurities must be removed before the CO_2 can be stored or utilised which will incur further energy consumption, not included within this assessment. It is suggested that this additional energy use will bring the energy demand for the adsorption methods more in-line with that estimated for chemical absorption.

Physical absorption was considered to have the lowest level of CO_2 capture of all the capture methods considered. Because of the gas pressures involved with this capture method, an expansion turbine can be added to the flowsheet to recover energy from the treated gas stream. But even with this electrical energy recovery, physical absorption has the highest electrical energy requirement of all the CO_2 capture technologies. As with chemical absorption, detailed plant design will allow an increased capture rate and reduced energy consumption to be realised. Overall, this technology is the least favoured for treating blast furnace gas, due to the requirement to compress large volumes of gas to a high pressure.

The assessment that chemical absorption is a better fit for removing CO_2 from blast furnace gas is at odds with several literature sources (Kim, 2015 & Quader, 2016). It should be noted that these sources often do not consider the difference in availability between electricity and steam and therefore the negative influence of using large amounts of electricity to capture CO_2 from a gas stream.

A large range of storage and utilisation options were also considered to dispose of the CO_2 captured from the blast furnace gas. The work completed to date has highlighted that any utilisation of CO_2 will generally require a large energy source (either thermal or electrical). An example of this would be the regeneration of CO_2 using plasma catalysis. Whilst small scale applications appear promising in literature, a full scale plant would more than double the energy requirement of the blast furnace process. A further technology with clear disadvantages is the use of CO_2 to feed algae. Whilst the energy requirement is very low, the land usage is enormous. This has the potential to lead to competition for space with agricultural land and areas identified for re-forestation.

Alternatively, a scheme including a water gas shift step prior to the capture stage could be introduced to generate hydrogen. This would result in a reduced calorific

value of the gas available to the Steelworks Power Plant. The advantages of this technology are:

- Higher CO_2 capture (although this results in a bigger capture plant)
- Production of hydrogen which could be sold to offset the cost of CO_2 capture, injected into the blast furnace to reduce carbon fuels or used to produce directly reduced iron. This could either be fed to the blast furnace or an electric arc furnace.

It should also be noted that the required amount of steam would be approximately quadruple that of a system without the WGS step. This increase is unlikely to be easily accommodated by any existing Steelworks steam network and may require additional steam boilers to be installed utilising either waste heat sources or fuel gases.

The assessment of utility costs suggests that most of the cases considered will result in costs below that charged to emit CO_2 to the atmosphere. The study therefore indicates that there is a commercial case to investing and deploying carbon capture to treat blast furnace gas. It is worth noting that the derived utility costs for carbon capture in this work are lower than reported elsewhere. This could be due to the higher concentration of CO_2 in the blast furnace gas leading to a more efficient carbon capture process. Alternatively, it may indicate that the availability of certain utilities, such as steam, leads to a lower cost on the steelworks than considered in other work. Taking the case of chemical absorption, references (Gentile, 2022 & van Dijk, 2017) consider costs per tonne of CO_2 captured between 24 and 36 £/t_{CO2} whereas a figure of 26 £/t_{CO2} is estimated for case 1 in Figure 5.8.
For pressure swing absorption (ULCOS, 2009) a range of between 21.7 and 52 £/t_{CO2} is given for operating costs, which includes a cryogenic step to purify the captured CO_2. Case 26 in Figure 5.8 estimates a value of 34 £/t_{CO2} which sits between these values, although the case excludes the power consumption and therefore operating cost of the cryogenic step. This will likely push the true operating cost towards the maximum range defined by the equipment supplier.

Most research into chemical absorption reports (Brown, 2016 & Hamborg, 2014) operating costs as an energy consumption per tonne of CO_2. This would appear to consider solely the regeneration energy in the form of steam and ignore electrical energy consumption for gas compressors, water and solvent pumps. This makes direct comparison between these literature sources and this work tricky as the different authors may not report results on a like for like basis.

Overall, this chapter identifies chemical absorption as the most promising type of carbon capture for removing CO_2 from blast furnace gas. It highlights that there is the potential for a financial benefit by adopting this technology. The work considered basic factors for CO_2 capture rate and the determination of energy consumption required to regenerate the capture solvent. The next chapter will aim to challenge the assumptions made within this chapter through advanced process modelling of the capture plant equipment. Furthermore, different chemicals and blends will be considered to judge the effect on capital cost and energy requirement for such a plant.

Chapter 6. Chemical Absorption Plant Design

6.1 Chapter Introduction

In the previous chapter, an initial analysis of different technologies for capturing CO_2 from blast furnace gas was carried out. From the assessment, chemical absorption was highlighted as the most promising method for removing CO_2, considering the inlet gas conditions and available utilities. To challenge the basic assumptions made within the previous chapter, a specialised computer simulation of the chemical absorption process utilising Aspen HYSYS® was employed. This allowed a more accurate modelling of the process and an estimation of equipment sizing. The model setup and procedure are detailed within Chapter 3.

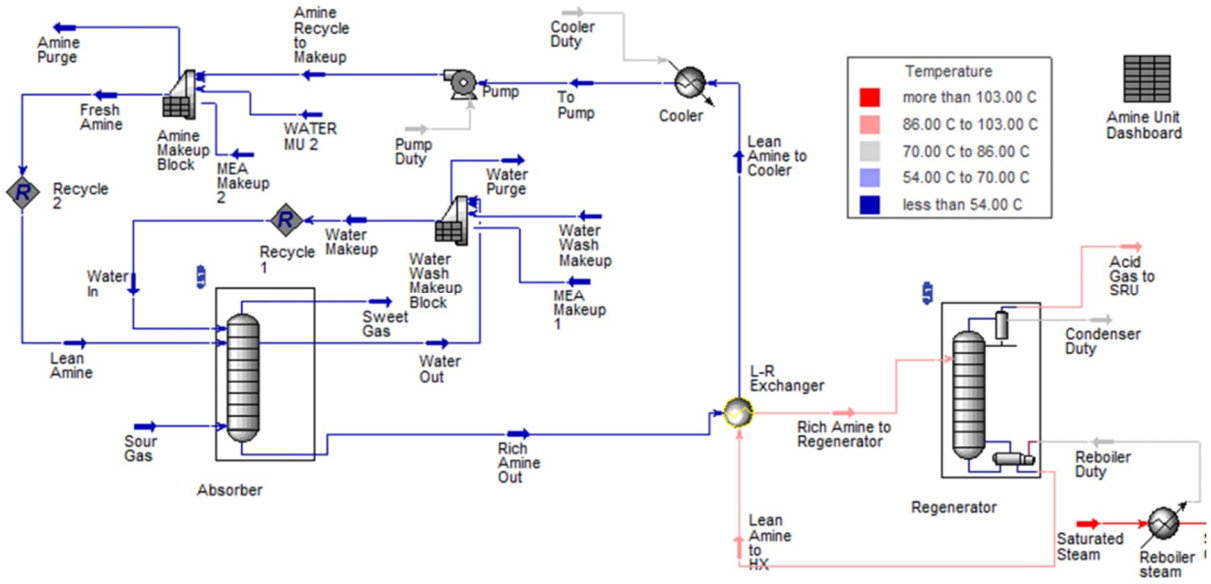

Figure 6.1: Flowsheet of chemical absorption based CO_2 capture

Figure 6.1, shows the flowsheet of the chemical absorption system used to remove CO_2 from blast furnace gas. The gas is contacted with a liquid containing an amine which chemically reacts with CO_2 and removes it from the gas stream. The absorber column, where the gas and liquid phases meet, is filled with a packing material to increase the contact area between the gas and liquid phases. The gas, which has had a portion of CO_2 removed, leaves from the top of the absorber column. Some further cooling and demisting of this gas stream may be required, based on the increase in gas temperature as it rises through the absorber column. The amine, rich in CO_2, leaves the absorber column from the base where it is pumped through a heat

exchanger to the regenerator column. The heat exchanger transfers heat from the lean amine stream leaving the base of the regenerator column to preheat the rich amine stream entering the top of the regenerator column. Furthermore, this also lowers the temperature of the lean amine and reduces the amine cooler duty. This not only reduces the physical size of the cooler unit and its cost but also reduces the volume of cooling water which must be supplied, hence reducing operating costs too.
In the regenerator column, part of the amine stream is heated in a reboiler and sent up the column to strip the CO_2 from the amine and allow the amine to be reused in the absorber column. The CO_2 leaves via the top of the regenerator column where it is passed through a condenser to remove and recover amine and water from the gas stream. The percent of CO_2 removed is determined by the gas volume and concentration of CO_2 leaving the condenser compared to the gas volume and concentration of CO_2 entering the absorber vessel.

6.2 Variation of Amine

Three different pure amines are considered in this work to determine the affect this choice has on the ability of an absorber column to remove CO_2 from a stream of blast furnace gas. The first is a primary amine, monoethanolamine (MEA), which is the benchmark amine for research into carbon capture. This is due to the large amount of data available within literature (Fosbøl, 2018 & Notz, 2012) on the ability of MEA to capture CO_2. A representation of the chemical structure of MEA is shown in Figure 6.2 below. It has a fast reaction with CO_2 but releases a large amount of heat during the chemical reaction. This in turn requires significant energy to reverse the reaction within the regenerator column. MEA can achieve CO_2 loadings as high as 0.53 mole/mole (Stec, 2015) but is susceptible to degradation by oxidising agents. The products of degradation are extremely corrosive, requiring more expensive stainless steel to be used for the construction of equipment.

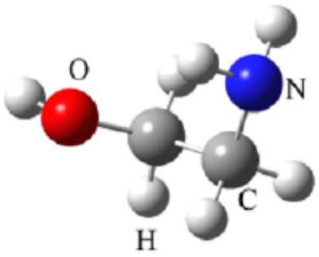

Figure 6.2: Representation of MEA (blue-N, grey-C, red-O, white-H) (Zhang, 2018)

The second is a cyclic amine, piperazine (PZ) shown in Figure 6.3 in which the carbon and nitrogen atoms form a ring-like structure. These structures maintain a fast reaction rate with CO_2 and can accommodate a higher CO_2 loading than MEA. A large amount of heat is also released on reaction with CO_2 which results in a high regeneration energy.

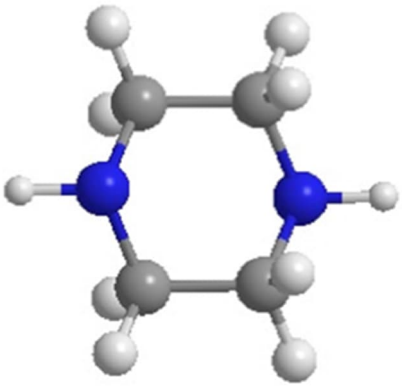

Figure 6.3: Representation of PZ (blue-N, grey-C, white-H) (Zhang, 2019)

Piperazine is not as prone to degradation as MEA and therefore does not form products corrosive to mild steel. Further research (Liu, 2020) has shown that PZ forms an inert layer of siderite ($FeCO_3$) on carbon steel which reduces corrosion rates. This allows higher concentrations to be used without damaging equipment or requiring more expensive construction materials.

A further option is a secondary amine, diglycolamine (DGA) as shown in Figure 6.4, which can be used in higher concentrations and therefore lead to lower recirculated liquid volumes.

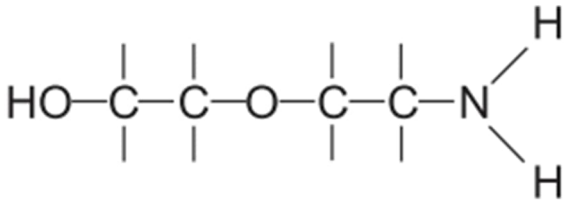

Figure 6.4: Molecular Structure of DGA (Yildirim, 2012)

This amine can lead to corrosion problems at high CO_2 loadings similar to those experienced with MEA. For this reason, loadings above 0.35 mole/mole should be avoided (Polasek, 1994). As with MEA and PZ, DGA also has a high heat of reaction with CO_2 which in turn increases the reboiler duty.

In addition to those amines described above, the following amines were also considered at an early stage. These were discounted after initial estimates showed that vastly taller absorber vessels would be required to remove 90% of the incoming CO_2 from the gas stream:

- 26 wt% diethanolamine (DEA)
- 40wt% diisopropanolamine (DIPA)
- 45wt% methyldiethanolamine (MDEA)
- 50wt% triethanolamine (TEA)

Despite displaying an underwhelming ability to capture CO_2 when used as the sole amine, MDEA was used in conjunction with MEA and PZ in a mixture of amines. This is an approach followed within available literature (Cuccia, 2019 & Zhao, 2017) to pair a slow reacting amine with a faster, promotor, amine. This allows the higher loading capacity and lower regenerator energies from the slower amines to be offset by the faster reacting amines.

The following amines and blends were considered due to their references of use within literature:

- Monoethanolamine (MEA) (Haribu, 2014)
- Piperazine (PZ) (Rochelle, 2019)

- Diglycolamine (DGA) (Sander, 1992)
- Mixture of MEA & PZ (Dugas, 2011)
- Mixture of MDEA & MEA (Cuccia, 2019)
- Mixture of MDEA & PZ (Zhao, 2017)

The above list considers the fact that amine concentrations should not be raised above certain limits as this can encourage extreme corrosivity or viscosity of the liquid leading to equipment damage or blockage. The concentrations of the amines should also sit within the validated range for the software used. Table 6.1 below identifies these ranges for amine concentration, operating temperature and CO_2 loading on a mole per mole basis.

Amine Type	Amine wt%	Temperature K	CO_2 loading mol/mol
MDEA	5.0 – 75	283 – 473	0.0004 – 1.68
DGA	20 – 65	297 – 433	0.003 – 1.41
MEA	6.5 – 40	273 – 423	0.002 – 2.15
PZ	1.7 - 30	298 - 393	0.05 – 1.69

Table 6.1: Validated range of amine concentrations, temperatures and CO_2 loadings (Dyment, 2015)

In cases where the chemical reaction between the amine and CO_2 increases absorber outlet gas temperatures over 55°C, a wash section is used at the top of the absorber column. Here, pure water is used to cool the gas stream and saturate the gas with water. By doing this a water balance is maintained within the system and losses of amine to the outgoing gas stream are limited. Of the 20 sections, or stages, within the absorber column, the wash section is assumed to occupy the top two. The remaining 18 stages are then left for CO_2 removal from the gas stream. The wash section is required as volatile amines can enter the gas stream at high temperatures. As well as increasing the consumption rate of chemicals, it also has the potential to be harmful to downstream users and to be emitted to atmosphere. In the case of CO_2 removal by blast furnace gas, the fuel gas stream leaving the absorber column will be burnt to raise steam or electricity or flared to maintain network pressure. All these

options will mean that any chemicals used to treat the gas stream would also be burnt and rendered harmless.

It should be noted, that even with the inclusion of a washing section, the purified gas temperature when MEA, PZ, and MDEA/MEA blends were considered as the amine, still rose above 45°C. The model blocks added to simulate this control the wash water chemistry to a fixed amine percent and total flowrate. It also determines a cooler duty to maintain the water temperature entering the absorber column at the top stage. The absorber was modified to drain the wash water from between the 2nd and 3rd column stage.

In cases where little increase of gas temperature rise is predicted, no wash section is included allowing CO_2 removal to occur at every stage within the absorber column and results in a shorter overall absorber column.

The amine is introduced to the absorber column at either the third stage (if a wash section is present) or at the first stage. The rich amine leaves the absorber column at the bottom stage where pump outlet pressure is adjusted to maintain a single phase stream through the rich/lean heat exchanger and into the top of the regenerator column.

None of the cases considered intercoolers within the absorber column design. An intercooler takes a portion of the liquid descending through the absorber column and cools it before returning it to the column. This allows the cooled liquid to react with more CO_2 and reduce the absorber column height. The cooling will limit the gas temperature increase and reduce amine loss to the gas stream leaving the absorber column.

The effect of compressing the inlet gas to the absorber column on equipment cost was also considered. It is anticipated that by using a higher pressure gas, the absorber column size can be reduced, resulting in an overall reduction in capital cost. This consideration is only made for MEA as a sole amine and has not been extended to other amine options.

Parameters kept constant in all model runs are recorded in Table 6.2:

Parameter	units	Value
Blast Furnace Gas Flow	kmol/h	13120
Blast Furnace Gas Temperature	°C	40
Blast Furnace Gas Pressure	bar	1.1
Blast Furnace Gas Composition		
CO_2	mol%	22.5
CO	mol%	23.2
N_2	mol%	45.0
H_2	mol%	2.7
H_2O	mol%	6.6
Lean Amine Temperature	°C	40
Lean Amine Pressure	bar	2
Gas Temperature leaving regenerator	°C	40
Column Packing Type		Metal Pall Rings
Column Stages		20
Absorber column packing size	mm	50
Absorber column packing size	mm	38

Table 6.2: Parameters kept constant within Aspen HYSYS® Models

A target of 90% CO_2 removal was achieved in the models by adjusting the Absorber packing height and lean amine flow to the absorber. The gas pressure drop through the column was limited to 35mbar to give a minimum outlet gas pressure of 1.065 bar by varying the absorber diameter. This pressure was targeted as it is in line with typical gas network pressures within a steelworks to allow the gas to be used elsewhere, such as the on-site boilers to raise steam and generate electricity.

The CO_2 removal was defined as given in Equation 6.1 below:

$$CO_2 \text{ Removal} = \frac{Q_{AG} \times x_{AG}CO_2}{Q_{SG} \times x_{SG}CO_2} \qquad \text{Equation 6.1}$$

Where:

Q_{AG} is the flow of Acid Gas leaving the condenser at the top of the Regenerator Column (kgmol/h).

Q_{SG} is the flow of Sour Gas entering the Absorber Column (kgmol/h)

$x_{AG}CO_2$ is the mole fraction of CO_2 in the Acid Gas (mol/mol)

$x_{SG}CO_2$ is the mole fraction of CO_2 in the Sour Gas (mol/mol)

Capital cost will be reported as ratioed figures and adopt the same material of construction for all cases. In practice, some of the amines assessed may require more expensive materials or corrosion resistant linings to be used.

No assessment of amine toxicity or flammability has been considered within this work as this should be made during the design phase of a project considering the locally applicable regulations. For this work, it is presumed that any amine escaping the absorber column within the gas stream will ultimately be burnt with the gas either at an onsite power plant or gas flare. It is therefore expected that any amine lost in this manner will pose little threat to the environment or surrounding communities.

6.3 Results

The model results for each amine or mixture of amines based on the fixed parameters in Table 6.2 are reported in the following sections. The results indicate the amine flowrate, absorber and regenerator column height required to reach the target CO_2 removal percent.

Reboiler duties to regenerate the amines and blends considered is significant and higher than estimated in the work reported in the previous chapter. The results also indicate loss of amine to the purified gas stream which was not considered in the assessment of operating costs.

Another factor excluded in the assessment in Chapter 5 is the cooling requirement of both the lean amine before it enters the absorber column and the gas stream leaving the regenerator column. The sum of these cooling duties is of a similar scale of magnitude to the heating duty of the reboiler which will add further operating costs to the capture plant.

6.3.1 MEA

Using MEA as the sole active component for capture of CO_2 exemplifies the fast, exothermic reaction between MEA and CO_2. This results in an increased sweet gas temperature leaving the absorber column. Because of this, the vaporisation and loss of amine into the purified gas stream increases. The highlighted output data from the modelling with MEA is included in the following Table 6.3. Three cases are

considered to identify the effect of amine concentration on equipment size. In addition, the third case also increases liquid flowrate through the absorber column to limit purified gas temperature and remove the requirement for a wash section at the top of the absorber column.

Parameter	**Units**	**Case 1**	**Case 2**	**Case 3**
Amine		MEA	MEA	MEA
Amine Concentration	mass%	28	20	25.5
Liquid Flowrate	m^3/h	2500	2500	3000
Lean Amine CO_2 Loading	mass/mass	0.149	0.118	0.142
Rich Amine CO_2 Loading	mass/mass	0.373	0.346	0.347
Sweet Gas Flow	kgmol/h	10723	10959	10228
Sweet Gas Temperature	°C	48.4	51.3	40.4
Sweet Gas Pressure	Bar abs	1.074	1.068	1.070
Sweet Gas CO_2 content	mol%	2.60	2.70	2.76
Acid Gas Flow	kgmol/h	2775	2760	2772
Acid Gas Pressure	Bar abs	1.974	1.972	1.963
Acid Gas CO_2 content	mol%	96.17	96.11	96.14
Amine temperature at regenerator	°C	109	109	105
Reboiler Duty	MW	179.8	175.9	200.6
Condenser Duty	MW	72.5	72.0	72.4
Amine Cooler Duty	MW	99.5	96.0	136.5
Amine Make-Up Rate	m^3/h	0.13	0.07	0.07
Absorber packing Height	m	9.0	11.3	8.2
Absorber column Diameter	m	9.0	9.0	9.0
Regenerator packing Height	m	9.5	9.5	9.5
Regenerator column Diameter	m	8.0	8.0	8.0
CO_2 Removal	%	90.4	89.9	90.3

Table 6.3: Results from modelling of carbon capture using MEA

The table above shows that around 90% of the incoming CO_2 can be captured using a range of MEA concentrations. The first case minimises liquid flow through the absorber column to provide the lowest capital cost solution. The low liquid flow and

high MEA concentration leads to an increase in gas temperature as it passes through the absorber column. A temperature of 48.4°C is observed after the wash section which is only slightly above the gas temperature entering the absorber column.

For the second case, the amine concentration is lowered from 28% to 20% to observe what changes are required to still capture approximately 90% of the incoming CO_2. The liquid flowrate is maintained and the results show that there is relatively little change in reboiler, condenser and cooler duty compared to the first case. But the absorber column height must increase by 2.3m to maintain a similar CO_2 capture rate as reported in case 1. The sweet gas temperature leaving the absorber column in the lower concentration, case 2, is 3.9°C higher than for the higher amine concentration case.

The third case increases the liquid flow by 500m^3/h from that considered in case 1 and decreases the MEA concentration. The increase in flow allows a greater volume of liquid to absorb the same level of heat from the reaction between MEA and CO_2. The resulting sweet gas temperature rise through the absorber column is then minimised which allows the removal of the wash section at the top of the absorber vessel. This in turn lowers the overall height of the absorber column by almost 10% compared to case 1. The duty of both the reboiler and cooler units increase as both must cater for an increased liquid flowrate. The results indicate that, despite the significantly lower sweet gas temperature in case 3, the make-up rate of MEA is very similar to that reported in case 2. For this reason, the third case within Table 6.3 was not considered in the capital cost analysis reported in section 6.4.

Predicted CO_2 loadings of the lean and rich amine streams are all below the validated range for the software model reported previously in Table 6.1.

6.3.2 PZ

When PZ is the sole amine for CO_2 capture, the reaction with CO_2 is both faster and more energetic than with MEA. The gas temperature leaving the absorber column is also higher with a correspondingly increased loss of amine to the sweet gas stream. Despite higher temperatures within the absorber column, using PZ allows the lowest liquid flows, resulting in benefits to equipment size, heat requirement and electrical consumption from pumps. A summary of the calculated data is included in the following Table 6.4. As with MEA, three cases are considered to give an understanding of the impact of amine concentration on absorber height.

Case 1 considers a higher PZ concentration to minimise equipment size. Sweet gas temperatures are predicted to reach 64°C even with the inclusion of a wash section at the top of the absorber column. This gas temperature leads to the highest amine make-up rate reported of all the cases considered by this work which may represent a high operating cost to replace the lost amine.

Case 2 considers the same liquid flowrate as in case 1 but for a lower PZ concentration. A wash section is still required in the case at the top of the absorber vessel to cool the sweet gas. The predicted gas temperature is 10°C lower than for case 1 with a decrease in amine make-up rate also observed. The absorber column height increases by around a third to maintain a similar CO_2 capture rate as in case 1. By doing this the reduction in PZ concentration is offset by a longer gas residence time within the absorber vessel to meet the ~90% CO_2 removal target.

Finally, case 3 considers an increase in liquid flowrate and decrease in PZ concentration compared to the other cases. This is to develop a scenario where the gas temperature rise through the absorber column is reduced and removes the requirement for a wash section at the top of the absorber column. To achieve this though, the liquid flowrate more than doubles and the PZ concentration is lowered beneath that considered in case 2 in order to reduce the gas temperature rise. These two changes result in an absorber vessel of greater height than in case 1 but shorter than in case 2. Reboiler duty for case 3 is similar to that reported for case 2 but amine cooler duty is the highest of all three cases. The aim of reducing gas temperatures throughout the absorber column do appear to limit the required make-up rate of PZ, with case 3 reporting the lowest rate of all the cases. In terms of equipment size, case 3 represents a midpoint between cases 1 and 2 for absorber column size. Therefore, this case will not be considered within in the capital cost analysis reported in section 6.4.

Parameter	Units	Case 1	Case 2	Case 3
Amine		PZ	PZ	PZ
Amine Concentration	mass%	26	15	13
Liquid Flowrate	m^3/h	1400	1350	3000
Lean amine CO_2 Loading	mass/mass	0.154	0.136	0.162
Rich amine CO_2 Loading	mass/mass	0.771	0.790	0.762
Sweet Gas Flow	kgmol/h	12273	11143	10170
Sweet Gas Temperature	°C	64.13	54.16	40.64
Sweet Gas Pressure	Bar abs	1.089	1.076	1.071
Sweet Gas CO_2 content	mol%	2.04	2.45	1.69
Acid Gas Flow	kgmol/h	2811	2784	2887
Acid Gas Pressure	Bar abs	1.984	1.975	1.982
Acid Gas CO_2 content	mol%	96.19	96.16	96.17
Amine temperature at Regenerator	°C	108	108	111
Reboiler Duty	MW	161.6	171.8	172.8
Condenser Duty	MW	73.3	72.2	75.2
Lean Amine Cooler Duty	MW	61.4	77.9	98.7
Amine Make-Up Rate	m^3/h	0.56	0.13	0.04
Absorber packing Height	m	6.4	9.2	8.5
Absorber column Diameter	m	9	9	9
Regenerator packing Height	m	9.5	9.5	8.5
Regenerator column Diameter	m	8	8	8
CO_2 Removal	%	91.6	90.7	94.1

Table 6.4: Results from modelling of carbon capture using PZ

The lean and rich amine CO_2 loadings for all three cases sit within the validated range for PZ within the software model reported previously in Table 6.1.

6.3.3 DGA

A single case was considered using diglycolamine (DGA) to capture CO_2 due to a lower number of references within literature (Sander, 1992) of using DGA compared to MEA and PZ. The reboiler and amine cooler duties are lower than for MEA in case 1 despite considering a higher liquid flowrate. The results suggest that DGA has a

less exothermic reaction with CO_2 and that the greater concentration of DGA compared with MEA is a benefit to the regeneration energy. For the higher concentration, there is a reduced amount of water within the recirculated liquid which is also required to be heated at the reboiler.

To remove 90% of the incoming CO_2 the height of the absorber and regenerator columns is required to increase above that used for MEA. The diameters of these columns remain similar between the DGA and MEA cases. The amine make-up rate is the lowest of the three pure amine cases considered at only $0.5m^3$ per day. A reason for this is the gas temperature leaving the absorber column being around 15°C less than that for MEA case 1. The lower gas temperature means less of the volatile DGA is lost to the gas leaving the absorber column and that no wash section is required.

The CO_2 loading of the lean and rich amine is the lowest of all cases. This is due to the combination of the high amine flowrate and high concentration of DGA.

Most importantly, the predicted rich loading is below the recommended limit of 0.35 mole/mole given in Table 6.1. Due to the low loadings within the results in Table 6.5, no corrosion issues are foreseen when using this amine.

Parameter	Units	Case 3
Amine		DGA
Amine Concentration	mass%	33
Liquid Flowrate	m^3/h	3000
Lean Amine CO_2 Loading	mass/mass	0.0151
Rich Amine CO_2 Loading	mass/mass	0.2892
Sweet Gas Flow	kgmol/h	10270
Sweet Gas Temperature	°C	40.33
Sweet Gas Pressure	Bar abs	1.067
Sweet Gas CO_2 content	mol%	3.08
Acid Gas Flow	kgmol/h	2756
Acid Gas Pressure	Bar abs	1.985
Acid Gas CO_2 content	mol%	96.14
Amine temperature at regenerator	°C	116
Reboiler Duty	MW	164.6
Condenser Duty	MW	71.92
Lean Amine Cooler Duty	MW	94.79
Amine Make-Up Rate	m^3/h	0.02
Absorber packing Height	m	10.2
Absorber column Diameter	m	9
Regenerator packing Height	m	12
Regenerator column Diameter	m	9
CO_2 Removal	%	89.8

Table 6.5: Results from modelling of carbon capture using DGA

6.3.4 MEA & PZ

The two fastest reacting amines, MEA and PZ, could be combined to capture CO_2. The overall amine concentration is lower than considered with the pure amine cases 1 & 2, which results in a much lower absorber outlet gas temperature. This can be explained as there is more water within the system to absorb the heat of reaction between the amines and the CO_2. As the temperature increase of both gas and liquid phases is lower the loss of amine to the gas stream is also reduced to a similar level

to using DGA. As with previous amines, two cases are considered to determine the effect on absorber column size with varying amine concentration.

Parameter	Units	Case 1	Case 2
Amine		MEA & PZ	MEA & PZ
Amine concentration	mass%	20 & 2.5	15 & 2.5
Liquid Flowrate	m^3/h	2800	2800
Lean Amine CO_2 Loading	mass/mass	0.0924	0.780
Rich Amine CO_2 Loading	mass/mass	0.3538	0.3529
Sweet Gas Flow	kgmol/h	10252	10263
Sweet Gas Temperature	°C	40.98	40.54
Sweet Gas Pressure	Bar abs	1.084	1.081
Sweet Gas CO_2 content	mol%	2.78	2.84
Acid Gas Flow	kgmol/h	2779	2764
Acid Gas Pressure	Bar abs	1.97	1.99
Acid Gas CO_2 content	mol%	96.16	96.18
Amine temperature at Regenerator	°C	111	111
Reboiler Heat Addition	MW	175.5	172.4
Condenser Duty	MW	72.60	72.8
Lean Amine Cooler Duty	MW	104.33	105.2
Amine Make-Up Rate	m^3/h	0.02	0.01
Absorber packing Height	m	6.8	8
Absorber column Diameter	m	9	9
Regenerator packing Height	m	10	10
Regenerator column Diameter	m	8	9
CO_2 Removal	%	90.5	90.0

Table 6.6: Results from modelling of carbon capture using MEA & PZ

Case 1 in Table 6.6 above considers a higher concentration of the main amine, MEA, and the promotor PZ in order to minimise equipment size. Reboiler duty is lower than reported for the MEA cases in Table 6.3 but slightly higher than for the PZ cases in Table 6.4. Make up rate is much lower than that estimated for the PZ or MEA cases which is to be expected as the gas temperatures within the absorber column are

lower when a mixture of MEA and PZ is considered. This removes the requirement for a wash section at the top of the absorber column and reduces the height below that required when MEA is used as the sole amine for CO_2 removal.

Case 2 uses the same liquid flowrate as in case 1 but considers a lower concentration of both amines. This results in the absorber column height increasing by 1.2m to maintain a CO_2 removal rate of 90%. Unusually, the regenerator column diameter is also required to increase, due to the relatively large water content in the CO_2 capture liquid. The duties of the reboiler and amine cooler show little difference between the low and high concentration cases. Amine make-up rate is halved for case 2, compared to case 1, to reach one of the lowest values for amine make-up of all the cases considered in this work.

6.3.5 MDEA & MEA

These cases are based on a mixture of methyldiethanolamine (MDEA) with a small percentage of monoethanolamine (MEA) acting as a promoter. The MEA concentration is significantly lower than when MEA acts alone to capture CO_2. The overall amine concentration is higher though with MDEA forming most of the amine within the recirculated liquid. Because MDEA is a slow reacting amine, a higher liquid flowrate is required to reach 90% CO_2 removal from the inlet gas stream.

As with previous amines and mixtures, case 1 represents the higher concentration option to derive a smaller equipment size. The sweet gas temperature leaving the absorber column is reported to be high and therefore requires a wash section. Even with this step at the top of the absorber column, gas temperatures leaving the column will exceed 55°C for both cases. Compared to the MEA cases in Table 6.3, the height of both absorber and regenerator columns increases to maintain 90% CO_2 removal. The increased height provides an additional residence time for the MDEA to react with the CO_2 in the gas stream. As the liquid flowrate increases, the diameter of the absorber column also increases to maintain the outlet gas pressure above 1.065 bar. Despite the increased column sizes, blending MEA and MDEA lowers both the lean and rich CO_2 loading of the amines and results in a non-corrosive amine mixture.

The reboiler duty is also lower than when MEA is considered as the sole amine due to both the increase in amine concentration and the use of MDEA, the reduced reboiler duty means less steam is required to regenerate the solvent which reduces the operating cost. The lean amine cooler duty is also lower than when only MEA is

used which will reduce equipment size and the requirement for a cooling water supply.

Parameter	Units	Case 1	Case 2
Amine		MDEA & MEA	MDEA & MEA
Amine concentration	mass%	32 & 10	20 & 10
Liquid Flowrate	m^3/h	2300	2300
Lean Amine CO_2 Loading	mass/mass	0.0339	0.0310
Rich Amine CO_2 Loading	mass/mass	0.2879	0.3697
Sweet Gas Flow	kgmol/h	11470	11395
Sweet Gas Temperature	°C	57.36	56.29
Sweet Gas Pressure	Bar abs	1.072	1.065
Sweet Gas CO_2 content	mol%	2.58	2.63
Acid Gas Flow	kgmol/h	2783	2762
Acid Gas Pressure	Bar abs	1.939	1.954
Acid Gas CO_2 content	mol%	96.1	96.1
Amine temperature at Regenerator	°C	105	105
Reboiler Heat Addition	MW	162.2	172.0
Condenser Duty	MW	71.4	72.0
Lean Amine Cooler Duty	MW	77.0	86.9
Amine Make-Up Rate	m^3/h	0.07	0.04
Absorber packing Height	m	14.4	18.5
Absorber column Diameter	m	10.3	10.3
Regenerator packing Height	m	15	15
Regenerator column Diameter	m	8	8
CO_2 Removal	%	90.6	90.0

Table 6.7: Results from modelling of carbon capture using MDEA & MEA

Case 2 maintains the same liquid flowrate but with a lower concentration of MDEA. To maintain CO_2 capture percentage, the absorber column is required to increase by 4.1m in height. This results in the tallest absorber column of all cases considered, due to the requirement for a wash section and the use of the slower acting MDEA. The reboiler and lean amine cooler duties also increase compared to case 1 because

of the more dilute amine concentration. The gas temperature leaving the absorber column is very similar when comparing cases 1 and 2 in Table 6.7, which suggests it is a result of the MEA concentration which remain constant between the cases.

6.3.6 MDEA & PZ

The slowest reacting amine is paired with the fastest, namely MDEA with PZ acting as a promoter. The PZ concentration is significantly lower than that considered when PZ was used as a sole amine. The MDEA concentration is also higher than when used in conjunction with MEA.

This combination results in the highest liquid circulation flow through the capture system as the CO_2 capture is mostly achieved via the slower acting MDEA. Due to the high liquid flow though, the gas temperature rise through the absorber column is lower than using PZ on its own. This removes the need to include a wash section at the top of the absorber column. But the extra packing height required to capture CO_2 counteracts the savings, because of the removal of the wash section and results in an absorber column 3.1m taller than when PZ is used. The combination of MDEA and PZ results in the minimum of amine loss.

The combination of MDEA and PZ also results in the second lowest rich and lean amine CO_2 loadings, with only the use of DGA giving a lower CO_2 loading. This leads to the lowest reboiler energy of all the cases considered in this work. The amine cooler duty is close to the other mixed amine cases considered, but higher than the case considering PZ as the sole amine.

Case 1 considers a higher concentration of MDEA than case 2. Both cases maintain the same liquid flowrate through the system to observe the impact on absorber height. By comparing cases 1 and 2, it is observed that the absorber height must increase by 2m to counteract a reduction in MDEA concentration from 42 to 20wt%. For this combination of amines there is no notable change in reboiler duty for the two concentrations, which is due to the low lean amine CO_2 loading predicted for both cases.

The lean amine cooler duty also remains similar for both cases in Table 6.8, which might indicate that the liquid flowrate could be reduced in further analysis of this combination of amines.

Parameter	Units	Case 1	Case 2
Amine		MDEA & PZ	MDEA & PZ
Amine concentration	mass%	42 & 2.5	20 & 2.5
Liquid Flowrate	m^3/h	3750	3750
Lean Amine CO_2 Loading	mass/mass	0.0059	0.0124
Rich Amine CO_2 Loading	mass/mass	0.1846	0.3668
Sweet Gas Flow	kgmol/h	10219	10265
Sweet Gas Temperature	°C	40.36	40.38
Sweet Gas Pressure	Bar abs	1.089	1.087
Sweet Gas CO_2 content	mol%	2.78	2.71
Acid Gas Flow	kgmol/h	2782	2774
Acid Gas Pressure	Bar abs	1.928	1.980
Acid Gas CO_2 content	mol%	96.06	96.15
Amine temperature at Regenerator	°C	116	116
Reboiler Heat Addition	MW	143.7	143.8
Condenser Duty	MW	72.57	72.22
Lean Amine Cooler Duty	MW	72.68	73.48
Amine Make-Up Rate	m^3/h	0.00	0.1
Absorber packing Height	m	9.5	11.5
Absorber column Diameter	m	9.5	9.5
Regenerator packing Height	m	10	10
Regenerator column Diameter	m	8.5	8.5
CO_2 Removal	%	90.5	90.4

Table 6.8: Results from modelling of carbon capture using MDEA & PZ

6.4 Assessment of capital cost

Eleven different models (amine types and concentrations) described in the previous sections were interrogated using the Aspen process economic analyser to develop equipment costs. The costs for each case were then ratioed against the model considering 28t% MEA by weight to compare them and to avoid any common error in the costing. The ratios of the capital expenditure (capex) cost for each model against that for the 28%wt MEA case is included in Figure 6.5.

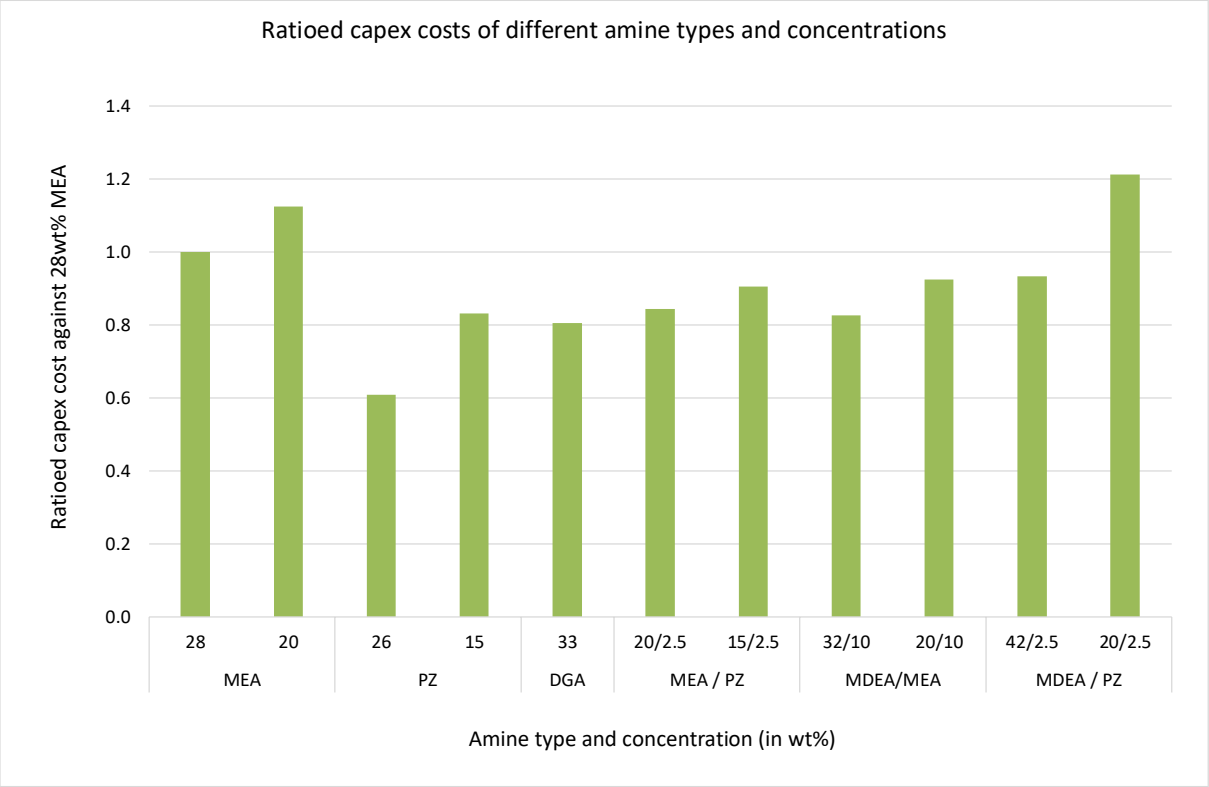

Figure 6.5: Graph of plant capital costs from 2018 for different amines and concentrations

Figure 6.5 above shows that only two of the options results in a capital equipment cost higher than the benchmark 28wt% MEA case. These are either when 20wt% MEA is considered (second column) or when a blend of 2.5wt% PZ and 20wt% MDEA is used (last column). The general trend, that a higher concentration of amine will result in lower capital costs is to be expected. This can be explained by the reduced size of absorber and regenerator vessels, but also pumps to circulate the amine, reboiler and heat exchangers. The trend is least pronounced when a combination of MEA and PZ is used to capture CO_2. By comparison, the trend is clearest when PZ is used as the sole amine or when used with MDEA.

The lowest capex option is the 26wt% PZ option (third column) due to the high reactivity of PZ leading to low recirculation volumes of amine and therefore smaller equipment size. The reboiler duty for this case is slightly lower than the 28wt% MEA case reported in section 6.3.1, but still one of the highest amongst the cases assessed.

The costings for the higher concentration options were then split down to observe the difference in individual equipment size for each of the higher amine concentration

cases. The true equipment costs developed using aspen economic analyser, following the methodology outlined in Chapter 3, are shown graphically within Figure 6.6. Owing to the database of equipment costs being from 2018, the costs should only be considered on a comparative, not absolute basis. Traditionally, engineering companies consider approximately a 3% increase in prices year on year of equipment. However, due to the longer lasting effects of COVID19 construction costs increased by approximately 1/3rd between 2018 and 2023 (Costmodelling, 2023) and prices for equipment also likely to have increased by a similar level.

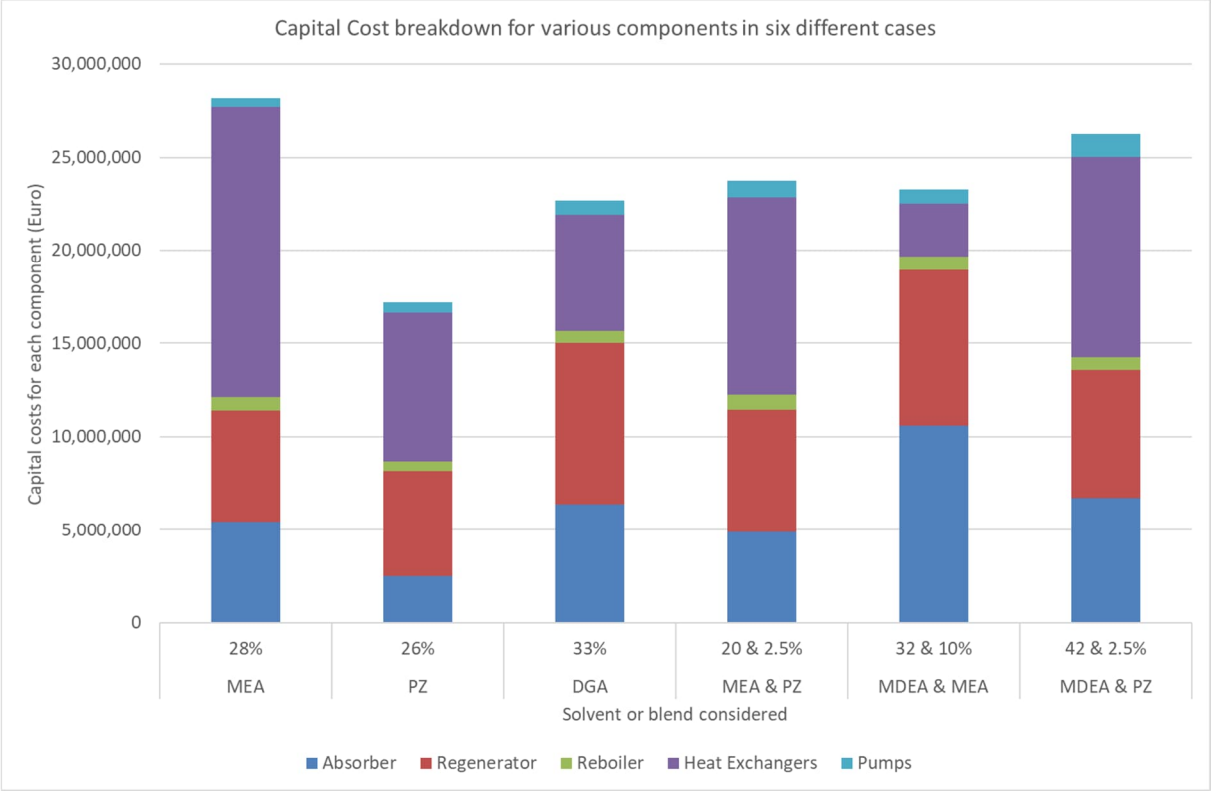

Figure 6.6: Graph of cost breakdown for individual elements of the capture plant

Within Figure 6.6 above, the heat exchanger category includes all equipment to transfer heat from the lean amine to the rich amine stream and cool lean amine and wash water streams. The pump category includes equipment for transferring rich amine from the absorber to the regenerator column and lean amine pumps for returning the, now lean, amine to the absorber column. Due to their significant contribution toward total capital cost, the absorber and regenerator column are split into their own categories.

The smallest impact on capital cost comes from the pumps required to circulate lean and rich amine around the carbon capture system. The estimated cost for this equipment varies only very slightly between the cases, despite a range of flowrates from 1300m^3/h to 3750m^3/h. The likely reason for this is the low capital cost for this equipment type, especially when compared to the absorber and regenerator vessels. The same can be said for the reboiler at the base of the regenerator column. The items with the most varying cost across the cases are the absorber column and heat exchangers. The absorber column would appear to vary in line with the reactivity of the amine or blend of amines. This is evident as the absorber column cost is lowest for PZ (the fastest acting amine) and highest for a mixture of MEA and MDEA.

For the heat exchanger costs, there is no obvious correlation between amine flow or reactivity with CO_2. A possible explanation for this is the different rich amine temperatures entering the regenerator column. These temperatures are set considering the thermal stability of the amines or blends which in turn influences the duty, and therefore cost, of the lean/rich heat exchanger. In cases where only a small transfer of heat from lean to rich amine streams is possible, the lean amine must undergo more cooling before it enters the absorber column. Finally, cases with a wash section at the top of the absorber column will include an additional heat exchanger in this cost category to control the water temperature entering the absorber column.

6.4.1 Benefit of inlet gas compression

As a variation to the 28%wt MEA case, a gas compressor was considered upstream of the absorber column to increase the gas pressure from 0.1 to 10 bar gauge. This was assessed as a higher gas pressure will increase the rate of CO_2 absorption and allow a reduction in absorber column diameter. It was intended to observe if the capital cost of the gas compressor would outweigh the reduction in capital cost due to the smaller absorber column. A gas cooler was added downstream of the compressor to control the gas temperature entering the column to 40°C to match the case without gas compression. Finally, a water drain was added downstream of the cooler to ensure that the gas was saturated at the specified temperature and pressure conditions. The results suggested a saving of approximately 47.4% in the cost of the CO_2 capture equipment due to reduction in the size of both absorber and regenerator columns but also the duties of the reboiler and lean amine cooler. The

cost of the gas compressor and auxiliaries is estimated to exceed 4.5 times the saving in capital cost by the capture equipment resulting in an overall increase in capital cost. Therefore, the use of a gas compressor is not seen as cost effective for the removal of CO_2 from blast furnace gas.

Parameter	**Units**	**Case 1**	**Case 2**
Amine		MEA	MEA
Amine Concentration	mass%	28	28
Amine Flowrate	m^3/h	2500	2300
Lean Amine CO_2 Loading	mass/mass	0.149	0.178
Rich Amine CO_2 Loading	mass/mass	0.373	0.420
Sweet Gas Flow	kgmol/h	10723	9652
Sweet Gas Temperature	°C	48.4	40.01
Sweet Gas Pressure	Bar abs	1.074	9.982
Sweet Gas CO_2 content	mol%	2.60	2.91
Acid Gas Flow	kgmol/h	2775	2784
Acid Gas Pressure	Bar abs	1.974	1.982
Acid Gas CO_2 content	mol%	96.17	95.95
Amine temperature at Regenerator	°C	109	117
Reboiler Duty	MW	179.8	152.8
Condenser Duty	MW	72.5	73.3
Amine Cooler Duty	MW	99.5	79.1
Amine Make-Up Rate	m^3/h	0.13	0.00
Absorber packing Height	m	9.0	4.3
Absorber column Diameter	m	9.0	4.85
Regenerator packing Height	m	9.5	5
Regenerator column Diameter	m	8.0	7
CO_2 Removal	%	90.4	90.5

Table 6.9: Results from modelling of carbon capture using MEA and considering inlet gas compression

6.5 Conclusions

Aspen HYSYS® was used to undertake a more detailed study of chemical absorption of CO_2 from blast furnace gas. Thirteen cases were considered using either a single

amine or a blend of two amines. The aim of the assessment was to ascertain what affect, if any, amine choice would have on equipment capital cost. Although the general flowsheet was kept constant for all the cases, models where MEA and PZ were used as the sole amine and the mixture of MEA and MDEA required the addition of a wash section at the top of the absorber column. In these cases, additional equipment was added to limit the gas temperature leaving the absorber column and therefore reduce amine losses from the capture system. Other factors investigated included the physical size of the absorber and regenerator column and the recirculating flowrate of amine. Finally, the regeneration energy and cooling duties of the various cases were also compared.

To rank the cases from most to least favourable, a rough capital cost for each case was developed based on the equipment sizing or duty. The results indicated the current benchmark of MEA does not provide the lowest capital cost solution for removing CO_2 from blast furnace gas. Instead, piperazine was determined to allow the lowest capital cost plant, whilst maintaining a 90% of the CO_2. When the total capital cost is split into categories, it became clear that the absorber cost drives this reduction in total cost. As PZ reacts quickly to capture CO_2 from the gas phase, less residence time is required to remove 90% which reduces the height and therefore cost of the absorber vessel. The fast and exothermic chemical reaction also leads to a large increase in gas temperature through the absorber vessel. Further work may recommend an intercooler be installed at the absorber column but this has not been considered within this work. It is hoped that the extra cost of the pump and heat exchangers would be outweighed by a further reduction in absorber column height.

Even with this additional consideration, the use of PZ remains controversial within the carbon capture community due to its marine toxicity. Therefore, the aim of this work is to show that amine choice does play a significant part in capture plant capital cost, rather than identify a specific amine for adoption by the steel industry.

This loosely agrees with the recommendations of a report (IEAGHG Technical Report, 2022) which identifies amine blends which included PZ as a promotor to be promising options for future chemical absorption plants. Furthermore, the report also concluded that no single amine investigated had a clear benefit in terms of capital or operating cost. Comparison to MEA within the report showed most amines to be slightly better or worse in terms of key performance indicators (KPIs) such as specific reboiler duty. However, the study indicated that PZ, MDEA and AMP displayed better

performance than MEA under the conditions studied. A final consideration made was that MEA is one of the most corrosive amines used to capture CO_2 which will likely increase both capital and operating cost of using MEA over alternatives.
By carrying out this analysis under dynamic conditions, it would allow the modelling to be better validated with operating data from trials. In such a case, the gas conditions, such as flow, temperature and composition into the absorber column would be varied to match the typical range seen in blast furnace gas.

To investigate whether gas compression would be beneficial, a single case based on using MEA was considered. This involved a further capital cost assessment which indicated the cost of the compressor would outweigh any saving in absorber and regenerator column cost. Although the ratio of these values may be different for other amines, it is expected that the compressor cost will always outweigh the saving in absorber column cost.

Finally, this assessment has been limited to pure amines or mixtures of two different amines. A variety of proprietary chemicals and blends are now being used to capture CO_2 at lab and commercial scale. Developers of these latest generation of amines claim they require less energy to regenerate the amine (Kamijo, 2023). As a result, there would be a further lowering of capital and operating costs, compared to the options considered here. The cost and the relatively low number of references remain an obstacle to adopting chemical absorption to remove CO_2 from blast furnace gas streams.

Chapter 7. Conclusions and Future Work

7.1 Conclusions from this work

The aim of this work has been to investigate methods to reduce the emissions of CO_2 per tonne of crude steel produced. This aim has been chosen due to the global focus on reducing CO_2 emissions from all human activities on the planet.

In Chapter 4 several different production routes for steel were considered and their effectiveness in reducing CO_2 emissions evaluated. The outcomes show that near zero emission routes would be possible through scrap recycling using renewable energy to power electric arc furnaces (EAFs). Neither the capacity of this route nor the available supply of scrap metal is expected to be sufficient to meet steel demand in the coming decades. For this reason, Chapter 4 concludes that a secondary (and tertiary) route will also be required to meet the demand for steel in the year 2050 and beyond.

These other routes may involve hydrogen fuelled directly reduced iron (DRI) plants to supplement the supply of scrap steel to the EAFs. This will place the steel industry in direct competition with a myriad of other consumers of this carbon free fuel source. Chapter 4 further hypothesises that even if sufficient hydrogen becomes available for these different users, the steel industry will be unable to secure the quantities necessary to support widescale adoption of hydrogen fuelled DRI facilities.

Alternatively, a new technology could be developed which emits a fraction of the emissions from the current blast furnace and basic oxygen furnace route. New technology would likely involve some form of carbon capture from its gas stream to reach low levels of CO_2 emissions. Such technology is not currently available commercially with possibilities still at a laboratory scale. The conclusion made within Chapter 4 was that the capacity of any new technology by 2050 will be limited, despite its potential to greatly reduce CO_2 intensity per tonne of steel produced.

As all the options above come with some limitations, the next chapters within this work focused on methods to reduce the carbon intensity of the existing blast furnace process. Identifying complimentary technologies which could be added to existing facilities would allow further development of new steel production methods to meet strict emission targets by 2050. Spreading the investment period for steel producers makes it more likely that these targets can be met.

In Chapter 5 further investigation was carried out into methods of decarbonising the most common current production route for steel, focusing on the blast furnace. The chapter reports the assessment of different carbon capture methods and carbon utilisation technologies within multiple flowsheet schemes at a high level. A total of six different metrics were used to identify the most promising options for technologies to reduce the carbon footprint of a blast furnace. The consumption of utilities was also used to generate an operating cost for the different options based on real utility costs from 2018.

Chapter 5 concluded that despite chemical absorption having the largest energy consumption per tonne of CO_2 captured, it also resulted in some of the lowest operating costs. This can be explained as chemical absorption requires steam which is more available and therefore lower cost than electricity within a steelworks. By comparison, CO_2 separation methods which rely on electrical energy are penalised by a relatively high cost for electricity.

Physical adsorption methods were assessed to remove the greatest proportion of CO_2 from blast furnace gas. This would appear to offer an advantage if reducing CO_2 is the sole criteria to installing carbon capture technology. Such methods, however also remove quantities of CO and H_2 from the blast furnace gas. For this reason chemical absorption was favoured as the CO_2 stream will require less purification before being sold or geologically stored. There will be less impact on the energy balance within the steelworks as a greater proportion of useful H_2 and CO can be retained and utilised by downstream consumers.

Finally, of all the capture methods considered only chemical absorption does not require compression of the blast furnace gas stream. This not only saves the operating costs to run the gas compressor but also significant capital investment to procure and install such a large electrically driven compressor.

The removal of CO_2 from blast furnace gas can be more than doubled by using a water shift gas reactor to convert CO and water vapour into CO_2 and H_2. The result is a higher concentration of CO_2 which is easier to remove from the gas stream and generates a stream of H_2 diluted with N_2. As more industries look to utilise H_2 as a carbon free energy source, using blast furnace gas in this way may become financially viable. By using blast furnace gas in this manner, some calorific value is lost and may need to be replaced using a purchased gas.

Flowsheets involving electrochemical regeneration of CO_2 to CO were also considered. As this reaction is unfavourable though, significant electrical energy is required which is unlikely to be available within the steelworks. This lack of availability is caused by the age of typical on site power generation facilities and the relatively low calorific value of gasses used. Both factors reduce the efficiency of producing electricity at such facilities.

Chapter 5 concluded that chemical absorption should be investigated further, due to not requiring gas compression and utilising an energy source more widely available within a steelworks than electrical energy. All the methods of CO_2 regeneration considered required an increase in energy requirement above what is estimated for gas compression for storage. For this reason, the conclusion reached was that blast furnaces equipped with carbon capture technology should be connected to carbon capture hubs to share infrastructure costs for geological storage.

Chapter 6 contains the results of the analysis of different amines and amine blends on the capital cost of a carbon capture plant for treating blast furnace gas. Other factors considered for the different cases included amine make-up rate and energy required to regenerate the amines. The setup of the models follows the information given in Chapter 3.

The results highlighted higher amine make-up rates for the primary and cyclic amine than for the tertiary amines studied. The extent of energy released during the reaction between the amine and CO_2 is likely to be the cause of this as primary and cyclic amines react more exothermically than secondary and tertiary amines. To limit amine loss to the gas stream an additional water wash circuit was required to be installed at the top of the absorber column which increased the height of this equipment. These amines offered low capital cost options for the capture of CO_2 from blast furnace gas. The explanation of this is that the slower acting amines required significantly greater residence times within the absorber column to reach a 90% CO_2 removal rate. Combining the different equipment capital costs into categories shows the absorber column, regenerator column and heat exchangers forms most of the overall plant capital cost. The various cases assessed resulted in a wide range of thermal energy requirements to regenerate the different amines. Although this will result in different operating costs, the reboiler capital cost remains relatively constant.

The lowest overall capital cost solution used piperazine as the CO_2 capture amine despite the extra water washing equipment required.

The results identify that the choice of amine does influence both operating and capital costs of a chemical absorption plant. By choosing a primary or cyclic amine a reduced capital cost is achievable due to smaller equipment, such as the absorber column, being required. This saving though may be counteracted by the increased operating cost coming from a higher amine make-up rate, amine cooler and reboiler duties. The alternatives of tertiary amines result in lower operating costs but higher capital costs.

7.2 Key Summary

The following points represent a key summary of the novel findings:

- Multiple production routes will be required to meet the predicted steel demand in 2050
- At least some steel production will remain via CO_2 intensive technologies such as the blast furnace
- To make significant reductions in CO_2 emissions from the global steel industry carbon capture will need to be applied
- Of the different carbon capture technologies, chemical absorption was identified as the most compatible with blast furnace gas
- A large amount of CO_2 could be removed if a water gas shift step was also introduced at the expense of a higher steam consumption
- By incorporating water gas shift, the steelworks could generate a gas stream with a high hydrogen content. This could be sold to other industries as a green fuel
- An assessment of different absorption chemicals indicated that the choice has a large effect on the physical size of a capture plant and therefore the capital cost
- Fast-acting chemical such as piperazine were identified as the best option to remove CO_2 from blast furnace gas due to the large gas volume
- The capital costs for a gas compressor were estimated to determine whether this would reduce overall capital cost
- The compressor cost was determined to be greater than the savings achievable in the remaining areas of plant

CO_2 emissions from every industry must be reduced globally by 2050. Some industries can substitute their current carbon intensive production methods for carbon free routes. The steel industry has a long-established reliance on carbon resulting in it being labelled as a “hard to abate” industry. There is now a focus on achieving the decarbonisation of this sector driven by the financial penalties for emitting CO_2 in Europe.

The results from the three parts of this investigation have shown that reducing emissions from steel production can be achieved by adopting new technologies to replace the currently dominant BF-BOF route. Many of these new technologies still require significant development and scale-up to compete with blast furnaces. This will limit the extent of uptake by 2050 and therefore the amount of steel production which can switch from the BF-BOF route. Based on this conclusion, there will still be a large amount of older BF-BOF facilities required to produce sufficient levels of steel. The results provide re-assurance to the steel industry that there are mature technologies available to reduce CO_2 emissions from these older facilities. These can be combined with the blast furnace to limit CO_2 emissions while the transition away from this long-established technology takes place. This intermediate step is essential if the steel industry is to meet, often legally binding, targets to reduce CO_2 emissions by 2050.

Based on the assumptions made in this work, Chemical absorption was identified as the most promising technology for treating blast furnace gas and detailed process models determined equipment sizes for such a plant. These results should give the industry confidence, that adopting carbon capture technology at existing blast furnace facilities is a valid strategy in the short term while development of alternative production routes is carried out. By following this philosophy, the steel industry will be able to meet the required reduction in CO_2 emissions by 2050, despite alternative technologies being unlikely to be available at commercial scale.

7.3 Recommended future work

The research undertaken during this work aimed to identify methods of significantly reducing CO_2 emissions from steelmaking. The conclusions drawn are reliant on the available data being viable for the range of operating conditions considered in this work. Suggested further work would be to challenge the assumptions made to test the conclusions made.

Within Chapter 4 the effects of conversion from natural gas to hydrogen fuelled Directly Reduced Iron were estimated. The true emission figures should be compared to the values used within this chapter, once more operating data is available from commercial scale plants currently under development by SSAB and others. Furthermore, emissions from new technologies should also be compared to the figures used in the assessment within Chapter 4. Such technologies have been based on HIsarna, which has yet to reach a commercial operating stage.

Chapter 5 uses multiple assumptions to simplify the various carbon utilisation and storage technologies considered. Chemical absorption is analysed in more detail to test these assumptions, but other technologies are based on limited information from laboratory scale research which may not be applicable for industrial scale applications. One technology showing promise was the water gas shift reaction to maximise both CO_2 and H_2 content of blast furnace gas. It is suggested that further work investigate blast furnace gas impurities to determine any impact on the life of the catalysts required for this reaction.

In Chapter 6 chemical absorption of CO_2 from blast furnace gas was studied theoretically in a steady state. Further work would involve validating Aspen HYSYS using operating data to confirm the results generated in this study. Alternatively, further pilot plant trials should be carried out using advanced, proprietary, amine mixtures.

Additional investigation should identify the benefits of absorber column intercooling to reduce both absorber column size and amine losses to the treated gas stream. By carrying out such an assessment the reduction in the cost of the absorber column could be compared to the additional cost for the amine pumps and heat exchangers which form the intercooling system.

Other methods of reducing operating cost should also be assessed to make adoption of chemical absorption in steelworks more attractive. These may include more advanced flowsheets, which have already been assessed for other sources of CO_2 but have not yet been assessed for treating blast furnace gas.

The work carried out to date has all been based on steady state conditions. Further research should investigate dynamic conditions using either Aspen or gPROMS software packages. This would vary the inlet gas conditions to the absorber column and estimate any effect on CO_2 removal performance. Such results could then be compared with pilot scale tests (Montañés, 2018 & Moser, 2020). Such research

should aim to develop an operating window for a chemical absorption plant for blast furnace gas by considering minimum and maximum gas flows and inlet CO_2 compositions. This would allow steelmakers to design suitable bypasses and safeguards when adopting this technology to remove CO_2 from blast furnace gas.

Finally, future development should engage with the suppliers of amines such as piperazine to ensure that the predicted quantities of this amine are available over the lifetime of multiple carbon capture plants. This work could also look to estimate the number of blast furnace facilities which would adopt carbon capture. This assessment would best be made based on location of the facility and the planned level of financial incentive for adopting CCS.

List of References

Afkhamipour, M., Mofarahi, M. (2013). 'Comparison of rate-based and equilibrium-stage models of a packed column for post-combustion CO_2 capture using 2-amino-2-methyl-1-propanol (AMP) solution' *Int. J. Greenh. Gas Control* 15, pp. 186–199

AISTech (2015). *Iron & Steel Technology*, March 2015, pp. 294-297

AISTech (2019). *Iron & Steel Technology*, March 2019, pp. 260-261

AISTech (2020). *Iron & Steel Technology*, March 2020, pp. 258-259

Allwood, J. M., Cullen, J. M., Milford, R. L. (2010) 'Options for achieving a 50% cut in industrial carbon emissions by 2050.' *Environ. Sci. Technol.*, 44 (6), pp. 1888−1894.

Arens M. and Worrell, E. (2014). 'Diffusion of energy efficient technologies in the German steel industry and their impact on energy consumption' *Energy*, 73, pp. 968–977

Arens, M., Worrell, E., Eichhammer, W., Hasanbeigi, A., & Zhang, Q. (2016). 'Pathways to a low-carbon iron and steel industry in the medium-term – the case of Germany.' *Journal of Cleaner Production*, 1990, pp. 1–15.

Aspentech. (2005). 'HYSYS® 2004.2 Operations Guide. Retrieved from https://sites.ualberta.ca/CMENG/che312/F06ChE416/HysysDocs/AspenHYSYSOperationsGuide.pdf on 10th June 2022.

Bachu, S. (2010). 'Screening and selection criteria, and characterisation techniques for the geological sequestration of carbon dioxide (CO_2)' *Developments and Innovation in CCS Technology*, Vol. 2, pp. 27–56. Woodhead Publishing Limited

Baranzini, A., Goldemberg, J. and Speck, S. (2000). 'A future for carbon taxes' *Ecological Economics*, 32, pp. 395–412.

Basile, A., Curcio, S., Bagnato, G., Liguori, S., Jokar, S. M., & Iulianelli, A. (2015). 'Water gas shift reaction in membrane reactors: Theoretical investigation by artificial neural networks model and experimental validation.' *International Journal of Hydrogen Energy*, 40(17), pp. 5897–5906.

Birat, J.-P. (2010). 'Carbon dioxide (CO_2) capture and storage technology in the iron and steel industry' *Developments and Innovation in Carbon Dioxide (CO_2) Capture and Storage Technology*, 16, pp. 492–521.

Blostein, P., Devaux, M. and Grant, M. (2011). 'Use of industrial gases in blast-furnace operation' *Metallurgist*, 55, pp. 552–557.

Bottoms, R. R. (1930). United States Patent No. 1783901, 'Process for separating acid gases'.

Brigman, N., Shah, M. I., Falk-Pedersen, O., Cents, T., Smith, V., De Cazenove, T., et al. (2014). 'Results of amine plant operations from 30 wt% and 40 wt% aqueous MEA testing at the CO_2 Technology Centre Mongstad' *Energy Procedia*, 63, pp. 6012–6022.

British Steel. (2018). "Energy Standard Prices 2015/16 – 2017/18"

Brown, S., Campbell, K. S., Gadikota, G., Howe, A. and Mac Dowell, N. (2016). 'CCS Forum Report'

Brunke, J. C. and Blesl, M. (2014). 'A plant-specific bottom-up approach for assessing the cost-effective energy conservation potential and its ability to compensate rising energy-related costs in the German iron and steel industry' *Energy Policy*, 67, pp. 431–446.

Cairns, C.J., de Chily, H.C. (1998). 'Energy Use in the Steel Industry' Committee on Technology, International Iron and Steel Institute, Brussels

Carpenter, A. (2012). 'CO_2 abatement in the iron and steel industry' Retrieved from www.ketep.re.kr/home/include/download.jsp?fileSID=6566 accessed December 13, 2019

Chang, Y., & Dyment, J. (2018). 'Jump Start Guide: Acid Gas Cleaning in Aspen HYSYS ® A Brief Tutorial (and supplement to and online documentation).' Retrieved from https://www.aspentech.com/en/resources/jump-start-guide/acid-gas-cleaning-in-aspen-hysys accessed 20 September 2018.

Chen, W. H., Lin, M. R., Leu, T. S., & Du, S. W. (2011). ‚An evaluation of hydrogen production from the perspective of using blast furnace gas and coke oven gas as feedstocks.' *International Journal of Hydrogen Energy.* 36(18), pp. 11727–11737.

Chen, W., Yin, X. and Ma, D. (2014). 'A bottom-up analysis of China's iron and steel industrial energy consumption and CO_2 emissions' *Applied Energy*, 136, pp. 1174–1183

Chung, W., Roh, K. and Lee, J. H. (2018). 'Design and evaluation of CO_2 capture plants for the steelmaking industry by means of amine scrubbing and membrane separation' *International Journal of Greenhouse Gas Control*, 74 (May), pp. 259–270.

Colclough, T. P. (1959). 'Developments in Blast Furnace Practice.' *Indian Construction News*, August 1959, pp. 222 – 228.

Conejo, A. N., Birat, J. P. and Dutta, A. (2020). 'A review of the current environmental challenges of the steel industry and its value chain' *Journal of Environmental Management*, 259, 109781.

Costa, M. M., Schaeffer, R. and Worrell, E. (2001). 'Exergy accounting of energy and materials flows in steel production systems' *Energy*, 26, pp. 363–384.

Costmodelling (2023). From https://costmodelling.com/construction-indices accessed on 23/08/2023.

Cuccia, L., Dugay, J., Bontemps, D., Louis-louisy, M., & Morand, T. (2019). 'Monitoring of the blend monoethanolamine / methyldiethanolamine / water for post-combustion CO2 capture.' *International Journal of Greenhouse Gas Control*, 80, pp. 43–53.

Danloy, G., Berthelemot, A., Grant, M., Borlée, J., Sert, D.; Van der Stel, J., Jak, H., Dimastromatteo, V., Hallin, M., Eklund, N., et al. (2009) 'ULCOS-Pilot testing of the low-CO_2 blast furnace process at the experimental BF in Luleå.' *Rev. Mét. Inter. J. Metall.* 106, pp. 1–8

de Mare, C. (2012). 'Why Both Hydrogen and Carbon Are Key for Net-Zero Steelmaking.' *Iron & Steel Technology,* September 2021.

Department for Energy Security & Net Zero (2023). 'Quarterly Energy Prices' Retrieved from https://www.gov.uk/government/collections/quarterly-energy-prices accessed on 14/04/2023

Doyle, A., Voet, T. (2021). 'The DRI dilemma: Could raw material shortages hinder the steel industry's green transition?' Retrieved from https://www.mckinsey.com/industries/metals-and-mining/our-insights/the-dri-dilemma-could-raw-material-shortages-hinder-the-steel-industrys-green-transition accessed on 25/09/2021

Dri, M., Sanna, A. and Maroto-Valer, M. M. (2014). 'Mass and energy balance of NH_4-salts pH swing mineral carbonation process using steel slag' *Energy Procedia*, 63, pp. 6544–6547.

Duarte, P. (2019) ‘Hydrogen-based steelmaking’ *Millennium Steel*, pp 18-22

Dugas, R.E., Rochelle, G.T., (2011). ‚CO_2 absorption rate into concentrated aqueous monoethanolamine and piperazine.’ *J. Chem. Eng. Data.* 56, pp. 2187–2195.

Dyment, J., Watanasiri, S., & Rumyantseva, I. (2015). ‘Acid Gas Cleaning using Amine Solvents: Validation with Experimental and Plant Data.’ Aspen Technology Inc,.

Elfving, J., Bajamundi, C., Kauppinen, J., & Sainio, T. (2017). ‘Modelling of equilibrium working capacity of PSA, TSA and TVSA processes for CO_2 adsorption under direct air capture conditions.’ *Journal of CO_2 Utilization*, 22, pp. 270–277.

Elmquist, S.A., Weber, P., Eichberger, H. (2002) ‘Operational results of the Circored fine ore direct reduction plant in Trinidad’ *STAHL UND EISEN*, 2002, pp 59–64.

Ember, retrieved from https://ember-climate.org/data/data-tools/carbon-price-viewer/ accessed 07/09/2022

Esmaeili, A., Tamuzi, A., Borhani, T. N., Xiang, Y., & Shao, L. (2022). ‘Modeling of carbon dioxide absorption by solution of piperazine and methyldiethanolamine in a rotating packed bed.’ *Chemical Engineering Science*, 248, 117118.

Eurofer (2014). ‘A Steel Roadmap for a Low Carbon Europe 2050’. *The European Steel association,* Brussels

European Commission (2010). Final Report of the Set-Plan workshop on Technology Innovations for Energy efficiency and Greenhouse Gas (GHG) emissions reduction in the Iron and Steel Industries in the EU-27 up to 2030.

Fan, Z. and Friedmann, S. J. (2021). ‘Low-carbon production of iron and steel: Technology options, economic assessment, and policy’ *Joule*, pp. 1–34.

Fernández, J.R., Martínez, I., Abanades, J.C., Romano, M.C. (2017). ‘Conceptual design of a Ca–Cu chemical looping process for hydrogen production in integrated steelworks.’ *Int. J. Hydrogen Energy*. 42, pp. 11023–11037.

Fischer, K. B., Daga, A., Hatchell, D. and Rochelle, G. T. (2017). ‘MEA and Piperazine Corrosion of Carbon Steel and Stainless Steel’ *Energy Procedia*, 114, pp. 1751–1764

Fosbøl, P. L., Neerup, R., Rezazadeh, A., Almeida, S., Gaspar, J., Knarvik, A. B. N., Flø, N. E. (2018). ‘Results of the fourth Technology Centre Mongstad campaign: LVC

testing' *14th International Conference on Greenhouse Gas Control Technologies,* pp 9-27

Ford, M. R. and Kench, P. S. (2015). 'Multi-decadal shoreline changes in response to sea level rise in the Marshall Islands' *Anthropocene*, 11, pp. 14–24.

Freguia, S., & Rochelle, G. T. (2003). 'Modeling of CO2 capture by aqueous monoethanolamine' *AIChE Journal*, 49(7), pp. 1676–1686.

Gentile, G., Bonalumi, D., Pieterse, J. A. Z., Sebastiani, F., Lucking, L., & Manzolini, G. (2022). 'Techno-economic assessment of the FReSMe technology for CO_2 emissions mitigation and methanol production from steel plants.' *Journal of CO_2 Utilization*, 56.

Gielen, D., Saygin, D., Taibi, E. and Birat, J. P. (2020). 'Renewables-based decarbonization and relocation of iron and steel making: A case study' *Journal of Industrial Ecology*, 24, pp. 1113–1125.

Global CCS Institute (2011). 'Accelerating The Uptake Of CCS: Industrial Use Of Captured Carbon Dioxide' March 2011

Goto, K., Okabe, H., Chowdhury, F. A., Shimizu, S., Fujioka, Y. and Onoda, M. (2011). 'Development of novel absorbents for CO_2 capture from blast furnace gas' *International Journal of Greenhouse Gas Control*, 5, pp. 1214–1219.

Griffin, P. W. and Hammond, G. P. (2019). 'Analysis of the potential for energy demand and carbon emissions reduction in the iron and steel sector' *Energy Procedia*, 158, pp. 3915–3922.

Hamborg, E. S., Smith, V., Cents, T., Brigman, N., Falk-Pedersen, O., De Cazenove, T., Chhanganlal, M., Feste, J., Ullestad, Ø., Ulvatn, H., Gorset, O. Askestad, I., Gram, L., Fostås, B., Shah, M., Maxson, A. and Thimsen, D. (2014). 'Results from MEA testing at the CO_2 Technology Centre Mongstad. Part II: Verification of baseline results' *Energy Procedia*, 63, pp. 5994–6011.

Han, K., Ahn, C. K. and Lee, M. S. (2014). 'Performance of an ammonia-based CO_2 capture pilot facility in iron and steel industry' *International Journal of Greenhouse Gas Control*, 27, pp. 239–246.

Haribu, I.V., Imle, M., Hasse, H., (2014). 'Modelling and simulation of reactive absorption of CO_2 with MEA: results for four different packings on two different scales.' *Chem. Eng. Sci.* 105, pp. 179–190.

Hasanbeigi, A., Arens, M., & Price, L. (2014). 'Alternative emerging ironmaking technologies for energy-efficiency and carbon dioxide emissions reduction: A technical review.' *Renewable and Sustainable Energy Reviews*. 33, pp. 645-658

Hai, A., Vengatesan, M. R., Zain, J. H., Abou-Khousa, M., & Banat, F. (2020). 'Design and optimization of a concentric setup for the separation of Heat Stable Salts from industrial lean amine solution using electromagnetic forces.' *International Journal of Greenhouse Gas Control*, 101.

He, H., Guan, H., Zhu, X. and Lee, H. (2017). 'Assessment on the energy flow and carbon emissions of integrated steelmaking plants' *Energy Reports*, 3, pp. 29–36.

HM Government. (2011). 'The Carbon Plan: Delivering our Low Carbon Future.' HM Government, Department of Energy & Climate Change, London, UK.

Ho, M. T., Bustamante, A., & Wiley, D. E. (2013). 'Comparison of CO_2 capture economics for iron and steel mills.' *International Journal of Greenhouse Gas Control*. 19, pp. 145–159.

Horii, K., Tsutsumi, N., Kato, T., Kitano, Y., & Sugahara, K. (2015). 'Overview of iron/steel slag application and development of new utilization technologies' *Nippon Steel & Sumitomo Metal Technical Report*, 109, pp. 5–11.

Hu, C., Han, X., Li, Z. and Zhang, C. (2009). 'Comparison of CO_2 emission between COREX and blast furnace iron-making system' *Journal of Environmental Sciences*, 21, S116–S120.

Humbert, P.S., Castro-Gomes, J. (2019). 'CO_2 activated steel slag-based materials: a review' *J. Clean. Prod.*, 208, pp. 448–457,

Hummel, H., Canapa, R., (2012). 'Steel Roadmap EU 2050'. IEAGHG.

IEA, (2004). 'Impact of Impurities on CO2 Capture, Transport and Storage Greenhouse Gas R&D programme' Report No. PH4/32.

IEA. (2020). Iron & Steel Roadmap.

IEAGHG, 'Prime Solvent candidates for next generation of PCC plants' 2022-03, February 2022

IPCC, (2005). Special Report on CCS. Cambridge University Press, UK

IPCC (2013). IPCC Report, 2013. URL http://www.ipcc.ch/ assessed on 27/10/2019

Isa, F., Zabiri, H., Harun, N., Shariff, A. M., Ng, N. K. S., & Afian, M. A. A. (2021). 'Simulation Comparison Between Equilibrium and Rate-Based Approach for CO_2 Removal Via Promoted K_2CO_3 with Glycine.' *E3S Web of Conferences*, 287, pp. 1–6.

Jassim, M. S. (2002). 'Process Intensification: Absorption and Desorption of Carbon Dioxide from Monoethanolamine Solutions Using Higee Technology', PhD thesis, Newcastle University

JFE Steel. (2013). 'Research and development for enhancing the use of low-quality ferrous scrap' NEDO Energy Efficiency Technology Forum 2013.

Jin, P., Jiang, Z., Bao, C., Hao, S. and Zhang, X. (2017). 'The energy consumption and carbon emission of the integrated steel mill with oxygen blast furnace' *Resources, Conservation and Recycling*, 117, pp. 58–65.

Jones, D. L. (2012). 'Available and Emerging Technologies for Reducing Greenhouse Gas Emissions from the Iron and Steel Industry' Retrieved from http://www.epa.gov/nsr/ghgdocs/ironsteel.pdf. Accessed 02/10/2021

Joss, L., Gazzani, M., & Mazzotti, M. (2017). 'Rational design of temperature swing adsorption cycles for post-combustion CO_2 capture.' *Chemical Engineering Science*, 158, pp. 381–394.

Kamijo, T., & Uemura, M., Agraniotis, M. (2023) 'Post combustion CO_2 capture technology of Mitsubishi Heavy Industries (KM CDR process™). Experience recent advancements and potential applications for steel industry' *METEC & 6th ECIC 2023 conference proceedings.* Accessed 28th June 2023.

Khallaghi, N., Abbas, S. Z., Manzolini, G., De Coninck, E., & Spallina, V. (2022). 'Techno-economic assessment of blast furnace gas pre-combustion decarbonisation integrated with the power generation.' *Energy Conversion and Management*, 255(January), 115252.

Kim, D. H., Han, S. W., Yoon, H. S., & Kim, Y. D. (2014). 'Reverse water gas shift reaction catalyzed by Fe nanoparticles with high catalytic activity and stability.' *Journal of Industrial and Engineering Chemistry*, 23, pp. 67–71.

Kim, H., Lee, J., Lee, S., Lee, I. B., Park, J. Hyoung, & Han, J. (2015). 'Economic process design for separation of CO_2 from the off-gas in ironmaking and steelmaking plants.' *Energy*, 88, pp. 756–764.

Kumar, B., Roy, G. G. and Sen, P. K. (2020). ‘Comparative exergy analysis between rotary hearth furnace-electric arc furnace and blast furnace-basic oxygen furnace steelmaking routes’ *Energy and Climate Change*, 1, 100016.

Kunze, C., Spliethoff, H. (2010) ‘Modelling of an IGCC plant with carbon capture for 2020’ *Fuel Process Technol.* 91, pp. 934–941

Lampert, K. and Ziebik, A. (2007). ‘Comparative analysis of energy requirements of CO_2 removal from metallurgical fuel gases’ *Energy*, 32, pp. 521–527.

Lefebvre, K., Aubry, N., Cameron, I. and Ellis, B. (2021). ‘Top Gas Recycling Revisited to Reduce Blast Furnace CO_2 Emissions’ *AISTech 2021 – Proceedings of the Iron & Steel Technology Conference*, pp. 1432–1444.

Leung, D. Y. C., Caramanna, G. and Maroto-Valer, M. M. (2014). ‘An overview of current status of carbon dioxide capture and storage technologies’. *Renewable and Sustainable Energy Reviews*, 39, pp. 426–443.

Liu, C.-.T., Fischer, K.B., Rochelle, G.T. (2020). ,Corrosion by aqueous piperazine at 40–150◦C in pilot testing of CO_2 capture.’ *IECR* 59 (15), pp. 7189–7197.

Lv, W., Sun, Z. and Su, Z. (2019). ‘Life cycle energy consumption and greenhouse gas emissions of iron pelletizing process in China, a case study’. *Journal of Cleaner Production*, 233, pp. 1314–1321.

MacPhee, J.A., Gransden, J.F., Giroux, L., Price, J.T. (2009) ‘Possible CO_2 mitigation via addition of charcoal to coking coal blends’ *Fuel Process Technol*, 90(1), pp. 16–20.

Markewitz, P., Bongartz, R. (2015) ‘Carbon capture technologies’ Carbon Capture, Storage and Use. Springer International.

Mathur, P, C., von Schéele, J. (2021) , Decarbonizing Solutions for Sustainable Steelmaking’ *Steel Times International*, April 2021

McBrien, M., Serrenho, A. C. and Allwood, J. M. (2016). ‘Potential for energy savings by heat recovery in an integrated steel supply chain’. *Applied Thermal Engineering*, 103, pp. 592–606.

Mei, D., Zhu, X., Wu, C., Ashford, B., Williams, P. T. and Tu, X. (2016). ‘Plasma-photocatalytic conversion of CO_2 at low temperatures: Understanding the synergistic effect of plasma-catalysis’. *Applied Catalysis B: Environmental*, 182, pp. 525–532.

Meijer, K., Zeilstra, C., Teerhuis, C., Ouwehand, M., Dry, R. and Pilote, J. (2014). 'The HIsarna ironmaking process'. *European Steel Environment & Energy Congress (ESEC) 2014*.

Melorose, J., Perroy, R. and Careas, S. (2015). 'The Paris Protocol – A blueprint for tackling global climate change beyond 2020'.

Metz, B., Davidson, O., de Coninck, H., Loos, M., Meyer, L. (2005) 'IPCC Special Report on Carbon Dioxide Capture and Storage, Intergovernmental Panel on Climate Change

Miller, B. R. and Kuijpers, L. J. M. (2011) 'Projecting future HFC-23 emissions' *Atmos. Chem. Phys.*, 11, pp. 13259–13267

Millner, R., Ofner, H., Boehm, C., Ripke, S. J., Metius, G. (2017), presented at ESTAD, Vienna, Austria, June 2017

Mimura, T., Shimojyo, S., Suda, T., Iijima, M., Mitsuoka, S. (1995). 'Development of energy-saving absorbents for the recovery of carbon dioxide from boiler flue gas' *Kagaku Kogaku Ronbunshu* 21 (3), pp. 478–485

Miyamoto, O., Maas, C., Tsujiuchi, T., Inui, M., Hirata, T., Tanaka, H., Yonekawa, T., and Kamijo, T. (2017). 'KM CDR Process™ Project Update and the New Novel Solvent Development'. *Energy Procedia*, 114, pp. 5616–5623.

Mohamadirad, R., Hamlehdar, O., Boor, H., Monnavar, A. F. and Rostami, S. (2011). 'Mixed amines application in gas sweetening plants'. *Chemical Engineering Transactions*, 24, pp. 265–270.

Montañés, R. M., Flø, N. E., & Nord, L. O. (2018). ‚Experimental results of transient testing at the amine plant at Technology Centre Mongstad: Open-loop responses and performance of decentralized control structures for load changes' *International Journal of Greenhouse Gas Control*, 73, pp. 42–59.

Morken, A. K., Nenseter, B., Pedersen, S., Chhaganlal, M., Feste, J. K., et al. (2014). 'Emission Results of Amine Plant Operations from MEA Testing at the CO_2 Technology Centre Mongstad'. *Energy Procedia*, 63, pp. 6023–6038.

Moser, P., Wiechers, G., Schmidt, S., Garcia Moretz-Sohn Monteiro, J., Charalambous, C., Garcia, S. and Sanchez Fernandez, E. (2020). ‚Results of the 18-month test with MEA at the post-combustion capture pilot plant at Niederaussem – new impetus to solvent management, emissions and dynamic behaviour'. *International Journal of Greenhouse Gas Control*, 95, 102945.

Myhre, C. L. (2012). 'Monitoring of greenhouse gases and aerosols at Svalbard and Birkenes: Annual report 2010' (Report number TA-2902/2012)

NOAA/ESRL data servers, retrieved from ftp://ftp.cmdl.noaa.gov/ccg/co2/in-situ/ Accessed 17/01/2016

Notz, R., Mangalapally, H. P. and Hasse, H. (2012). 'Post combustion CO_2 capture by reactive absorption: Pilot plant description and results of systematic studies with MEA'. *International Journal of Greenhouse Gas Control*, 6, pp. 84–112.

OECD 2021 - Bataille, C., et al. (2020). Low and zero emissions in the steel and cement industries BARRIERS, TECHNOLOGIES AND POLICIES (OECD). https://www.oecd-ilibrary.org/ environment/low-and-zero-emissions-in-the- steel-and-cement-industries_5ccf8e33-en.

Oh, S.-Y., Binns, M., Cho, H. and Kim, J.-K. (2016). 'Energy minimization of MEA-based CO2 capture process'. *Applied Energy*, 169, pp. 353–362.

Øi, L. E. (2007). 'Aspen HYSYS Simulation of CO_2 Removal by Amine Absorption from a Gas Based Power Plant' SIMS2007 *Conference Proceedings*, Gøteborg. From https://ep.liu.se/ecp/027/008/ecp072708.pdf accessed on 22nd August 2023

Onda, K., Takeuchi, H., Okumoto, Y., (1968). 'Mass transfer coefficients between gas and liquid phases in packed columns.' *J. Chem. Eng. Jpn.*, 1, pp. 56-62.

Pardo, N., Moya J.A. and Vatopoulos, K. (2012). 'Prospective Scenarios on Energy Efficiency and CO_2 Emissions in the EU Iron & Steel Industry.'

Paulussen, S., Verheyde, B., Tu, X., De Bie, C., Martens, T., Petrovic, D., Bogaerts, A., Sels, B. (2010) 'Plasma Sources' *Sci. Technol.* 19, 034015.

Peacey, J. G. & Davenport, W. G. (1979). 'The Iron Blast Furnace - Theory and Practice.' 1st ed. *Pergamon Press,* Oxford, pp. 1-266

Pettersson, M., Sikström, P., & Eklund, N. (2012). 'Final evaluation of the ulcos tgr-bf pilot tests performed at the lkab experimental blast furnace.' *6th International Congress on the Science and Technology of Ironmaking 2012*, ICSTI 2012.

Pickering, S.J.; Hay, N.; Roylance, T.F.; Thomas, G.H. (1985). 'New process for dry granulation and heat recovery from molten blast furnace slag' *Ironmak. Steelmak.* 12, pp. 14–21.

Piketty, M. G., Wichert, M., Fallot, A. and Aimola, L. (2009). ‘Assessing land availability to produce biomass for energy: The case of Brazilian charcoal for steel making’. *Biomass and Bioenergy*, 33, pp. 180–190.

Polasek, J., & Bullin, J. (1994). ‘Selecting Amines for Sweetening Units’ *Process Considerations in Selecting Amine*. Gas Processors Association.

Pouladi, B., Nabipoor Hassankiadeh, M., & Behroozshad, F. (2016). ‘Dynamic simulation and optimization of an industrial-scale absorption tower for CO_2 capturing from ethane gas’ *Energy Reports*, 2, pp. 54–61.

Primetals Technologies Limited. Icons of various steelmaking processes. From company intranet. Accessed 26/02/2021

Progressive Energy (2015). TVU CCS Pre FEED WP1 – SSI Process Study. Concept Report. AMEC Project No. 1720 2000

Quader, M. A., Ahmed, S., Ghazilla, R. A. R., Ahmed, S. and Dahari, M. (2015). ‘A comprehensive review on energy efficient CO_2 breakthrough technologies for sustainable green iron and steel manufacturing’. *Renewable and Sustainable Energy Reviews*, 50, pp. 594–614.

Abdul Quader, M., Ahmed, S., Dawal, S. Z., & Nukman, Y. (2016). ‘Present needs, recent progress and future trends of energy-efficient Ultra-Low Carbon Dioxide (CO2) Steelmaking (ULCOS) program.’ *Renewable and Sustainable Energy Reviews*, 55, pp. 537–549.

Ramírez-Santos, Á. A., Castel, C. and Favre, E. (2018). ‘A review of gas separation technologies within emission reduction programs in the iron and steel sector: Current application and development perspectives’. *Separation and Purification Technology*, 194, pp. 425–442.

Rechberger, K., Spanlang, A., Sasiain Conde, A., Wolfmeir, H. and Harris, C. (2020). 'Green Hydrogen-Based Direct Reduction for Low-Carbon Steelmaking’. *Steel Research International*, 91, pp. 1–10.

Reddy, S., Scherffius, J. and Freguia, S. (2003). ‘Fluor ’s Econamine FG Plus SM Technology: An Enhanced Amine-Based CO_2 Capture Process’. *Second National Conference on Carbon Sequestration*, pp. 1–11.

Rhee, C. H., Kim, J. Y., Han, K., Ahn, C. K. and Chun, H. D. (2011). ‘Process analysis for ammonia-based CO_2 capture in ironmaking industry.’ *Energy Procedia*, 4, pp. 1486–1493.

Ribbenhed, M., Thorén, M., Sternhufvud, C. (2008). 'CO_2 emission reduction costs for iron ore-based steelmaking in Sweden.' *J. Cleaner Prod*. 16, pp. 125–134.

Riesbeck, J., Hooey, L., Kinnunen, K., Lilja, J., Hallin, M. and Sandberg, J. (2013). 'Global effects of closing down sinter plant at Ruukki Raahe integrated steelworks'. *The Iron and Steel Institute of Japan - Proceedings of the ISIJ -VDEh - Jernkontoret Joint Symposium*, 15-16 April, 2013, Osaka, Japan.

Rochelle, G. T., Wu, Y., Chen, E., Akinpelumi, K., Fischer, K. B., Gao, T., et al. (2019). 'Pilot plant demonstration of piperazine with the advanced flash regenerator.' *International Journal of Greenhouse Gas Control*, 84, pp. 72–81.

Rosenbauer, R. J. and Thomas, B. (2010). 'Carbon dioxide (CO_2) sequestration in deep saline aquifers and formations'. *Developments and Innovation in Carbon Dioxide (CO_2) Capture and Storage Technology*, 3, pp. 57–103.

Sachde, D. and Rochelle, G. T. (2014). 'Absorber intercooling configurations using aqueous piperazine for capture from sources with 4 to 27% CO_2'. *Energy Procedia*, 63, pp. 1637–1656.

Saima, H., Mogi, Y., Haraoka, T., & Saima, H.; Mogi, Y; Haraoka, T. (2013). 'Development of PSA System for the Recovery of CO2 from Blast Furnace Gas.' *Energy Procedia*, 37, pp. 7152–7159.

Sander, M., Mariz, C., (1992). 'The Fluor Daniel Econamine FG process: Past experience and present day focus.' *Energy Convers. Manage.* 33 (5), pp. 341–348.

Santos, S. (2013). 'Iron and Steel CCS Study (Techno-economics Integrated Steel Mill).' IEAGHG, Report number 2013/04

Sanz, A., Nieva, D., & Dufour, J. (2015). 'Steam-Iron process as an alternative to Water Gas Shift reaction in biomass gasification.' *International Journal of Hydrogen Energy*, 40(15), pp. 5074–5080.

Saravanan, A., Senthil kumar, P., Vo, D. V. N., Jeevanantham, S., Bhuvaneswari, V., Anantha Narayanan, V., Yaashikaa, P. R., Swetha, S., Reshma, B. (2021). 'A comprehensive review on different approaches for CO_2 utilization and conversion pathways.' *Chemical Engineering Science*, 236, 116515.

Sen, P. K. (2013). 'CO_2 accounting and abatement: An approach for iron and steel industry.' *Transactions of the Indian Institute of Metals*, 66, pp. 711–721.

Song, Y., Chen, C.-C., (2009). ‘Symmetric Electrolyte Non-random Two-Liquid Activity Coefficient Model.’ *Ind. Eng. Chem. Res.* 2009, 48, pp. 7788-7797

Srinivasa Rao R T (2007) ‘Environment & energy aspects of Corex at JSW Steel Ltd.’ Presentation at: 3rd steel workshop of the Asia-Pacific Partnership on Clean Development and Climate, Wollongong, NSW, Australia, 25 Oct 2007

Stec, M., Tatarczuk, A., Więcław-Solny, L., Krótki, A., ̄ciązko, M., & Tokarski, S. (2015). ‘Pilot plant results for advanced CO2 capture process using amine scrubbing at the Jaworzno II Power Plant in Poland’ *Fuel*, 151, pp. 50–56.

Stel, J. Van Der. (2013). ‘Development of ULCOS-Blast Furnace: Working toward technology demonstration.’ Iron *and Steel Industry CCUS and Process Integration Workshop*.

Stel, J. Van Der, Sert, D., Hirsch, A., Eklund, N., and Ökvist, L. S. (2020). ‘Top Gas Recycle Blast Furnace developments for low CO_2 ironmaking.’

Styring, P., Jansen, D., de Coninck, H., Reith, H. and Armstrong, K. (2011). ‘Carbon Capture and Utilisation in the green economy.’ In *Centre for Low Carbon Futures*.

Sun A., R. Davis, M. Starbuck, A. Ben-Amotz, R. Pate, and P. T. Pienkos (2011). ‘Comparative cost analysis of algal oil production for biofuels’ *Energy* 36, pp. 5169 – 5179.

Sun, J., Rongwong, W., Liang, Z., Gao, H., Idem, R. O., & Tontiwachwuthikul, P. (2015). ‘Simulation Studies of Process Improvement of Three-Tower Low-Temperature Distillation Process to Minimize Energy Consumption for Separation of Produced Gas of CO2-Enhanced Oil Recovery (EOR).’ *Canadian Journal of Chemical Engineering*, 93(7), pp. 1266–1274.

Sundqvist, M., Biermann, M., Normann, F., Larsson, M., & Nilsson, L. (2018). ‘Evaluation of low and high level integration options for carbon capture at an integrated iron and steel mill.’ *International Journal of Greenhouse Gas Control*, 77, pp. 27–36.

Suzuki, K., Hayashi, K., Kuribara, K., Nakagaki, T. and Kasahara, S. (2015). ‘Quantitative evaluation of CO_2 emission reduction of active carbon recycling energy system for ironmaking by modeling with aspen plus.’ *ISIJ International*, 55, pp. 340–347.

Takeuchi, M., (2009). 'The Status of Recycling in the Basic Materials Industry and the Limiting Factors'. In Japanese. *Kagaku Gijutsu Doukou*.

Tan, Y., Nookuea, W., Li, H., Thorin, E. and Yan, J. (2016). 'Property impacts on Carbon Capture and Storage (CCS) processes: A review.' *Energy Conversion and Management*, 118, pp. 204–222.

Thimsen, D., Maxson, A., Smith, V., Cents, T., Falk-Pedersen, O., Gorset, O., Hamborg, E. S. (2014). 'Results from MEA testing at the CO_2 Technology Centre Mongstad. Part I: Post-Combustion CO_2 capture testing methodology.' *Energy Procedia*, 63, pp. 5938–5958.

Tobiesen, F. A., Svendsen, H. F. and Mejdell, T. (2007). 'Modeling of blast furnace CO_2 capture using amine absorbents.' *Industrial and Engineering Chemistry Research*, 46, pp. 7811–7819.

Trading Economics, https://tradingeconomics.com/commodity/natural-gas accessed 07/09/2022

Tu, X., Whitehead, J. C. (2012). 'Plasma-catalytic dry reforming of methane in an atmospheric dielectric barrier discharge: Understanding the synergistic effect at low temperature.' *Applied Catalysis B: Environmental*, 125, pp. 439–448.

Turan, G. (2020). 'Are stars finally aligning for CCS in Europe?' From https://www.euractiv.com/section/energy-environment/opinion/are-stars-finally-aligning-for-ccs-in-europe/. Accessed on 03/12/2020.

UKCOP26 (2021) from https://ukcop26.org/. Accessed on 07/10/20022.

ULCOS New Blast Furnace Process. (2009). Final Report - Contract Number: RFS-CR-04005

Van Dijk, H. A. J., Cobden, P. D., Lundqvist, M., Cormos, C. C., & Watson, M. J. (2017). 'Cost effective CO_2 reduction in the Iron & Steel Industry by means of the SEWGS technology: STEPWISE project.' *Energy Procedia*, 114, pp. 6256–6265.

Van Dijk, H. A. J., Cobden, P. D., Lukashuk, L., Van De Water, L., Lundqvist, M., Manzolini, G., Cormos, C.-C., Van Dijl, C., Mancuso, L., Johns, J., Bellqvist, D. (2018). 'Stepwise project: Sorption-enhanced water-gas shift technology to reduce carbon footprint in the iron and steel industry.' *Johnson Matthey Technology Review*, 62, pp. 395–402.

Van Paasen, S., Infantino, M., Yao, J., Leenders, S. H. A. M., van de Graaf, et al. (2021). 'Development of the solid sorbent technology for post combustion CO_2 capture towards commercial prototype.' *International Journal of Greenhouse Gas Control*, 109.

Steel Institute VDEh, 2009. Statistics of the European Iron & Steel Sector. http:// www.vdeh.de (accessed 20/07/2019)

Visser, E., Hendricks, C., Barrio, M., Mölnvik, M., Koeijer, G., Liljemark, S., et al. (2008). 'DYNAMIS CO_2 quality recommendations.' *Int J Greenh Gas Control*, 2. pp. 478–484.

von Schéele, J., Gartz, M., Lantz, M.T., Riegert, J.P., Söderlund, S. (2008). 'Flameless oxyfuel combustion for increased production and reduced CO_2 and NOx emissions.' *stahl und eisen,* 128 (7), pp. 35–42

Watakabe, S., Miyagawa, K., Matsuzaki, S., Inada, T., Tomita, Y., Saito, K., Osama, M., Sikström, P. Ökvist, L., Wikstrom, J.-O. (2013). 'Operation Trial of Hydrogenous Gas Injection of COURSE50 Project at an Experimental Blast Furnace.' *ISIJ International*, 53, pp. 2065–2071.

Wiencke, J. et al. (2018). 'Electrolysis of iron in a molten oxide electrolyte' *Journal of Applied Electrochemistry*, Vol. 48, pp. 115-126.

Wilson, M., Tontiwachwuthikul, P., Chakma, A., et al. (2004). 'Evaluation of the CO_2 capture performance of the University of Regina CO_2 technology development plant and the boundary dam demonstration plant.' *Proceedings of the 7th International Conference on Greenhouse Gas Control*.

Woertler, M., Schuler, F., Voigt, N., Schmidt, T., Dahlmann, P., Luengen, H. B., & Ghenda, J.-T. (2013). 'Steel's Contribution to a Low-Carbon Europe 2050.'

WorldSteel (2020). '2020 World Steel in Figures'. *World Steel Association*, Brussels.

WorldSteel (2023). '2023 World Steel in Figures'. *World Steel Association*, Brussels. Retrieved from https://worldsteel.org/wp-content/uploads/World-Steel-in-Figures-2023-3.pdf on 24th June 2023

Xie, D. (2010) 'Second life for slag.' *Materials World*, 18(8), pp. 27-28

Xu, C. and Cang, D. (2010). 'A Brief Overview of Low CO_2 Emission Technologies for Iron and Steel Making.' *Journal of Iron and Steel Research International*, 17, pp. 1–7.

Yang, L. Z., Jiang, T., Li, G. H. and Guo, Y. F. (2017). 'Discussion of Carbon Emissions for Charging Hot Metal in EAF Steelmaking Process.' *High Temperature Materials and Processes*, 36, pp. 615–621.

Yildirim, Ö., Kiss, A. A., Hüser, N., Leßmann, K., & Kenig, E. Y. (2012). ‚Reactive absorption in chemical process industry: A review on current activities.' *Chemical Engineering Journal*, 213, pp. 371–391.

Yilmaz, C., Wendelstorf, J., & Turek, T. (2017). ‚Modeling and simulation of hydrogen injection into a blast furnace to reduce carbon dioxide emissions.' *Journal of Cleaner Production*, 154, pp. 488–501.

Zeilstra, C., Teerhuis, C., van der Stel, J., Meijer, K., Ouwehand, M., Keilman, G., & Treadgold, C. (2014). The HIsarna ironmaking process.' *European Steel Environment & Energy Congress (ESEC)* 2014, (June).

Zhang, Y., Chen, H., Chen, C.-C., Plaza, J. M., Dugas, R., Rochelle, G. T. (2009). 'Rate-Based Process Modelling Study of CO_2 Capture with Aqueous Monoethanolamine Solution.' *Ind. Eng. Chem. Res.* 48, pp. 9233-9246.

Zhang, Y., Chen, C.-C. (2011). 'Thermodynamic modelling for CO_2 Absorption in Aqueous MDEA Solution with Electrolyte NRTL Model.' *Ind. Eng. Chem. Res.* 50, pp. 163-175.

Zhang, Y., Que, H., Chen, C.-C. (2011). 'Thermodynamic Modelling for CO_2 absorption in Aqueous MEA Solution with Electrolyte NRTL model.' *Fluid Phase Equilibria*. 311, pp. 68-76.

Zhang, X., Zhang, R., Liu, H., Gao, H. and Liang, Z. (2018). 'Evaluating CO_2 desorption performance in CO_2-loaded aqueous tri-solvent blend amines with and without solid acid catalysts.' *Applied Energy*, 218, pp. 417–429.

Zhang, Q., Xu, J., Wang, Y., Hasanbeigi, A., Zhang, W., Lu, H., & Arens, M. (2018). 'Comprehensive assessment of energy conservation and CO 2 emissions mitigation in China's iron and steel industry based on dynamic material flows.' *Applied Energy*, 209, pp. 251–265.

Zhang, Q., Wei, Z., Ma, J., Qiu, Z., & Du, T. (2019). ‚Optimization of energy use with CO_2 emission reducing in an integrated iron and steel plant.' *Applied Thermal Engineering*, 157(April), 113635.

Zhang, X., Jiao, K., Zhang, J., & Guo, Z. (2021). 'A review on low carbon emissions projects of steel industry in the World.' *Journal of Cleaner Production*, 306, 127259.

Zhao, B., Liu, F., Cui, Z., Liu, C., Yue, H., Tang, S., et al. (2017). ‘Enhancing the energetic efficiency of MDEA / PZ-based CO_2 capture technology for a 650 MW power plant: Process improvement.’ *Applied Energy*, 185, pp. 362–375.

Appendix

1. Determination of CO_2 intensity of steel

Within Chapter 4 of the thesis, the average CO_2 emissions per tonne of crude steel produced is determined considering multiple different production routes to meet the predicted demand. This work builds from the data shared within the literature review in section 2.2. A worked example of the analysis steps from reference data to that reported in Chapter 4 is included below:

The emissions from the Coke Ovens are considered to be generated by the combination of:

- Amount of waste gas multiplied by the mass percent of CO_2 in the gas.
- Amount of coke oven gas multiplied by the CO_2 mass percent.
- Minus the effect of dry gas quenching estimated at 27.5 kg_{CO2} per tonne of coke produced.

Using the values in Table 2.2 from Santos (2013), this equates to:

2130 * 22.06% + 140 * 90% - 0.001* 27.5 = 0.57 t_{CO2} / t_{coke}.

As 0.386 kg coke are required to produce 1 tonne of steel through the BF-BOF route, this results in 0.57 * 0.39 = 0.22 t_{CO2}/t_{steel}

The emissions from the sinter plant are calculated based on the following:

- Waste gas amount multiplied by the mass percentage of CO_2
- Minus the effect of flue gas recirculation estimated at 34 kg_{CO2} per tonne of sinter produced.

Using the values in Table 2.3 from McBrien (2016), this equates to:

650 * 14.6% - 0.001 * 34 = 0.06 t_{CO2} / t_{sinter}

As 1 tonne of sinter is required per tonne of steel produced through the BF-BOF route, this results in 0.06 t_{CO2}/t_{steel}

The emissions from the pellet plant are calculated based on the following:

- 58.5 kg_{CO2} per tonne of pellets produced or 0.0585 t_{CO2} per tonne pellets.

As 0.45 tonnes of pellets are consumed to produce 1 tonne steel through the BF-BOF route, this results in 0.03 t_{CO2}/t_{steel}.

Emissions from the blast furnace are calculated based on the following:

- Mass of flue gas multiplied by the CO_2 mass percent
- Mass of blast furnace gas multiplied by the CO_2 mass percent
- Minus the effect of installing a TRT estimated as 19.6 kg_{CO2} per tonne of hot metal

When CCS is applied to blast furnace gas, the following is also considered:

- Minus 90% of the mass of blast furnace gas multiplied by the CO_2 mass percent

Using the values in Table 2.5 from Santos (2013), this equates to:

1110kg * 37.81% CO_2 + 1513kg * 59% CO_2 – 0.001 * 19.6 kg CO_2 = 1.28t_{CO2}/tHM

As 900 kg hot metal is required to produce 1 tonne of steel via the BF-BOF route this results in 1.16 t_{CO2}/t_{steel}.

Emissions from the DRI plant are calculated based on the following:

- 435 kg_{CO2} per tonne of pellets produced or 0.435 t_{CO2} per tonne pellets.

As 1.05 tonnes of DRI are consumed to produce 1 tonne steel through the DRI-EAF route, this results in 0.46 t_{CO2}/t_{steel}.

Emissions from New Technology are calculated based on the following:

- The CO_2 emissions calculated from a blast furnace multiplied by 20%

It is assumed that the new technology will produce the same quality of hot metal as a blast furnace and that 900 kg hot metal is required to produce 1 tonne of steel in the BOF process. This results in 0.23 t_{CO2}/t_{steel}.

Emissions from the BOF plant are calculated based on the following:

- Mass of blast furnace gas multiplied by the CO_2 mass percent

Using the values in Table 2.11 from Santos (2013), this equates to:

104kg * 87.8% CO_2 = 0.09 t_{CO2}/t_{steel}

Emissions from the EAF plant are calculated based on the following:

- Mass of flue gas multiplied by the CO_2 mass percent

Using the values in Table 2.13 from Kumar (2020), this equates to:

0.878 * 0.08 = 0.07 t_{CO2}/t_{steel}

In a production route involving coke ovens, sinter plant, pellet plant, blast furnace and BOF the total CO_2 emissions per tonne of steel will be 0.22 + 0.06 + 0.02 + 1.16 + 0.09 = 1.56 to which 0.04 tonnes of CO_2 will be added from electrical energy generation. This leads to the value reported in Table 4.2 of 1.6 t_{CO2}/t_{steel}.

In case 1 of Chapter 4, approximately 1,390 million tonnes of steel are predicted to be produced via the BF-BOF route. This gives CO_2 emissions of 2.19 billion tonnes, or 1.63 billion tonnes if CCS is applied to blast furnace gas.
A further 500 million tonnes of steel will be produced by the EAF route from scrap generating 0.07 billion tonnes of CO_2. The DRI-EAF route will be used to account for the remaining steel production of approximately 210 million tonnes. This will generate a further 0.16 billion tonnes of CO_2. By summating the emissions from the three production routes, a total and average emissions intensity can be determined. The total is 2.42 billion tonnes of CO_2 which gives an average intensity of 1.15 t_{CO2}/t_{steel}.

The DRI-EAF route is able to use hydrogen to greatly reduce it's CO_2 emissions. In this case, emissions from the DRI plant are calculated as follows:
DRI: 1000 * 0.435 / 10 = 0.04t_{CO2}/t_{DRI} or 0.05t_{CO2}/t_{steel}.
For the CCS values for the Business as Usual case in section 4.3.1, emissions from the BF-BOF and DRI-EAF routes drop to 1.63 and 0.08 billion tonnes of CO_2 respectively. With the unchanged emissions from the EAF route, this leads to total CO_2 emissions of 1.78 billion tonnes with an average emissions intensity of 0.85 t_{CO2}/t_{steel}.
This same logic is applied to all the cases presented in Chapter 4, where the percentage split of steel production varies across possible production routes. This affects the total emissions from each route and therefore the total emissions from steel production for a single year.

2. Example Flowsheet

Within Chapter 5 of the thesis, flowsheets were used to determine technologies which may be able to reduce the CO_2 emissions from a blast furnace. Figure 1 shows a typical flowsheet of the type used in for this analysis. This particular flowsheet is for case 3, in which vacuum pressure swing adsorption is used to remove CO_2 from the blast furnace gas. Chemical absorption, physical absorption, pressure swing adsorption and temperature swing adsorption were also analysed.

The flowsheet is shown graphically in the top part of the figure with the gas flow, composition, temperature and pressure given for each numbered stream. Information for the Cold blast, Hot blast, Dirty BFG, Clean BFG, Coke and Coal (streams 1-4, 20 & 21) for all cases comes from the Primetals Technologies proprietary blast furnace heat and mass balance model for blast furnaces.

The enthalpy of the cold and hot blast streams in kCals/Nm^3 is calculated based on Primetals Technologies procedures detailed below. The difference between these values represents the minimum amount of energy which must be supplied to the hot blast stoves to heat the cold blast before it enters the blast furnace.

$$\text{Cold Blast Enthalpy} = 47.65 \times O_2\% + 46.8 \times N_2\% + 54.13 \times H_2O\% \quad (2)$$

$$\text{Hot Blast Enthalpy} = 410.85 \times O_2\% + 389.55 \times N_2\% + 481.3 \times H_2O\% \quad (3)$$

The calorific values of the combustion gas streams are also calculated based on Primetals Technologies procedures summarised below. This value for the exported gas streams is used to determine the amount of exported chemical energy from the flowsheet. This amount of export energy is one of the criteria used to assess the different flowsheet cases.

$$\text{Gas Calorific Value} = 25.751 \times H_2\% + 30.161 \times CO\% + 85.544 \times CH_4\% \quad (4)$$

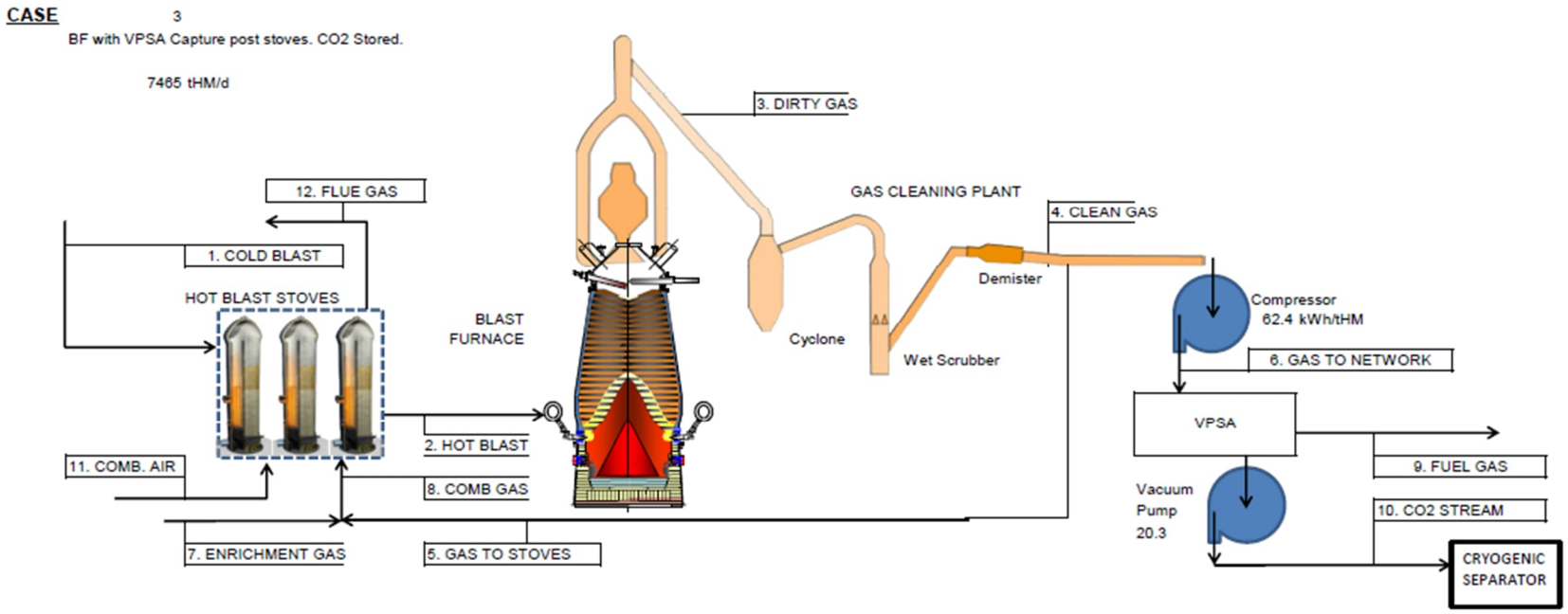

STREAM	Gas Flow (Nm3/tHM)	Gas Composition O2	CO2	N2	CO	H2	H2O	CH4	Temp °C	Pressure bar g.	Enthalpy kCals/Nm³	CV kCals/Nm³		dH MCals/tHM	tCO2/tHM	
1 Cold Blast	947	25.5%	-	71.1%	-	-	3.4%	-	150	4	47.27			-		
2 Hot Blast	947	25.5%	-	71.1%	-	-	3.4%	-	1150	4	398.10			332		
3 Dirty BFG	1466	0.0%	23.3%	46.6%	24.0%	2.8%	3.3%	0.0%	150	2.5		795.0			1.36	424 tCO2/h
4 Clean BFG	1528	0.0%	22.4%	44.7%	23.0%	2.7%	7.3%	0.0%	40	2.2		762.8			1.36	
5 BFG to Stoves	583	0.0%	22.4%	44.7%	23.0%	2.7%	7.3%	0.0%	40	0.1		762.8	38.2%		0.52	
6 BFG to network	945	0.0%	22.4%	44.7%	23.0%	2.7%	7.3%	0.0%	40	4		762.8			0.84	
7 Stoves Enrich	42	0.0%	1.5%	3.8%	6.2%	59.3%	4.2%	24.9%	30	0.15		3846.5			0.03	
8 Comb. Gas	625	0.0%	21.0%	42.0%	21.9%	6.5%	7.0%	1.7%	39	0.1	25.19	970.8	80.0%	623	0.55	
9 BFG Fuel	660	0.0%	1.0%	64.0%	31.3%	3.8%	0.0%	0.0%	40	2		1041.0			0.42	
10 Separated CO2	285	0.0%	72.0%	0.0%	3.8%	0.1%	24.1%	0.0%	40						0.42	
11 Comb. Air	586	20.6%	0.0%	77.5%	0.0%	0.0%	1.9%	0.0%	35	0.1					0.00	
12 Stove Flue Gas	1123	1.0%	24.8%	63.8%	0.0%	0.0%	10.4%	0.0%	300	0.02					0.55	
20 Coke	362	kg/tHM														
21 Coal	120	kg/tHM														
			Compression & Storage		115 kWh/tCo2			352 g/kWh							0.02	

Figure 1: View of a typical flowsheet used to determine possible technologies for reducing CO2 from blast furnaces

The combustion gas stream sent to the hot blast stoves is dependant on the calorific value of the gas from the blast furnace. If it is too low to achieve a target flame temperature, then coke oven gas is added. If the calculated flame temperature is too high, then nitrogen is added to dilute the gas from the blast furnace. The calculation method for determining flame temperature is based on the standard calculation method from Primetals Technologies. The energy within the combustion gas stream to the hot blast stoves is combined with the calculated flow of combustion air required to give an energy input to the stoves. A thermal efficiency of 80% is taken to determine the flow of combustion gas to the hot blast stoves.

Separate tabs are included to calculate the electrical duty of the chemical absorption plant, gas compressors for physical adsorption and gas expanders to recover energy from high pressure gas streams. Details of the gas compressor calculation are given in Figure 2. Details of the gas expander calculation based on Primetals Technologies standard calculation procedure are given in Figure .

3. Gas Compressor Duty

The calculation in Figure 2 takes gas inlet conditions such as volumetric flowrate, temperature, pressure and composition from the overall summary tab shown in Figure 1. This information is used to determine an electrical energy consumption to meet a specified outlet pressure. The calculation follows a standard procedure by Primetals Technologies and assumes a mechanical efficiency of 80%.

The resulting electrical energy consumption is used to determine the electrical and total energy consumption per tonne of CO_2 captured from blast furnace gas.

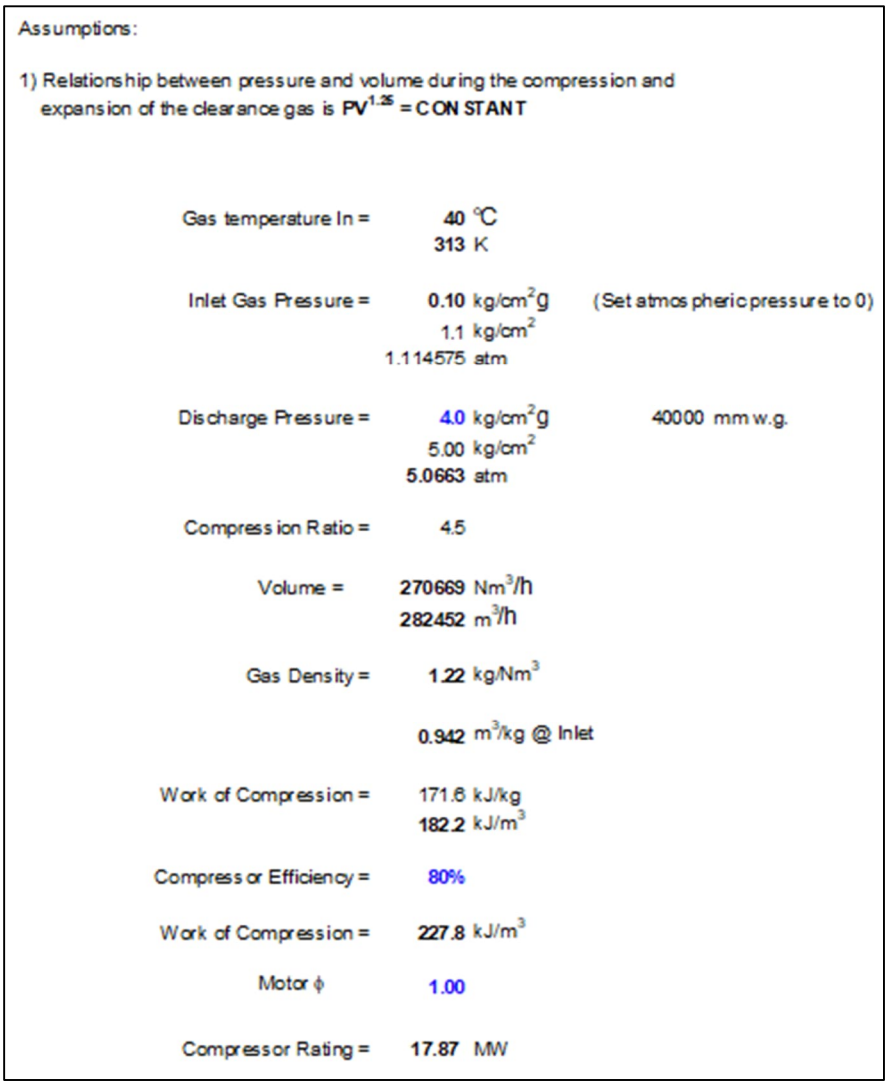

Figure 2: Gas compressor duty Calculation

The key calculations within Figure 2 are included below:

$$E_{\text{compressor}} = Q_{\text{gas}} \times work_{\text{compression}} / (eff_{\text{mech}} \times eff_{\text{elec}}) \quad 5$$

Where:

$E_{\text{compressor}}$ = electrical energy consumption of the gas compressor (MW)

Q_{gas} = Flowrate of gas stream (m^3/s)

$work_{\text{compression}}$ = work of compression (MJ/m^3)

eff = efficiency split into mechanical (80%) and electrical (100%)

$$work_{\text{compression}} = 100 \times P_{\text{in}} * 2 * \left(\frac{1.25}{0.25}\right) \times \left(\left(\frac{P_{\text{out}}}{P_{\text{in}}}\right)^{\left(\frac{0.25}{2.5}\right)} - 1\right) \quad 6$$

Where:

$work_{\text{compression}}$ = work of compression (MJ/m^3)

P_{in} = gas inlet pressure (bar)

P_{out} = gas outlet pressure (bar)

4. Gas Expander

In cases where gas streams are generated with high pressures, such as with Physical Absorption, a gas expander is added into the flowsheet to recover electrical energy. The amount of energy which can be generated is calculated in a gas expander sub-model following a calculation procedure from Primetals Technologies. The calculation takes gas information such as volumetric flow, gas composition, temperature and pressure from the summary sheet. By specifying an outlet pressure and conversion efficiencies, an electrical power output can be derived. The layout of the calculation is given in Figure . The key calculation from this sheet is summarised below:

$$E_{\text{TRT}} = Q_{\text{gas}} \times \rho \times Sp.Heat \times \left(T_{\text{gas}} \times \left(1 - \left(\frac{P_{\text{out}}}{P_{\text{in}}}\right)^{\frac{(SHR-1)}{SHR}}\right)\right) \times (eff_{\text{mech}} \times eff_{\text{elec}}) \quad 7$$

Where:

E_{TRT} = Electrical energy generated by gas expander (MW)

Q_{gas} = Flowrate of gas stream (m^3/sec)

ρ = gas density (kg/m^3)

Sp. Heat = Specific heat capacity of gas (MJ/kg.K)

T_{gas} = Temperature of gas (K)

P_{in} = gas inlet pressure (bar)

P_{out} = gas outlet pressure (bar)

SHR = Specific Heat Ratio (unitless)

eff = efficiency split into mechanical (85%) and electrical (97%)

Generator Output

Inputs :	Gas volume (dry)	Nm^3/h	312506
	Specific gravity (gas)	kg/Nm3	1.2203
	Specific heat	kcal/kg°C	0.2557
	Inlet gas temperature	°K	40
	Furnace top pressure	kg/cm^2g	4
	Inlet gas pressure	bar abs	4.9
	Outlet gas pressure	bar abs	1.11325
			0.23
	Specific heat ratio		1.37
			0.67
	Turbine efficiency	%	85.00%
	Generator efficiency	%	97.00%

Output at generator = 1238 kWh

Figure 3: Calculation of power generation from gas expander

5. Other Calculations

Several other calculations were used within the analysis given in Chapter 5. These are summarised below.

5.1. Chemical Absorption

In flowsheet cases 1, 5, 9-11, 15, 18, 22, 26, 30, 31, 35, 41 and 47-50 where chemical absorption was used to remove CO_2 from the blast furnace gas, the flowrate of amine required was estimated. This flow was also used to determine an electrical energy requirement to recirculate the amine using electrically driven pumps.

$$Q_{\text{solvent}} = (mol_{\text{CO2}} \times M_{\text{MEA}})/(0.3 \times \rho_{\text{MEA}} \times y_{\text{MEA}}) \quad (8)$$

Where:

$Q_{solvent}$ = Flow of capture solvent (m^3/h)

mol_{CO2} = moles of CO_2 captured (kmol/h)

M_{MEA} = Molecular weight of MEA (kg/kmol)

y_{MEA} = Volume percent of MEA (vol%)

ρ_{MEA} = Density of MEA (kg/m^3)

$$E_{\text{pump}} = (Q_{\text{solvent}} \times dP)/(work_{\text{compression}} \times eff) \quad 9$$

Where:

E_{pump} = electrical energy consumption by solvent pumps

$Q_{solvent}$ = Flow of capture solvent (m^3/s)

dP = differential pressure of the pump (bar)

$work_{compression}$ = work of compression taken as 36.7 (m^3.bar/MJ)

eff = pump efficiency, taken as 75%

The quantity of steam required to regenerate the amine within the chemical absorption plant was also determined using the quantity of CO_2 removed from the blast furnace gas. The formula to estimate the steam consumption is given below.

$$Steam_{\text{MEA}} = Q_{\text{CO2}} \times y_{\text{CO2}} \times \rho_{\text{CO2}} \times Regen_{\text{energy}}/H_{\text{Steam}} \quad 10$$

Where:

$Steam_{MEA}$ = steam requirement for regeneration of MEA (kg/tHM)

Q_{CO2} = Flow of CO_2 rich gas leaving chemical absorption plant (m^3/tHM)

y_{CO2} = Volume percent of CO_2 in outlet gas (vol%)

ρ_{CO2} = Density of CO_2 (kg/m^3)

$Regen_{energy}$ = Energy required to regenerate MEA taken as 2.5 (MJ/kg)

H_{Steam} = Enthalpy of Steam (MJ/kg)

5.2. Algae

In case 9 where CO_2 is used to grow algae, the approximate land usage was determined based on the amount of CO_2 captured and a land utilisation factor as below:

$$Land\_use = Q_{CO2} \times y_{CO2} \times \rho_{CO2} / Utilisation \quad 11$$

Where:

Land_use = area of land required to utilise the CO_2 amount (km^2)

Q_{CO2} = Flow of CO_2 rich gas leaving chemical absorption plant (m^3/day)

y_{CO2} = Volume percent of CO_2 outlet gas (vol%)

ρ_{CO2} = Density of CO_2 (t/m^3)

Utilisation = Utilisation Factor (50 t/d/km^2)

5.3. Water Gas Shift (WGS)

In cases 18-25, a water gas shift (WGS) process is used to convert CO and water into CO_2 and H_2. This increases the amount of CO_2 which can be removed from the blast furnace gas but requires additional steam. The formulae overleaf are used to determine the outlet gas conditions from the WGS process. The calculations consider the full conversion of CO to CO_2:

$$Q_{OUT} = Q_{IN} \times (y_{CO2} + y_{N2} + 2y_{CO} + y_{H2} + y_{H2O}) \quad 12$$

Where:

Q_{OUT} = Flow of gas leaving the WGS process (m^3/h)

Q_{IN} = Flow of gas entering the WGS process (m^3/h)

y_i = Volume percent of species 'i' in inlet gas (vol%)

$$x_i = (y_i + y_{CO}) \times \left(\frac{Q_{IN}}{Q_{OUT}}\right) \quad 13$$

Where:

x_i = Volume percent of CO_2 or H_2 in outlet gas (vol%)

y_i = Volume percent of CO_2 or H_2 in inlet gas (vol%)

y_{CO} = Volume percent of CO in inlet gas (vol%)

Q_{OUT} = Flow of gas leaving the WGS process (m^3/h)

Q_{IN} = Flow of gas entering the WGS process (m^3/h)

In addition, the steam requirement is estimated by the equation below. This quantity of steam is added to that required by other processes such as chemical absorption or temperature swing adsorption to give a total steam requirement per flowsheet case.

$$Steam_{\mathrm{WGS}} = y_{\mathrm{CO}} \times Q_{\mathrm{IN}} \times \rho_{\mathrm{steam}} \quad 14$$

Where:

$Steam_{WGS}$ = Flow of steam required for the WGS process (kg/h)

y_{CO2} = Volume percent of CO_2 in inlet gas (vol%)

Q_{IN} = Flow of gas entering the WGS process(m^3/h)

ρ_{steam} = Density of Steam (kg/m^3)

5.4. Solid Oxide Electrolysis Cell (SOEC)

In cases 26-29 a solid oxide electrolysis cell (SOEC) is used to regenerate CO_2 separated from blast furnace gas into a mixture of CO and CO_2. This regenerated gas is then used as a fuel gas at the hot blast stoves. The formulae which estimate the electrical energy requirement and outlet gas conditions from this step are given overleaf:

$$E_{\mathrm{SOEC}} = Energy \times eff \times y_{\mathrm{CO2}} \times mol_{\mathrm{CO2}} \quad 15$$

Where:

E_{SOEC} = electrical energy requirement for SOEC (kWh/tHM)

Energy = electrical energy per mole of CO_2 taken as 189 (kWh/kmol)

eff = SOEC process efficiency taken as 62.8%

y_{CO2} = Volume percent of CO_2 in inlet gas (vol%)

mol_{CO2} = molar flowrate of inlet gas stream (kmol/tHM)

$$x_{\mathrm{CO2}} = y_{\mathrm{CO2}} - (y_{\mathrm{CO2}} \times eff) \quad 16$$

Where:

x_{CO2} = Volume percent of CO_2 in outlet gas (vol%)

y_{CO2} = Volume percent of CO_2 in inlet gas (vol%)

eff = SOEC process efficiency taken as 62.8%

$$x_{\mathrm{CO}} = y_{\mathrm{CO}} + (y_{\mathrm{CO2}} \times eff) \quad (17)$$

Where:

x_{CO} = Volume percent of CO in outlet gas (vol%)

y_{CO} = Volume percent of CO in inlet gas (vol%)

y_{CO2} = Volume percent of CO_2 in inlet gas (vol%)

eff = SOEC process efficiency taken as 62.8%

5.5. Reverse Water Gas Shift (RWGS)

In cases 30 to 38, the reverse water gas shift reaction is used to regenerate CO_2 separated from blast furnace gas into a mixture of CO and CO_2. A portion of this regenerated gas is then used as a fuel gas at the hot blast stoves with the remainder exported to the gas network. The formulae which estimate the pure H_2 flow required and outlet gas conditions from this step are given below:

$$Q_{\mathrm{H2}} = Q_{\mathrm{IN}} \times y_{\mathrm{CO2}} \quad (18)$$

Where:

Q_{H2} = volumetric flow of H_2 gas (m^3/h)

Q_{IN} = inlet gas flow to RWGS step (m^3/h)

y_{CO2} = inlet volume percent of CO_2 (vol%)

$$Q_{\mathrm{OUT}} = Q_{\mathrm{IN}} + Q_{\mathrm{H2}} \quad (19)$$

Where:

Q_{OUT} = outlet gas flow from RWGS step (m^3/h)

Q_{IN} = inlet gas flow to RWGS step (m^3/h)

Q_{H2} = volumetric flow of H_2 gas (m^3/h)

$$x_{\mathrm{CO}} = y_{\mathrm{CO2}} \times eff \times \frac{Q_{\mathrm{IN}}}{Q_{\mathrm{OUT}}} \quad (20)$$

Where:

x_{CO} = outlet gas CO volume percent (vol%)

y_{CO2} = inlet volume percent of CO_2 (vol%)

eff = efficiency of RWGS process taken as 20%

Q_{IN} = inlet gas flow to RWGS step (m^3/h)

Q_{OUT} = outlet gas flow from RWGS step (m^3/h)

$$x_{\mathrm{H2}} = \frac{Q_{\mathrm{H2}} - (x_{\mathrm{CO}} \times Q_{\mathrm{OUT}})}{Q_{\mathrm{OUT}}} \quad 21$$

Where:

x_{H2} = outlet gas H_2 volume percent (vol%)

Q_{H2} = flow of Hydrogen required (m^3/h)

x_{CO} = outlet gas CO volume percent (vol%)

Q_{OUT} = outlet gas flow from RWGS step (m^3/h)

$$x_{\mathrm{CO2}} = \left(y_{\mathrm{CO2}} - (y_{\mathrm{CO2}} \times eff)\right) \times \frac{Q_{\mathrm{IN}}}{Q_{\mathrm{OUT}}} \quad 22$$

Where:

x_{CO2} = outlet gas CO_2 volume percent (vol%)

y_{CO2} = inlet gas CO_2 volume percent (vol%)

eff = efficiency of RWGS process taken as 20%

Q_{IN} = inlet gas flow to RWGS step (m^3/h)

Q_{OUT} = outlet gas flow from RWGS step (m^3/h)

$$x_{H2O} = \frac{y_{\mathrm{H2O}} \times Q_{\mathrm{IN}} + x_{\mathrm{CO}} \times Q_{\mathrm{OUT}}}{Q_{\mathrm{OUT}}} \quad 23$$

Where:

x_{H2O} = outlet gas H_2O volume percent (vol%)

y_{H2O} = inlet gas H_2O volume percent (vol%)

Q_{IN} = inlet gas flow to RWGS step (m^3/h)

x_{CO} = outlet gas CO volume percent (vol%)

Q_{OUT} = outlet gas flow from RWGS step (m^3/h)

5.6. Temperature Swing Adsorption (TSA)

In cases 39 and 40, temperature swing adsorption (TSA) is used to separate CO_2 from blast furnace gas. This technology uses thermal energy in the form of steam to regenerate the adsorbant material once it has reached its capacity to remove CO_2 from the gas stream. Calculations used to determine the steam requirement are included below.

$$Steam_{\mathrm{TSA}} = \frac{y_{\mathrm{CO2}} \times \rho_{\mathrm{CO2}} \times Q_{\mathrm{IN}} \times Regen_{\mathrm{energy}}}{H_{\mathrm{Steam}}} \quad 24$$

Where:

$Steam_{TSA}$ = Flow of steam required for the TSA process (kg/h)

Q_{IN} = flow of gas entering TSA process (m^3/h)

y_{CO2} = inlet gas CO_2 volume percent (vol%)

ρ_{CO2} = Density of CO_2 (kg/m^3)

$Regen_{energy}$ = Energy required to regenerate adsorbant taken as 4.4 (MJ/kg)

H_{Steam} = Enthalpy of Steam (MJ/kg)

5.7. Plasma Catalysis

In cases 47-49, plasma catalysis is used to regenerate the CO_2 removed from blast furnace gas into a mixture of CO, O_2 and CO_2. A portion of this regenerated gas is then used as a fuel gas at the hot blast stoves with the remainder exported to the gas network. The formulae which estimate the electrical energy required and outlet gas conditions from this step are given overleaf:

$$E_{\mathrm{plasma}} = (eff \times mol_{\mathrm{CO2}})/(Energy \times 3600) \quad 25$$

Where:

E_{plasma} = electrical energy requirement for SOEC (kWh/tHM)

eff = efficiency of plasma catalysis step taken as 38%

mol_{CO2} = molar flow of CO_2 into the plasma catalysis step (mol/tHM)

Energy = energy required to convert CO_2 taken as 0.6 (kW/mol)

$$Q_{\mathrm{OUT}} = Q_{\mathrm{IN}} + (Q_{\mathrm{IN}} \times y_{\mathrm{CO2}} \times 0.5eff) \quad 26$$

Where:

Q_{OUT} = flow of gas leaving the Plasma Catalysis process (m^3/h)

Q_{IN} = flow of gas entering Plasma Catalysis process (m^3/h)

y_{CO2} = inlet gas CO_2 volume percent (vol%)

eff = efficiency of plasma catalysis step taken as 38%

$$x_{\mathrm{CO}} = \frac{y_{\mathrm{CO2}} \times eff \times Q_{\mathrm{IN}}}{Q_{\mathrm{OUT}}} \quad (27)$$

Where:

x_{CO} = outlet gas CO volume percent (vol%)

y_{CO2} = inlet gas CO_2 volume percent (vol%)

eff = efficiency of plasma catalysis step taken as 38%

Q_{IN} = flow of gas entering Plasma Catalysis process (m^3/h)

Q_{OUT} = flow of gas leaving the Plasma Catalysis process (m^3/h)

$$x_{\mathrm{O2}} = 0.5 x_{\mathrm{CO}} \quad (28)$$

Where:

x_{O2} = outlet gas O_2 volume percent (vol%)

x_{CO} = outlet gas CO volume percent (vol%)

$$x_{\mathrm{CO2}} = \left(y_{\mathrm{CO2}} - (y_{\mathrm{CO2}} \times eff)\right) \times \frac{Q_{\mathrm{IN}}}{Q_{\mathrm{OUT}}} \quad (29)$$

Where:

x_{CO2} = outlet gas CO_2 volume percent (vol%)

y_{CO2} = inlet gas CO_2 volume percent (vol%)

eff = efficiency of plasma catalysis step taken as 38%

Q_{IN} = flow of gas entering Plasma Catalysis process (m^3/h)

Q_{OUT} = flow of gas leaving the Plasma Catalysis process (m^3/h)